

Zory Vlad Todres

Organic Chemistry in Confining Media

 Springer

Organic Chemistry in Confining Media

Zory Vlad Todres

Organic Chemistry in Confining Media

 Springer

Zory Vlad Todres
Belmont, MA
USA

ISBN 978-3-319-00157-9 ISBN 978-3-319-00158-6 (eBook)
DOI 10.1007/978-3-319-00158-6
Springer Cham Heidelberg New York Dordrecht London

Library of Congress Control Number: 2013937188

© Springer International Publishing Switzerland 2013

This work is subject to copyright. All rights are reserved by the Publisher, whether the whole or part of the material is concerned, specifically the rights of translation, reprinting, reuse of illustrations, recitation, broadcasting, reproduction on microfilms or in any other physical way, and transmission or information storage and retrieval, electronic adaptation, computer software, or by similar or dissimilar methodology now known or hereafter developed. Exempted from this legal reservation are brief excerpts in connection with reviews or scholarly analysis or material supplied specifically for the purpose of being entered and executed on a computer system, for exclusive use by the purchaser of the work. Duplication of this publication or parts thereof is permitted only under the provisions of the Copyright Law of the Publisher's location, in its current version, and permission for use must always be obtained from Springer. Permissions for use may be obtained through RightsLink at the Copyright Clearance Center. Violations are liable to prosecution under the respective Copyright Law. The use of general descriptive names, registered names, trademarks, service marks, etc. in this publication does not imply, even in the absence of a specific statement, that such names are exempt from the relevant protective laws and regulations and therefore free for general use.

While the advice and information in this book are believed to be true and accurate at the date of publication, neither the authors nor the editors nor the publisher can accept any legal responsibility for any errors or omissions that may be made. The publisher makes no warranty, express or implied, with respect to the material contained herein.

Printed on acid-free paper

Springer is part of Springer Science+Business Media (www.springer.com)



This book is dedicated to my parents. To my father, who despite having been imprisoned in the whirlwind of Stalin's Great Terror, did not yield to his captors and did not implicate other innocent people. To both my mother and my father, who survived the horrors of war and political repression and were able to keep their three children alive and healthy, and gave them a good education.

Preface

This treatise considers the chemistry of confined organic and organometallic compounds. When molecules are confined, their reactivity is changed. These conditions provide a shielding effect which confines and inhibits undesirable interactions and increases the desired chemical capabilities.

This book is devoted to an important and well-developed area of organic and organometallic chemistry, which is now an indispensable part of this science. Calixarenes, pillararenes, cyclodextrins, cucurbiturils, and zeolites as confining agents are well known, but the corresponding new and demonstrative publications now deserve fresh attention. Inclusion of these topics is also important as a general approach to the themes considered.

This book has several distinctive features. First, it considers the unprecedentedly wide range of confinement effects. Second, emphasis is put on examples, which are representative for each kind of effect discussed. Third, the book includes previously avoided discussions concerning transformations within micelles, porous materials, solvent cages, hydrogen-bond or charge-transfer complexes, and resin-docking and template effects of organometallic compounds. Fourth, the author summarizes sorption effects, the role of solvents, crystal-lattice phenomena, and stereochemical changes upon confinement. Finally, relevant practical applications of confinement effects in microelectronics, pharmacchemistry, petrochemistry, and related fields are also considered. This is a comprehensive picture of the chemistry of confined organic and elemento-organic compounds, and I hope that it will be a valuable resource for a wide range of readers.

Further Readings

There are already a wide range of books devoted to confinement by organic cavities such as calixarenes, cyclodextrins, and cucurbiturils, which testifies to the importance of this research area. For further reading, please see the following titles:

Gutsche (1989, 1998), Vicens and Boehmer, eds. (1991), Usawa and Yonemitsu, eds. (1992), Cram and Cram (1994), Easton and Lincoln (1999), Mandolini and Ungaro, eds. (2000), Asfari et al. eds. (2001), Guisnet and Gilson (2002), Vicens and Harrowfield, eds. (2006), Dodziuk, ed. (2008), Sliwa and Kozlowski (2009), Brinker and Miesset, eds. (2010), and Kim et al. (2011).

Contents

1	Encapsulation Effects	1
1.1	Introduction	1
1.2	Calixarenes as Hosts	2
1.3	Pillararenes and Pillarquinones	7
1.4	Concaves as Hosts	9
1.5	Carcerands as Hosts	11
1.6	Cyclodextrins as Hosts	17
	1.6.1 Native Cyclodextrins	17
	1.6.2 Modified Cyclodextrins	28
1.7	Cucurbiturils as Hosts	36
1.8	Tweezers as Hosts	49
1.9	Dendrimers as Hosts	53
1.10	Closing Remarks	57
	References	57
2	Resin-Docking, Polymer-Penetration, and Surface-Engrafting Effects	65
2.1	Introduction	65
2.2	Resin-Docking Effects	65
2.3	Polymer-Penetration Effects	66
2.4	Surface-Engrafting Effects	68
2.5	Closing Remarks	69
	References	70
3	Reactions Within Charge-Transfer Complexes	71
3.1	Introduction	71
3.2	Specific Characteristics of Reactions Within Charge-Transfer Complexes	71
3.3	Cyclization Within Charge-Transfer Complexes	72
3.4	Substitution Within Charge-Transfer Complexes	74
3.5	Geometrical Isomerization of Alkenes Within Charge-Transfer Complexes	76

3.6	Role of Charge-Transfer Complexation in Vinylic Nucleophilic Substitution	78
3.7	Role of Charge-Transfer Interaction in Oxidative Polymerization	80
3.8	Organic Reactivity Within Crystals Containing Charge-Transfer Complexes	81
3.9	Closing Remarks	84
	References	86
4	Effects of Hydrogen Bonding	89
4.1	Introduction	89
4.2	Host–Guest Arrangement in Hydrogen-Bond Complexes	89
4.3	Hydrogen-Bonding Effects on Reactivity of Confined Guests	92
4.4	Hydrogen-Bonding Effects in Organic Co-Crystals	96
4.5	Closing Remarks	101
	References	101
5	Effects of Coordination to Metals	103
5.1	Introduction	103
5.2	Organic-Ligand Isomerization Within Metallocomplexes	103
5.3	Metal-Coordination Assemblage	104
5.4	Closing Remarks	111
	References	112
6	Effects of Sorption	115
6.1	Introduction	115
6.2	Chemisorption	115
6.3	Physisorption	117
6.4	Absorption at Water Surface	119
6.5	Adsorption at Electrode Surfaces	120
6.6	Confinement by Monolayers or Clathrates	124
6.7	Closing Remarks	126
	References	127
7	Micellar Effects	129
7.1	Introduction	129
7.2	Micellar Effects on Guest Reactivity	129
7.3	Micellar Effects in Regulation of Guest Reactivity	131
7.4	Drug-Protective and Drug-Delivery Properties of Polymer-Based Micelles	133
7.5	Closing Remarks	134
	References	134

8	Cage Effects of Solvents, Proteins, and Crystal Lattices	137
8.1	Introduction	137
8.2	Solvent-Cage Effects.	137
8.3	Interplay Between Salt- and Solvent-Cage Effects	138
8.4	Protein-Cage Effects	139
8.5	Cage Effects of Crystal Lattices	140
8.6	Closing Remarks	141
	References	141
9	Pore Effects	143
9.1	Introduction	143
9.2	Porous Organic Frameworks	143
9.3	Porous Organometallic Frameworks	144
9.4	Silica Porous Materials	148
9.5	Single Crystals as Porous Materials	151
9.6	Zeolites as Confining Materials	152
9.7	Confinement Within Porous Metal Oxides.	163
9.8	Confinement Within Carbon and Polymer Nanopores	164
9.9	Closing Remarks	165
	References	165
10	Stereochemical Outcomes of Confinement	169
10.1	Introduction	169
10.2	Effects of Guest Confinement on Host Configurations	169
10.3	Stereochemical Changes of Guests Upon Their Inclusion into Hosts	172
10.4	Closing Remarks	176
	References	176
11	The Role of Solvents in Confined Organic and Organometallic Reactions.	179
11.1	Introduction	179
11.2	Hydration/Dehydration Upon Confinement	179
11.3	Organic Solvents	183
11.4	Mixed Solvents	184
11.5	The Specific Role of Organic Solvents in Trapping by Porous Materials	185
11.6	Solvent–Matrix Effects	186
11.7	Closing Remarks	186
	References	187
12	Conclusions	189
	Index	191

About the Author

Zory Vlad Todres holds a Ph.D. in Chemical Technology and Sc.D. (a doctor habilitatus) in Physical Organic Chemistry. He has published several hundred papers on electron- and charge-transfer phenomena, on metal-coordination assemblage, and on reactions of organic substrates influenced by sorption.

He has published the following books: “Organic Ion-Radicals”, “Chalcogen-adiazoles”, “Organic Mechanochemistry”, and “Ion-Radical Organic Chemistry”. Through his books, Z. V. Todres aspires to engraft new and practically important branches onto the great tree of organic chemistry. This book on confined effects in organic chemistry is also a step in this direction. His published books are much in demand and have been well received by the chemical community.

Chapter 1

Encapsulation Effects

1.1 Introduction

Consideration of supramolecular systems which provide a confined nanospace for the formation of discrete inclusion complexes with reactive guests is based on new and principally important data. Encapsulation effects are inherent to concave molecules named cavitands. Cavitands are spherical, hollow hosts with inner cavities that are large enough to accommodate one or more guest molecules. The cavity of the cavitand allows it to engage in host–guest chemistry with guest molecules of complementary shape and size. Examples include cyclodextrins, cucurbiturils, calixarenes, resorcinarenes, pillararenes, etc. Cavitands are used as molecular flasks to study the effects of confinement on reactions involving encapsulated guests.

Encapsulation is usually considered as host–guest complexation or an inclusion reaction. Reversibly encapsulated complexes are systems in which molecular guests are more or less surrounded by hosts, which themselves were either ready-made or self-assembled. The formation of host–guest inclusion complexes takes place in accordance with the principles of geometric and energetic complementarity, with noncovalent forces being responsible for the binding. Weak intermolecular interactions hold the guest–host system together: hydrogen bonds, hydrophobic effects, salt bridges, coordinative and dispersion forces, and dipole–dipole and electrostatic interactions.

Under confinement conditions, a site-specific substrate can be located in the correct position, orientation, and conformation. Being incorporated into an open cavity, an organic guest may stay there for much longer than 1 μ s. This time is significantly longer than the lifetime of commonly encountered photoexcited molecules (Zhang et al. 2002). When the reacting guest is completely imprisoned, it can only escape from the “prison” at elevated temperature. Depending on the relative sizes of the host and guest molecules, more than one guest can be accommodated and chemistry between the imprisoned guests becomes possible. On the basis of the preference for filling empty cavities and according to the experimental data, Mecozzi and Rebek (1998), Adjami and Rebek (2007), and Rekharsky et al. (2007) estimated that the

confined molecules can take up $55 \pm 0.09\%$ of the cavity volume. The paper by Al-Sou'od (2008) gives a typical example of multivariate approaches to detect the formation of inclusion complexes.

The literature gives examples where chemical reactants lower their energies by forming encapsulated complexes. Inside such complexes, the reactant interactions proceed faster and are more selective. The azide–alkyne 1,3-dipolar cycloaddition is one such example (Mock et al. 1989; Tuncel and Steinke 1999; Carlqvist and Maseras 2007; Liu et al. 2008a). In other words, encapsulation is related to enzymatic catalysis, which is also attracting heightened interest.

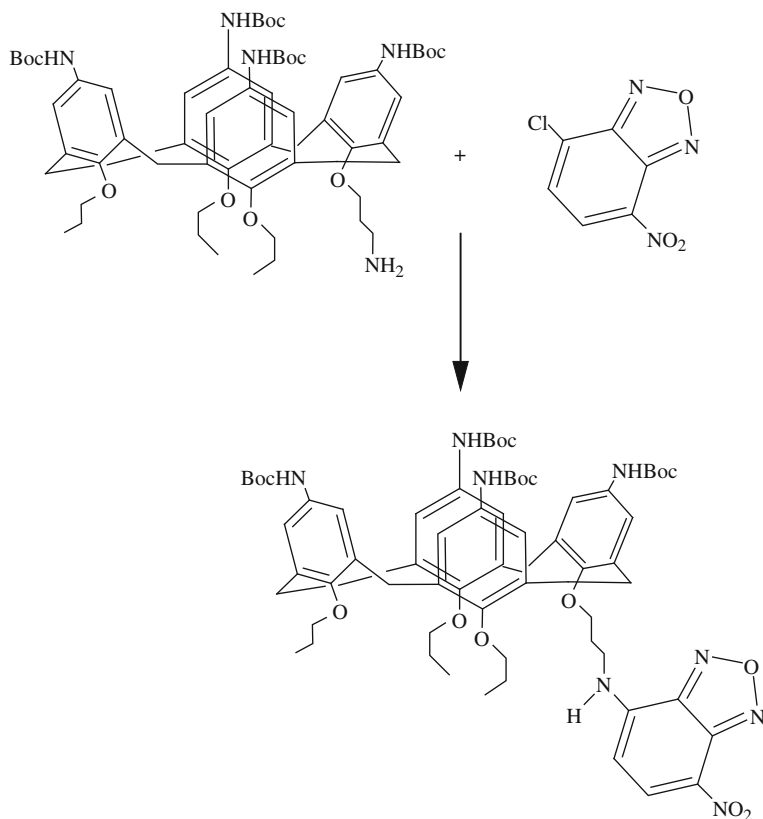
1.2 Calixarenes as Hosts

Calixarenes are cyclic oligomers of aryl compounds, and their structures resemble a molecular bowl with a hydrophobic cavity. Reversibly assembled capsules are developed for anionic, cationic, and neutral species to provide a cavity for guests. Inclusion of guest molecules into calixarene frameworks is typically achieved either in solution via convection and solvation-based molecular recognition or in solid via simple diffusion. Once inside the calixarene cavity, organic guests change their reactivity.

For instance, inclusion of the 1,1'-dimethyl-4,4'-dipyridyl cation-radical (the cation-radical of methylviologen) into a sulfocalixarene cavity prevents the disadvantageous π dimerization. This is important for more effective use of viologens as components for electrochromic displays and electric conductors (Guo et al. 2007 and references therein). In this case, the donoric particle is included into the acceptoric cup of the cyclodextrin.

The donoric-cup aminocyclodextrin reacts with the strong acceptor nitrochlorobenzofurazan of Scheme 1.1 in another way: Instead of possible inclusion, nucleophilic substitution takes place, and the amino group bonded to cyclodextrin dislodges the chlorine (Lalor et al. 2008). The nitrochlorobenzofurazan of Scheme 1.1 is often used in substitutions of this type to endow biologically important compounds with fluorescence properties acceptable for spectral determination with high reliability (Todres 2011, pp. 55–59). The fluorescent probe (and potential drug-delivery system) of the final product of Scheme 1.1 does not affect overall cell viability (Lalor et al. 2008).

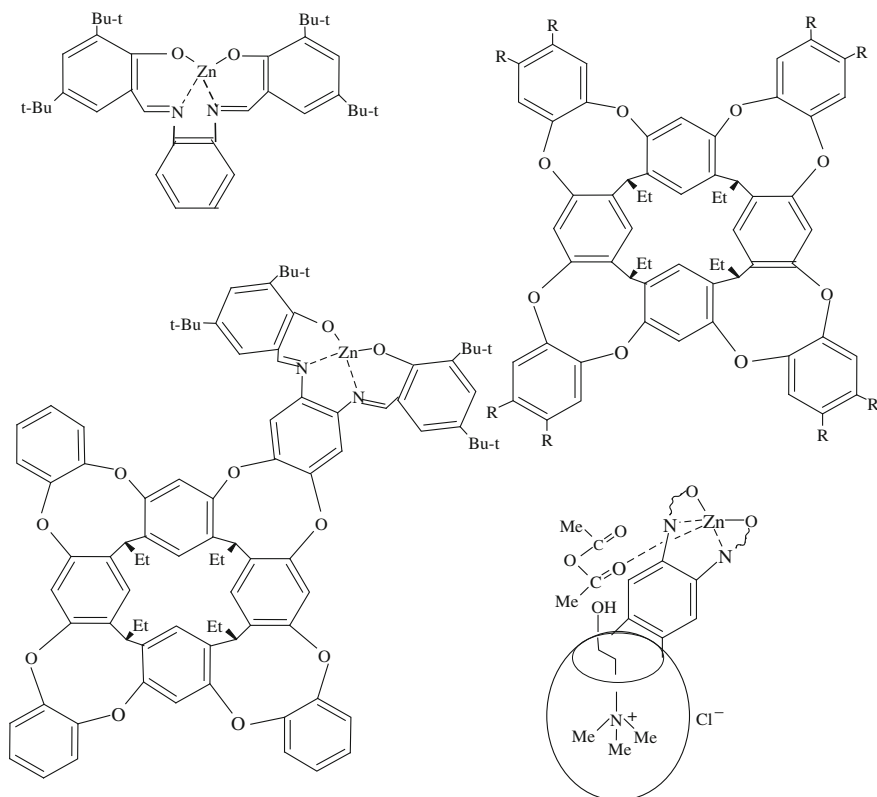
Guests bearing trimethylammonium end are well positioned within the resorcinarene cavity. Choline chloride (β -hydroxyethyltrimethylammonium chloride) belongs to this class of guests. Its transformation into *O*-acetyl derivative is a biomedically important reaction. In metabolic chains, choline reacts with acetyl coenzyme A to generate *O*-acetylcholine. The latter is a neurotransmitter. Zelder and Rebek (2006) measured the kinetics of the reaction between choline and acetic anhydride, on the one hand, and, on the other hand, the kinetics of acetic anhydride reactions with choline encapsulated by resorcinarene-based cavitands or by the zinc-salen complex without any cavitand (Scheme 1.2). Two cavitands were tested: the simple cavitand



Scheme 1.1 Aminocyclodextrin-chloronitrobenzofurazan substitution reaction

(top-right structure in Scheme 1.2) and the Zn-salen-modified cavitant (bottom-left structure in Scheme 1.2). As it turned out, no reaction was observed between choline and acetic anhydride in the presence of the simple cavitant. Meanwhile, in the presence of a small amount (2 mol%) of the Zn-salen-modified cavitant, acetylation does take place. As compared with the choline reaction with acetic anhydride with no cavitant, the confined acetylation proceeds 1,900 times faster. The rate of the reaction considered dropped up to 23 times when the zinc-salen complex not covalently attached to the cavitant was used as a catalyst in 2 mol% amount. This complex is depicted in the top right of Scheme 1.2; here, the schematic structure in the bottom right represents the prereaction arrangement of the participants that causes such a high catalytic effect to be observed. This effect undoubtedly illustrates one more type of organic reactivity in confined environments.

Interesting results were obtained during electrochemical oxidation of ferrocene included in the simple cavitant (top-right structure in Scheme 1.2). As shown, ferrocene is fully included in the aromatic cavity of the host. Whereas ferrocene as a free depolarizer is very easily oxidized into ferrocenium cation, the encapsu-



Scheme 1.2 Nature of catalytic effect on acetylation of choline confined in zinc-salen cavitand

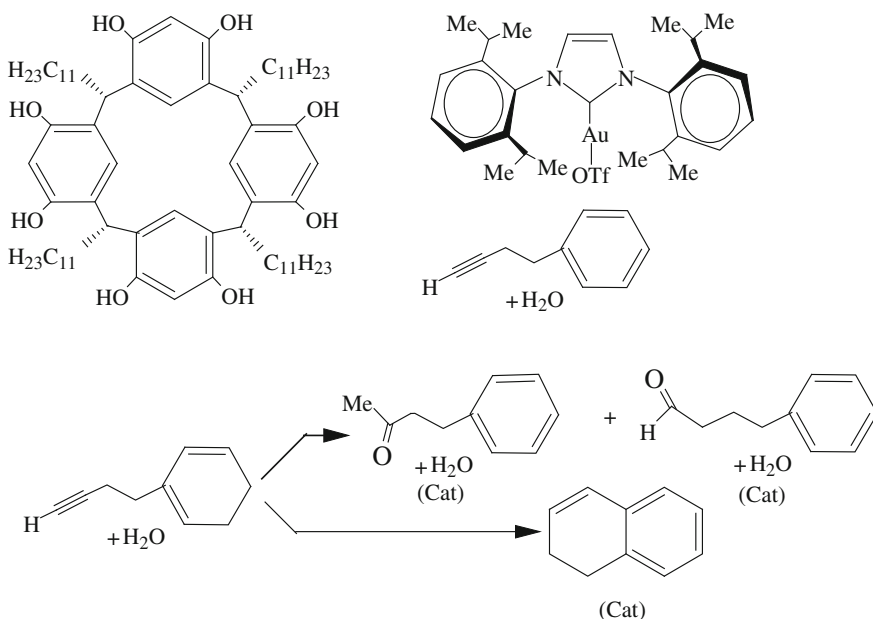
lated ferrocene was voltammetrically silent in this case (Podkoscielny et al. 2008). The fact that the ferrocene complex mentioned is not electroactive can be explained by the screening effect from encapsulation. However, other explanations are also possible: The complex is too bulky to go into the double electric layer or the distance is too long between the encapsulated redox center and the electrode surface at the time of the heterogeneous electron transfer.

Sulfonylcalix[4]arenes bearing hydroxyl groups at the lower rim and *tert*-butyl substituents at *para*-positions of phenyl rings (at the upper rim) react with manganese, cobalt, or nickel diacetate. As a result, the starting calixarene container occurs bound with a metalorganic knot, where four phenoxo and four sulfonyl oxygen atoms coordinate to four metal ions that are further bound by four acetate groups and one μ_4 -hydroxo oxygen (Dai and Wang 2012). In other words, the compound obtained has both *endo* and *exo* domains. The authors replaced acetate by 1,3,5-benzenetricarboxylate and obtained the metalorganic domains as nanosized capsules. These symmetric and unique coordination capsules contain both internal and surface cavities, a trademark feature of viruses, which use the enclosed space to store genetic material (i.e., DNA or RNA) and the surface binding sites to recognize the specifi-

cally targeted hosts. This makes the metalorganic sulfonylcalixarenes promising for allosteric catalysis, biosensing, and controlled drug delivery.

Water-soluble sulfocalixarenes have attracted interest in recent years due to their ability to form host–guest complexes that are used in therapeutic practice and bioanalytical procedures. As for cyclodextrins and cucurbiturils, size–shape fitting effects, electrostatic, cation– π , hydrogen bonding, van der Waals, hydrophobic, and other interactions are important for sulfocalixarene complexation with guests. When the size–shape demands are satisfied, the relative role of other factors depends on the structure of the guest. Zhou et al. (2008) note that, in aqueous media, the sulfocalixarene reaction with vitamin K₃ (2-methyl-1,4-naphthoquinone) is defined by hydrophobic interaction whereas electrostatic interaction plays an important role in the inclusion of lomefloxacin [(*RS*)-1-ethyl-6,8-difluoro-7-(3-methoxypiperazin-1-yl)-4-oxoquinoline-3-carboxylic acid].

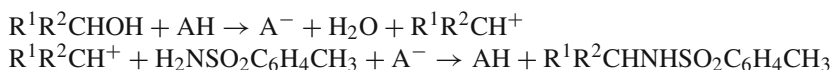
Being mixed in water, the reaction participants of Scheme 1.3 undergo some specific self-organization (Cavarzan et al. 2011). The self-organized composition includes six molecules of resorcin[4]arene gathered into a huge bowl and, in the cavity formed, the gold complex (a catalyst), and reactants (4-phenylbutyne with water). The huge bowl cavity has a volume of about 1.4 nm³. The gold complex has a molecular volume of about 0.4 nm³ and consequently occupies about 30 % of the volume of the cavity. This means that up to four water molecules are encapsulated to ensure stable complexation, in agreement with the general 55 % occupancy rule



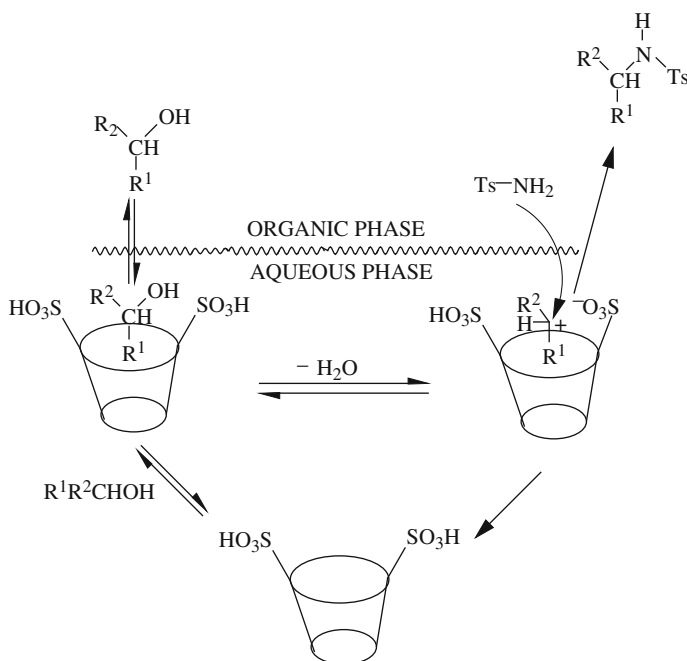
Scheme 1.3 Reaction between water and phenylbutyne confined within calixarene upon catalytic assistance of gold-complex

proposed by Mecozzi and Rebek (1998). Scheme 1.3 shows products formed inside the capsule. When the reaction is performed in the absence of resorcin[4]arene, almost exclusive and quantitative formation of methyl-ethyl(2-phenyl) ketone takes place. The nanoenvironment provided by the self-assembled capsule as host leads to the formation of not only the ketone but also (2-phenyl)ethanal as the additional product of 4-phenylbutyne hydration. In the confined reaction, formation of 1,2-dihydronaphthalene was also observed. The authors ascribed the dihydronaphthalene formation to intramolecular rearrangement of 4-phenylbutyne on the catalyst with no participation of water (Cavarzan et al. 2011).

A promising method is that for dehydrative amination of alcohols in aqueous solution using water-soluble calix[4]resorcinolarene sulfonic acid (Shirakawa and Shimizu 2008). For the dehydration, a Brønsted acid (A^-) is needed:



In the pair of *trans*-1,3-diphenylprop-2-en-1-ol and *p*-toluenesulfonamide ($H_2NSO_2C_6H_4CH_3$ or H_2N-Ts), common Brønsted acids such as acetic, trifluoroacetic, and *p*-toluenesulfonic acid were not effective. However, a water-soluble calix[4]resorcinolarene disulfonic acid made the reaction possible with almost quantitative yield. Scheme 1.4 describes the course of the reaction (Shirakawa and Shimizu 2008).



Scheme 1.4 Alcohol dehydrative amination within sulfocalixarene (Reproduced with permissions from Georg Thieme Verlag of September 11, 2012)

As seen from Scheme 1.4, inclusion of the alcohol in the sulfocalixarene capsule secures dehydration and the very reaction on the phase boundary. The sulfocalixarene works not only as a Brønsted acid catalyst but also as an inverse phase-transfer catalyst.

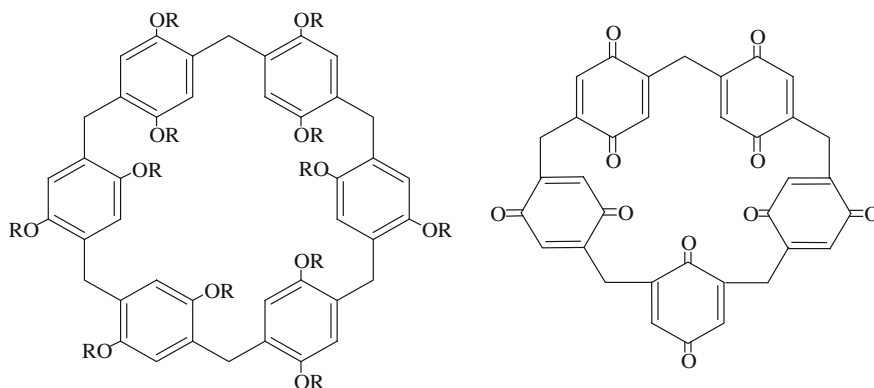
Dsouza and Nau (2008) described complexation that takes place in mixtures consisting of *p*-sulfonatocalix[4]arene (exaggeratedly depicted in Scheme 1.4) and 2,3-diazabicyclo[2,2,2]oct-2-ene or its 1-methyl-4-isopropyl derivative. The investigation was run in the absence and presence of Zn^{2+} . In the absence of Zn^{2+} , the corresponding host–guest complexes are formed. When 2,3-diazabicyclo[2,2,2]oct-2-ene was a guest, this host–guest compound transforms into a zinc disulfonate. When 1-methyl-4-isopropyl-2,3-diazabicyclo[2,2,2]oct-2-ene was a guest, the Zn^{2+} -disulfonate was formed with the host whereas the guest was displaced from the cavity in the outer sphere. In the first case, there is a sufficient vacant space at the upper rim to allow Zn^{2+} to dock and to reinforce the resulting complex through the formation of strong zinc-sulfonato bonds and a weak metal–ligand bond with the azo group of 2,3-diazabicyclo[2,2,2]oct-2-ene. In the second case, steric constraints prevent the formation of such a ternary complex and 1-methyl-4-isopropyl-2,3-diazabicyclo[2,2,2]oct-2-ene is displaced from the cavity in favor of the formation of the binary metal–calixarene complex.

Of special note is the formation of host–guest complexes and nanocapsules with large internal void volumes. Thus, saturation of *C*-propyl pyrogallol[4]arene in liquid 1-ethyl-3-methylimidazolium ethylsulfate results in the formation of two dissimilar host–guest complexes (Fowler et al. 2012). In one complex, 1-ethyl-3-methylimidazolium is horizontally seated at the base of the pyrogallol cavity. In the other complex, 1-ethyl-3-methylimidazolium keeps only the ethyl group in the base of the cavity, i.e., is positioned vertically. The *C*-propyl pyrogallol[4]calixarene macrocycles within both complexes take on very similar shapes during the cation binding, without being influenced by the different position of the imidazolium guest. It is noteworthy that 1-ethyl-3-methylimidazolium ethylsulfate is an ionic liquid. Encapsulation of ionic liquids in calixarenes can endow the host–guest complexes with electric conductivity. This may open a way to new sensor devices.

AlHujran et al. (2012) synthesized a new class of homooxalixarene based on functionalized acenaphthene. One of these hosts was studied by X-ray diffraction. It was revealed that it exists in a 1,3-alternate conformation. This macrocycle formed a 1:1 complex with C_{60} fullerene in toluene. The fullerene is a bulky guest. Supposedly, acenaphthenic homooxalixarenes can serve as good “flasks” for reactions in confined media.

1.3 Pillararenes and Pillarquinones

Pillararenes and pillarquinones are hexamers or pentamers of hydroquinone or quinone derivatives conjuncted with methylene groups. The corresponding examples are presented in Scheme 1.5. These new calixarene analogs were first synthesized in



Scheme 1.5 Structures of pillar[6]arene and pillar[5]quinone

2008 by Ogoshi et al. and recently appeared in the supramolecular world. Naturally, not many such materials have been accumulated yet, and most of them correspond to host–guest complexation (e.g., Li et al. 2011a; Cao et al. 2009; Yu et al. 2012; Ma et al. 2012).

Being calixarene analogs, pillararenes and pillarquinones differ from them in the following important regards: They are highly symmetrical and rigid, which affords their selective binding to specially designed guests. They have no basket structure, but contain functional groups inside holes. Guests can interact with these functional groups, showing altered reactivity with respect to reactants entering the collection boxes. The host–guest properties of pillararenes can easily be tuned by introduction of different substituents on the benzene rings. There is every reason to expect new and interesting confined organic chemistry within these hosts newly put into circulation.

For instance, Yao et al. (2012) synthesized an amphiphilic pillar[5]arene bearing five amino groups as the hydrophilic head and five alkyl chains as the hydrophobic tail. Being placed in water, this pillararene forms bilayer vesicles after 1 min and multiwalled microtubes after aging during 4 months. The vesicles can encapsulate calcein (fluorexon) within their interiors under neutral conditions and release it in response to a decrease of pH. The microtubes, which have primary amino groups on their surface, can adsorb trinitrotoluene through donor–acceptor interaction (Yao et al. 2012).

In terms of cavity size (Yu et al. 2012), the diameter of the internal cavity of pillar[6]arene is ca. 0.67 nm, close to that of β -cyclodextrin (ca. 0.60 nm). The diameter of the internal cavity of pillar[5]arene is ca. 0.47 nm, equal to that of α -cyclodextrin (ca. 0.47 nm). Accordingly, bromide of 4-(methylenetrिमethylammonium)-*trans*-azobenzene can be encapsulated by its azobenzene fragment into pillar[6]arene, but not into pillar[5]arene (Yu et al. 2012). It should be noted that α -cyclodextrin with similar internal cavity size is able to bind azobenzene derivatives in water (Yu et al. 2012). A possible reason is that pillar[5]arene has a rigid pillar structure, while α -cyclodextrin has a flexible truncated conic structure. Being encapsulated

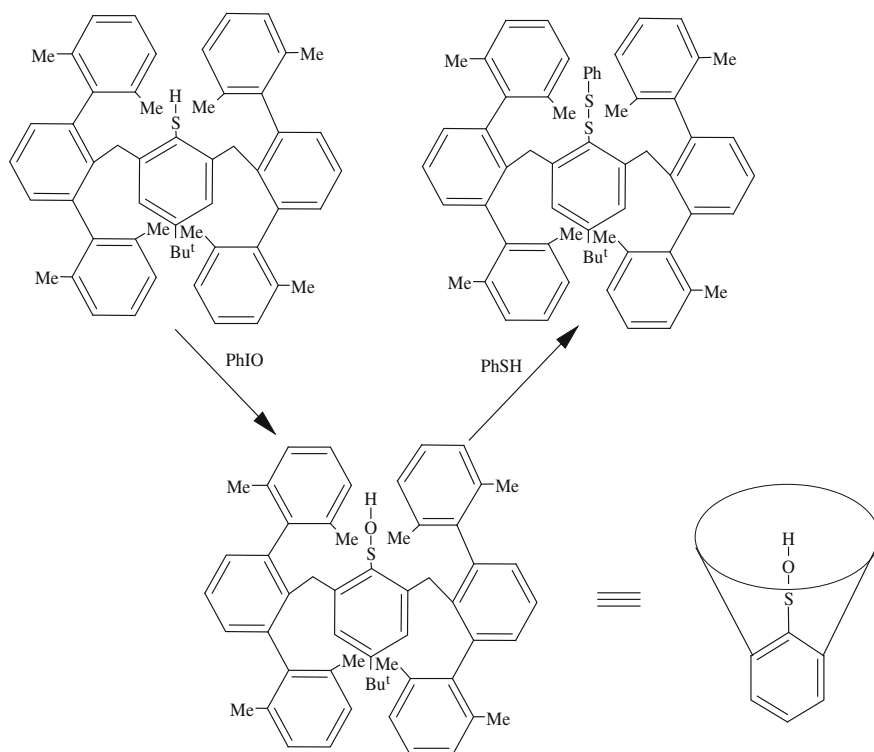
by pillar[5]arene, the *trans*-azobenzene guest undergoes usual photoisomerization into its *cis* isomer, but at a decreased rate compared with the *trans*–*cis* conversion of the nonencapsulated guest. Within the complex, photoisomerization is geometrically restricted. In bromide of 4-(methylenetrimethylammonium)-*cis*-azobenzene, as the size of the *cis*-azobenzene moiety is larger than that of the pillar[6]arene cavity, the formed *cis* isomer is decomplexed. The trimethylammonium group of 4-(methylenetrimethylammonium)azobenzene is bound by a rim of pillar[6]arene, while the azobenzene remainder of this new “guest” is outside the cavity (Yu et al. 2012).

The complexation between 1,4-dimethoxypillar[5]arene and *N*-octyl-*N*-ethylammonium hexafluorophosphate in chloroform is an interesting reaction because the guest encapsulation can be switched off by adding Cl^- (Han et al. 2012). When this complex is treated with tetrabutylammonium chloride, decomplexation takes place and the uncomplexed pillararene returned. Compared with PF_6^- , Cl^- is a smaller and charge-convergent anion. On contact with the encapsulated *N*-octyl-*N*-ethylammonium cation, the chloride anion forms an intimate ion pair in chloroform. For the cation, such ion pairing results in loss of its dwelling: the intimate ion pair is inadmissibly large for the cavity of the pillararene. On the other hand, the hexafluorophosphate anion is larger and charge divergent, forming a relatively loose ion pair with the *N*-octyl-*N*-ethylammonium cation in chloroform. In this loose ion pair, the cation is more or less independent and is easily accepted by the pillararene.

Ogoshi et al. (2012) prepared an ionic liquid using pillar[5]arene in its core. Starting from bis(1-bromopropoxy)benzene, the authors performed cyclization with paraform in the presence of trifluoride diethyl etherate. The final product was *per*-1-bromopropylated pillar[5]benzene. Reaction with 1-methylimidazole bromide provides a bromide salt of propoxypillar[5]benzene containing ten methylimidazolium end groups. Exchange reaction of the bromide salt with excess of lithium bis(trifluoromethylsulfonyl)amide leads to a salt with this new anion as a liquid at 25 °C. When solid tetracyanoethylene was mixed with the prepared ionic liquid, the 1:1 inclusion complex was formed. Consequently, the ionic liquid containing a macrocyclic pillar[5]arene in its core possesses solvent-free complexation ability. Host–guest complexation usually proceeds in solution. The solvent-free complexation between a solid guest and a liquid host demonstrated by Ogoshi et al. (2012) is a new concept that is simple and green. The complex obtained by the authors manifests ionic conductivity of 5.00×10^{-6} S/cm. This level of conductivity can be improved by means of modification of pillar[5]arene arms. Ionic conductivity induced by pillar–guest complexation can find applications in sensory devices.

1.4 Concaves as Hosts

Concaves constitute bowl-shaped structures that can be considered as pails with bottoms. Pails without bottoms are typical for calixarenes, cyclodextrins, and cucurbiturils. The concave effect is clearly demonstrated by the oxidation of arylmercaptane



Scheme 1.6 Concave protection of unstable arylsulfenic acids formed during arylmercaptane oxidation

of Scheme 1.6 by iodosobenzene to arylsulfenic acid (Goto et al. 1997). Without concave protection, such acids are unstable and immediately transform into symmetrical disulfides. As seen from Scheme 1.6, two rigid *m*-terphenyl units surround the sulfenyl group like the brim of a bowl. In other words, sulfenic acids can be synthesized by direct oxidation of mercaptanes under protection by encapsulation. Protection of this kind does not abolish the possibility of reaction of the sulfenyl group with other small molecules: The encapsulated sulfenic acid reacts with thiophenol, giving the unsymmetrical disulfide in 85 % yield (Goto et al. 1997).

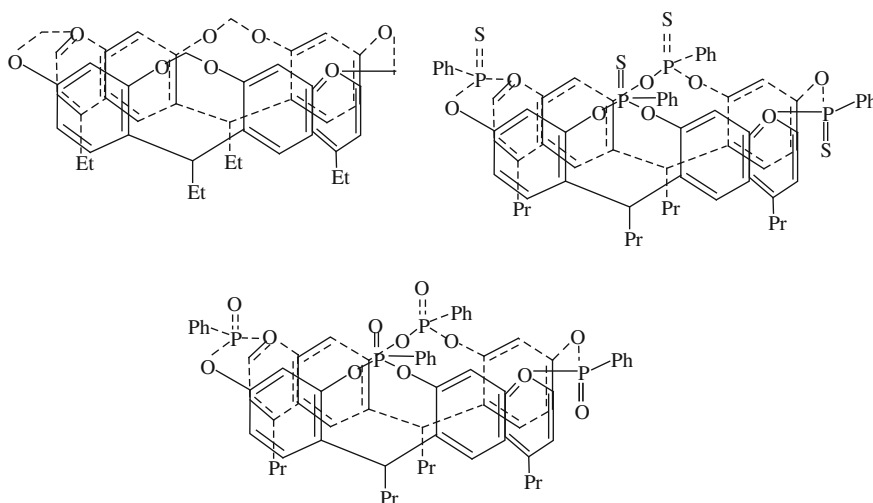
Another important application of the concave influence can be demonstrated by highly selective monomethylation of primary amines (Yebeutchou and Dalcanale 2009). *N*-Monomethylated amines are widely used as intermediate products in the preparation of pharmaceuticals and dyes. Usually, direct *N*-monoalkylation of primary amines is complicated by the formation of *N*-multialkylated amines or requires the use of special catalysts, solid bases, and nonconventional alkylating agents. Harsh reaction conditions, poor yields, and low selectivity are the major limitations.

Yebeutchou and Dalcanale (2009) used variable concaves as hosts to achieve strong selectivity of monomethylation. The reaction conditions were very simple: It

was sufficient to add a concave (1 equivalent) and an alkyl iodide (3 equivalents) to a solution of an aliphatic, cycloaliphatic, or aromatic primary amine (0.035 M) in chloroform at room temperature. In all cases, the monoalkylated product was the only compound formed, thus eliminating the need for tedious purification procedures to recover it in its pure form. Yields depend on the relative stability of the corresponding concave–methylammonium complexes. In the case of methylation with no concave, the yield of butylmonomethylamine [determined by means of gas chromatography (GC)] does not exceed 25%. Among concaves tested, one containing no phosphonate groups stands at the lower end of complexing ability, as it binds the guest (*n*-butylamine) only through $\text{CH}_3\text{-}\pi$ interaction. In the case of this concave, the yield of butylmonomethylamine was determined by GC as 45%. Tetrathiophosphonate concave occupies an intermediate position: In addition to $\text{CH}_3\text{-}\pi$ interaction, it offers the guest weak hydrogen-bonding and ion–dipole interaction. In this “middle” case, the GC yield of butylmonomethylamine rises to 65%. The best active concave is the tetraphosphonic one, increasing the GC yield up to 100%. Indeed, the substitution of weakly polarized $\text{P}=\text{S}$ moieties with highly polarized $\text{P}=\text{O}$ units further increases ion–dipole and hydrogen-bonding interactions, making the intermediary ammonium complex much more stable. Scheme 1.7 depicts the structures of concaves under consideration.

1.5 Carcerands as Hosts

The name “carcerand” is derived from the Latin word *carcer*, which means “prison.” Multiply linking concaves leads to carcerands. A large variety of carcerands have been synthesized by connecting two cavitands with four appropriate linkers. To be



Scheme 1.7 Phosphonate-containing concave as stabilizer of intermediary ammonium complex during amine selective monomethylation

incarcerated, a guest is introduced into a concave, and this filled concave is linked to an empty concave. A depth of approximately 1 nm is easily achieved for cavitands (Gibb and Gibb 2011); this means 2 nm for the height of inner cavities in homocarcerands. Successful attempts have been made to further deepen the dimensions of these cavities (Yamauchi et al. 2011).

Sometimes, two reaction partners can be imprisoned in the carcerand cavity, where chemistry between them takes place. In other cases, one reactant can be cleaved within the cavity, e.g., producing gaseous and condensed products. The gaseous component can leak through the carcerand shell, whereas the condensed counterpart is released during heating. At elevated temperature, the host shell opens to liberate the product formed.

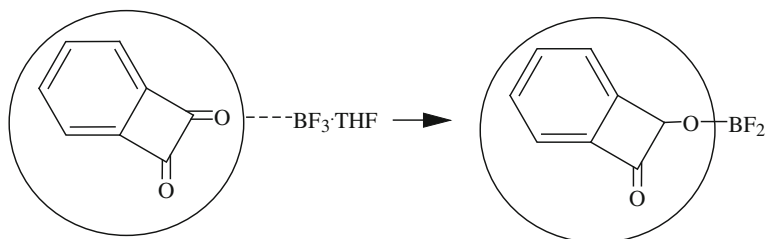
In electron-transfer reactions, the incarcerated guests are able to interact with molecules outside the inclusion complex with rate constants considerably smaller than those found for free guest in solution (Chen et al. 2008). These interactions are most efficient through the overlap of the orbitals of the incarcerated guest through the carcerand's orbitals with the orbitals of molecules present outside. The electron transfer considered is also possible due to tunneling over long distance.

Porel et al. (2012) studied photoinduced electron transfer between 4,4'-dimethyl-*trans*-stilbene (a donor) incarcerated within the octa acid bowl-lid pair and dimethylviologen (dication) electrostatically outwardly bound to the negatively charged octa acid. Upon photoexcitation, the direct and back electron transfers take place, and both processes are rapid.

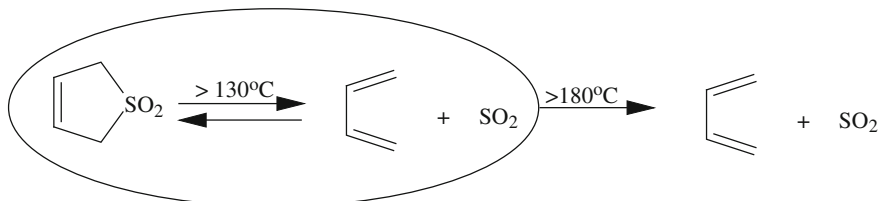
Robbins and Cram (1993) considered the reaction of nitrobenzene (free or incarcerated) with samarium diiodide dissolved in methanol. The free nitrobenzene is reduced upon action of SmI₂ into aniline. The reduction of the incarcerated nitrobenzene with SmI₂, at temperatures much lower than those required to liberate the initial or final product, stops at the formation of *N*-phenylhydroxylamine. The carcerand employed was constructed from pyrogallol (1,2,3-trihydroxybenzene). The product obtained is specifically stabilized by hydrogen bonding with the walls of the carcerand used. Hydrogen bonding between the wall oxygen and hydroxylamine preserves this product from subsequent reduction. The interior of the carcerand is too small to accommodate both reactants—nitrobenzene and samarium diiodide—in the same capsule, and electron tunneling seems to be a very reasonable mechanism for the reduction considered.

When a reaction center of the guest is located just at the slit trench of the host, a through-shell interaction with a small reactant from the bulk phase turns out to be possible. As an example, regioselective addition of borane tetrahydrofuranate to incarcerated benzocyclobutadione can be mentioned (Warmuth et al. 2003). As seen from Scheme 1.8, one carbonyl of this dione is shielded. The other carbonyl is perfectly positioned for through-shell reaction inside an entryway. After addition to the exposed C=O, coordination of the boron atom to a host's ether oxygen hinders guest rotation and prevents exposure of the second C=O, leaving it inaccessible for the second addition of the outer reactant.

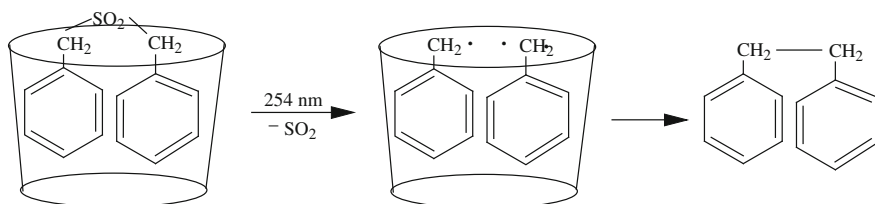
Incarceration can also establish an unusual equilibrium. When free 3-sulfolene is heated at 100–130 °C, irreversible extrusion of sulfurous anhydride and 1,3-butadiene



Scheme 1.8 Regioselectivity in addition of borane to incarcerated benzocyclobutadione



Scheme 1.9 Thermolytic equilibrium of incarcerated sulfone



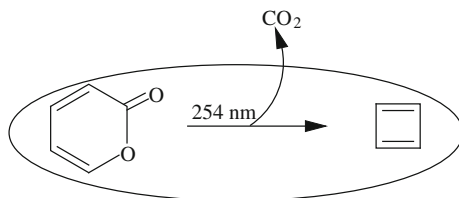
Scheme 1.10 Dibenzylsulfone photolysis within cyclodextrin

takes place. Being incarcerated and heated at temperature above $130\text{ }^{\circ}\text{C}$, this sulfone undergoes thermal destruction with the formation of the same products. In the carcer, these products keep close contact and acquire the possibility to reversibly unite. Scheme 1.9 shows the equilibrium mentioned. Upon heating above $180\text{ }^{\circ}\text{C}$, one of the carcerand bowls goes outward and the equilibrium is disturbed. The products of thermolysis leave their jail (Scheme 1.9) (van Wageningen et al. 1997).

In a similar manner, dibenzyl sulfone encapsulated in β -cyclodextrin undergoes photoextrusion of SO_2 upon irradiation of the 1:1 solid complex. Encapsulation, most probably, follows Scheme 1.10; extrusion of SO_2 leaves a benzyl radical pair inside the cavity. Although these radicals are relatively stable, they are not able to diffuse apart: Both partners are constrained by the walls of the host structure. Recombination of the radicals takes place inside the cavity and results in the formation of *sym*-diphenylethane (Scheme 1.10) (Pitchumani et al. 1995).

In Scheme 1.9, a calix[4]arene-based carcerand was used as the host. The “windows” in the host are not wide enough to pass SO_2 . Cram et al. (1991) used a calix[4]arene-based carcerand whose “windows” (orifices) were wide enough to allow CO_2 out. The authors built an inclusion compound, in which this carcerand contained α -pyron. Photolysis of the “construction” led to release of CO_2 and cyclobuta-

Scheme 1.11 Stabilization of labile cyclobutadiene by calixarene-based carcerand during photolysis of encapsulated pyron



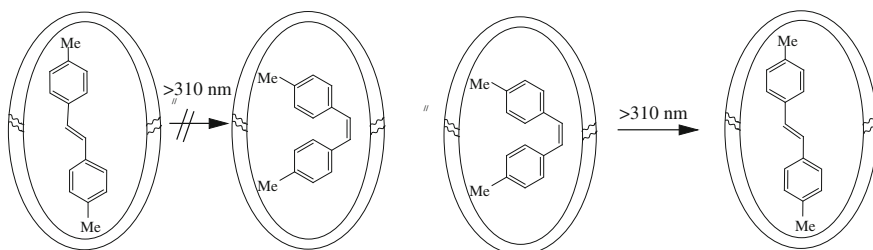
diene. The latter remained inside the carcer. Because cyclobutadiene itself is severely angle-strained in addition to being antiaromatic, this compound could not be obtained in a free state. However, within the carcerand and in the absence of oxygen, cyclobutadiene was stable up to 60 °C. Cyclobutadiene was characterized for the first time by proton magnetic resonance spectroscopy just within the carcerand inclusion complex. Scheme 1.11 presents the generation and stabilization of cyclobutadiene described.

As carcerands, resorcinolarenes and octa acid present special cases: These carcerands are formed only in the presence of hydrophobic guests of complementary size. Octa acid possesses an external coat of eight carboxylic groups. The conical bowl of octa acid has the following geometric parameters: height ca. 1 nm, upper circle diameter ca. 1 nm, dead bottom diameter ca. 0.55 nm (Parthasarathy et al. 2007). It should be particularly emphasized that the entrance to the cavity constitutes a wide hydrophobic rim that dimerizes upon guest encapsulation. On penetration into the hydrophobic cavities, the guest holds two capsules together. Nondirectional π - π stacking interaction between the aromatic rings on the wide hydrophobic rim of the two cavitands can also play a definite role in formation of a carcer with a prisoner inside (Gibb and Gibb 2004). For the octa acid case, a guest molecule functions as a molecular glue to bind a macrocycle as a single-complex architecture.

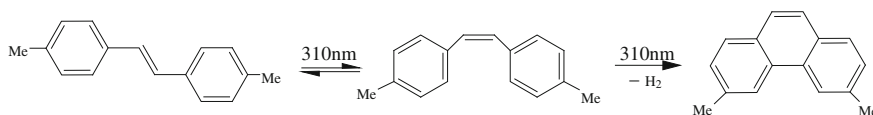
Generally speaking, carcerands resulting from self-assembled capsules can surround their guests and isolate them from each other and the bulk solution. These carcerands feature a nonspherical inner space, which can accommodate long, narrow, and flexible guests.

Dimerization of the host, as depicted in Scheme 1.12, becomes impossible when the guest-bound polar groups such as carboxylate remain at the entrance of one bowl binding site. This orientation maximizes the solvation/hydration of the carboxylate, and hence inhibits the host dimerization with carcerand formation (Sun et al. 2008).

An important problem is that of temporary disassembly of the bis(octaacid) complex that already contains an appropriate guest. This “breathing” of the complex allows an additional small molecule to enter and touch the guest, i.e., defines the reactivity of this guest. Using a fluorescence technique, Tang et al. (2012) revealed that the mechanism of pyrene–octa acid binding involves rapid (<1 ms) formation of a 1:1 complex followed by slower formation of a 1:2 (octa acid–pyrene–octa acid) complex. The dissociation of the latter capsular complex occurs with a lifetime of 2.7 s, five orders of magnitude slower than the microsecond opening/closing (“breathing”) time adopted in the literature. It is clear that this lifetime defines the very possibility for small reactants to enter the capsule and encounter the incarcerated guest inside this capsule.



Scheme 1.12 Selective *cis*-to-*trans* photoisomerization of dimethyl stilbene confined in octa-acid



Scheme 1.13 Dimethylphenanthrene formation during photolysis of non-confined *trans*-dimethylstilbene

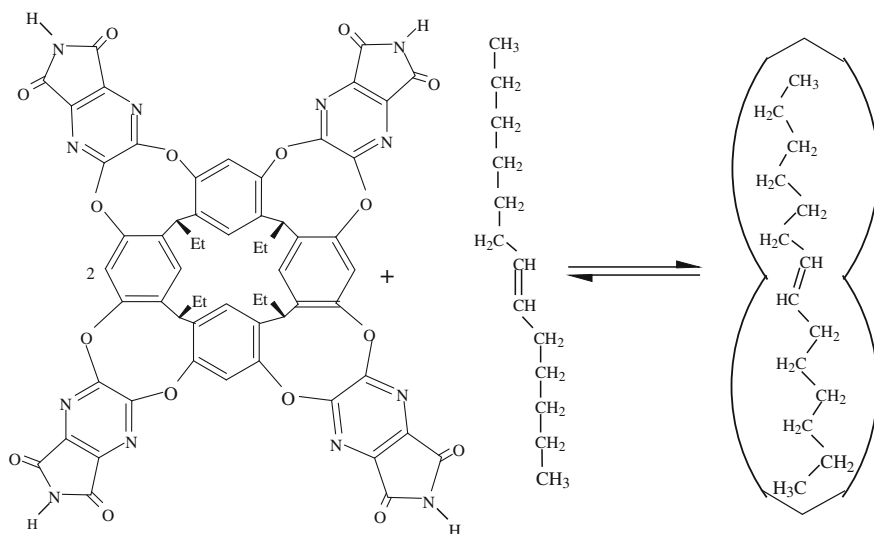
Octa acid incarceration controls photochemical isomerization of 4,4'-dimethyl-*cis*-stilbene into the *trans* isomer, making *trans* \rightarrow *cis* conversion impossible (Parthasarathy et al. 2007). Upon addition of octa acid, the turbid water (borate buffer) solutions of dimethylstilbene isomers become transparent. Inclusion compounds are formed, so that one molecule of stilbene occurs covered from the top and the bottom with two molecules of octa acid. Both isomers are located in the carcer differently. Scheme 1.12 shows that there are differences in the available free space around the two isomers: As compared with the *cis* isomer, the *trans* counterpart almost rests on the tapered ends of the double bowls, and this provides a barrier for the relocation of the two methyl groups from the narrower top/bottom to the broader middle region of the built capsule. For the *cis* isomer, such a barrier is absent. Upon photoirradiation at >310 nm, the *cis* form isomerizes into the *trans* form, whereas the *trans* \rightarrow *cis* transition is not observed.

Upon light exposure (>310 nm) in hexane without octa acid, *trans*-4,4'-dimethylstilbene easily turns into the *cis* isomer and, upon continued irradiation, into 3,6-dimethylphenanthrene (Scheme 1.13) (Parthasarathy et al. 2007).

It is the supramolecular effects provided by the host two-bowl cavity that are responsible for the change in photochemistry depicted in Schemes 1.12 and 1.13.

It is interesting to compare the results depicted by Scheme 1.13 with the outcome of photolysis at 312 nm of aqueous 4,4'-bis(dimethylammoniomethyl)-*trans*-stilbene solutions containing either β - or γ -cyclodextrin. In the case of β -cyclodextrin, the reaction outcome is the same as in Scheme 1.13 (the inclusion complex has 1:1 stoichiometry). γ -Cyclodextrin forms a 1:2 complex with the substrate, and [2+2] cycloaddition takes place, leading to the tetraphenylcyclobutane derivative bearing bis(dimethylammoniomethyl) groups at all four *para*-positions (Herrmann et al. 1997).

Resorcinolarene dimerization in the presence of 7-*trans*-tetradecene is shown in Scheme 1.14 (Adjami and Rebek 2009). The authors estimated that the tapered ends



Scheme 1.14 Acquiring of zigzag conformation upon tetradecene incarceration

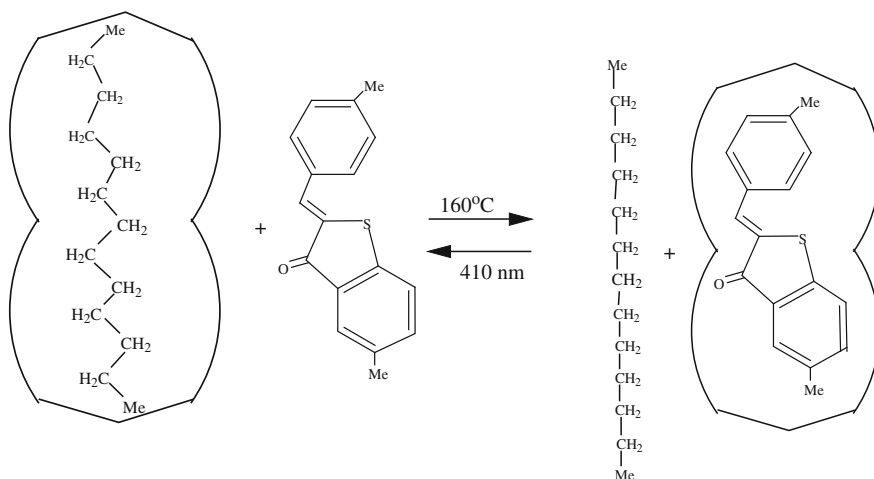
limit the length of the dimeric carcerands to under 0.15 nm. The guest is coiled during inclusion into the dimeric carcerand, acquiring a length of 0.146 nm. Therefore, the guest fits into the available space of the host and is truly encapsulated.

For instance, the *n*-alkanes from C₉ to C₁₄ as guests in the carcerand of Scheme 1.14 are all fully incarcerated but assume different shapes inside; namely, the C₉, C₁₀, and C₁₁ alkanes keep their extended form, while the C₁₂, C₁₃, and C₁₄ alkanes acquire coiled conformation (Jiang et al. 2012).

It was shown for tetradecene that coiling shortens the hydrocarbon length and increases its steric energy. This applies pressure to the ends of the dimeric carcerand capsule (Adjami and Rebek 2009). This phenomenon may be important for the intrinsic behavior of other molecules confined to limited spaces. In particular, this takes place in biology, where long-chain fatty acids are seen in contorted conformations in protein interiors and must exert pressure on them. As a concrete example, high-resolution X-ray crystallography revealed such features for nonspecific lipid binding in maize lipid-transfer protein complexes (Han et al. 2001).

Scheme 1.15 describes the guest exchange from the filled carcerand of Scheme 1.14 (Dube and Rebek 2012). Heating a mixture of encapsulated *n*-tridecane and free hemithioindigo leads to incarceration of the free guest and liberation of the guest formerly encapsulated. Photoexcitation of the newly obtained mixture restored the starting state. The thermal exchange obviously includes opening of the host shell, liberation of the alkane guest, and incarceration of hemithioindigo. The mechanism of the photoinitiated exchange remains, however, unclear.

Analyzing the phenomenon of host two-bowl cavities, Rebek (2005) underlines that guest molecules must be appropriately filled inside the cavities. The guests can be held within the space of a double capsule for lifetimes ranging from milliseconds



Scheme 1.15 Tridecane straightening after displacement from carcerated cavity

to days. “A molecule appears frozen in time and in space while inside a capsule. Its interaction with other encapsulated molecules are extended and, compared to the random and rapid collisions and exchange of partners that occur in bulk solution, are intensified or amplified in the capsule.” (Rebek 2005).

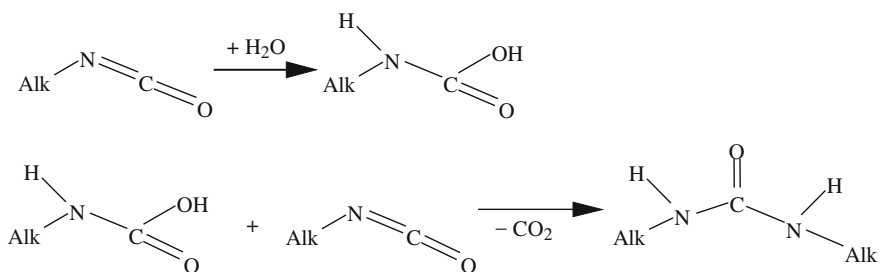
Thus, a bimolecular Diels–Alder reaction between *p*-quinone and cyclohexadiene in bulk solution requires more than 1 year duration at millimolar concentrations in deuterated *p*-xylene solution. However, after addition of the capsule (Kang and Rebek 1997) to the reactants at these concentrations, the product is formed after only 1 day. The Diels–Alder adduct is the best guest available for the double capsule, and the generation of a catalytic cycle is prevented by product inhibition. Nonetheless, acceleration takes place, reaching about 200-fold (Kang and Rebek 1997).

In the presence of glycouril, the joining capsule can elongate. Glycouril serves as a gasket between the two joining half-capsules. As a result, several and different reactant molecules can be incorporated in close vicinity to each other. This strongly facilitates the reaction between them. Hydration of isocyanates in an expanded, self-assembled capsule is a relevant example. The reaction follows the sequence depicted in Scheme 1.16 and leads to *N*, *N*'-dialkylurea (Taira et al. 2012).

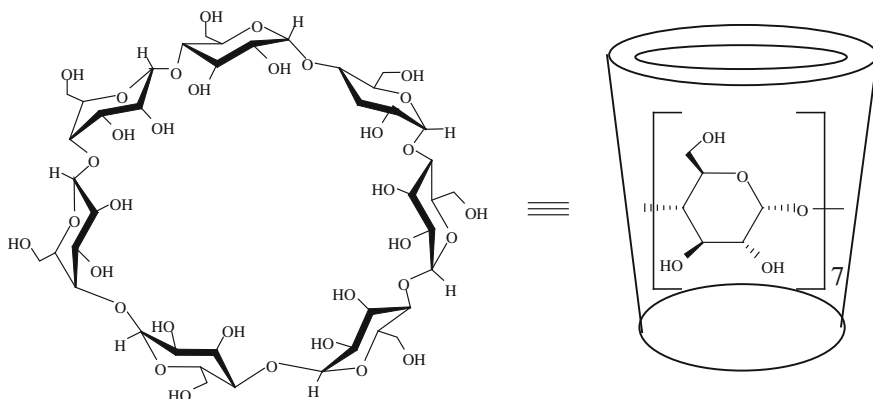
1.6 Cyclodextrins as Hosts

1.6.1 Native Cyclodextrins

Enzymatic hydrolysis of starch usually results in the formation of glucose, maltose, and a wide range of linear and branched dextrans. Some microorganisms and



Scheme 1.16 Formation of dialkylurea upon hydration of alkylisocyanates inside carcerand

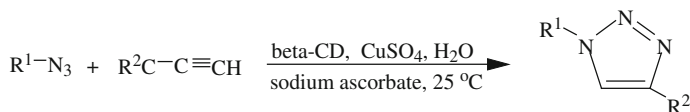


Scheme 1.17 Structures of cyclodextrins and their graphic representation

plants, however, produce certain enzymes, called cyclodextrin glucosyltransferases, which degrade starch through an intramolecular chain splitting sequence. The cyclic products formed have a common name: cyclodextrins. Scheme 1.17 presents β -cyclodextrin as an example. For the sake of graphical simplicity, Scheme 1.17 shows the truncated cone as a conical barrel.

The most abundant natural cyclodextrins are α -cyclodextrin (α -CD), β -cyclodextrin (β -CD), and γ -cyclodextrin (γ -CD), containing six, seven, and eight glucopyranose units, respectively. (Of these three CDs, β -CD appears to be the most useful pharmaceutical complexing agent because of its complexing abilities, low cost, and other specific properties.)

Cyclodextrins and their derivatives are primarily known for their ability to form inclusion complexes in aqueous solutions and in the crystalline state with molecules that are able to fit completely or partially into their central cavity. Unsubstituted cyclodextrins are naturally occurring molecular tubes that contain ring-shaped polymerized D-(+)-glucosopyranose units in an α -(1,4) linkage. Due to the chair structure of the glucopyranose units, the cyclodextrin molecules are shaped like a truncated cone rather than a perfect cylinder. Structurally, the cyclic nature of a cyclodextrin forms a torus, or donut-like shape, having an inner apolar or hydrophobic cavity. The secondary hydroxyl groups are situated on one side of the cyclodextrin torus, and



Scheme 1.18 Cyclodextrin catalytic effect on triazole formation from azides and terminal alkynes

the primary hydroxyl groups are situated on the other side of the torus. The side on which the secondary groups are located has a wider diameter than the side on which the primary hydroxyl groups are located. On each end of the torus there is a belt of hydrogen bonds. This molecular arrangement confers a hydrophobic character to the cyclodextrin cavities relative to the external surface, which is hydrophilic.

The hydrophobic and restrictive cavities combined with hydrophilic external walls provide specific microenvironments in terms of complexation between cyclodextrins and guest molecules. In contrast to water-insoluble free organic compounds, their cyclodextrin inclusion complexes are completely soluble: The poly-hydroxyl moieties of the dextrin keep the complex in water solution. By using this feature, cyclodextrin and cyclodextrin derivatives have been used as phase-transfer catalysts in organic synthesis.

Thus, 1,4-disubstituted 1,2,3-triazoles were obtained in excellent yields from azides and terminal alkynes in water if β -cyclodextrin was introduced in the reaction mixture in catalytic amounts. The reaction proceeds at ambient temperature in the presence of copper sulfate and sodium ascorbate. The latter two compounds are not included in β -cyclodextrin. Scheme 1.18 outlines the transformation (Shin et al. 2012).

Cyclodextrin complexes may impart beneficial modifications of guest molecules. Besides solubility enhancement, cyclodextrins can provide stabilization of labile guests, physical isolation of incompatible compounds, and control of volatility and sublimation. Encapsulation of stilbene and tolan by cyclodextrins greatly enhances their fluorescence, as has been established for the complexes where encapsulation of the multiple-bond fragments was fixed by stoppers at both *para*-positions of protruding phenyl rings (Stanier et al. 2001).

The number of glucose units defines the dimension and size of the cavity. As mentioned above, the most commonly used are cyclodextrins with numbers of D-glucose units of six, seven, or eight.

For α -, β -, and γ -CDs, the dimensional parameters were reported as follows: The cavity volumes are 0.17, 0.26, and 0.47 nm³ (Szejtli 1998). Li and Purdy (1992) proposed the following geometrical values for α -, β -, and γ -CDs: External diameters are 1.37, 1.53, and 1.69 nm, and internal diameters are 0.57, 0.78, and 0.95 nm, respectively. The cavity depth is common for all of the cyclodextrins and is equal to 0.79 nm. This rim-to-rim dimension varies with the conformation, and cyclodextrins often pack closer than this is in the solid state through hydrogen-bonding interactions to form channel structures. For this reason, cyclodextrins can accommodate molecules of relatively large volume. Because of the relatively nonpolar character of the

cavity in comparison with the polar exterior, cyclodextrins can form inclusion complexes with a wide variety of guest molecules, predominantly due to hydrophobic (solvophobic) interactions. In general, each weak interaction such as hydrophobic, van der Waals, or hydrogen bonding is not sufficient individually to stabilize an inclusion complex. The driving force responsible for the inclusion phenomenon is the sum of such interactions.

The dipole–dipole and ion–dipole interactions play a crucial role in the inclusion phenomenon and in guest–host orientation. Cyclodextrins have dipole moments. The positive end of this dipole moment is directed to the narrower rim of the cyclodextrin cavity (with primary hydroxyls), whereas the negative end is oriented to the wider rim (with secondary hydroxyls). Robust complexes are formed when host molecules also have significant dipole moments. Understandably, the dipole moment vectors of guests and hosts are oriented in an antiparallel fashion.

Thus, *p*-nitrobenzenediazonium is encapsulated into β -cyclodextrin such that its ($-\text{N}_2^+$) group is located in the vicinity of the rim bearing the secondary hydroxy groups with the negative end of the host dipole. Interestingly, upon one-electron reduction, *p*-nitrobenzenediazonium forms *p*-nitrobenzenediazenyl radical ($p\text{-O}_2\text{NC}_6\text{H}_5\text{N}_2\cdot$) fixed within the host cavity (Gonzalez-Romero et al. 2004). Without encapsulation, *p*-nitrobenzenediazonium loses N_2 just after acquiring one electron and transforms into *p*-nitrophenyl radical ($p\text{-O}_2\text{NC}_6\text{H}_5\cdot$).

Accordingly, the binding of β -cyclodextrin with 4-nitrophenol or 4-nitroaniline is much stronger than that with phenol or aniline (Yang et al. 2001). The dipole moment of 4-nitrobenzoic acid or 4-nitrobenzaldehyde is less than that of benzoic acid or benzaldehyde. Respectively, the binding constants with β -cyclodextrin are less for the guests whose dipole moments are smaller (Yang et al. 2001).

Note that, in the crystalline complex between β -cyclodextrin and *p*-aminobenzoic acid, the guest molecule is deeply included into the cavity of the host. Because of conjugation, the electron density in the guest is shifted to the carboxylic group so that the amino group bears a partial positive charge whereas the carboxylic group becomes more negative. Accordingly, the amino group protrudes from the wide (negative) side of the β -cyclodextrin cavity and the carboxylic group is located on the narrow (positive) side (Zhang et al. 2008).

In the crystalline complex between β -cyclodextrin and *p*-nitrobenzoic acid, both the nitro and carboxylic groups protrude from the cavity. Interestingly, the nitro group protrudes from the region of the secondary hydroxyl groups, i.e., at the wide (negative) side of the cyclodextrin. Hydrogen bonding between the nitro group and the secondary hydroxyl group of β -cyclodextrin is absent. In contrast, the carboxylic group protrudes from the region of the primary hydroxyl groups, i.e., at the narrow (positive) side. Such mutual orientation of the carboxylic group of the nitrobenzoic acid and the primary hydroxyl group of cyclodextrin is favorable for hydrogen bonding between them. This fixes the noted position of the guest in the host (Fan et al. 2007).

The stability of the inclusion complexes between β -cyclodextrin and alkyl nitrobenzoates is identical for the *meta* and *para* isomers (for equal length of alkyl chain). It is an alkylbenzoate that enters the cyclodextrin cavity, being oriented to the

wider side of the sleeve (Tee et al. 1993). In alkyl nitrobenzoates, the dipole vector is directed toward the nitrobenzoic fragment, in just the opposite direction to that of the cyclodextrin dipole vector.

Aside from hydrogen bonding, charge-transfer interaction during cyclodextrin complexation is important as well. To confirm this statement, comparison of binding constants is relevant. The binding constant of the α -cyclodextrin complex with the 1,4-dicyanobenzene anion-radical is 45 times larger than that with the neutral 1,4-dicyanobenzene complex (Kano et al. 1990). The binding constant of the β -cyclodextrin complex with neutral 10-methylphenothiazine is 35 times smaller than that with the 10-methylphenothiazine cation-radical (Liu et al. 2000). The presence of β -cyclodextrin during photolysis of nitrosogluthathione mixture with 5,5-dimethyl-1-pyrroline *N*-oxide in water of pH 7 permits stabilization of the spin adduct formed. This enhances the signal intensity in electron spin resonance spectra and opens the possibility of using the spin-trapping method to study glutathyl radicals in vivo (Polovyanenko et al. 2008).

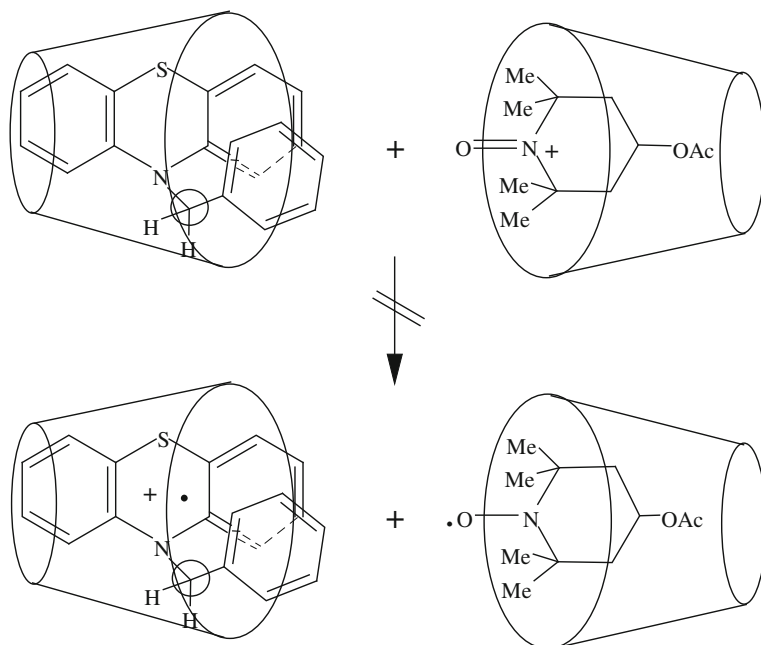
The cyclodextrin cavity is linked by glycosidic oxygen bridges. The nonbonding electron pairs of the glycosidic oxygen bridges are directed toward the inside of the cavity, producing a high electron density and lending it some Lewis-base character. As a result of this special arrangement of the functional groups in the cyclodextrin molecules, the cavity is rather hydrophobic while the external faces are hydrophilic. In the cyclodextrin molecules, a ring of hydrogen bonds is also formed intramolecularly between the 2-hydroxyl and the 3-hydroxyl groups of adjacent glucose units. This hydrogen-bonded ring gives the cyclodextrin a more or less rigid structure.

The cavity of a cyclodextrin offers a hydrophobic environment for guest molecules. The energy of the guest molecules increases due to the inclusion, which implies immobilization and sometimes changes of conformation. Oxygen atoms of cyclodextrins generate enriched electronic density of the cavity, which affects the electronic energy states of the guest molecules.

To be encapsulated, the guest size must correspond to the diameter and depth of the cavity. Thus, β -cyclodextrin forms an inclusion complex with 1,3-propanediyl-1-(1-pyrenyl)-3-[(*N*-adamantyl)amide], in which the adamantyl, but not pyrenyl, is accommodated into the host cavity (Liu et al. 2008b).

In view of the wide variety of guest types that can be included, there are diverse driving forces of inclusion reactions. The contributions of these forces can vary widely. In particular, van der Waals forces, hydrophobic/hydrophilic interaction, and release of strain energy are important. To underline this, cyclodextrins are characterized by an apolar cavity and a polar external surface formed by numerous hydroxyl groups. This defines the manner of guest inclusion and the physicochemical properties of the complexes formed.

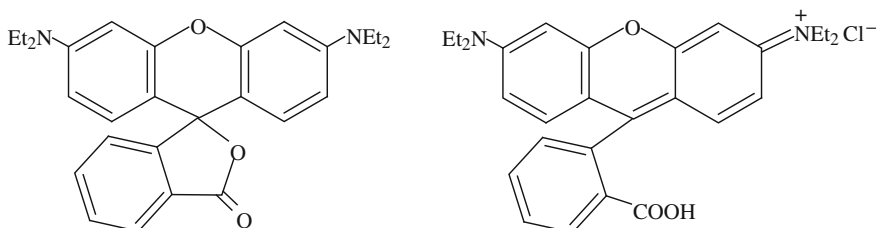
Special consideration should be addressed to changes in reactivity caused by inclusion of organic molecules into the cyclodextrin cavity. Oxidation of *N*-substituted phenothiazines encapsulated by β -cyclodextrin with concentrated nitric acid leads to the corresponding encapsulated cation-radicals. As guests, *N*-phenylphenothiazine, *N*-benzylphenothiazine, and *N*-(phenylethyl)phenothiazine were used (Zheng et al. 1999). Used as free substrates, these phenothiazine derivatives also give rise to cation-



Scheme 1.19 Stereoarrangement of benzylphenothiazine inside cyclodextrin

radicals upon oxidation with 4-acetoxy-2,2,6,6-tetramethyl-1-oxopiperidinium hexachloroantimonate. Nevertheless, if a phenothiazine and oxopiperidinium were separately imprisoned in β -cyclodextrin, some selectivity was observed in oxidation. Namely, *N*-phenylphenothiazine and *N*-(phenylethyl)phenothiazine formed the corresponding cation-radicals, whereas *N*-benzylphenothiazine was inert (Zheng et al. 1999). Such results were reproduced electrochemically (Wang et al. 2003). The individuality of *N*-benzylphenothiazine consists in its conformation within the host, which is depicted in Scheme 1.19. Explicitly, in the complex, the rotation of *N*-CH₂Ph fragment is restricted by the β -CD wall; the thiazine cycle, the oxidation center, is just under the shielding of the benzyl group and the β -CD wall. The oxidation is blocked. This blockade is negligible for *N*-phenylphenothiazine (a compact guest) and for *N*-(phenylethyl)phenothiazine (a guest with more flexible -CH₂-CH₂- binder).

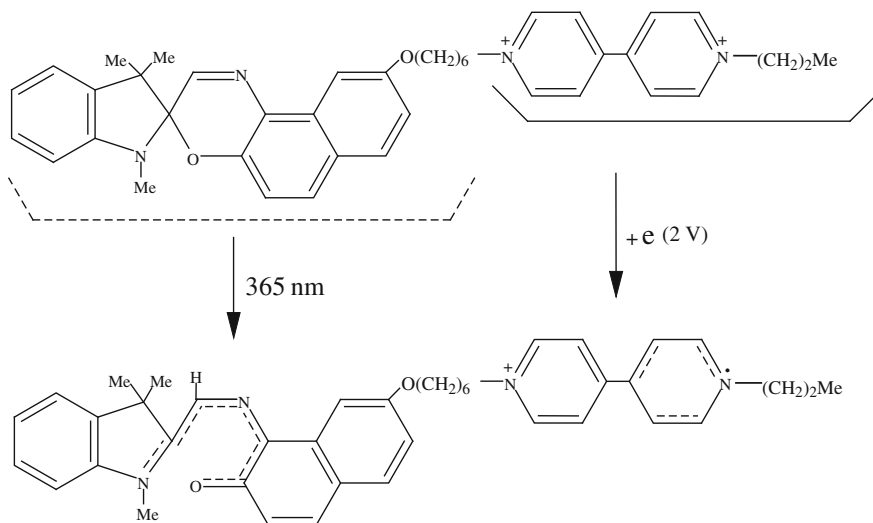
The fact that nitric acid is able to oxidize *N*-benzylphenothiazine inside the β -CD cavity is explained by the small volume of nitric acid. It can therefore enter the β -CD cavity of the β -CD@*N*-benzylphenothiazine complex to oxidize the guest even though it is still encapsulated. (The nitrate ion in nitric acid solutions acts as an oxidizing agent because nitrogen is small and electronegative.) If *N*-benzylphenothiazine is included into the larger cavity of γ -CD, it is easily oxidized by β -CD@oxopiperidinium complex (Zheng et al. 1999). Within γ -CD, steric hindrance does not play any role.



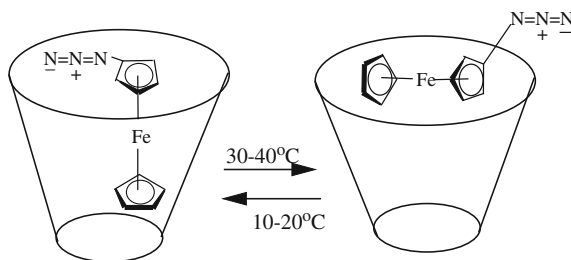
Scheme 1.20 Neutral and positively-charged forms of Rhodamine

In aqueous phosphate buffer (pH 7.2), native β -CD preferred to bind with the uncharged (colorless) lactonic form of rhodamine B, but not with the positively charged dye, i.e., the ammonium form (Zhao et al. 2008). Scheme 1.20 shows the difference between the lactonic (left) and corresponding ammonium (right) structures.

At this point, the photochromism and electrochromism of the heterobifunctional dye of Scheme 1.21 should be considered. The dye consists of two active parts, namely the spiroxazine and viologen moieties. The former moiety rearranges into the ring-opened (colored) merocyanine form upon ultraviolet irradiation. The latter moiety gives the viologen (colored) cation-radical upon one-electron reduction. Both processes are depicted in Scheme 1.21. This means that the dye can be used in optical electronic sensors. First-order kinetics, however, indicates that the closed-to-open reaction of spiroxazine occurs more rapidly than the generation of the viologen cation-radical. The faster reaction can be restricted by addition of β -cyclodextrin to



Scheme 1.21 Preference of photochromism over electrochromism for dye encapsulated in cyclodextrin



Scheme 1.22 Temperature effect on ferrocenylazide location inside cyclodextrin

the solution of the dye in dimethylsulfoxide: The confining cyclodextrin encapsulates the neutral spiroxazine rather than the doubly charged viologen (Son et al. 2007).

It is worth mentioning the temperature effect on the orientation of a guest, ferrocenyl azide, which has been encapsulated by β -CD in aqueous dimethylsulfoxide (Walla et al. 2006). Scheme 1.22 illustrates the effect. At lower temperatures, the ferrocenyl fragment adopts preferentially a “vertical” arrangement. This arrangement is not the most convenient due to the polar nature of the azide group. This group should be expelled as far from the CD cavity as possible. After weak activation by mild heating, Walla et al. (2006) obtained the expected change. They reported the “vertical”-to-“horizontal” rearrangement of the ferrocenyl fragment. According to the authors, the polar azide group is removed from the CD cavity. It should be noted, however, that an increase of temperature could also bring about relocation of the guest beyond or beneath the β -CD cavity.

From the point of view indicated by Scheme 1.22, it is relevant to mention the results of computational analysis on encapsulation of ferrocene bearing two $\text{CH}_2\text{N}^+(\text{CH}_3)_3$ groups in both five-membered carbocycles (Moghaddam et al. 2009). This dication is predicted not to bind to β -CD despite the guest–host compatibility in their sizes. Meanwhile, the same dication is predicted to bind with cucurbit[7]uril, and encapsulation takes place very snugly. The following consideration shows that this host, cucurbit[7]uril, preferentially confines *charged*, but not neutral species. In the case just mentioned, each ammonium group is able to locate at the electronegative portals of cucurbit[7]uril (Rekharsky et al. 2007).

Adamantane bearing $\text{CH}_2\text{N}^+(\text{CH}_3)_3$ group is similar to ferrocene in its size and hydrophobic character. This compound also shows extremely high affinity to cucurbit[7]uril, with very good encapsulation constant and other thermodynamic parameters. Note that the guest contains a cationic substituent at only one electronegative portal of the host. The guest has no metal atom. Consequently, the observed, remarkably high affinity of the ferrocene-based guest need not be attributed to metal-specific interaction with cucurbit[7]uril (Moghaddam et al. 2011).

Of course, encapsulation can also be governed by other factors besides charge control. Thus, the anion-radical of fullerene C_{60} exhibits better inclusion ability by cyclodextrins than neutral C_{60} (Liu et al. 2007a). The polarizability of the anion-radical is much larger than that of the neutral fullerene. This factor enhances dispersion forces and assists encapsulation of the charged particle by cyclodextrin.

On the other hand, hydrophobic forces can also play the dominant role. The relevant example is 1,3-bis(adamantyl)-1-imidazolium chloride. The cation of this salt participates in fast hydrogen–deuterium exchange in D₂O. In the presence of β -cyclodextrin, the inclusion complex is formed and the isotope exchange decelerates. The cause lies in confinement of the guest by two hosts. Within the 1:2 complex, there are no direct interactions between the imidazolium hydrogen at position 2 and the host. Hydrophobic interaction is responsible for the imidazolium cation hiding. Moreover, the formation of a hydrogen-bond network between the two cyclodextrins creates a steric barrier around the imidazolium cation. This barrier modifies the kinetics of hydrogen–deuterium exchange (Leclercq and Schmitzer 2009).

Encapsulation by means of cyclodextrins is used to stabilize rapidly metabolized drugs, to increase oral bioavailability, to decrease toxicity, to prevent immune response in mammals, and to achieve water solubility of cyclodextrin@drug complexes. Cyclodextrins have seen increased application in pharmaceutical formulations in recent years due to their approval by various regulatory agencies (Thompson 1997; Hedges 1998).

Let us consider here the problem of water solubility of lipophilic compounds such as sodium dicloxacillin. It was shown that inclusion of sodium dicloxacillin into γ -cyclodextrin highly protects the drug from the undesirable hydrolysis of its amide group (Echezarreta-Lopez et al. 2008). Being included in α -, β -, or γ -cyclodextrin, tenoxicam (a nonsteroidal anti-inflammatory medication) is protected from hydrolysis, and the rate of its photodegradation is reduced (Rawashdeh et al. 2008b). Analogous improvement of curative properties was described for the inclusion of 3*S*-1,2,3,4-tetrahydro- β -carboline-3-carboxylic acid into β -cyclodextrin. This drug was identified as an active antiplatelet aggregation ingredient. However, its very poor water solubility and disadvantage of being oxidized easily to the pharmacologically less active byproduct reduce the therapeutic effectiveness and seriously limit the clinical application of the drug. Li et al. (2008) reported that the complex of this drug with β -cyclodextrin differs from the free medication in its improved solubility in water, enhanced “in vitro antioxidation stability and therefore increased the in vitro antiplatelet aggregation and in vivo antithrombotic activity.”

Progesterone has been used in antibirth control and postmenopausal therapy. Therapeutic use of progesterone is limited since it is slightly water soluble and poorly absorbed by oral ingestion unless micronized or dissolved in oil. The latter formulation may cause allergic reactions in some people. The formation of inclusion complexes with various cyclodextrins showing notable improvement of solubility has been reported and reviewed by Caballero et al. (2008).

A further example springs from the improvement of human diet (Jullian et al. 2008 and references therein). Morin (2',3,4',5,7-pentahydroxyflavone) is a flavonoid widely distributed in tea, coffee, cereal grains, and a variety of fruits and vegetables. Morin manifests anti-inflammatory, antineoplastic, and cardioprotective activity. Inclusion within cyclodextrin increases the water solubility and, more importantly, antioxidative activity of this flavonoid.

In oral preparations, coadministration of cyclodextrins increases the adsorption and efficiency of poorly soluble medications. Enhancing drug solubility is an

alternative to use of high doses, generally associated with adverse side-effects. Drug pharmacological action is prolonged upon encapsulation into dextrans. The dextrin size should provide adequate space to accommodate the drug but should not be large enough to provide retention of the molecule accommodated. It is useful, however, to keep in mind that the water solubility of β -CD is lower than that of α -CD and γ -CD. The solubility pattern correlates with the increase in flexibility according to the sequence β -CD, α -CD, and γ -CD. At 25 °C, the solubilities of these CDs in 10 ml water are 0.18, 1.3, and 2.6 g, respectively (Sabadini et al. 2008 and reference therein). Due to its cavity size, β -CD is best suited for many pharmaceuticals, agricultural chemicals, cosmetics, and foods. Nevertheless, its low intrinsic solubility in water makes it impractical for use. Addressing the phenomenon of the unexpectedly low solubility of β -CD, Naidoo et al. (2008) found that the order of the water structure around β -CD is higher than in the case of α -CD or γ -CD. A possible molecular origin for this is the difference in their glycosidic conformation space. β -CD is the least flexible of the three CDs compared.

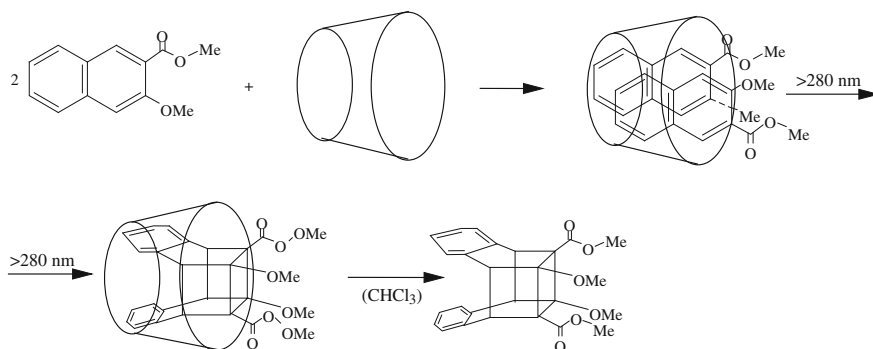
Having been encapsulated by γ -cyclodextrin, Solvent Green 7 (i.e., pyranine) exhibits slower dissociation dynamics in aqueous solution. The activation energy of hydroxyl proton release from the encapsulated pyranine is significantly higher than that from the free guest (Radozkowicz et al. 2008).

There are also examples where hydroxyl groups of a cyclodextrin activate the guest compounds, allowing reaction between the guests. Thus, Narender et al. (2006) proposed a mild and efficient method to transform oximes into ketones at room temperature with ketone yields of 84–90%. Oximes are highly stable, being used for protection of carbonyl functionalities. Oximes can also be prepared from noncarbonyl starting materials. The Barton reaction is one route to such oximes.

To prepare carbonyl compounds from oximes, Narender et al. (2006) used iodosobenzene (PhIO) and potassium bromide in the presence of β -cyclodextrin in water. After the reaction, β -cyclodextrin was recovered and reused. No reaction was observed in the absence of cyclodextrin. Reaction of 4-hydroxyacetophenone oxime within the cyclodextrin leads to 4-hydroxyacetophenone. Usually, phenolic hydroxy groups are readily oxidized with iodosobenzene. Being included into cyclodextrin, the hydroxy group of 4-hydroxyacetophenone is stabilized by hydrogen bonding with one of the cyclodextrin hydroxyls and survives under the oxidation. As for the iodosobenzene, its oxygen atom forms a hydrogen bond with another hydroxyl of cyclodextrin that results in specific activation of the oxidizer.

Scheme 1.23 shows that γ -cyclodextrin can encapsulate two molecules of methyl 3-methoxynaphthalene-2-carboxylate. Photoirradiation of this inclusion complex results in dimerization (Luo et al. 2009). The reaction proceeds in water solution under ambient temperature and pressure. The product has *anti*-head-to-head orientation and *e,e*-enantioselectivity as high as 48%. The authors suppose that the enantioselectivity obtained originates from the close proximity and fixed orientation of the guest within the host as well as from the tight fit of the photoproduct within the host cavity. All these features are reflected in Scheme 1.23.

It should be noted that some guests can form micelles in water. Addition of cyclodextrins results in extraction of the guests from the micelles. The extraction is



Scheme 1.23 Photodimerization of two methoxynaphthalenes confined in one cyclodextrin

reversible. This reversibility was observed for the interaction between 1-alkyl derivatives of 4,4'-bipyridinium and α -cyclodextrin in water. The competitive formation of the aqueous micelles and the cyclodextrin inclusion complexes was established. Heating the reaction solution to 60 °C caused re-formation of the micelles into the inclusion complexes. Recooling the solution to 25 °C restores micellization. Repetition of the temperature change between 25 and 60 °C allows switching between the mentioned forms (Suzaki et al. 2010).

Micellization is often accomplished by participation of surfactants. Sometimes, the surfactant can compete with a guest to complex with cyclodextrin. In such cases, surfactant–cyclodextrin complexation reduces the host cavity and reduces the micelles available for hosting the guest (Nogueiras-Nieto et al. 2009). Of course, the very ability of cyclodextrins to include surfactant depends on their size congruence. Thus, introduction of α -CD into the self-neutralized binary micelle of sodium perfluorooctanoate and octyltrimethylammonium bromide results in selective encapsulation of octyltrimethylammonium bromide, but not sodium perfluorooctanoate. In the absence of encapsulation, both surfactants form a homogeneous aqueous mixture. Although both have nearly equal chain length, the diameters of their head groups are different: The methyl group has diameter of 0.4 nm, whereas the trifluoromethyl group has diameter of 0.7 nm (Xing et al. 2008). The selectivity in encapsulation derives from the fact that the cavity diameter of α -CD is about 0.5 nm. The thermodynamic characteristics of cetyltrimethylammonium bromide inclusion into β -CD in water:butanol mixture are very favorable (Rafati and Safatian 2008).

CDs promote some transformations that are specific for polymer chemistry. Thus, Chen et al. (2012) proposed a simple approach to form supramolecular hydrogels: They used the ability of γ -cyclodextrin to encapsulate two pyrene molecules. This opened a route to introduce into the cavity two pyrene terminals, each of them being bound with poly(ethylene glycol) star polymer. Such double encapsulation resulted in physical cross-linking of the polymer chains. In the presence of water, these physically cross-linked and partially confined polymer pairs form a hydrogel. Since only pyrene terminals were involved in the complexation with γ -cyclodextrin, the

gelation is a rapid process, taking place in a few seconds after mixing of the star polymer, γ -cyclodextrin, and water.

Free-radical polymerization of *N*-vinylimidazolium cations in water has been well established for decades. The resulting polycations are of broad interest because of their many practical applications, e.g., in cosmetics or as flocculants (see references in the paper by Amajjahe and Ritter 2008). These authors used complexation with β -CD to improve 1-butyl-3-vinylimidazolium bis(trifluoromethylsulfonyl)imide [(bvim)(Tf₂N)] solubility in water. In this system, the 1:1 complex is formed. The β -CD host exclusively accommodates the Tf₂N anion, leaving the bvim cation spatially separated from the anion. These quasinaked bvim cations do not polymerize in water because the “naked” positively charged particles undergo strong mutual repulsion. However, addition of lithium chloride to the reaction system actuates polymerization (Amajjahe and Ritter 2008). The addition of the salt leads to shielding of the charges of the monomers in solution. The chloride anions are localized close to the bvim cations. The repulsion of these cations is substantially compensated, and polymerization is carried out easily.

Liu et al. (2008c) synthesized an inclusion complex of β -cyclodextrin with bornyl-4-(6-acryloyloxyhexyloxy) phenyl-4'-benzoate and performed its polymerization upon ultraviolet irradiation. The final product was obtained in the columnar architecture. The columnar structure originates from the self-assembly interaction between the terminal acryloyl, bornyl groups, and hydroxy groups of β -cyclodextrin. Polar-polar interactions between the carbonyl groups, π - π interactions between the vinyl groups, and hydrogen bonding between the hydroxy groups on β -cyclodextrin are the main factors drawing the molecules together and leading to the formation of the columnar architecture. Such structures can be used as dopants in preparation of polymer films and other plastic devices.

1.6.2 Modified Cyclodextrins

There are several routes to modify the dimensional parameters of cyclodextrin cavities. Ivanov and Jaime (2004) reported cyclodextrin-like macrocycles containing up to 48 glucopyranose units. Li et al. (2011b) tuned the cavity and overall size of β -CD by replacing a single oxygen atom in its macroring skeleton by a disulfide unit. Before that, Kikuzawa et al. (2007) inserted a disulfide unit into the macrorings of permethylated α - and β -CDs. Those authors showed that the disulfide unit is reduced with dithiothreitol in aqueous solutions at room temperature. Splitting of the cyclodextrin macroring can, naturally, liberate a guest from the host cavity.

Rodriguez-Lucena et al. (2008) modified α -CD by replacing oxygen as a linkage between glucose units with a thiourea fragment. This modification endows the macroring with higher adaptability toward potential guest molecules of appropriate size, primarily on the basis of the capability to orient the NH protons to the inside or outside of the cavity. Due to the hydrophilic character of the thiourea moieties, the cavity decreases its hydrophobicity. The authors also noted the higher confor-

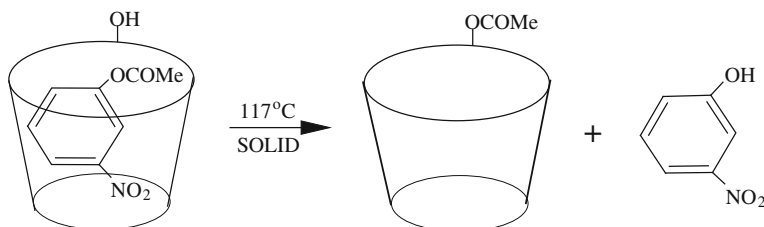
mational adaptability of the thiourea analog compared with the natural cyclodextrin counterpart.

Many publications describe cyclodextrins differing from the native ones by the presence of functional groups. Because the narrower rim of the cyclodextrin cavity corresponds to the positive end of the dipole and the wide rim corresponds to the negative dipole part, positively charged groups engrafted onto the narrower end occur outside the CD cavity. In the case of wider-end engrafting, self-complexation leads to drawing of the positively charged substituents into the cavity. Such a regularity was described by Park et al. (2005) for β -CDs, in which the viologen cation-radical moiety (1-methyl-4,4'-bipyridinium group reduced by a single electron) was separately connected to either the narrower or wider end by an octamethylene chain.

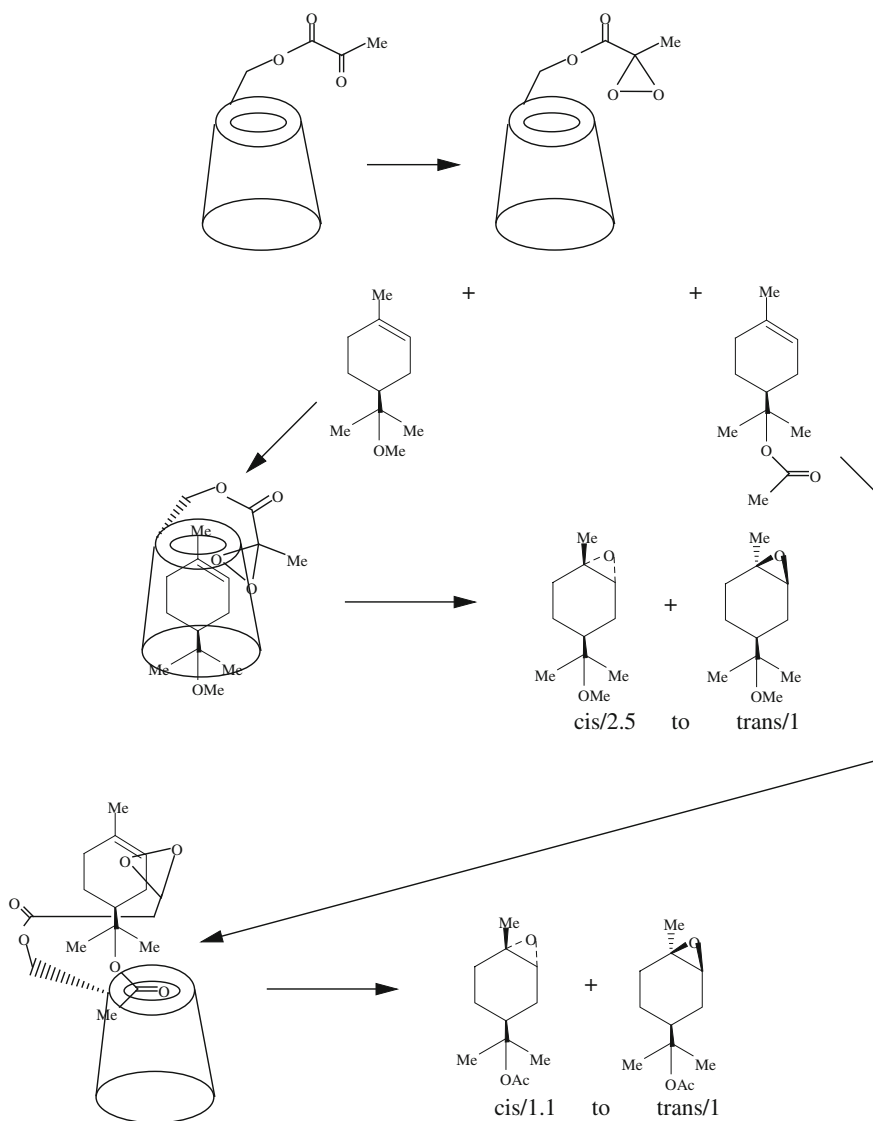
Scheme 1.24 presents participation of a cyclodextrin hydroxyl group in saponification of nitrophenyl acetates. According to the mutual orientation of dipole moments, *m*-nitrophenyl acetate is included into α -CD such that its carbonyl group occurs in close proximity to a nucleophilic α -CD secondary hydroxylic group (VanEtten et al. 1967a). Scheme 1.24 shows that the reaction proceeds as transesterification.

For Scheme 1.24, the reaction selectivity depends on the aggregative state of the reactants. Being heated at 117 °C under dry nitrogen, the *solid* α -CD complex of *m*-nitrophenyl acetate takes part in the reaction considered. Under the same conditions, transesterification of *p*-nitrophenyl acetate develops undetectably slowly (Wernick et al. 1988). When the reaction of Scheme 1.24 was conducted in alkaline aqueous solution of pH 10.6 at 25 °C, the *p*-nitrophenyl acetate saponification also ran, albeit still more slowly than that of *m*-nitrophenyl acetate: The rate of *p*-nitrophenyl acetate saponification turned out to be only 27 times slower than that of *m*-nitrophenyl acetate (VanEtten et al. 1967b). As seen, solid-state reactions can sometimes exhibit enhanced selectivity.

Contino et al. (2008) reported the formation of a fairly stable inclusion complex of anthraquinone-2-sulfonate with γ -cyclodextrin that bears the amino group at cyclodextrin position 3. The complexation was accomplished in water solution of pH 4.8. In the same solution, the *underivatized* γ -cyclodextrin forms a complex with anthraquinone-2-sulfonate that is not so stable. Evidently, the amino residue, which is protonated at pH 4.8, serves as an anchoring point for the negatively charged sulfonate group of the guest, thus leading to a more stable inclusion complex.



Scheme 1.24 Transesterification between nitrophenyl acetate guest and hydroxyl of cyclodextrin host



Scheme 1.25 Stereoregulation of epoxidation in a cyclodextrin host upon guest epoxidation

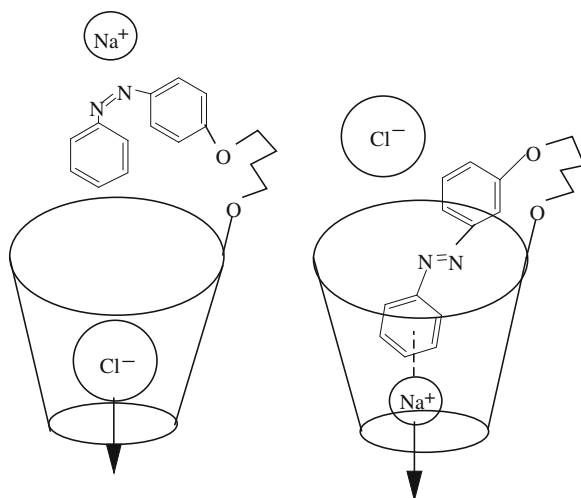
A cyclodextrin modified with the ketoester function provides a unique opportunity to follow the stereochemistry of alkene epoxidation depending on the degree of guest penetration. Scheme 1.25 shows how a ketoester-modified β -cyclodextrin is transformed into the covalently tethered cyclodextrin dioxirane. The dioxirane is generated in situ from the ketocyclodextrin and oxone. Oxone is potassium peroxy-monosulfate (RHSO_5).

The cyclodextrin dioxirane was used in oxidation of *O*-methyl or *O*-acetyl derivatives of (*S*)- α -terpineol (Chan et al. 2003). These derivatives are distinguished by their degree of immersion into the cyclodextrin cavity, which defines the stereoselectivity of the epoxidation. As seen from Scheme 1.25, the more deeply immersed *O*-methyl guest transforms into epoxide with higher *cis/trans* isomeric ratio, namely (2.5):1. The guest bearing *O*-acetyl group is less well locked into the cavity, and its epoxidation stereoselectivity is lower, the ratio of *cis/trans* products being only (1.1):1.

Marinescu et al. (2005) and Lopez et al. (2007) grafted carbon chains bearing aldehyde or keto groups onto a natural cyclodextrin. The functionalized carbon chains were fastened at both sides of the cone and were kept just above the cavity. Such cyclodextrin derivatives were used for oxidation of 2-hydroxyaniline into 2-aminophenoxazin-2-one with hydrogen peroxide in aqueous solution at pH 7.0 and 25 °C (Marinescu et al. 2005; Lopez et al. 2007). The carbonyl group of the fastened chain reacts with hydrogen peroxide. The hydroperoxide adduct is formed. This adduct is a very active oxidant and transforms the encapsulated 2-hydroxyaniline into 2-aminophenoxazin-2-one. As a result, oxidation of the amine inside the cavity proceeds 400–1,500 times faster than in the absence of confinement. This method of acceleration is practically important, especially for drug synthesis. Oxidation of amines to phenazine derivatives has been performed using many different oxidants, but with respect to price and environmental friendliness, hydrogen peroxide is preferred. However, reactions using nonconfined hydrogen peroxide require high activation energy. Inclusion of hydrogen peroxide into carbonyl-bearing cyclodextrins allows this obstacle to be avoided.

This approach had been proposed as far back as in 1969 by Breslow and Campbell: Interaction of anisole with hypochlorous acid in aqueous solution results in the formation of *para* and *ortho* chloroanisoles. In the presence of α -cyclodextrin, *para*-regioselectivity of the chlorination increases by 20 times. According to the authors, one of the hydroxyl groups of the cyclodextrin reacts with HOCl to give the hypochlorite functional group that further acts as a chlorinating part. Because this modified Cl–O group hangs over the included anisole right next to its *para*-position, *para*-regioselectivity of the reaction is strongly facilitated. Encapsulation enhances the accessibility of the *para* position and shields the *ortho* positions of anisole. The same effect was reported in 2003 by Dumanski et al. for cyclodextrin-assisted bromination of anisole by means of pyridinium dichlorobromate in water. The effect is observed for Cl–O derivatives of both α - and β -cyclodextrins (Dumanski et al. 2003).

Tachikawa et al. (2005) studied one-electron oxidation of alkylaromatic sulfides (AlkSAr). The substrates were encapsulated into hydroxypropyl β -cyclodextrin (HP- β -CD). The bromine anion-radicals ($\text{Br}_2^{\cdot-}$, generated by pulse radiolysis) acted as one-electron oxidants. The bromine anion-radical is a strong oxidant, and the redox potential of the $\text{Br}_2^{\cdot-}/2\text{Br}^-$ pair is 1.6V against saturated calomel electrode (Neta et al. 1988). However, inhibition of one-electron oxidation was clearly observed when compared with the same process in the absence of HP- β -CD. The binding affinity of $(\text{AlkSAr})^+$ with HP- β -CD was much lower than that of AlkSAr. Comparison



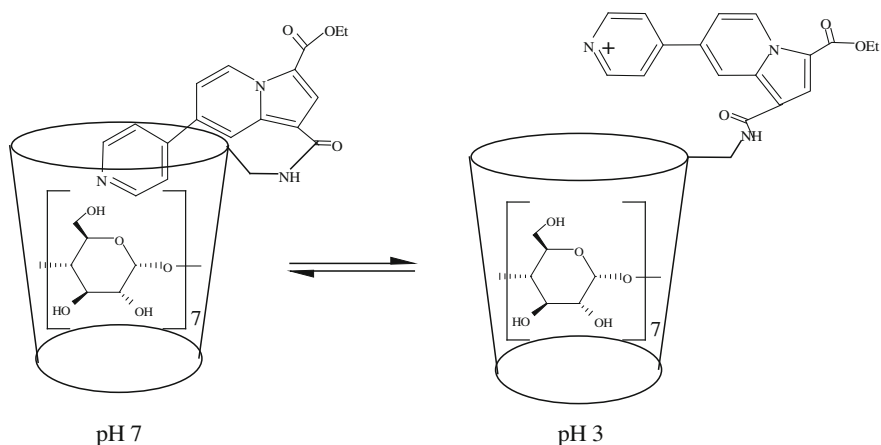
Scheme 1.26 Transferability of Na^+ or Cl^- in dependence on location of azobenzene substituent relatively to conjugated cyclodextrin

between the rates of AlkSAr and $(\text{AlkSAr})^+$ exclusion from the HP- β -CD nanocavity confirms this deduction. In other words, the encapsulation forces of cyclodextrins are stronger with respect to neutral species than to charged ones.

Covalent linkage of bioactive molecules to cyclodextrins is also widely used in medicinal practice. The merits of such bioconjugated drugs lie outside the scope of this book, but are well documented in the medicinal literature. As an example, one can mention the enhanced bioavailability and antioxidant activity of the β -cyclodextrin conjugate with homocarnosine (Amorini et al. 2007).

With an eye toward using cyclodextrins as synthetic ion channels, the conjugate between α -cyclodextrin and azobenzene was tested for its ion transport rate with regard to sodium chloride (Jog and Gin 2008). Scheme 1.26 shows the difference between the permeability of cyclodextrins conjugated with *cis*- and *trans*-azobenzenes. Namely, the *cis* compound is auspicious for anion transport, whereas the *trans* compound is favorable for cation transport. Scheme 1.26 makes the difference mentioned quite lucid: In the *cis* case, the CD channel remains open and provides an easy path for the bulky chloride ion; in the *trans* case, the CD channel is closed, but the azobenzene fragment is accommodated together with the much smaller sodium cation bound by cation- π interaction. For ion transport rates, the attenuation is possible through geometrical conversion from *trans* to *cis* upon ultraviolet irradiation or from *cis* to *trans* upon charge/electron transfer. (For instance, stimulating redox states are often present within diseased cells but not in healthy cells.) This phenomenon is applicable to the construction of switching components in implantable medical devices.

A conjugate constructed from β -cyclodextrin and pyridin-4-yl indolizine derivative manifests interesting dependence of its fluorescent properties on the pH of the



Scheme 1.27 Fragmental exclusion from cyclodextrin cavity upon protonation of pyridyl indolizine

water medium. Namely, at pH 7 the pyridyl indolizine moiety keeps its hydrophobic nature and is oriented inside the cyclodextrin cavity. The system displays strong ultraviolet fluorescence. At pH 3, protonation of free pyridyl nitrogen takes place, and the conjugated moiety acquires hydrophilic character. This causes its motion to the bulk water environment, and the fluorescence emission is switched off. The emission can be restored by return to neutral conditions upon alkalization (Scheme 1.27) (Becuwe et al. 2007).

β -Cyclodextrin conjugated to the N-side of nonapeptide oxytocin was synthesized by Bertolla et al. (2008). The nonapeptide is not included into the cyclodextrin cavity, leaving it vacant for other drugs to be encapsulated. The authors underline that this compound has a double interest as a component of pharmacological formulations. First, inclusion of approved uterotonic drugs such as prostone or carboprost could improve the stability and reduce the systematic side-effects of these drugs, since they will be mainly driven to the uterus level, an oxytocin-receptor-rich tissue in case of pregnancy and delivery. The other interest of this conjugate is to form a host-guest complex with anticancer drugs used in therapy of cervical cancer. This strategy could drive anticancer medication to the uterus and so limit its side-effects.

As already emphasized, β -CD is the most appropriate container for medications, but differs in its low water solubility. Demands include coadministration of β -CD@(drug) complexes in water solutions. To improve the water solubility of β -CD, its randomly methylated derivative is commonly used. Alkylation increases the aqueous solubility by almost 30 times (Sabadini et al. 2008 and reference therein).

While the solubility of native cyclodextrins in water increases with temperature, the opposite is true for their methylated derivatives. The latter are better soluble in cold water than in hot water. In other words, the solubility coefficient in water is negative for methylated cyclodextrins, but it is positive for native ones, as their solubility rises with increasing temperature. Kusmin et al. (2008) showed that the

negative solubility coefficient of methylated cyclodextrins in water is associated with the hydrophobic effect. Note that water molecules can also find themselves inside the cyclodextrin cavity (despite its hydrophobicity).

It should be underlined that the inclusion of correctly selected small organic molecules into drug–cyclodextrin complexes strengthens them and enhances their water solubility. Thus, the ocular bioavailability of acetazolamide is strongly hampered by its low aqueous solubility. However, the hydrophilicity of this drug was improved by combined use of hydroxypropyl- β -cyclodextrin and triethanolamine. Simultaneous complexation and salt formation between acetazolamide and triethanolamine significantly increased the hydroxypropyl- β -cyclodextrin solubilizing power by forming a multicomponent system, enhancing the acetazolamide availability in aqueous hydroxypropyl- β -cyclodextrin solutions. This opens the way to more effective drug delivery to the cornea surface (the transparent front part of the eye). Triethanolamine is an effective additive for corneal transport of acetazolamide in aqueous eyedrops (Granero et al. 2008).

Modification of cyclodextrins is sometimes used to control the regioselectivity and stereospecificity of photocyclodimerization; For instance, anthracene-2-carboxylic acid forms the 9,10-dimer on light excitation. The dimerization can proceed in head-to-tail (*anti* and *syn*) or head-to-head (*anti* and *syn*) fashion. Yang et al. (2008) carried out photocyclodimerization of anthracene-2-carboxylic acid within γ -cyclodextrin capped by a biphenyl-4,4'-disulfonyl bridge, $-\text{O}-\text{SO}_2\text{C}_6\text{H}_4\text{C}_6\text{H}_4\text{SO}_2-\text{O}-$. The mentioned cap was grafted to the two hydroxyls at the narrower rim of the cyclodextrin. This kind of γ -cyclodextrin modification made the dimerization more head-to-tail regioselective (up to 45 %) and more *syn*-stereospecific (*e*, *e* 58 %) as compared with photocyclodimerization of free anthracene-2-carboxylic acid. Owing to the capping, the first included guest molecule orients its hydrophilic carboxylate group to the wider rim of the host, with the anthracenic moiety being hidden beneath the cap. The size of γ -cyclodextrin is not large enough to completely accommodate the second molecule of anthracene-2-carboxylic acid. Due to mutual repulsion of the two carboxylate groups, the second molecule adjoins the first one by its hydrophobic part, at the hydrophobic capped rim having the carboxylate group outside of the cavity. These features predetermine the structure of the product formed.

Modified cyclodextrins (CDs) also play an important role in the chemistry of polymers. Zhang et al. (2012) selectively transformed the hydroxyl groups on the primary face of β -CD to iodine atoms via reaction with PPh_3/I_2 . The iodine substituents were subsequently converted into thiol groups via reaction with thiourea. The obtained $\text{CD}(\text{SH})_7$ was then reacted with different (meth)acrylic monomers or vinyl-terminated polymers to give cyclodextrin-centered star polymers. What is more, the hydroxyl groups on the secondary face of CD remained unchanged during the reaction and were employed as an initiator of ϵ -caprolactam ring-opening polymerization (Zhang et al. 2012).

Cyclic ethers tethered to CDs undergo ring-opening polymerization, and the CD moiety initiates this reaction. The polymers have the structure of pseudo-polyrotaxane, being obtained in high yields without cocatalysts or solvents (Harada et al. 2008; Kikuzawa et al. 2008).

As applied to lactones tethered to CDs, several steps were revealed for the mechanism of polyester-tethered CD formation. The first step is inclusion of lactone in the CD cavity to form the 1:1 encapsulated complex. The carbonyl carbon of the encapsulated lactone is activated by forming a hydrogen bond between the lactone carbonyl oxygen and the CD hydroxyl group. A secondary hydroxyl group at the C₂-position of a CD nucleophilically attacks the activated carbonyl carbon of the lactone to cleave the carbonyl-oxygen bond and form an ester bond. The monomer-attached CD is formed in the initial step. Further, the hydroxyl group of the monomer-attached CD attacks the carbonyl group of the included lactone in the CD cavity to form a disubstituted CD. Then, the hydroxyl group of the monomer moiety immediately attacks the carbonyl carbon of the other monomer moiety so as to insert the lactone into the ester bond between the CD and the polymer chain (Harada et al. 2008). CDs show high activity for the lactone polymerization described.

By means of encapsulation into cyclodextrins, specific polymer cross-linkage can be performed. This is so-called physical cross-linking: The network is retained by nonpermanent and reversible interactions between the polymer chains; For instance, a self-assembling poly(ethylene glycol) (PEG) hydrogel system was described by van de Manakker et al. (2008). The system was based on inclusion complexes between β -CD and cholesterol. Hydrogels are formed after hydration of a mixture of the star-shaped eight-arm PEG end, modified with β -cyclodextrin groups, and the same star-shaped PEG end modified with cholesterol moieties. The gel formation is caused due to β -cyclodextrin-cholesterol inclusion complexes that form physically cross-linked networks. Because of their biocompatibility and physiological clearance, these hydrogels are attractive as drug-delivery matrices and for other pharmaceutical and biomedical applications.

Molecular polymeric wires inside cyclodextrins are attractive because they can have the following ideal features (Terao et al. 2012): (1) a π -conjugated polymer chain with a high degree of insulation, (2) a rigid polymer with high linearity, (3) high solubility in organic solvents, (4) high charge mobility, and (5) high regioregularity. Thus, polymerization of tolan derivatives included into a permethylated α -CD leads to high-molecular main chains with outer coats. The rigidity is caused by intramolecular inclusion of the polymer main chain into the cyclodextrin cavity. Terao et al. (2009) thereby synthesized insulated molecular wires as rigid π -conjugated polymers with high degree of insulation and linearity. The polymers differ in their high charge mobility and easy processability (their organic solubility is unprecedented).

When water is added dropwise into dimethylformamide solution of polyether imide with β -CD building block (containing rigid chains at both ends) under ultrasonication, polymeric vesicles are formed (Guo et al. 2008). Seemingly by means of hydrogen bonding, the chains pack radially into a monolayer membrane, forming a circular locked cavity. This cavity can serve as a specific carcerand for appropriate reactions in a confined environment. Reactions in vesicles and in liposomes have significant importance in bioorganic chemistry. Such reactions lie outside the scope of the present treatise. The reader interested in this field may refer to recently published reviews by Stuart and Engberts (2010) as well as by Stano and Luisi (2010).

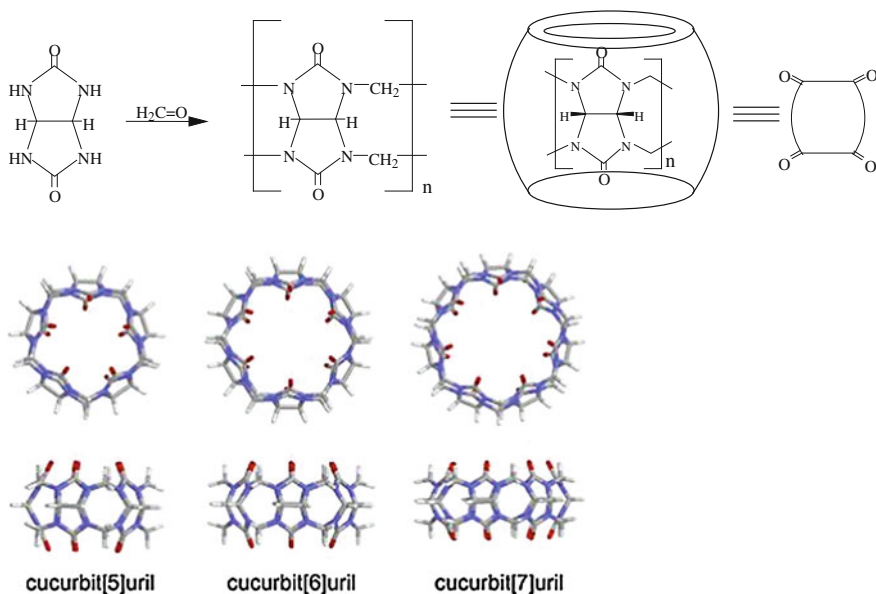
Promising effects were observed with modified cyclodextrins that are intercalated in layered double hydroxides. Based on divalent (M^{2+}) and trivalent (M^{3+}) metal cations, hydroxyl, and anion A, the double hydroxides had a structure of $[M_{1-x}^{2+}M_x^{3+}(\text{OH})_2]^{x+}(\text{A}^{n-x/n}) \cdot m\text{H}_2\text{O}$. These layered double hydroxides are also known as anionic clays. Liu et al. (2008d) constructed novel nanocage structures derived from carboxymethyl- β -cyclodextrins intercalated in layered double hydroxides, whose gates can be regulated by the process of swelling/drying the composition. The extent of opening of these nanocages can be controlled by swelling in different solvents. Dodecylbenzene as the guest molecule has been incorporated into the nanocages. Compared with the confinement effect produced by cyclodextrin only, this double confinement imposes stronger restrictions on the mobility of the guest molecule, which leads to a blueshift of the fluorescence spectrum and increases the decay time of the fluorophore. The authors assume that such “nanocages might have potential applications as adsorbents, synergistic agents, and storage vessels for neutral molecules” (Liu et al. 2008d).

1.7 Cucurbiturils as Hosts

The cucurbit[n]urils (CB[n], $n = 5-8, 10$) are a family of cyclic host molecules comprising n glycouril units bridged by $2n$ methylene groups. The portals of the hydrophobic cavity are lined with ureido carbonyl groups, which afford ion–dipole, dipole–dipole, and hydrogen-bonding interactions with the guest. The first part of the name “cucurbituril” originates from the Latin word *cucurbita*, alluding to the capsule shape of a gourd or pumpkin (Scheme 1.28). The second part of the name appears because cucurbit[n]urils are composed of n glycouril units linked by a pair of methylene groups (Scheme 1.28).

The notable peculiarity of cucurbiturils consists in the relative orientation of the glycouril hydrogen atoms of C–H bonds, which point out of the cavity (Freeman et al. 1981). Recently, diastereomeric cucurbiturils were reported, in which a single pair of methylene C–H groups point into the central cavity (Isaacs et al. 2005; Isaacs 2009). Cucurbiturils also contain carbonyl-fringed portals that have considerable negative charge density, facilitating the binding of positively charged species. For the same reason, cucurbiturils do not bind species charged negatively (Kaifer et al. 2012). Because of the negative electrostatic potential, both at the portals and within the cavity, interaction with cationic guests is preferred. With cationic guests, the stability constants of cucurbit[n]urils are larger than those of cyclodextrins of corresponding size. These constants can be several orders of magnitude larger when the guest is a cation. The nonpolarizable cavity preferably accommodates hydrophobic moieties.

According to Lagona et al. (2005), all of the cucurbiturils have a common depth of 0.91 nm. The most frequently used cucurbit[8]uril has a large cavity of 0.48 nm^3 , equatorial diameter of 0.88 nm, and portal diameter of 0.69 nm. Cucurbit[6]uril is a relatively rigid, hollow, barrel-shaped molecule with cavity volume of 0.16 nm^3 , equatorial diameter of 0.58 nm, and portal diameter of 0.39 nm. Those data had also



Scheme 1.28 Structures of cucurbiturils and their graphical representation

been reported by Freeman et al. (1981) and Marquez et al. (2004). Cucurbit[7]uril has cavity volume of 0.279 nm^3 , equatorial diameter of 0.73 nm , and portal diameter of 0.54 nm (Lagona et al. 2005; Wheate et al. 2008). As seen, carbonyl-rimmed portals are narrower than the cavity equatorial section. This produces a significant steric barrier to binding and dissociation of various guests. In other words, the appropriate cucurbituril (the reaction flask) should be so selected that the reaction product formed can eject from the cavity, whose exit is guarded by the narrower rim. All cucurbiturils present highly symmetrical structures with two identical openings, and this distinguishes them from cyclodextrins.

Synthesis of cucurbit[6]uril was performed by Behrend et al. in 1905 by condensation of glycouril (acetylene urea) and formaldehyde in concentrated HCl. In 1981, Mock's group reinvestigated the report by Behrend et al. and disclosed the remarkable macrocyclic structure comprising 6 glycouril units and 12 methylene bridges (Freeman et al. 1981). Moreover, the aforementioned reaction results in the formation of 24 new C–N bonds and 6 eight-membered rings, all with complete control over the relative orientation of the glycouril C–H atoms. As just mentioned, all these hydrogen atoms point out of the cavity. Bakovets et al. (2008) calculated thermodynamic functions and used them for a description of the cyclization mechanism leading to the formation of cucurbit[6]uril. Isaacs (2009) formulated the mechanism of CB[*n*] formation as a step-growth cyclooligomerization.

The behavior of cucurbiturils in terms of solubility is somewhat astonishing. According to Isaacs (2009), “odd” cucurbit[5 and 10]urils are nicely soluble in neutral water whereas “even” cucurbit[6, 8, and 7]urils are poorly water soluble at pH 7.

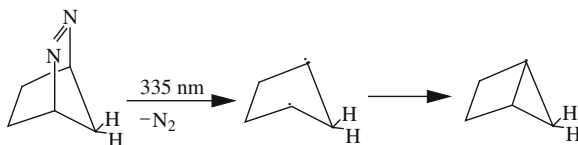
Thus, the dimethyl derivative of CB[7] is highly soluble in water. As a result of the high intrinsic solubility, Me₂CB[7] is able to solubilize the insoluble benzimidazole drug albendazole (Vinciguerra et al. 2012). Meanwhile, all of the urils exhibit good aqueous solubility under acidic conditions or in the presence of certain metal cations such as Na⁺.

Binding of Na⁺ to cucurbituril portals is equivalent to the appearance of a lid, so that the addition of a salt to a water solution of the developing host–guest complex effectively triggers guest release from the capsule (Florea and Nau 2011). At the same time, coordination of Na⁺ to the carbonyl portals increases steric hindrance and blocks guest entry into the cavity. On the other hand, addition of cations that bind to the cucurbituril portals decreases the concentration of free host available to bind a guest and therefore decreases the association process. Thus, the magnitude of the association rate constant of the *R*-(+)-1-(2-naphthyl)ethylammonium cation with the binary complex CB[7]@Na⁺ is at least 40 times lower than that with CB[7] alone (Tang et al. 2011).

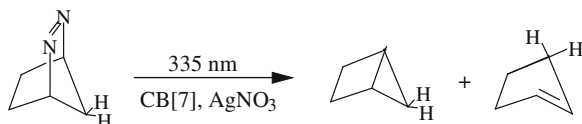
Cucurbit[*n*]urils have a hydrophobic cavity and two identical carbonyl-laced portals. Cucurbit[7]uril actively sucks protons into the cavity from water environment. In water, thiabendazole, i.e., 4-(2-benzimidazolyl)thiazole, remains unprotonated in its uncomplexed form, but becomes protonated after inclusion in cucurbit[7]uril (Saleh et al. 2008). There are also other examples of this host-assisted guest protonation; see, e.g., works by Bakirci et al. (2006) and Praetorius et al. (2008). This phenomenon has been used to monitor the enzymatic activity of lysine decarboxylase (Praetorius et al. 2008).

Koner et al. (2011) described unexpected photoreaction of 2,3-diazabicyclo[2.2.1]hept-2-ene included in cucurbit[7]uril. The reaction proceeds in water–toluene mixture upon excitation at 335 nm. The specificity of the reaction can be seen from the comparison between Schemes 1.29 and 1.30. Upon excitation, diazabicyclo[2.2.1]hept-2-ene affords 100 % bicyclo[2.1.0]pentane (housane). This product is invariably obtained from uncomplexed diazabicyclo[2.2.1]hept-2-ene in aqueous or toluene solution, or from its inclusion complex with cucurbit[7]uril, or from diazabicyclo[2.2.1]hept-2-ene in the presence of Ag⁺.

It is important to note that the binding constant between Ag⁺ and diazabicyclo[2.2.1]hept-2-ene is very low, not exceeding 23 M⁻¹. This binding constant increases by about three orders of magnitude when Ag⁺ is complexed with diazabicyclo[2.2.1]hept-2-ene already encapsulated in cucurbit[7]uril (Koner et al. 2011). The carbonyl portals of the host coordinate Ag⁺ close by the diaza fragment of the guest. Such activation causes the reactivity outlined in Scheme 1.30: Cyclopentene and bicy-



Scheme 1.29 Housane generation during photolysis of diazabicycloheptene

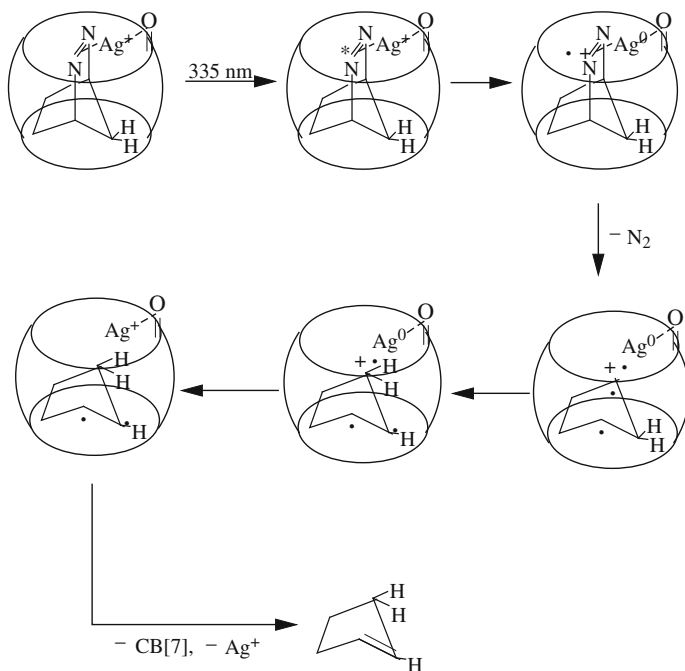


Scheme 1.30 Housane and cyclopentene formation upon photoexcitation of diazabicycloheptene and Ag⁺ co-jointly included into cucurbituril

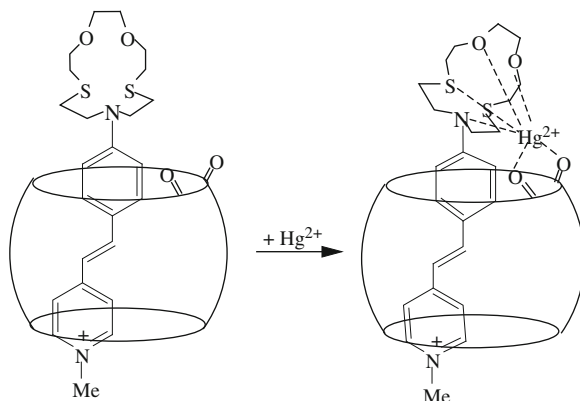
clo[2.1.0]pentane are obtained as final products, with yields of 41% and 59%, respectively.

Koner et al. (2011) proposed the following mechanism: The silver ions complexed to the CB[7] portals facilitate a highly exergonic one-electron oxidation of singlet diazabicyclo[2.2.1]hept-2-ene. Elimination of nitrogen from the resulting aza cation-radical afforded the 1,3-cyclopentadienyl cation-radical, which underwent a rapid 1,2-H shift to give the cyclopentene cation-radical. The latter was reduced, again in an exergonic reaction, by the (still portal-associated) silver atom to yield cyclopentene and a regenerated silver ion. Scheme 1.31 outlines the mechanism proposed by Koner et al. (2011).

It was underlined “that the singlet excited state of 2,3-diazabicyclo[2.2.1]hept-2-ene is far too short-living to undergo bimolecular electron transfer with additives,



Scheme 1.31 Confinement effect on Ag⁺-promoted of diazabicycloheptene photolytic transformation



Scheme 1.32 Cucurbituril role in reinforcement of Hg^{2+} coordination with styryl pyridinium bearing dithia dioxo monoaza crown substituent

which accounts for the fact that cyclopentene is not formed upon direct photolysis. It is likely to do so, however, when firmly held in place in immediate proximity to the oxidizing silver ion within the ternary cucurbituril complex... This demonstrates the potential for metal catalysis at the cucurbituril rim and the concomitant exploitation of the same macrocycles in inverse phase-transfer catalysis.” (Koner et al. 2011).

The ternary complex depicted in Scheme 1.32 is formed in water mixture containing CB[7], 1-methyl-4-styryl pyridinium dye derivatized with dithia-dioxo-monoaza-15-crown-5-residue, and double-charged mercury cation (Chernikova et al. 2012). In the complex, Hg^{2+} ion coordinates to ureidyl $\text{C}=\text{O}$ portals of CB[7] and to the crown-ether moiety of the guest dye. The authors estimate the Hg^{2+} affinity for the binary complex that starts the equation of Scheme 1.32 as about 25 times greater than the Hg^{2+} affinity for the free dye nonencapsulated into CB[7].

Many of the ready-made cucurbituril@guest complexes are easily soluble in water. Cucurbit[6]uril readily encapsulates organic ammonium ions in water (Rekharsky et al. 2007; Huang et al. 2008). However, the host-guest dimension agreement is crucial in this case, too: The ammonium salt formed from *p*-methylbenzylamine is smoothly encapsulated by cucurbit[6]uril. Under the same conditions, no binding was detected for *o*-methyl- or *m*-methylbenzylamines because they cannot easily fit within the cucurbit[6]uril sleeve (Lagona et al. 2005).

According to Dearden et al. (2009), similar shape selectivity exists for isomeric phenylenediamine salts: only the 1,4-isomer binds in the interior when coming into contact with cucurbit[6]uril in the gas phase. Dearden et al. (2009) analyzed thermodynamic factors governing the inclusion process in solution and in the gas phase: “In solution, at least some of driving force for host-guest binding arises because expulsion of solvent from the host binding cavity, and/or disruption of interactions between solvent and guest, is entropically favorable. If the guest has difficulty entering the host cavity, no solvent is expelled, entropic benefits are decreased, and complexation may not be observed. In the gas phase, no entropic stabilization from solvent is avail-

able. Rather, the loss of translational freedom that occurs upon complexation is also unfavorable. Hence, entropy frequently favors complex formation in solution, but always disfavors complexation in the absence of solvent. Enthalpy can either favor or disfavor complexation in solution, depending on the balance between solvation enthalpies of host and guest and the interaction enthalpy associated with complex formation. On the other hand, in the gas phase there is no competition between solvation and complex formation, so interaction enthalpy is always favorable and tends to be the dominant factor in gas-phase complexation” (reproduced with permission by D.V. Dearden, the Author, of September 19, 2012).

The water solubility of CB[6] can be seriously improved by inclusion of imidazolium compounds; For instance, encapsulation of bis(1-ethylimidazolium)-3,3'-(octyl-1,8-diyl) dibromide by CB[6] allows monoxidizing (functionalizing) of the host with ammonium persulfate in water. After oxidation, the guest can be easily removed by refluxing in methylene chloride (Zhao et al. 2012).

N-Methyl-4-(4-substituted benzoyl)pyridinium cations can, in principle, enter the cavity by the pyridinium end or by the central carbonyl fragment and, partially, by the adjacent aromatic rings. Concerning the equilibrium of Scheme 1.33 in water solution, encapsulation of the pyridinium end cannot result in any change in the equilibrium position. At the same time, this equilibrium must be shifted toward the keto form, because the carbonyl group turned out to be protected by the CB[7] cavity. This was the effect revealed experimentally. Incorporation of the carbonyl, but not pyridinium, fragment was also elucidated by ^1H nuclear magnetic resonance (NMR) (Rawashdeh et al. 2008b). Clearly, the benzoyl group, despite the possible hydrogen bonding with the solvent through the carbonyl oxygen, prefers to retreat into the hydrophobic cavity, where it can benefit from greater stabilization through hydrophobic interaction.

Thangavel et al. (2012) examined the location of 2,6-disubstituted 4-phenylpyridiniums encapsulated by CB[7] or CB[8] from water solution. In all of the cases, only 4-phenyl group is drawn into the cavity. These supramolecular complexes show promising photoluminescence suitable for electroluminescent devices.

Note, cyclodextrins and cucurbiturils provide different opportunities for binding of neutral, cationic, or anionic forms of the guest. Cucurbiturils provide electrostatic and hydrophobic driving forces for encapsulation. Electrostatic forces are stronger than hydrophobic ones, but the latter also can play a role in encapsulation. Thus, 4',6-diamino-2-phenylindole dication, being encapsulated into cucurbit[7]uril in water solution, is displaced from the cavity by 1-alkyl-3-methylimidazolium ionic liquid (Miskolczy et al. 2009). While the 4',6-diamino-2-phenylindole dication is bound



Scheme 1.33 Reversibility in hydration of benzoyl pyridinium

to the host with solely electrostatic forces, alkylmethylimidazoliums are retained by both electrostatic and hydrophobic forces. The presence of head alkyl groups in the imidazolium fragment of the ionic liquids adds the hydrophobic interaction to the electrostatic ones. At the same time, the anion of the ionic liquids is not included in the encapsulation by cucurbit[7]uril (Miskolczy et al. 2009). The reason consists in the significant negative charge density of the carbonyl-laced portals of the host, which hinders interaction with the anion. Moreover, the cavity is not very polar, which disfavors ion pairing.

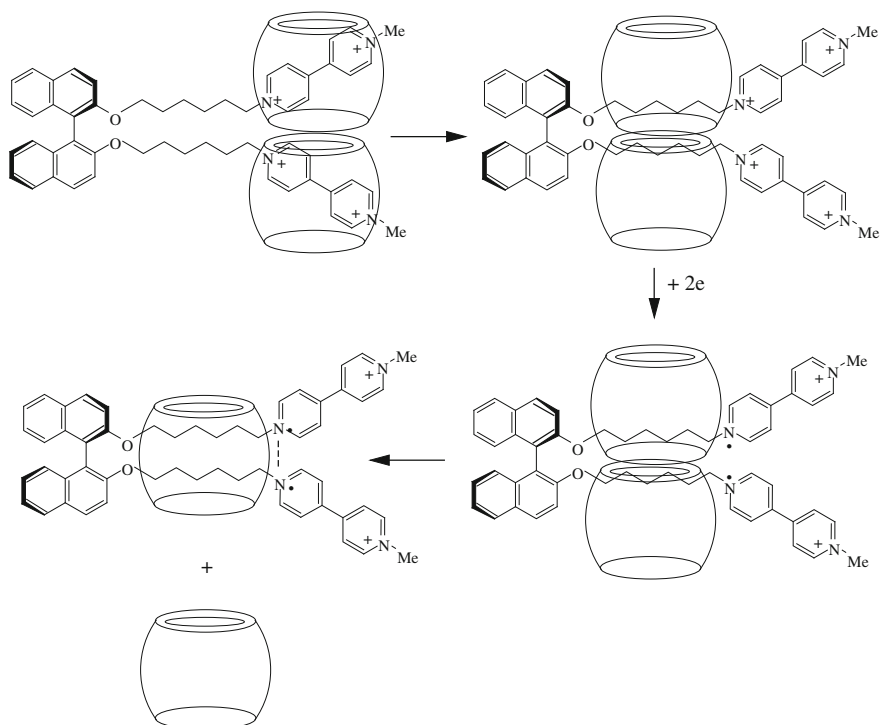
In contrast, β -cyclodextrin has a more polar cavity. Chloride, tetrafluoroborate, and hexafluorophosphate of 1-butyl-3-methylimidazolium are accommodated in this cavity as ion pairs with totally embedded imidazolium cation (He and Shen 2008). It is also probable that inclusion of the imidazolium moiety is directed by a cooperative two-step binding process with the anion playing the role of an effector (see, for analogy, Menand and Jabin 2009).

Tetrakis(4-methylpyridiniumyl)porphyrin reacts at once with four equivalent cucurbit[7]urils due to the strong affinity between the host and each of the four *N*-methylpyridinium groups. This kind of encapsulation disrupts the intramolecular charge transfer between the *N*-methylpyridinium ring and the central porphyrin moiety and changes the porphyrin fluorescence spectrum (Mohanty et al. 2008).

Kalmar et al. (2012) measured fast kinetics of the reaction between CB[7] and the viologen dication bearing the tri(ethylene glycol) arm on one nitrogen atom and the methylene-(*m*-xylyl) substituent on the opposite nitrogen atom of viologen. The guest was chosen in order to compare the affinity of the arm and the substituent to the CB[7] host. The exact name of the guest is 1-[(methoxytri(ethylene glycol)-1'-[(3,5-dimethylphenyl)methyl]-4,4'-bipyridinium dication. It was established that two complexes are formed: one in which CB[7] docks near the more hydrophobic xylyl-substituted end of the viologen, and a second in which an additional CB[7] associates around the ethylene glycol end of the viologen. The xylyl-centered inclusion complex is more stable than the ethylene-glycol counterpart.

Gao et al. (2012) studied complexation of cucurbit[8]uril with the bromide–iodide salt of Scheme 1.34 in water. The salt was composed of two 4,4'-bipyridium arms connected by means of hexyl chains to an *R*-2,2'-dioxy-1,11-binaphthyl. The binaphthyl acted as a hinge. The salt associated with two CB[8] molecules (i.e., each pyridinium unit became encircled by a CB[8]). Hydrophobic interaction promoted the formation of the complex in which CB[8] surrounds the two hexyl chains. The encirclement of both bipyridium units and/or the two hexyl chains by bulky CB[8] macrocycles generates steric hindrance which forces the two dioxy arms to move away. This intriguing result was obtained after treatment of the 1:2 complex with sodium dithionite in water solution: Monoreduction of nearly all the bipyridinium units occurred, and at least 65% of them dimerized. That caused a change in the complex stoichiometry (from 1:2 to 1:1) with the release of one equivalent of CB[8] (Gao et al. 2012).

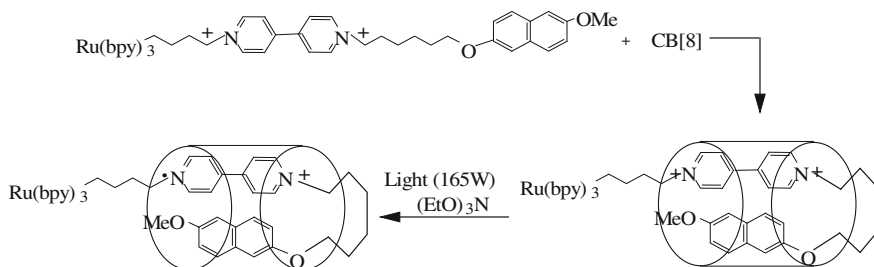
Other intriguing results were obtained with *N,N'*-dioctylviologen, i.e., *N,N'*-dioctyl-4,4'-dipyridinium dication. Due to hydrophobic interaction, reaction of this dication with cucurbit[7]uril in aqueous solution results in docking of the uril at one of the octyl moieties. However, addition of α -cyclodextrin pushes the uril from the



Scheme 1.34 Cucurbituril shift from dipyridinium to hexyl chain fragments in dioxybinaphthyl derivative and guest dimerization upon monoreduction of dipyridinium units

octyl moiety of dioctyl viologen to the pyridinium moiety (Liu et al. 2007b). Stability of the resulting inclusion complex is caused by docking of the two different capsules at the most appropriate parts of the viologen molecule. Namely, the cyclodextrin is anchored to the uncharged octyl group, and the uril at the positively charged pyridinium fragment.

When included in cucurbiturils, viologens readily undergo one-electron reduction to yield monomeric cation-radicals (Jeon et al. 2002). The viologen cation-radicals bind strongly to cucurbit[7]uril. The binding constant of the viologen cation-radical with cucurbit[7]uril is only twofold lower as compared with that of the viologen dication with the same host (Ong et al. 2002). In aqueous solution, a methylviologen derivative was more easily reduced when it was inserted into the cavity of cucurbit[8]uril (Sun et al. 2008). In the presence of cucurbit[8]uril, one-electron reduction of viologen leads to the formation of a complex including the viologen cation-radical in its *dimeric* form (Coulston et al. 2011). The formation of the dication-radical in the cucurbit[8]uril capsule is one important cause of the reduction promotion. The reasons for the stability of the complex between the dication-radical dimer and cucurbit[8]uril include the interaction between two π systems of the two cation-radical



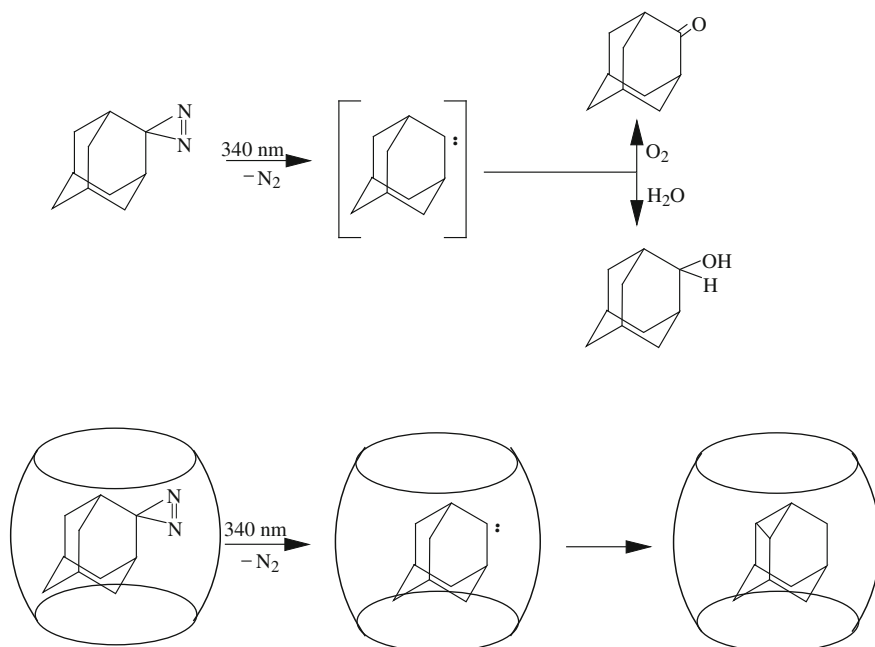
Scheme 1.35 Viologen-dihydroxynaphthalene photoinduced charge transfer and dimerization of ruthenium complex confined in cucurbituril

parts, and contacts of the cation-radical aromatic surfaces with the inner cavity surface coupled with hydrophobic interaction (Senler et al. 2012).

Lee et al. (2003) described a 1:1:1 ternary inclusion complex between cucurbit[8]uril and an acceptor–donor pair of the viologen dication and 2,6-dihydroxynaphthalene. The major driving force for the complex formation is the strong charge-transfer interaction of the acceptor with the donor inside the host cavity. Their close contact within the cavity was established by X-ray crystallography. Without CB[8], this charge-transfer interaction is very weak. Cerium ammonium nitrate, in some way, reaches the encapsulated complex, oxidizes 2,6-dihydroxynaphthalene to 2,6-naphthoquinone, and annihilates the donor–acceptor interaction mentioned above (Lee et al. 2003).

When the viologen and 2,6-dihydroxynaphthalene moieties are parts of the same molecule, both of them are encapsulated by the CB[8] host (Scheme 1.35) (Zou et al. 2008). The encapsulated parts form a charge-transfer complex (inside the capsule). No changes were observed during photoexcitation of the hidden charge-transfer complex. However, photoexcitation in the presence of triethanolamine and Ru(II)(bpy)₃ results in generation of the viologen cation-radical partnering with the close neighboring naphthalene. Light stimulates the ruthenium complex to give the excited state $[\text{*Ru(II)(bpy)}_3]$ bound with the rest of the system. This excited state is capable of transferring an electron intramolecularly to the viologen moiety, generating Ru(III)(bpy)₃ fragment and the viologen cation-radical confined within the guest. However, the back electron transfer from the cation-radical just formed to the Ru(III) is so fast that no changes in the hidden charge-transfer complex can be observed. In the presence of (EtO)₃N electron donor, Ru(III) is reduced to Ru(II). This restrains the back electron transfer from the viologen cation-radical to Ru(III)(bpy)₃. The formation of the stabilized (confined) viologen–dihydroxynaphthalene partner radical becomes detected.

It should be underlined that cucurbiturils provide high preservation of unstable intermediates generated from guests. Thus, adamantanediazirine, a precursor of adamantylidene, forms a 1:1 complex with CB[7] or CB[8] in water. While photolysis of free adamantanediazirine in water gave mainly adamantanone and adamantanol via adamantanylidene as intermediate, the 1:1 complex of adamantanediazirine with



Scheme 1.36 Cucurbituril effect on photolytic transformation of adamantanyl diazirine

CB gave intramolecular C–H insertion product of adamantanylidene in excellent yield (Scheme 1.36) (Gupta et al. 2012). Significant control of carbene reactivity and equilibrium between singlet and triplet forms was achieved when the precursor was encapsulated within a tight inert cavity.

The strength of the binding to cucurbiturils depends on the state of the guest protonation. Cyclodextrins, rimmed with not so polar hydroxyl groups, prefer neutral or anionic guests over cationic species. The cucurbiturils contain a hydrophobic interior cavity, with more polar carbonyl groups surrounding the two restrictive portals. These polar carbonyl groups have affinity to cationic guest forms. The best demonstrative examples are organic guests containing protons at nitrogen, oxygen, and carbon centers. Through dipole–dipole, ion–dipole, and hydrogen-bonding interactions, stabilization of the corresponding cationic forms takes place. Thus, inclusion of protonated 2-aminoanthracene into cucurbit[7]uril diminishes its acidity. This is a result of hydrogen bonding between the ammonium fragment and the portal carbonyl moieties. Both the ground and excited states undergo diminution of acidity, resulting in a switch of fluorescence from green to blue (Wang et al. 2005).

It was found by the same research group that, in aqueous solutions, the pK_a of novocaine changes from 2.28 to 3.55 in the presence of cucurbit[7]uril. The same effect was observed for other anesthetics such as tetracaine, dibucaine, and prilocaine (Wyman and Macartney 2010). The effect described for anesthetics is important for medical practice. The point is that only the neutral form of the injected anesthetic

is able to diffuse across nerve membranes and block sodium channels. At sites of inflammation (acidosis), a more acidic environment is observed. The anesthetic is protonated, and its fixation by polar parts of the surroundings is secured. This phenomenon has a crucial influence on the pharmacokinetics of local anesthetics.

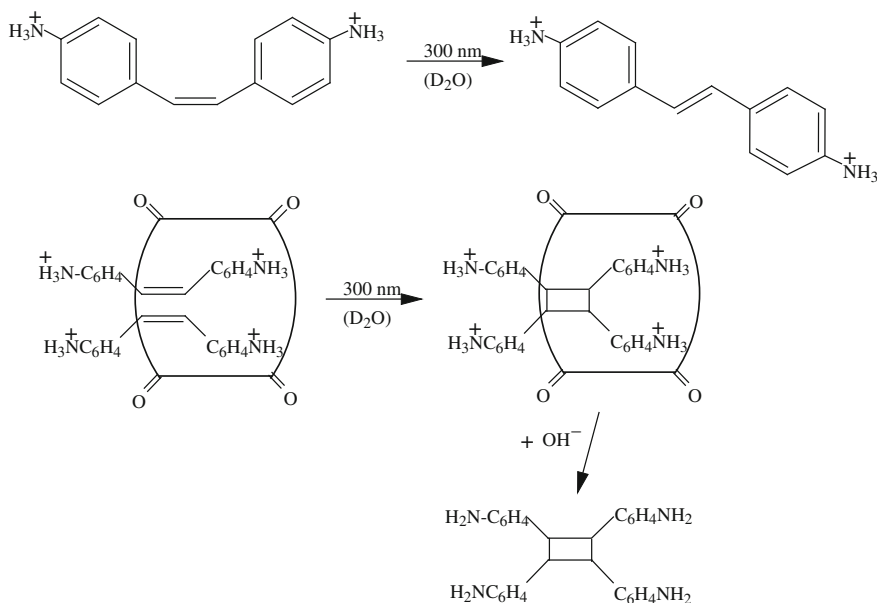
For alkanediammonium ions, the stability of their complexes with cucurbiturils depends on the alkane length. When the distance between the ammonium termini matches the distance between the electrostatically negative ureidyl C=O portals of CB[6], tight binding (due to a combination of hydrophobic effect and ion–dipole interactions) is observed. Alkanediammonium ions with shorter or longer alkane are connected to CB[6] significantly less tightly (Isaacs 2009). Interestingly, cucurbit[7]uril binds NR_4^+ , PR_4^+ , and SR_3^+ cations ($\text{R} = \text{Me}, \text{Et}, n\text{-Pr}, n\text{-Bu}$), with smaller alkyl chains *inside* its cavity, rather than at the carbonyl-lined portals. Considerable size selectivity was noted (St-Jacques et al. 2008).

N,N' -Bis(ferrocenylmethyl)- N,N' -dimethyl-1,5-hexylenyl diammonium [$\text{Fc-CH}_2\text{-N}^+(\text{CH}_3)_2\text{-(CH}_2)_6\text{-N}^+(\text{CH}_3)_2\text{-CH}_2\text{-Fc}$] and N,N' -bis(ferrocenylmethyl)- N,N' -dimethyl-1,4-bis(methylenephenyl) diammonium [$\text{Fc-CH}_2\text{-N}^+(\text{CH}_3)_2\text{-CH}_2\text{-C}_6\text{H}_4\text{-CH}_2\text{-N}^+(\text{CH}_3)_2\text{-CH}_2\text{-Fc}$] are encapsulated into a cucurbituril in such a way that the host soaks up the fragments containing dimethylammonium units. The ferrocenyl moieties remain outward. Anodic oxidation transforms the ferrocenyl moieties to ferrocenium fragments through two-electron removal. Four-charged particles are formed without any changes in the encapsulation manner (Sobransingh and Kaifer 2006). The cavity attracts only the two ammonium parts because the ammonium positive charge density is stronger than that of the terminal ferrocenium one. N -(Ferrocenylmethyl)- N,N,N -trimethylammonium [$\text{Fc-CH}_2\text{-N}^+(\text{CH}_3)_3$] forms a remarkably stable inclusion complex with cucurbituril, and the whole guest molecule is encapsulated (Jeon et al. 2005).

Yuan and Macartney (2007) used aqueous solution of bis(2,6-pyridinedicarboxylato)cobaltate for comparative oxidation of free and encapsulated compounds. (This oxidant does not associate with cucurbituril.) As it turned out, encapsulation significantly reduced the rate constants for the ferrocene–ferrocenium transition. One of the important causes of the observed retardation is steric hindrance due to the close approach of the oxidant to the encapsulated ferrocene (Yuan and Macartney 2007).

Reaction between *cis*-stilbene-4,4'-diammonium dichloride and the octameric cucurbituril homolog cucurbit[8]uril, CB[8], is demonstrative from the viewpoint of accommodation of two arylammonium compounds. When the mentioned host and guest compounds are mixed in 1:1 stoichiometry, the 1:2 inclusion complex is formed as the major product. CB[8] can include two ammonium compounds, even though a half of the CB[8] amount remains unfilled (Jon et al. 2001).

Jon et al. (2001) compared photochemical transformation of free *cis*-stilbene-4,4'-diammonium dichloride and the same compound doubly encapsulated by CB[8]. For the free diammonium dichloride, the main reaction pathway upon irradiation at 300 nm is isomerization into the *trans*-isomer according to Scheme 1.37. Under the same conditions, the 1:2 complex produces a [2 + 2] adduct, almost solely. No formation of isomerization product, i.e., the *trans*-stilbene, was observed. The adduct formation is depicted in Scheme 1.37. This is a prominent demonstration of



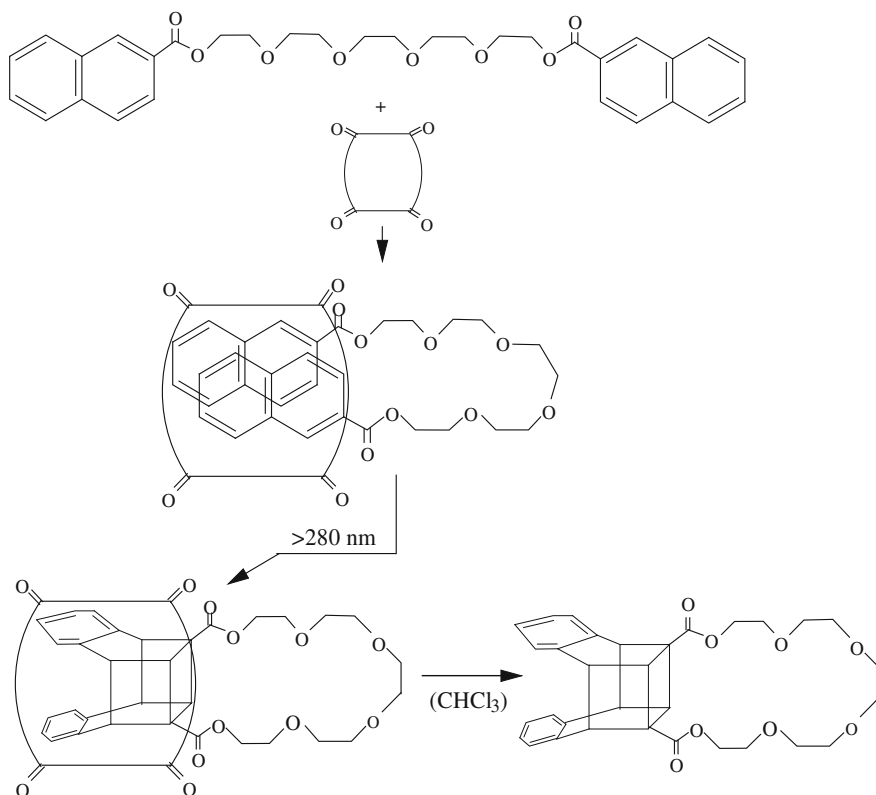
Scheme 1.37 Photolysis of *cis*-diaminostilbene and its doubly encapsulated complex with cucurbituril

the effects of confinement on organic reactivity. The ability of the host to stabilize the two guest molecules with parallel orientation of the olefinic group in close proximity leads to the experimental photodimerization. Scheme 1.37 shows the inclusion of a macrocycle guest in a macrocycle host that resembles the famous Russian matryoshka dolls.

Interestingly, not so huge cyclic guests (the smaller macrocycles) can form transition-metal complexes with Cu(II) or Zn(II) while still being encapsulated in CB[8] (Lee et al. 2003).

Another interesting example is the interaction between CB[8] and water-insoluble neutral 2-naphthyl-labeled polyethylene glycol (Scheme 1.38) (Wu et al. 2008). There is some attraction between these compounds: The terminal naphthyl groups are hydrophobic, and the CB[8] cavity is hydrophobic, too. By inclusion, CB[8] encapsulates the polyethylene glycol to position the two end naphthyl groups in proximity. (CB[8] is able to accommodate two aromatic molecules within the cavity; the polyetheral chain of the glycol is flexible and can bend.) Irradiation with light of wavelength longer than 280 nm results in the formation of a dimer through the two carbonyl-neighboring benzene rings of each naphthalenyl moiety. After 12 min of irradiation, the authors extracted the free (nonencapsulated) dimeric product by chloroform with yield of 96% (Scheme 1.38) (Wu et al. 2008).

It is worth mentioning the protective properties of cucurbiturils. Cystine–cysteine, i.e., disulfide–thiol, interconversion proceeds readily as either a chemical reaction or metabolic transformation. Berbeci et al. (2008) established that CB[6] completely



Scheme 1.38 Photodimerization of ethylene glycol bearing two terminal naphthylcarbonyl groups within cucurbituril

preserves the disulfide bond from reduction and the thiol group from oxidation. Namely, CB[6] forms stable complexes with 2-aminoethanethiol (cysteamine) or with the related cystamine disulfide. In these complexes, the thiol or the disulfide group is encapsulated inside the host cavity. The CB-complexed thiols turned out to be resistant against oxidants, while the CB[6]-bound disulfides are stable under the action of reductants.

Rotaxane-type architectures have been proposed for the construction of frictionless rotary motors (Ben Shir et al. 2008). The authors used CB[6] as a macrocyclic cavitand and a 1,6-diammonium-2,4-hexadiyne bis(hydrosulfate), 1,6-dipiperdinium-2,4-hexadiyne dichloride, or 1,6-dipyrrolidinium-2,4-hexadiyne dichloride rod as a rotor. Each diyne rod floats at the center of the macrocyclic host with no apparent van der Waals contacts between the guest and host.

Inclusion of organic guests into cucurbituril cavities rids the guests of forces causing their aggregation that takes place in noncomplexed states. Thus, two cyanine dyes, pinacyanol and pseudoisocyanine, form aggregates in water solutions. The dyes were encapsulated by CB[7] in their monomeric forms. Disruption of the

intermolecular forces responsible for the aggregation led to changes in the visible and fluorescence emission spectra of the dyes (Gadde et al. 2008). This phenomenon may find applications, for instance, in the development of new optical sensors.

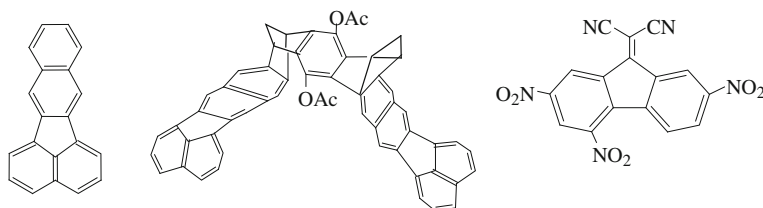
1.8 Tweezers as Hosts

Molecular tweezers and clips containing aromatic sidewalls are able to form stable complexes with aromatic and aliphatic molecules or ions. The driving force for the formation of these adducts is based on charge-transfer interactions coupled to CH- π and π - π interactions and, in some cases, on electrostatic forces. Tweezers containing two metallocomplexes [e.g., bis(zinc^{II} porphyrin)] as sidewalls incorporate guests [e.g., (1*R*,2*R*)-1,2-diphenylethylenediamine] through addition coordination of these guests as ligands to the central metal. The work by Brahma et al. (2012) is a case in point.

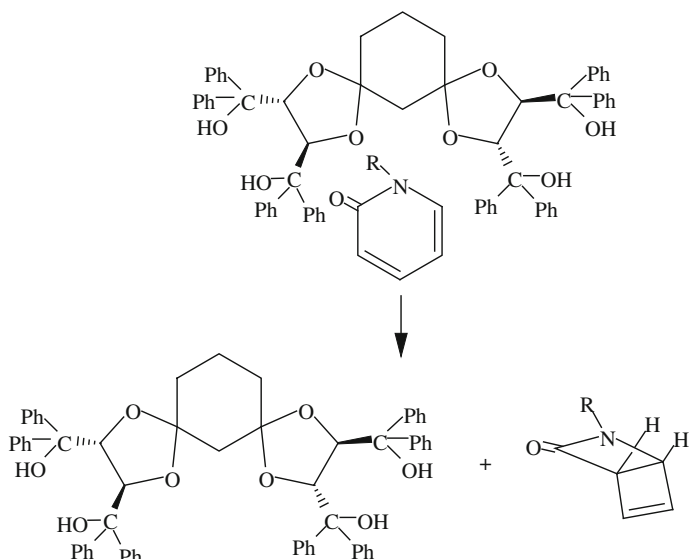
Scheme 1.39 exemplifies suction of a guest into tweezers (clips). The left structure in Scheme 1.39 represents benzo[*k*]fluoranthene; this structure forms two sidewalls of the tweezers (clips). The host is represented by the middle structure in Scheme 1.39. The guest is 9-dicyanomethylene-2,4,7-trinitrofluorene, the right structure in Scheme 1.39. As reported by Branchi et al. (2008), the host and the guest mentioned form a stable host-guest complex of charge-transfer type. Upon one-electron oxidation or one-electron reduction, the complex is reversibly disassembled.

The tweezers of Scheme 1.40 hold 1-alkylpyridin-2-one, forming 1:1 inclusion complexes. In the solid state, both constituents of the complex occupy a fixed mutual arrangement. Upon irradiation by a high-pressure mercury lamp, the solid complexes undergo cyclization of the guests to form the corresponding β -lactams in good yield. The lactam is obtained in *e*, *e*-conformation, and the enantiomeric purity reaches 99.5% (Tanaka et al. 2002).

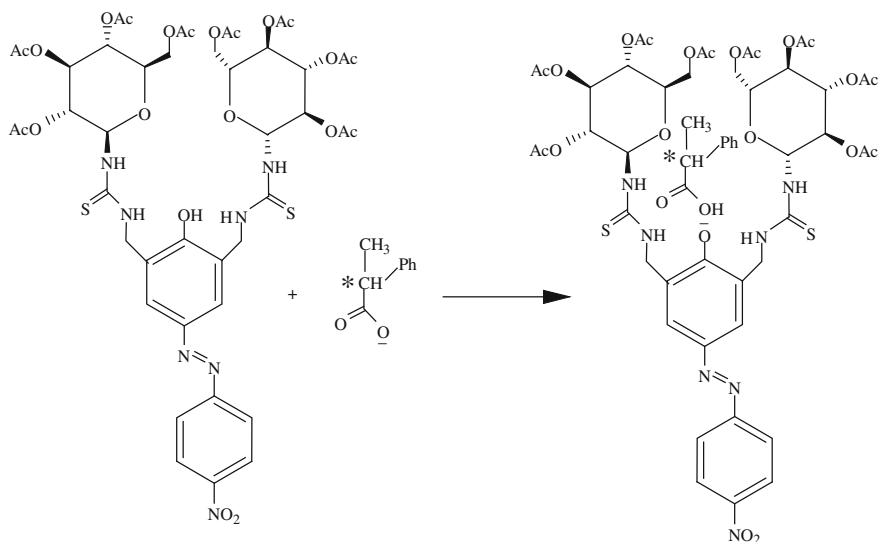
Choi et al. (2008) prepared the tweezers of Scheme 1.41, which are especially oriented for chiral recognition of guest enantiomers. The tweezers accommodate a combination of three different functional groups such as a chromophore (azophenol dye), binding moieties (two thiourea groups), and a chiral barrier from two glucopyranosyl units. Accepting organic anions, the tweezers experience a large bathochromic shift (up to 150 nm in the ultraviolet spectra) and change their color.



Scheme 1.39 Structures of dicyanomethylene benzofluorene guest and tweezers



Scheme 1.40 Molecular rearrangement of pyridinone confined by tweezers upon photoexcitation



Scheme 1.41 Molecular recognition of phenylpropionic acid enantiomers by tweezers

This bathochromic shift can be attributed to deprotonation of the azophenol fragment (left part of Scheme 1.41). The deprotonation can provoke photoinduced charge transfer. The chiral carboxylate anions showed larger association constants for (*S*)-enantiomers (K_S) than those (K_R) for (*R*)-enantiomers. 2-Phenylpropionic acid, shown as a guest in Scheme 1.41, demonstrates a ratio $K_S/K_R = 2.95$. The tweezers

considered also displayed moderate selectivity (3.60) for the (*S*)-enantiomer over the (*R*)-enantiomer of naproxen (Choi et al. 2008). Naproxen is 2-(6-methoxynaphth-2-yl)propionic acid. Naproxen is administrated as a nonsteroidal anti-inflammatory drug. For its (*S*)-enantiomer, pharmacological activity is greater compared with that of the (*R*)-enantiomer.

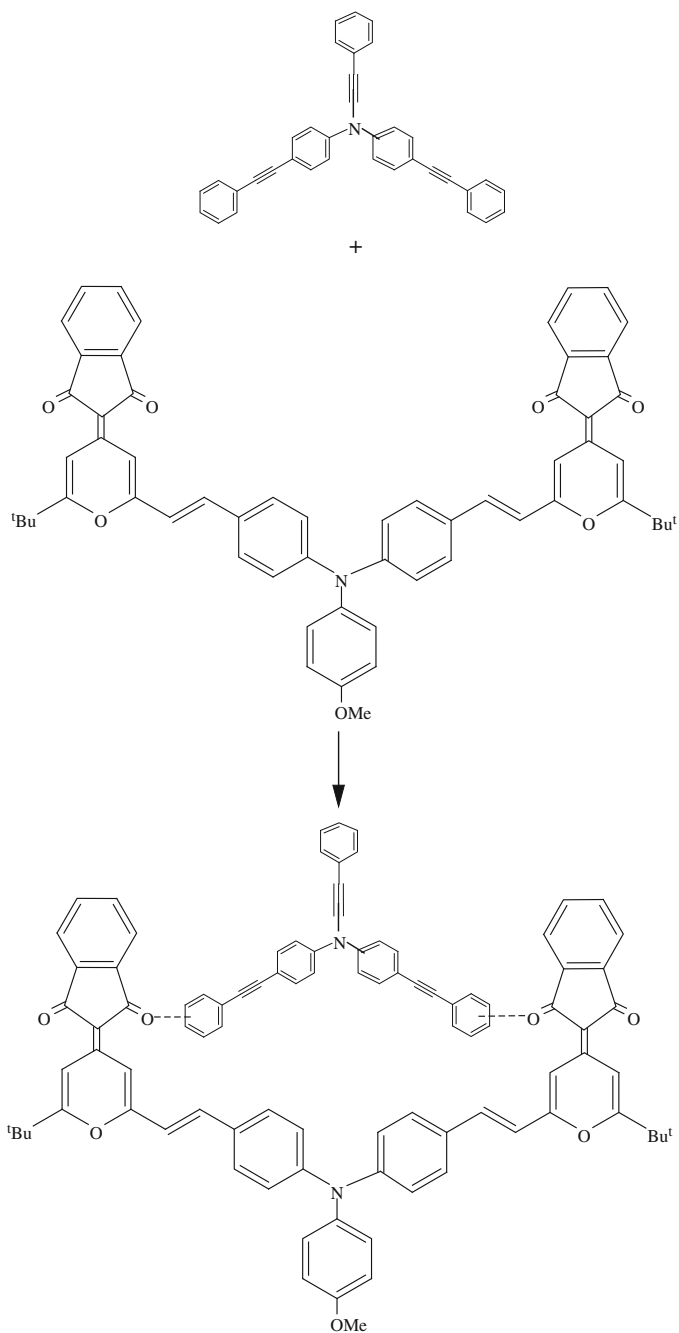
On inclusion in a tweezers-like complex, an organic compound can change its polarizability. This problem is as important for academia as it is for use of the technique. Xiao et al. (2008) presented an example of this change. Organic light-emitting devices have attracted much attention owing to their advantages of low power consumption, high brightness, and strong contrast. All these properties are needed for applications in color flat-panel displays. Regrettably, for full color, some deficit is observed in the red color components. The pyrrolidinyll indandione derivative of Scheme 1.42 does emit red light, but its brightness is insufficient.

To enhance the brightness, formation of a charge-transfer complex was performed using tris(diphenylacetylenyl)amine as donor. Note that the acetylene fragment is a straight rod; it cannot be bent. The confining (acceptor) indanedione molecule has a hollow similar to tweezers. Due to the rigid structure of the donor, it enters the hollow as it is. Donor-to-acceptor charge transfer takes place. This increases the polarizabilities of both constituents and markedly enhances the emitted brightness to the level needed. The confinement and charge-transfer phenomena are depicted in Scheme 1.42 (Xiao et al. 2008).

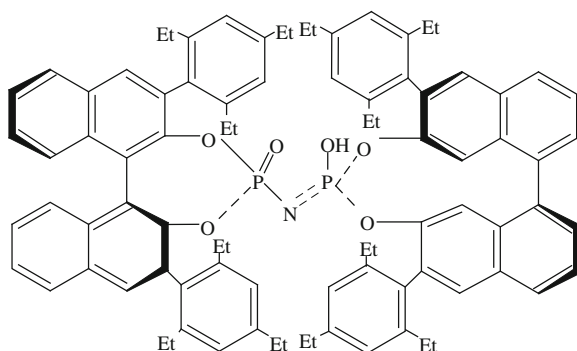
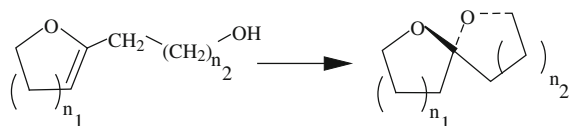
Of course, geometrical compatibility is crucial for a guest to be clamped by tweezers. Thus, resorcinol is clamped by the pyridine arms connected with the 1,2,4,5-benzenediimide system over its surface. In the case of 1,7-naphthalenediol, complexation of the two guest molecules takes place by turning the pyridine arms over so that each arm is above or below the 1,2,4,5-benzenediimide system surface and is H-bonded with 7-hydroxyl of 1,7-naphthalenediol (Rasberry et al. 2008).

The requirement for geometrical guest–tweezers compatibility opens ways for improvement of many organic syntheses; For instance, spiroacetalization of enol cyclic ethers upon action of phosphoric acid typically proceeds with relatively large substrates only. Small substrates are not good for this reaction due to insufficient interactions with the phosphoric acid catalyst. Coric and List (2012) included a phosphoric acid derivative (namely, the imidodiphosphoric acid fragment) in the basic axle of the tweezers, as depicted in the bottom line of Scheme 1.43. This hidden catalyst possesses an extremely demanding chiral environment. It is ineffective for large substrates, but with small ones ($n_1 = 1-3$, $n_2 = 1, 2$) yields of the spiroacetals are 62–89% with enantioselectivity of 96–99%. The spiroacetalization under consideration is shown by the upper equation of Scheme 1.43. The catalyst from Coric and List (2012) has understandable difficulties in handling relatively large substrates, which do not fit into the catalytic cavity.

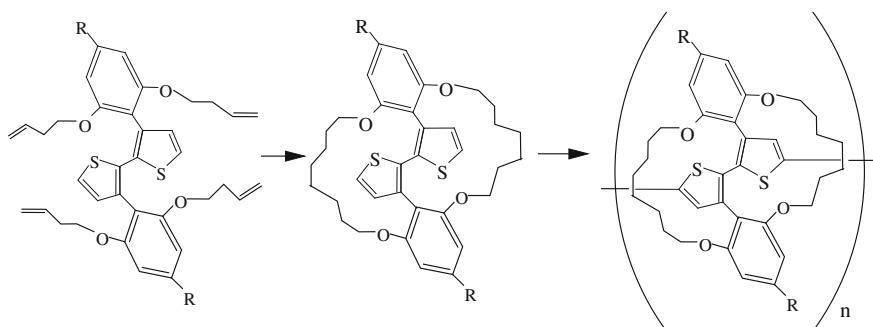
Another principal example concerns a synthetic strategy that has been implemented to prepare a unique three-dimensional architecture that resembles rotaxanes, but the “ring” and the “axis” are covalently connected with the molecular carcass. Scheme 1.44 presents the main phases of the five-step synthesis. The final product was obtained with ca. 60% yield. Each unit of the resulting polythiophene backbone



Scheme 1.42 Charge-transfer confinement of tris(diphenylethynyl) amine with pyrrolidinyliodonium by tweezers



Scheme 1.43 Stereospecificity of alkanole-heterocycle spiroacetalization upon confinement by tweezers



Scheme 1.44 Main route in formation of polythiophene confined in its own cyclic side chain

is actually confined in its own cyclic side-chain. This prevents π - π stacking interaction between the backbones even in the solid state. The polythiophene backbone exhibits extended π -electron delocalization, sheathed within defect-free “insulated” layers. Such a confined polymer intrinsically has excellent intrachain hole mobility (Sugiyasu et al. 2010).

1.9 Dendrimers as Hosts

Dendrimers are highly branched globular molecules which are generally well defined, effectively monodispersed, and symmetric. Simplistically, these molecules can be regarded as uniformly sized, globular objects, in which the hyperbranched arms

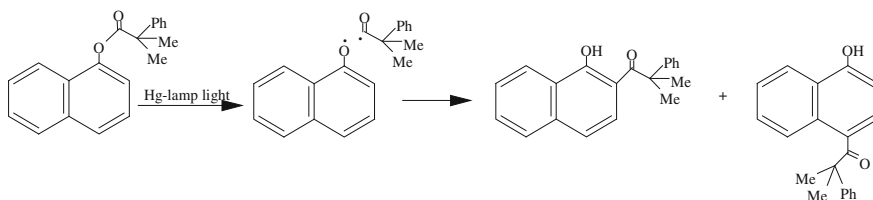
efficiently fill space around the molecular core. A dendrimer is composed of three structural regions: a main chain, branched repeating units derived from the core, and groups on the periphery of the molecule. These regions provide an interior space that is sterically protected from solvent molecules and can accommodate small organic molecules and control their release from the cavities. Noncovalent (inside the cavities of dendrimers) and covalent attachment (to the outer terminal groups of dendrimers) are used to deliver drugs in chemotherapy. The drug-filled dendrimers have the same size as serum protein and hence are capable of directly entering the microvasculature. These nanocarriers are efficient in reducing drug leakage, hemolytic toxicity, and renal filtration while raising in vivo stability and biocompatibility.

Thus, the poorly water-soluble anticancer drug 10-hydroxycamptothecin was encapsulated within biodendrimer composed from poly(glycerol-sodium succinate). This dendrimer is biocompatible and degradable in vivo to natural metabolites. The formulation acquired good aqueous solubility. Cytotoxicity assays of this drug with human breast cancer cells showed a significant reduction in the viability of tumor cells. The drug retains its anticancer activity even upon encapsulation within the dendritic nanocarrier (Carnahan and Grinstaff 2001; Morgan et al. 2003).

The interactions between dendrimers and organics can be subdivided into the following three types: internal encapsulation (involving physical encapsulation, hydrophobic interaction, and hydrogen bonding), external electrostatic interaction, and covalent conjugation. Whereas covalent conjugation, physical encapsulation, hydrophobic interaction, and hydrogen bonding have already been considered as confining factors, external electrostatic interaction deserves to be independently illustrated. Beeby et al. (2002) studied the interaction between 1,4-dimethoxybenzene or related oligomers with a dendrimer containing tetrathiafulvalene end groups. No confinement takes place when the tetrathiafulvalene termini remain neutral. To confine the guest, it was sufficient to transform those terminal groups into the cation-radical state. (Tetrathiafulvalene cation-radicals are very stable.)

The loading/encapsulating ability of a dendrimer depends not only on the properties of the organic guest molecule, but also on the dendrimer architecture. Dendrimers with more hydrophobic repeated units or cavities can encapsulate more neutral and hydrophobic participants in their interior rather than adsorb them on the surface. Last but not least, the aggregation into assembled clusters due to dendrimer–dendrimer interactions provides micelle-like combinations with a specific opportunity to encapsulate organic reactant pairs.

Two specific host–guest dendrimeric copolymers should be mentioned here; for both of them, the applicative importance was foretold. Firstly, a dendrimer was formed by an adamantane dimer and two β -cyclodextrin trimers in aqueous solution (Galantini et al. 2008). Secondly, oligoethyleneamine dendrons bond to a β -cyclodextrin core via 1,2,3-triazole linkers (Srinivasachari et al. 2008). While the dendritic wings can act as tweezers, the β -cyclodextrin hydrophobic cup can be exploited to host adamantane groups substituted with poly(ethylene glycol) chains to increase the stability against aggregation, increase the circulation lifetime of administered drugs, and/or enable tissue-specific targeting of nanoparticles for enhanced therapeutic selectivity and specificity.



Scheme 1.45 Photolysis of naphthyl phenacyl ester confined in poly(alkyl aryl ether) dendrimer

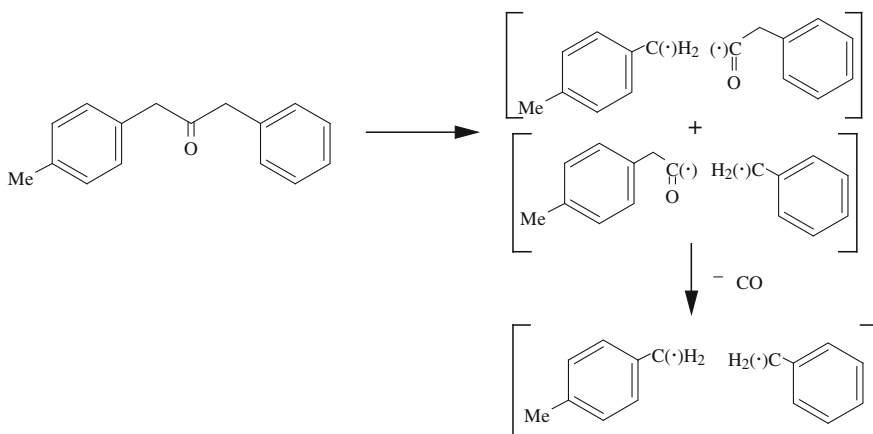
Kaanumalle et al. (2004) explored poly(alkyl aryl ether) dendrimers as hosts for 1-naphthyl phenacyl ester as a guest. Photolysis of the host–guest aggregate in aqueous dendrimer media results in the formation of the radical pair depicted in Scheme 1.45.

Recombination of the radicals proceeds within the dendrimer and, as seen from Scheme 1.45, leads to only two products. When photolysis of the same guest is performed in hexane without a dendrimer host, seven different products of radical recombination are formed (Kaanumalle et al. 2004). Thus, reaction within the dendrimer cage proceeds much more selectively. Under the cage protection the formed radical pair remains encapsulated, its mobility is reduced, and the two moieties can better recombine.

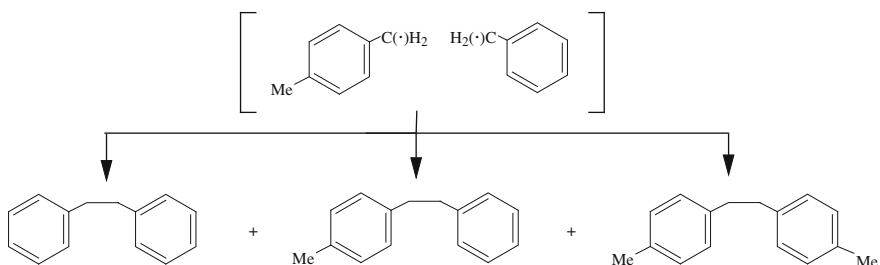
Similar results were obtained from photolysis (450-W Hg lamp) of 1-phenyl-3-(4-methylphenyl)-propan-2-one. Homolysis takes place between the carbonyl part and one of the adjacent methylene groups according to Scheme 1.46 (Natarajan et al. 2011).

In hexane without a dendrimer, carbonyl-containing radicals are unstable and expel carbon monoxide so that only diaryl ethanes are eventually formed (Scheme 1.47).

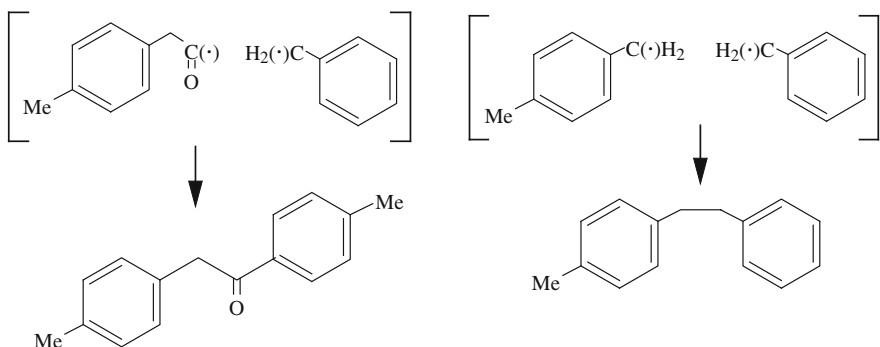
In basic aqueous solution of poly(alkyl aryl ether) dendrimer of third generation (C_5G_3), the carbonyl-containing radicals were stabilized and the final products turned



Scheme 1.46 Homolysis of phenyl (methylphenyl) propanone upon photoexcitation



Scheme 1.47 Diarylethane formation from phenyl (methylphenyl) propanone during photolysis



Scheme 1.48 Phenyl (methylphenyl) propanone photolytic transformation upon control with poly(alkyl aryl ether) dendrimer

out to be the aryl benzyl ketone and diaryl ethane of Scheme 1.48 (Natarajan et al. 2011).

Natarajan et al. (2011) studied photochemical isomerization of *trans*-stilbene incorporated into poly(alkyl aryl ether) dendrimers in aqueous solutions. Direct irradiation in the region of *trans*-stilbene absorption led to *trans* → *cis* isomerization and, what is more, to the formation of phenanthrene in considerable amounts. For successful cyclization, the linker lengths constituting the dendrimer must be increased, which provides deeper penetration of the guest into an inner part of the tweezers. As a rule, dendrimers with longer linkers afford higher rigidities to reactive intermediates. This reduces the “leakiness” of intermediates to the bulk environment, facilitating product formation with high selectivity.

Dendrimers are often considered to be “stable static unimolecular micelles.” Kaanumalle et al. (2004) performed photolysis of 1-naphthyl phenacyl ester in water micelle with sodium dodecyl sulfate. In this case, homolysis proceeds less selectively than for the reaction within dendrimers. Consequently, dendrimeric media offer much better confinement than the micelles.

1.10 Closing Remarks

This chapter has presented plenty of cavitands that differ by their internal volume and depth, complexation–decomplexation equilibrium, molecular recognition ability, and the very driving forces for encapsulation. This varied picture was used to analyze the behavior of encapsulated organic and organometallic compounds, and their stereochemical changes and reactivity. The outcome of encapsulation consists in the unpredictable formation of reaction products and stabilization of intermediates which were unthinkable as independent species in routine chemistry. It should also be underlined that encapsulation of medications confers them solubility in water, enhances their bioavailability, and prolongs their periods of action. Thus, use of cucurbit[7]uril to encapsulate temozolomide leads to a 400 % increase in the activity of the drug against glioblastoma multiforme cancer cells. Furthermore, the stabilization of the drug in the complex with cucurbit[7]uril enhances the propensity of the drug to cross the blood–brain barrier and its adsorption into cells, thereby increasing its efficacy for this kind of chemotherapy (Appel et al. 2012). All these features permit a decrease of administered drug doses and their undesirable side-effects.

References

- Adjami, D., & Rebek, J. (2007). *Proceedings of the National Academy of Sciences of the United States of America*, 104, 16000.
- Adjami, D., & Rebek, J. (2009). *Nature Chemistry*, 1, 87.
- AlHujran, T. A., Dawe, L. N., & Georghiou, P. E. (2012). *Organic Letters*, 14, 3530.
- Al-Sou'od, Kh. A. (2008). *Journal of Solution Chemistry*, 37, 119.
- Amajjahe, S., & Ritter, H. (2008). *Macromolecules*, 41, 716.
- Amorini, A. M., Bellia, F., Di Pietro, V., Giardina, B., La Mendola, D., Lazzarino, G., et al. (2007). *European Journal of Medicinal Chemistry*, 42, 910.
- Appel, E. A., Rowland, M. J., Loh, X.-J., Heywod, R. M., Wattas, C., & Scherma, O. A. (2012). *Chemical Communications*, 48, 9843.
- Asfari, Z., Boehmer, V., Harrowfield, J., & Vicens, J. (Eds.). (2001). *Calixarenes*. Kluwer, Dordrecht.
- Bakirci, H., Koner, A/L., Schwarzlose, Th., & Nau, W.M. (2006). *Chemistry: A European Journal*, 12, 4799.
- Bakovets, V. V., Masliy, A. N., & Kuznetsov, A. M. (2008). *Journal of Physical Chemistry B*, 112, 12010.
- Becuwe, M., Cazier, F., Bria, M., Woisel, P., & Delattre, F. (2007). *Tetrahedron Letters*, 48, 6186.
- Beeby, A., Bryce, M. R., Christensen, Ch., Cooke, C., Duclairoiroir, F. M. A., & Rotello, V. M. (2002). *Chemical Communications*, 24, 2950.
- Behrend, R., Meyer, E., & Rusche, F. (1905). *Liebigs Annalen der Chemie*, 339, 1.
- Ben Shir, I., Sasmal, S., Mejuch, T., Sinha, M. K., Kapon, M., & Keinan, E. (2008). *Journal of Organic Chemistry*, 73, 8772.
- Berbeci, L. S., Wang, W., & Kaifer, A. E. (2008). *Organic Letters*, 10, 3721.
- Bertolla, C., Rolin, S., Evrard, B., Pochet, L., & Masereel, B. (2008). *Bioorganic & Medicinal Chemistry Letters*, 18, 1855.
- Brahma, S., Iqbal, S. A., Dey, S., & Rath, S. P. (2012). *Chemical Communications*, 48, 4070.
- Branchi, B., Balzani, V., Ceroni, P., Kuchenbrandt, M. C., Klaerner, F.-G., Blaeser, D., et al. (2008). *Journal of Organic Chemistry*, 73, 5839.

- Breslow, R., & Campbell, P. (1969). *Journal of the American Chemical Society*, *91*, 3085.
- Brinker, U. H., & Miesset, J.-L. (Eds.). (2010). *Molecular encapsulation. Organic reactions in confined system*. Hoboken, NJ: Wiley.
- Caballero, J., Zamora, C., Aguayo, D., Yanez, C., & Gonzalez-Nilo, F. D. (2008). *Journal of Physical Chemistry B*, *112*, 10194.
- Cao, D., Kou, Y., Liang, J., Chen, Zh., Wang, L., & Meier, H. (2009). *Angewandte Chemie International Edition*, *48*, 9721.
- Carlqvist, P., & Maseras, F. (2007). *Chemical Communications*, 748.
- Carnahan, M. A., & Grinstaff, M. W. (2001). *Macromolecules*, *34*, 7648.
- Cavarzan, A., Scarso, A., Sgarbossa, P., Strukul, G., & Reek, J. N. H. (2011). *Journal of the American Chemical Society*, *133*, 2848.
- Chan, W.-K., Yu, W.-Y., Che, Ch-M., & Wong, M.-K. (2003). *Journal of Organic Chemistry*, *68*, 6576.
- Chen, J. Y.-C., Jayaraj, N., Jockusch, S., Ottaviani, M. F., Ramamurthy, V., & Turro, N. J. (2008). *Journal of the American Chemical Society*, *130*, 7206.
- Chen, B., Liu, K. L., Zhang, Zh., Ni, X., Goh, S. H., & Li, J. (2012). *Chemical Communications*, *48*, 5638.
- Chernikova, E., Berdnikova, D., Fedorov, Yu., Fedorova, O., Peregudov, A., & Isaacs, L. (2012). *Chemistry Communications*, *48*, 7256.
- Choi, M. K., Kim, H. N., Choi, H. J., Yoon, J., & Hyun, M. H. (2008). *Tetrahedron Letters*, *49*, 4522.
- Contino, A., Cucinotta, V., Giuffrida, A., Maccarrone, G., Messina, M., Puglisi, A., & Vecchio, G. (2008). *Tetrahedron Letters*, *49*, 4765.
- Coric, I., & List, B. (2012). *Nature*, *483*, 315.
- Coulston, R. J., Jones, S. T., Lee, T.-Ch., Appel, E. A., & Scherman, O. A. (2011). *Chemical Communications*, *47*, 164.
- Cram, D. J., & Cram, J. M. (1994). *Container Molecules and Their Guests*. Cambridge, UK: The Royal Society of Chemistry.
- Cram, D. J., Tanner, M. E., & Thomas, R. (1991). *Angewandte Chemie International Edition*, *30*, 1024.
- Dai, F.-R., & Wang, Zh. (2012). *Journal of the American Chemical Society*, *134*, 8002.
- Dearden, D. V., Ferrell, T. A., Asplund, M. C., Zilch, L. W., Julian, R. R., & Jarrold, M. F. (2009). *Journal of Physical Chemistry A*, *113*, 989.
- Dodziuk, H. (Ed.). (2008). *Cyclodextrins and their complexes*. Weinheim, Germany: Wiley-VCH.
- Dsouza, R. N., & Nau, W. M. (2008). *Journal of Organic Chemistry*, *73*, 5305.
- Dube, H., Rebek, J. (2012). *Angewandte Chemie International Edition*, *51*, 3207.
- Dumanski, P. G., Easton, C. J., Lincoln, C. F., & Simpson, J. S. (2003). *Australian Journal of Chemistry*, *56*, 1107.
- Easton, C. J., & Lincoln, S. F. (1999). *Modified cyclodextrins, scaffolds and templates for supramolecular chemistry*. London, UK: Imperial College Press.
- Echezarreta-Lopez, M. M., Otereo-Mazoy, I., Ramirez, H. L., Villalonga, R., & Torres-Labandeira, J. J. (2008). *Current Drug Discovery Technologies*, *5*, 140.
- Fan, Zh., Diao, Ch.-H., Guo, M.-J., Du, R.-J., Song, Yu.-F., Jing, Z.-L., et al. (2007). *Carbohydrate Research*, *342*, 2500.
- Florea, M., & Nau, W. N. (2011). *Angewandte Chemie International Edition*, *50*, 9338.
- Fowler, D. A., Teat, S. J., Baker, G. A., & Atwood, J. L. (2012). *Chemical Communications*, *48*, 5262.
- Freeman, W. A., Mock, W. L., & Shih, N.-Y. (1981). *Journal of the American Chemical Society*, *103*, 7367.
- Gadde, S., Batchelor, E. K., Weiss, J. P., Ling, Y., & Kaifer, A. E. (2008). *Journal of the American Chemical Society*, *130*, 17114.
- Galantini, L., Jover, A., Leggio, C., Meijide, F., Pavel, N. V., Tellini, V. H. S., et al. (2008). *Journal of Physical Chemistry B*, *112*, 8536.

- Gao, Ch., Silvi, S., Ma, X., Tian, H., Venturi, M., & Credii, A. (2012). *Chemical Communications*, 48, 7577.
- Gibb, C. L. D., & Gibb, B. C. (2004). *Journal of the American Chemical Society*, 126, 11408.
- Gibb, C. L. D. & Gibb, B. C. (2011). *Journal of the American Chemical Society* 133, 7344.
- Gonzalez-Romero, E., Fernandez-Calvar, B., & Bravo-Diaz, C. (2004). *Progress in Colloid and Polymer Science*, 123, 131.
- Goto, K., Holler, M., & Okazaki, R. (1997). *Journal of the American Chemical Society*, 119, 1460.
- Granero, G. E., Maitre, M. M., Garnero, C., & Longhi, M. R. (2008). *European Journal of Medicinal Chemistry*, 43, 464.
- Guisnet, M., & Gilson, J.-P. (2002). *Zeolites for cleaner technologies*. London, UK: Imperial College Press.
- Guo, D-Sh., Wang, L.-H., & Liu, Y. (2007). *Journal of Organic Chemistry*, 72, 7775.
- Guo, M., Jiang, M., & Zhang, G. (2008). *Langmuir*, 24, 10583.
- Gupta, Sh., Choudhury, R., Krois, D., Brinker, U. H., & Ramamurthy, V. (2012). *Journal of Organic Chemistry*, 77, 5155.
- Gutsche, C. D. (1989). *Calixarenes*. Cambridge, UK: The Royal Society of Chemistry.
- Gutsche, C. D. (1998). *Calixarenes revisited*. Cambridge, UK: The Royal Society of Chemistry.
- Han, G. W., Lee, J. Y., Song, H. K., Chang, Ch., Min, K., Moon, J., et al. (2001). *Journal of Molecular Biology*, 308, 263.
- Han, Ch., Yu, G., Zheng, B., & Huang, F. (2012). *Organic Letters*, 14, 1712.
- Harada, A., Osaki, M., & Yamaguchi, H. (2008). *Accounts of Chemical Research*, 41, 1143.
- He, Y., & Shen, X. (2008). *Journal of Photochemistry and Photobiology*, 197, 253.
- Hedges, A. R. (1998). *Chemical Reviews*, 98, 2035.
- Herrmann, W., Wehrle, S., & Wenz, G. (1997). *Chemical Communications*, 18, 1709.
- Huang, W.-H., Zavalij, P. V., & Isaacs, L. (2008). *Journal of the American Chemical Society*, 130, 8446.
- Isaacs, L. (2009) *Chemical Communications*, 6, 619.
- Isaacs, L., Park, S.-K., Liu, S., Ko, Y. H., Selvapalam, N., Kim, Y., et al. (2005). *Journal of the American Chemical Society*, 127, 18000.
- Ivanov, P. M., & Jaime, C. (2004). *Journal of Physical Chemistry B*, 108, 6261.
- Jeon, W. S., Kim, H. J., Lee, C., & Kim, K. (2002). *Chemical Communications*, 1828.
- Jeon, W. S., Moon, K., Park, S. H., Chun, H., Ko, Y. H., Lee, J. Y., et al. (2005). *Journal of the American Chemical Society*, 127, 12984.
- Jiang, W., Ajami, D., & Rebek, J. (2012). *Journal of the American Chemical Society*, 134, 8070.
- Jog, P. V., & Gin, M. S. (2008). *Organic Letters*, 10, 3693.
- Jon, S. Y., Ko, Y. H., Park, S. H., Kim, H.-J., & Kim, K. (2001) *Chemical Communications*, 19, 1938.
- Jullian, C., Orosteguis, T., Perez-Cruz, F., Sanches, P., Mendizabal, F., & Olea-Azar, C. (2008). *Spectrochimica Acta Part A*, 71, 269.
- Kaanumalle, L. S., Nithyanandhan, J., Pattarbiraman, M., Jayaraman, N., & Ramamurthy, V. (2004). *Journal of the American Chemical Society*, 126, 8999.
- Kaifer, A. E., Li, W., Silvi, S., & Sindelar, V. (2012). *Chemical Communications*, 48, 6693.
- Kalmar, J., Ellis, Sh. B. & Halterman, R. L. (2012). *Organic Letters*, 14, 3248.
- Kang, J., & Rebek, J. (1997). *Nature*, 385, 50.
- Kano, K., Mori, K., Uno, B., Goto, M., & Kubota, T. (1990). *Journal of the American Chemical Society*, 112, 8645.
- Kikuzawa, A., Kida, T., & Akashi, M. (2007). *Organic Letters*, 9, 3909.
- Kikuzawa, A., Kida, T., & Akashi, M. (2008). *Macromolecules*, 41, 3393.
- Kim, K., Ko, Y. H., & Selvapalam, N. (2011). *Cucurbiturils: Chemistry, supramolecular chemistry and applications*. London, UK: Imperial College Press.
- Koner, A. L., Marquez, C., Dickman, M. N., & Nau, W. M. (2011). *Angewandte Chemie International Edition*, 50, 545.

- Kusmin, A., Lechner, R. E., Kammel, M., & Saenger, W. (2008). *Journal of Physical Chemistry B*, *112*, 12888.
- Lagona, J., Mukopadhyay, P., Chakrabarti, S., & Isaacs, L. (2005). *Angewandte Chemie*, *117*, 4922; *Angewandte Chemie International Edition*, *44*, 4844.
- Lalor, R., Bailie-Johnson, H., Redshaw, C., Mathews, S. E., & Mueller, A. (2008). *Journal of the American Chemical Society*, *130*, 2892.
- Leclercq, L., & Schmitzer, A. R. (2009). *Journal of Physical Organic Chemistry*, *22*, 91.
- Lee, J. W., Samal, S., Selvapalam, N., Kim, H.-J., & Kim, K. (2003). *Accounts of Chemical Research*, *36*, 621.
- Li, S., & Purdy, W. C. (1992). *Chemical Reviews*, *92*, 1457.
- Li, L., Cui, G., Zhao, M., Wang, H., Li, W., & Peng, Sh. (2008). *Journal of Physical Chemistry B*, *112*, 12139.
- Li, Ch., Shu, X., Li, J., Chen, S., Han, K., Xu, M., et al. (2011a). *Journal of Organic Chemistry*, *76*, 8458.
- Li, W.-W., Claridge, Th. D. W., Li, Q., Wormald, M. R., Davis, B. G., & Bayley, H. (2011b). *Journal of the American Chemical Society*, *133*, 1987.
- Liu, L., Li, X.-S., Mu, T.-W., Guo, Q.-X., & Liu, Y.-Ch. (2000). *Journal of Inclusion Phenomena and Macrocyclic Chemistry*, *38*, 199.
- Liu, W., Zhang, Y., & Gao, X. (2007a). *Journal of the American Chemical Society*, *129*, 4973.
- Liu, Y., Li, X.-Y., Zhang, H.-Y., Li, Ch.-Y., & Ding, S. (2007b). *Journal of Organic Chemistry*, *72*, 3640.
- Liu, Y., Yang, Z.-X., & Chen, Y. (2008a). *Journal of Organic Chemistry*, *73*, 5298.
- Liu, Y., Yu, Zh.-L., Zhang, Y.-M., Guo, D.-Sh., & Liu, Y.-P. (2008b). *Journal of the American Chemical Society*, *130*, 10431.
- Liu, J.-H., Hung, H.-J., & Harada, A. (2008c). *Langmuir*, *24*, 7442.
- Liu, X. L., Wei, M., Wang, Zh. L., Evans, D. G., & Duan, X. (2008d). *Journal of Physical Chemistry C*, *112*, 17517.
- Lopez, O. L., Marinescu, L., & Bols, M. (2007). *Tetrahedron*, *63*, 8872.
- Luo, L., Liao, G.-H., Wu, X.-L., Lei, L., Tung, Ch.-H., & Wu, L.-Zh. (2009). *Journal of Organic Chemistry*, *74*, 3506.
- Ma, Y., Chi, X., Yan, X., Liu, J., Yao, Y., Chen, W., et al. (2012). *Organic Letters*, *14*, 1532.
- Mandolini, L., & Ungaro, R. (Eds.). (2000). *Calixarenes in actions*. London, UK: Imperial College Press.
- Marinescu, L., Molbach, M., Rousseau, C., & Bols, M. (2005). *Journal of the American Chemical Society*, *127*, 17578.
- Marquez, C., Hudgins, R. R., & Nau, W. N. (2004). *Journal of the American Chemical Society*, *126*, 5806.
- Mecozzi, S., & Rebek, J. (1998). *Chemistry: A European Journal*, *4*, 1016.
- Menand, M., & Jabin, I. (2009). *Organic Letters*, *11*, 673.
- Miskolczy, Zs, Biczok, L., Megyesi, M., & Jablonikai, I. (2009). *Journal of Physical Chemistry B*, *113*, 1645.
- Mock, W. L., Irra, T. A., Wepsiec, J. P., & Adhya, M. J. (1989). *Journal of Organic Chemistry*, *54*, 5302.
- Moghaddam, S., Inoue, Y., Gilson, M. K. (2009). *Journal of the American Chemical Society*, *131*, 4012.
- Moghaddam, S., Yang, Ch., & Rekharsky, M. (2011). *Journal of the American Chemical Society*, *133*, 3570.
- Mohanty, J., Bhasikuttan, A. C., Choudhury, Sh. D., Pal, H. (2008). *Journal of Physical Chemistry B Letters 1-2*, 10782.
- Morgan, M. T., Carnahan, M. A., Imoos, C. E., Ribeiro, A. A., Finkelstein, S., Lee, S. J., et al. (2003). *Journal of the American Chemical Society*, *125*, 15485.
- Naidoo, K. J., Gamieldeen, V. R., Chen, J. Y.-J., Widmalm, G., & Maliniak, A. (2008). *Journal of Physical Chemistry B*, *112*, 15151.

- Narender, M., Reddy, M. S., Krishnaveni, N. S., Surendra, K., Nageswar, Y. V., & Rao, K. R. (2006). *Synthetic Communications*, 36, 1463.
- Natarajan, B., Gupta, Sh., Ramamurthy, V., & Jayaraman, N. (2011). *Journal of Organic Chemistry*, 76, 4018.
- Neta, P., Huie, P., & Rose, A. B. (1988). *Journal of Physical and Chemical Reference Data*, 17, 1027.
- Nogueiras-Nieto, L., Alvarez-Lorenzo, C., Sandez-Macho, I., Concheiro, A., & Otero-Espinar, F. J. (2009). *Journal of Physical Chemistry B*, 113, 2773.
- Ogoshi, T., Kanai, S., & Fujinami, Sh. (2008). *Journal of the American Chemical Society*, 130, 5022.
- Ogoshi, T., & Ueshima, N. (2012). *Chemical Communications*, 48, 3536.
- Ong, W., Gomez-Kaifer, M., & Kaifer, A. E. (2002). *Organic Letters*, 4, 1791.
- Park, J. W., Lee, S. Y., Song, H. J., & Park, K. K. (2005). *Journal of Organic Chemistry*, 70, 9505.
- Parthasarathy, A., Kaanumalle, L. S., & Ramanurthy, V. (2007). *Organic Letters*, 9, 5059.
- Pitchumani, K., Velusamy, P., Banu, H. S., & Srinivasan, C. (1995). *Tetrahedron Letters*, 36, 1149.
- Podkoscielny, D., Hooley, R. J., Rebek, J., & Kaifer, A. E. (2008). *Organic Letters*, 10, 2865.
- Polovyanenko, D. N., Marque, S. R. A., Lambert, S., Jicsinszky, L., Plysnin, V. F., & Bagryanskaya, E. G. (2008). *Journal of Physical Chemistry B*, 112, 13157.
- Porel, V., Jockusch, S., Parthasarathy, A., Rao, V. J., Turro, N. J., & Ramamurthy, V. (2012). *Chemical Communications*, 48, 2710.
- Praetorius, A., Bailey, D. M., Schwarzlose, Th., & Nau, W. V. (2008). *Organic Letters*, 10, 4089.
- Radozkowicz, L., Project, E., Gepshtein, R., Nachliel, E., Huppert, D., & Gutman, M. (2008). *Zeitschrift für Physikalische Chemie*, 222, 1247.
- Rafati, A. A., & Safatian, F. (2008). *Physics and Chemistry of Liquids*, 46, 587.
- Raspberry, R. D., Smith, M. D., & Shimizu, K. D. (2008). *Organic Letters*, 10, 2889.
- Rawashdeh, A. M., Mizyed, Sh., Mahmoud, S., & Marji, D. (2008a). *Spectrochimica Acta Part A*, 71, 562.
- Rawashdeh, A. M. M., Thangavel, A., Sotiriou-Leventis, Ch., & Leventis, N. (2008b). *Organic Letters*, 10, 1131.
- Rebek, J. (2005). *Angewandte Chemie International Edition*, 44, 2068.
- Rekharsky, M. V., Mori, T., Yang, C., Ko, Y. H., Selvapalam, N., Kim, H., et al. (2007). *Proceedings of the National Academy of Sciences of the United States of America*, 104, 20737.
- Robbins, T. A., & Cram, D. J. (1993). *Journal of the American Chemical Society*, 115, 12199.
- Rodriguez-Lucena, D., Beniti, J. M., Alvarez, E., Jaime, C., Perez-Miron, J., Mellet, C. O., et al. (2008). *Journal of Organic Chemistry*, 73, 2967.
- Sabadini, E., do Carmo Egidio, F., Fujiwara, F.Y., & Cosgrove, T. (2008). *Journal of Physical Chemistry B*, 112, 3328.
- Saleh, N., Koner, A. L., & Nau, W. M. (2008). *Angewandte Chemie International Edition*, 47, 5398.
- Senler, S., Cui, L., Broomes, A. M., Smith, E. L., Wilson, J. N., & Kaifer, A. E. (2012). *Journal of Physical Organic Chemistry*, 25, 592.
- Shin, J.-A., Lim, Y.-G., & Lee, K.-H. (2012). *Journal of Organic Chemistry*, 77, 4117.
- Shirakawa, S., & Shimizu, Sh. (2008). *SYNLETT*, 10, 1539.
- Sliwa, W., & Kozlowski, C. (2009). *Calixarenes and resorcinarenes: Synthesis, properties and applications*. Weinheim, Germany: Wiley.
- Sobransingh, D., & Kaifer, A. E. (2006). *Organic Letters*, 8, 3247.
- Son, Y.-A., Kim, B.-S., Choi, M.-S., & Kim, S.-H. (2007). *Dyes Pigments*, 75, 283.
- Srinivasachari, S., Fichter, K., & Reineke, Th. M. (2008). *Journal of the American Chemical Society*, 130, 4618.
- Stanier, C. A., O'Connell, M. J., Clegg, W., & Anderson, H. L. (2001). *Chemical Communications*, 5, 493.
- Stano, P., & Luisi, P. L. (2010). In U. H. Brinker, & J.-L. Miesusset (Eds.), *Molecular encapsulation. Organic reactions in constrained systems* (pp. 454–491). Chichester, UK: Wiley.
- St-Jacques, A. D., Wyman, I. W., & Macartney, D. H. (2008) *Chemical Communications*, 40, 4936.

- Stuart, M. C. A., & Engberts, J. B. F. N. (2010). In U. H. Brinker & J.-L. Mieusset (Eds.), *Molecular encapsulation. Organic reactions in constrained systems* (pp. 421–454). Chichester, UK: Wiley.
- Sugiyasu, K., Honsho, Yo, et al. (2010). *Journal of the American Chemical Society*, *132*, 14754.
- Sun, H., Gibb, C. L. D., & Gibb, B. C. (2008). *Supramolecular Chemistry*, *20*, 141.
- Suzaki, Yu., Taira, T., & Osakada, K. (2010). *Bulletin of The Chemical Society of Japan*, *83*, 378.
- Szejtli, J. (1998). *Chemical Reviews*, *98*, 1743.
- Tachikawa, T., Tojo, S., Fujitsuka, M., & Majima, T. (2005). *Journal of Physical Chemistry B*, *109*, 17460.
- Taira, T., Ajami, T., & Rebek, J. (2012). *Chemical Communications*, *48*, 8508.
- Tanaka, K., Fujiwara, T., & Urbanczyk-Lipkowska, Z. (2002). *Organic Letters*, *4*, 3255.
- Tang, H., Fuentealba, D., Ko, Y. H., Selvapalam, N., Kim, K., & Bohne, C. (2011). *Journal of the American Chemical Society*, *133*, 20623.
- Tang, H., & Santos de Oliveira, C. (2012). *Journal of the American Chemical Society*, *134*, 5544.
- Tee, O. S., Gadosy, T. A., & Giorgi, J. B. (1993). *Journal of the Chemical Society, Perkin Transactions*, *2*, 1705.
- Terao, J., Tsuda, S., Tanaka, Yu., Okoshi, K., Fujihara, T., et al. (2009). *Journal of the American Chemical Society*, *131*, 16004.
- Terao, J., Kimura, K., Seki, Sh., Fujihara, T., & Tsuji, Ya. (2012). *Chemical Communications*, *48*, 1577.
- Thangavel, A., Sotiriou-Leventis, Ch., Dawes, R., & Leventis, N. (2012). *Journal of Organic Chemistry*, *77*, 2263.
- Thompson, D. O. (1997). *Critical Reviews in Therapeutic Drug Carrier Systems*, *14*, 1.
- Todres, Z. V. (2011). *Chalcogenadiazoles—chemistry and applications*. Boca Raton, FL, USA: CRC Press, Taylor and Francis Group.
- Tuncel, D., & Steinke, J. H. G. (1999). *Chemical Communications*, *16*, 1509.
- van de Manakker, F., van der Pot, M., Vermonden, T., van Nostrum, C. F., & Hennink, W. F. (2008). *Macromolecules*, *41*, 1766.
- VanEtten, R. L., Clowes, G. A., Sebsation, J. F., & Bender, M. L. (1967a). *Journal of the American Chemical Society*, *89*, 3253.
- VanEtten, R. L., Sebsation, J. F., Clowes, G. A., & Bender, M. L. (1967b). *Journal of the American Chemical Society*, *89*, 3242.
- Vicens, J., & Boehmer, V. (Eds.). (1991). *Calixarenes: A versatile class of macrocyclic compounds*. Dordrecht, The Netherlands: Kluwer Academic Publishers.
- Vicens, J., & Harrowfield, J. (Eds.). (2006). *Calixarenes in the nanoworld*. Dordrecht, The Netherlands: Springer.
- Vinciguerra, B., Cao, L., Cannon, J. R., Zavalij, P. Y., Fenzelau, C., & Isaacs, L. (2012). *Journal of the American Chemical Society*, *134*, 13133.
- van Wageningen, A. V. A., Timmerman, P., van Duynhoven, J. P. M., Verboom, W., van Veggel, F. C. J. M., & Reinhoudt, D. N. (1997). *Chemistry: A European Journal*, *3*, 639.
- Walla, P., Arion, V. B., & Brinker, U. H. (2006). *Journal of Organic Chemistry*, *71*, 3274.
- Wang, Y.-H., Zhu, M.-Zh., Lio, T., & Guo, Q.-X. (2003). *Research on Chemical Intermediates*, *29*, 191.
- Wang, R., Yuan, L., & Macartney, D. H. (2005). *Chemical Communications*, *47*, 5867.
- Warmuth, R., Maverick, E. F., Knobler, C. B., & Cram, D. J. (2003). *Journal of Organic Chemistry*, *68*, 2077.
- Wernick, D. L., Savion, Z., & Levy, J. (1988). *Journal of Inclusion Phenomena and Macrocyclic Chemistry*, *6*, 483.
- Wheate, N. J., Kumar, P. G. A., Torres, A. V., Aldrich-Wright, J. R., & Price, W. S. (2008). *Journal of Physical Chemistry B*, *112*, 2311.
- Wu, X.-L., Luo, L., Lei, L., Liao, G.-H., Wu, L.-Zh., & Tung, Ch.-H. (2008). *Journal of Organic Chemistry*, *73*, 491.
- Wyman, I. W., & Macartney, D. H. (2010). *Organic & Biomolecular Chemistry*, *8*, 247.
- Xiao, J., Deng, Zh.-B., Yao, Y.-Sh., & Wang, X.-S. (2008). *Dyes Pigments*, *76*, 290.

- Xing, H., Lin, Sh.-Sh., Yan, P., & Xiao, J.-X. (2008). *Langmuir*, 24, 10654.
- Yamauchi, Y., Ajami, D., Lee, J.-Y., & Rebek, J. (2011). *Angewandte Chemie International Edition*, 50, 9150.
- Yang, Ch., Liu, L., Mu, T.-W., & Guo, Q.-X. (2001). *Journal of Inclusion Phenomena and Macrocyclic Chemistry*, 39, 97.
- Yang, Ch., Mori, T., & Inoue, Y. (2008). *Journal of Organic Chemistry*, 73, 5786.
- Yao, Y., Xue, M., Chen, J., Zhang, M., & Huang, F. (2012). *Journal of the American Chemical Society*, 134, 15712.
- Yebeutchou, R.M., & Dalcanale, E. (2009) *Journal of the American Chemical Society*, 131, 2452.
- Yu, G., Han, Ch., Zhang, Z., Chen, J., Yan, X., Zheng, B., et al. (2012). *Journal of the American Chemical Society*, 134, 8711.
- Yuan, L., & Macartney, D. H. (2007). *Journal of Physical Chemistry B*, 111, 6949.
- Zelder, F. H., & Rebek, J. (2006). *Chemical Communications*, 7, 753.
- Zhang, X., Gramlich, G., Wang, X., & Nau, W. M. (2002). *Journal of the American Chemical Society*, 124, 254.
- Zhang, Q., Li, G.-Zh., Becer, R., & Haddleton, D. M. (2012). *Chemical Communications*, 48, 2063.
- Zhang, Y., Yu, Sh., Bao, F. (2008). *Carbohydrate Research*, 343, 2504.
- Zhao, Y., Yang, Z. M., Chi, Sh M, Gu, J., Yang, Y. C., Huang, R., et al. (2008). *Bulletin of the Korean Chemical Society*, 29, 953.
- Zhao, N., Lloyd, G. O., & Scherman, O. A. (2012). *Chemical Communications*, 48, 3070.
- Zheng, X.-Q., Ruan, X.-Q., Wang, W., Zhang, H.-M., Guo, Q.-X., & Liu, Y.-Ch. (1999). *Bulletin of the Chemical Society of Japan*, 72, 253.
- Zhou, Y., Xu, H., Wu, L., Liu, Ch., Lu, Q., & Wang, L. (2008). *Spectrochimica Acta Part A*, 71, 597.
- Zou, D., Andersson, S., Zhang, R., Sun, Sh, Aekermark, B., & Sun, L. (2008). *Journal of Organic Chemistry*, 73, 3775.

Chapter 2

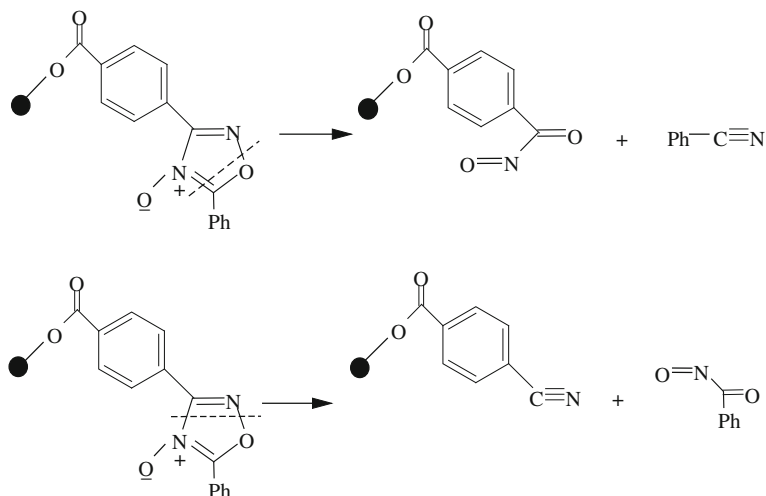
Resin-Docking, Polymer-Penetration, and Surface-Engrafting Effects

2.1 Introduction

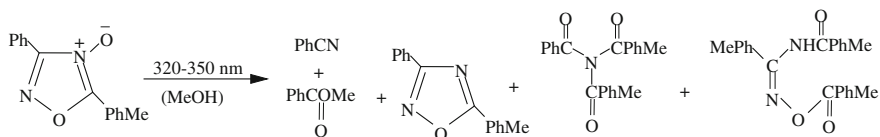
This chapter considers topics that up to now have remained beyond the scope of reviews or books relevant to confined chemistry. Among these are changes in organic reactivity resulting from docking to resins, transformations of substrates confined in polymer grinds (under conditions of ultrasmall scales), and polymer-penetration and surface-engrafting effects. Further development of these problems may provide innovative solutions for currently pressing problems related to energy, the environment, sustainability, and health.

2.2 Resin-Docking Effects

Docking resins contain only one side connected with organic substances. The literature does not pay much attention to effects of organic-substrate docking at resins. Nevertheless it exists, as shown by the following example. Quadrelli et al. (2005) studied photolytic splitting of 1,2,4-oxadiazole 4-oxide docked at Wang resin through the carboxy phenyl substituent (Scheme 2.1). The reactions were carried out in methanolic suspension at room temperature. The reaction depicted at the top of Scheme 2.1 shows the results of 2-h irradiation by an ultraviolet lamp. The nitroso-carbonyl was generated on the resin, while the benzonitrile was released in solution. The reaction at the bottom of Scheme 2.1 shows the results of 2-h exposure to sunlight. In this case, the nitroso-carbonyl was released in solution while the benzonitrile was generated on the resin. Consequently, the splitting direction depends on the intensity of photoexcitation. It is significant that the resin-supported reactions did not lead to deoxygenation of the *N*-oxide fragment as takes place upon light irradiation of free 1,2,4-oxadiazole 4-oxides (not docked at the resin) (cf. Scheme 2.2). Consequently, the resin docking changes the reactivity of the oxides, representing a kind of confinement effect.



Scheme 2.1 Light-irradiation intensity and splitting manner of oxadiazole docked at Wang resin

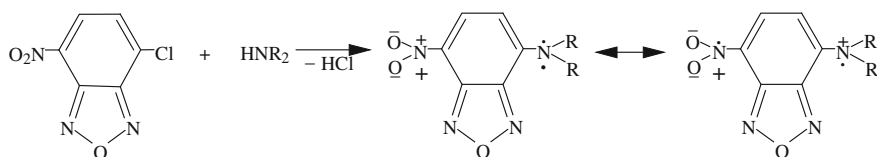


Scheme 2.2 Photolytic splitting and deoxygenation of oxadiazole N-oxide

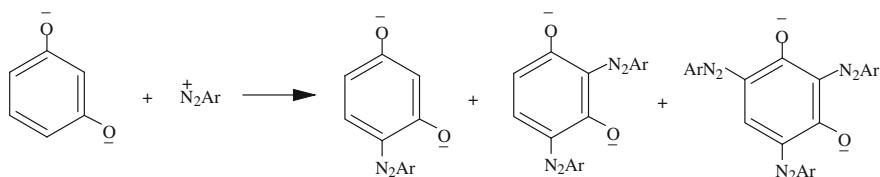
2.3 Polymer-Penetration Effects

It has been known for many years that polymer fibers can interact with each other after production. Anzenbacher and Palacios (2009) used the interaction between electrospun polyurethane fibers to deposit them in a rectangular grid and to overlay in a cross-hatch pattern. The authors doped the fibers with different reagents and heated the hatch or exposed it to solvent vapors. As a result, the fibers joined (welded) at the crossing points. The multiple junctions created during this process have a volume of a few attoliters (aL, 1 aL is 10^{-18} L). Because the polymer readily adsorbs hydrophobic compounds, these compounds occur very close to each other, in a confined space, and real chemistry is possible between them.

Scheme 2.3 shows the reaction between amines and α -chloro- α' -nitro-benzofurazan taking place in a nanofiber junction (Anzenbacher and Palacios 2009). The nucleophilic substitution leads to an intense intramolecular charge transfer, resulting in strong fluorescence; for analogs to this, see pp. 51, 52, 58, and 59 of Todres's monograph (2011). The fluorescent spectra registered in cases of ultrasmall-scale reactions are free from any artifacts caused by side-interactions. The reaction of Scheme 2.3 confirms not only that the content of the fiber junctions is physically mixed, but also that the reactant molecules diffuse close enough to enter into chemical interaction.



Scheme 2.3 Amine-chloronitrobenzofuran reaction within polymer nanofiber junction

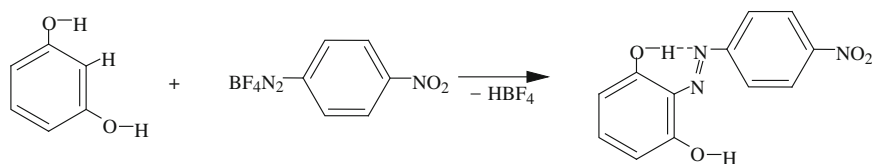


Scheme 2.4 Azocoupling of resorcinol

Resorcinol coupling with 4-nitrobenzenediazonium salts proceeds in alkali medium where the hydroxyl groups step forward in their high active anionic forms. Multiple substitution takes place: Even in the case of equimolar ratio of the azo and diazo components, resorcinol couples first at position 4, then easily transforms into a 2,4-bis(azo) compound and, eventually, into the 2,4,6-tris(azo) product (Scheme 2.4).

When resorcinol and 4-nitrobenzenediazonium tetrafluoroborate come into contact in a poly(ether-urethane) attoliter reactor, the hydroxyl groups of the azo component react in its neutral form and solely the monosubstituted product is obtained (Anzenbacher and Palacios 2009). According to the authors, the azocoupling proceeds at position 2. Obviously, the attoliter reactor cannot accommodate “shaggy” bis(azo) and tris(azo) compounds. Stabilization of the monoazo compound by intramolecular hydrogen bonding is also an important feature of the confined reaction (Scheme 2.5). This reaction provides another fundamental insight into the chemistry of confined spaces.

Carotenoids present some challenges in terms of their therapeutical application. The presence of a polyene chain and various terminal substituents in carotenoid molecules determines their near-zero inherent aqueous solubility, instability in the presence of oxygen, and high photosensitivity. Developing carotenoids into a pharmaceutical formulation requires a chemical delivery system that overcomes the problem



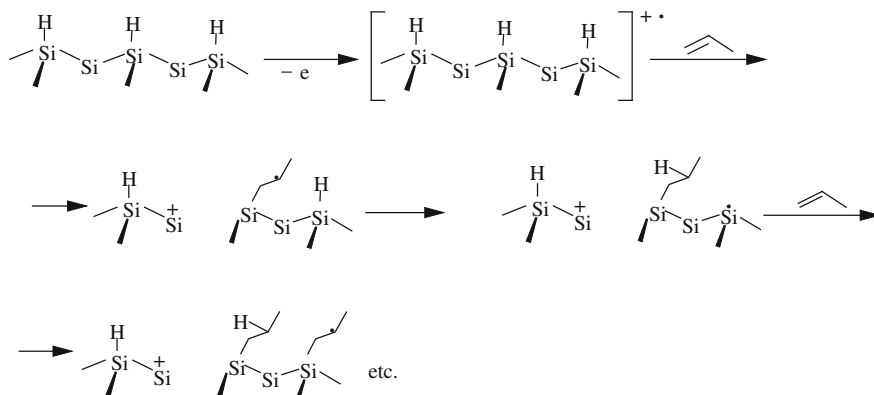
Scheme 2.5 Resorcinol coupling with nitrobenzene diazonium within poly(ether-urethane) nanofiber junction

with parenteral administration of a highly lipophilic, low-molecular-weight compound. Such a system was found in the complex between carotenoids and the natural polysaccharide arabinogalactan (Polyakov et al. 2009). This polysaccharide is a long, highly branched polymer composed of galactose and arabinose fragments in 6:1 ratio. Arabinogalactan is extracted from larch and approved for use by the U.S. Food and Drug Administration (FDA). Pharmaceutical-grade larch arabinogalactan is a fine, dry, beige powder with a slightly sweet taste and mild pine-like odor. It is low in viscosity, dissolves completely in water or juice, and is therefore easy to administer, even to children. Mixing a water solution of arabinogalactan with an ethanol solution of carotenoid did not result in complexation. However, it was found that an appropriate approach to complexation consists of cogrinding of a solid mixture of carotenoid crystals with arabinogalactan powder. This results in penetration of the carotenoid into the arabinogalactan polymer. Upon cogrinding, the crystal lattices of the starting materials are destroyed and reformed. The mechanochemical reaction leads to formation of supramolecular compounds or hybrid molecular crystals (Todres 2006). The resulting complexes are water soluble. Compared with pure carotenoids, these polysaccharide complexes showed enhanced photostability by a factor of 10 in water solution. A significant fall by a factor of 20 in the reactivity toward metal ions (Fe^{3+}) and reactive oxygen species was also detected. The carotenoid cation-radical imbedded into a polysaccharide host demonstrated greatly increased stability (Polyakov et al. 2009). The authors underline that this opens wide possibilities for application of these complexes in the design of artificial light-harvesting and photoredox devices.

2.4 Surface-Engrafting Effects

Surface-initiated and surface-confined polymerization has attracted great attention from specialists in material sciences. This approach provides rapid access to thick films or brushes with smooth surface and long-range order. The few defects and high precision of layers grown from the initiator-sown surface provide the possibility to generate a substantially enhanced photocurrent (Sakai et al. 2011). This approach can be exemplified by the work of Jones et al. (2002). In concrete language, the controlled radical polymerization of methyl methacrylate and glycidyl methacrylate from gold surface deserves to be mentioned. The gold surface was sown with mixed monolayers comprising undecanethiol (a confining component) and ω -mercaptoundecyl bromoisobutyrate (a fixed initiator of radical polymerization). The initiator density at the start of polymerization determines the ultimate “footprint” and hence the density of polymer molecules in the polymer brushes. The polymerization proceeds rapidly at room temperature in aqueous media. Sacrificial amounts of initiator are not needed, and polymerization in solution did not take place (Jones et al. 2002).

Jhon et al. (2008) used a flat silicon surface as a support and an initiator of styrene polymerization. The resulting polystyrene remained on the surface in the form of brushes. Bromination of the brushes led to substitution of the phenyl rings at their



Scheme 2.6 Alkene photoinoculation to silicon surface

para-positions. As that took place, the rate of reaction with the polystyrene brushes was much slower than bromination of free polystyrene in bulk solution. This behavior was attributed to steric hindrance due to the polystyrene confinement on the substrate.

Modification of the flat silicon surface is important for applications in electronic devices. Visible-light irradiation of Si(111) wafer in the presence of alkenes results in fast inoculation according to Scheme 2.6 (Rijksen et al. 2011). The reaction proceeds at room temperature and is distinguished by low activation energy. As seen from Scheme 2.6, the monolayer formation onto H-terminated Si progresses as cation-radical-induced initiation followed by radical recombination.

Adenier et al. (2005) grafted iron with 4-nitropobenzene diazonium cation so that a layer of 4-nitropolyphenylene was formed. The grafting was performed spontaneously by dipping the iron surface into 10 mM solution of the diazonium salt in acetonitrile. The immersion time governed the thickness of the layer: It was 2.8 nm after 1 min and 9.7 nm after 360 min. This simple method can be used to modify conductor and semiconductor surfaces.

2.5 Closing Remarks

Regardless of common opinion, chemical supports such as Wang resin really can change the reactivity of docked molecules. As seen from this chapter, the photoinduced splitting direction is different for docked oxadiazole oxides and for the same undocked compounds.

Polymer grinds readily absorb hydrophobic species, creating conditions of reactions in confined environments. These ultrasmall-scale reactions sometimes lead to products showing strong fluorescence, a property that can be used in practice without product isolation.

Penetration within polymers changes the physicochemical properties of organic compounds. Thus, carotenoids penetrated into arabinoglucan polymer become water soluble. Compared with pure carotenoids, these polysaccharide complexes showed enhanced photostability by a factor of 10 in water solution. A significant fall by a factor of 20 in the reactivity toward metal ions (Fe^{3+}) and reactive oxygen species is also important. This opens wide possibilities for application of these complexes in the design of artificial light-harvesting and photoredox devices.

By and large, further progress on the problems discussed in this chapter can bring about new developments of knowledge in organic and organometallic chemistry. At the same time, innovative developments that are potentially technologically useful can be made.

References

- Adenier, A., Cabet-Deliry, E., Chausse, E., Griveau, S., Mercier, F., Pinson, J., et al. (2005). *Chemistry of Materials*, *17*, 491.
- Anzenbacher, P., & Palacios, M. A. (2009). *Nature Chemistry*, *1*, 80.
- Jhon, Y. K., Semler, J. J., & Genzer, J. (2008). *Macromolecules*, *41*, 6719.
- Jones, D. M., Brown, A. A., & Huck, W. T. S. (2002). *Langmuir*, *18*, 1265.
- Polyakov, N. E., Leshina, T. V., Meteleva, E. S., Dushkin, A. V., Konovalova, T. A., & Kispert, L. D. (2009). *The Journal of Physical Chemistry B*, *113*, 275.
- Quadrelli, P., Scrocchi, R., Piccanello, A., & Caramella, P. (2005). *Journal of Combinatorial Chemistry*, *7*, 887.
- Rijksen, B., van Lagen, B., & Zuilhof, H. (2011). *Journal of the American Chemical Society*, *133*, 4998.
- Sakai, N., Lista, M., Kel, O., & Sakurai, S., Emery, D., Mareda, J., Vauthney, E., Matile, S. (2011). *Journal of the American Chemical Society*, *133*, 15224.
- Todres, Z. V. (2006). *Organic mechanochemistry and its practical applications*. Boca Raton: CRC Press, Taylor and Francis Group.
- Todres, Z. V. (2011) *Chalcogenadiazoles—chemistry and applications*. Boca Raton: CRC Press, Taylor and Francis Group.

Chapter 3

Reactions Within Charge-Transfer Complexes

3.1 Introduction

Charge-transfer complexation includes electron transfer from a donor to an acceptor molecule. This kind of complexation proceeds reversibly, and the notion of “electron-transfer degree” comes into play. Accordingly, charge-transfer complexes can be weak, medium or strong. In all cases, the electronic structures of the participants are somewhat changed, leading to some changes in reactivity. Examples of the specific reactivity within charge-transfer complexes are listed in this chapter. It is worth underlining the principal difference between electron-transfer reactions resulting in a release of the products formed, with a superfluous electron or electron–hole pair, on the one hand, and transformations of the participants within the charge-transfer complexes on the other hand. When relevant, such a difference is discussed in this chapter.

The formation of charge-transfer complexes can be revealed by a special charge-transfer band in electronic spectra, by changes in infrared, nuclear or spin magnetic resonance spectra, as well as by alteration of dipole moments and cathodic/anodic potentials. Such complexes provide signals in electronic paramagnetic resonance spectra only in cases where the charge-transfer degree is close to unity. Because charge-transfer complexes are species of increased polarity, their solubility in polar solvents is better than that of the individual components. High degrees of dilution can, however, give rise to dissociation of these complexes.

3.2 Specific Characteristics of Reactions Within Charge-Transfer Complexes

Reactions within charge-transfer complexes are characterized by special features. Namely, their rate becomes slower (not faster) with increasing reaction temperature. The first definitive case of such negative temperature dependence was reported by

Kiselev and Miller (1975), who showed that a negative activation enthalpy arises when the charge-transfer complex between 9,10-dimethylantracene and tetracyanoethylene was formed along the reaction pathway of the corresponding cycloaddition. In fact, donor–acceptor interaction does not lead to the formation of covalent bonds. Consequently, the first effect of increasing temperature is destruction (complete or partial) of the charge-transfer intermediate. Decreased temperature contributes to enhanced stability of charge-transfer complexes.

Another important characteristic of reactions within charge-transfer complexes is the appropriate difference in the donor and acceptor properties of the reactants.

Condensation of aldehydes with arylhydrazines is a well-known reaction that proceeds in the presence of sulfuric or hydrochloric acid. Using tetracyanoethylene (instead of these acids) results in marked acceleration of the condensation: The reactions are completed in 5–10 min, and hydrazones are formed in high (often quantitative) yields. Notably, the acceleration effect is observed only for aromatic aldehydes, but not for the aliphatic counterparts (Ryzhakov et al. 2003). Only with aromatic aldehydes, tetracyanoethylene forms charge-transfer (π, π) complexes, providing confinement environments and enhancing the reactivity of the substrates and reactants.

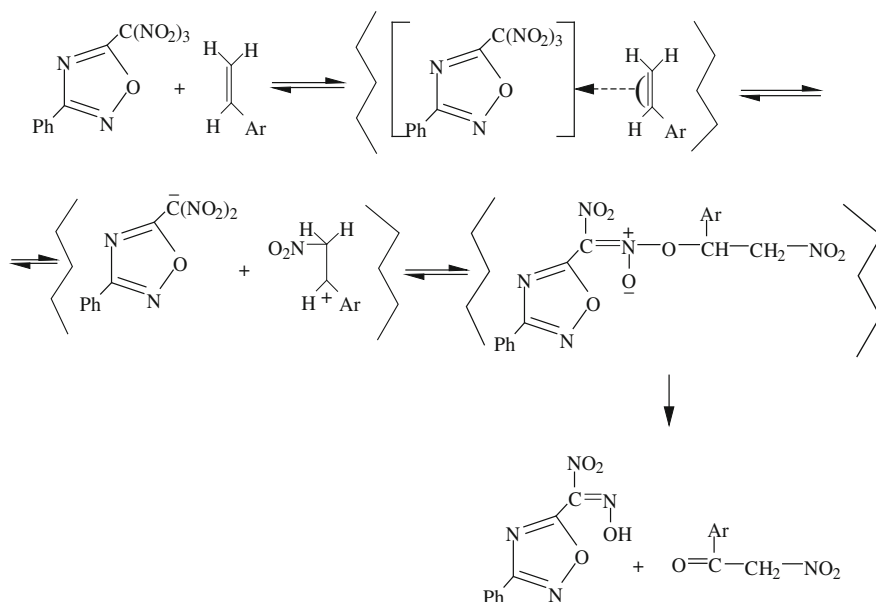
The electrophilicity of 1,2,4-oxadiazole allows it to form charge-transfer complexes with donor counterparts, especially when the oxadiazole bears electron acceptor substituents. With arylenes, 3-phenyl-5-trinitromethyl-1,2,4-oxadiazole forms charge-transfer complexes. Within the complexes, the arylenes pull a nitro group out from the trinitromethyl substrate, after which the resulting components are covalently bound with each other. The new compounds are unstable and break down, giving nitroketones and 3-phenyl-1,2,4-oxadiazole-5-methylnitronitrolic acid according to Scheme 3.1 (Tyrkov 2004).

Scheme 3.1 presents an example of such chemical reactions in a confined environment. It would be interesting to study reactions of 1,2,4-oxadiazoles within *inclusion* complexes, too; For instance, a molecular mechanics study by Al-Sou'od (2006) points out that the bulky 3,3'-bis[4-alkyl-1,2,4-oxadiazol-5(4*H*)-one] completely penetrates into the cavity of β -cyclodextrin. The driving forces for the formation of inclusion complexes are dominated by nonbonding van der Waals host–guest interactions with some electrostatic contribution. Organic reactions governing the inclusion of organic substrates into cyclodextrins are considered in Chap. 1.

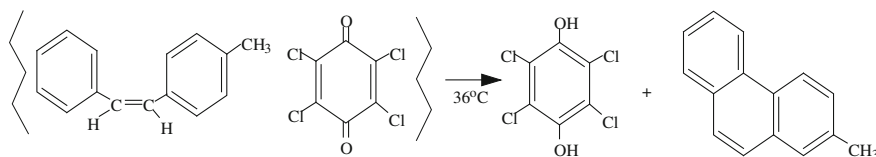
3.3 Cyclization Within Charge-Transfer Complexes

When confined within *p*-chloranil, 4-methyl-*cis*-stilbene is cyclized and converted (within a charge-transfer complex) into 3-methylphenanthrene. The cyclization takes place at a very moderate temperature (36 °C) without light irradiation. Scheme 3.2 depicts the cyclization in brief (Todres et al. 1990).

Charge-transfer complexation governs the asymmetric oxidation of benzylic carbon with 2,3-dichloro-5,6-dicyanobenzoquinone as outlined by Scheme 3.3. Charge transfer allows the reacting moieties of benzylic carbon and carboxylic



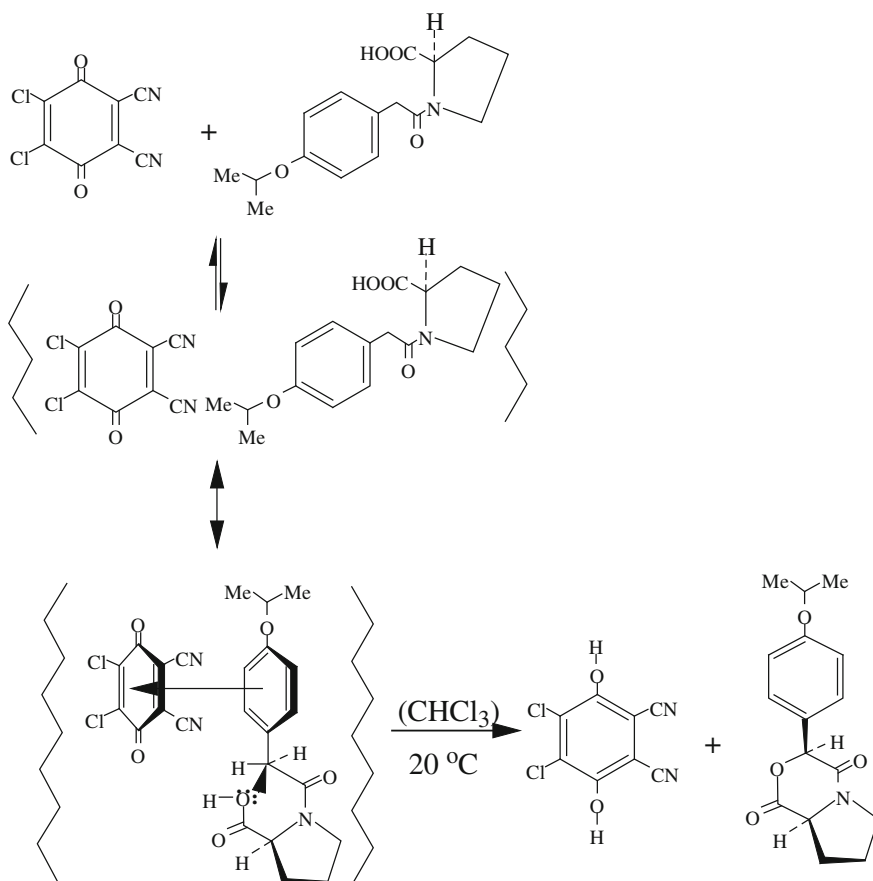
Scheme 3.1 Charge-transfer complexation and monodenitration during reaction of trinitromethyl oxadiazole with arylethylene



Scheme 3.2 Phenanthrene formation inside charge-transfer complex of *cis*-stilbene with chloranil

oxygen to be retained at specific locations. Cyclization eventually results in the formation of oxazine-dione with diastereomeric excess of 65 % (Lemaire et al. 1986).

Reaction of *p*-chloranil with 2-aminopyrimidine in methanol also takes place within a 1:1 charge-transfer complex according to Scheme 3.4 (Rabie et al. 2007). Chloranil, a π -acceptor, initially forms an outer-sphere charge-transfer complex with the pyrimidine donor. With time, the outer-sphere complex is reorganized into an inner-sphere complex and then into an anion-radical. The chemical reaction develops to yield the final cyclic product, 7,8-dichlorobenzo[4.5]imidazo[1,2-*a*]pyrimidine-6,9-dione.

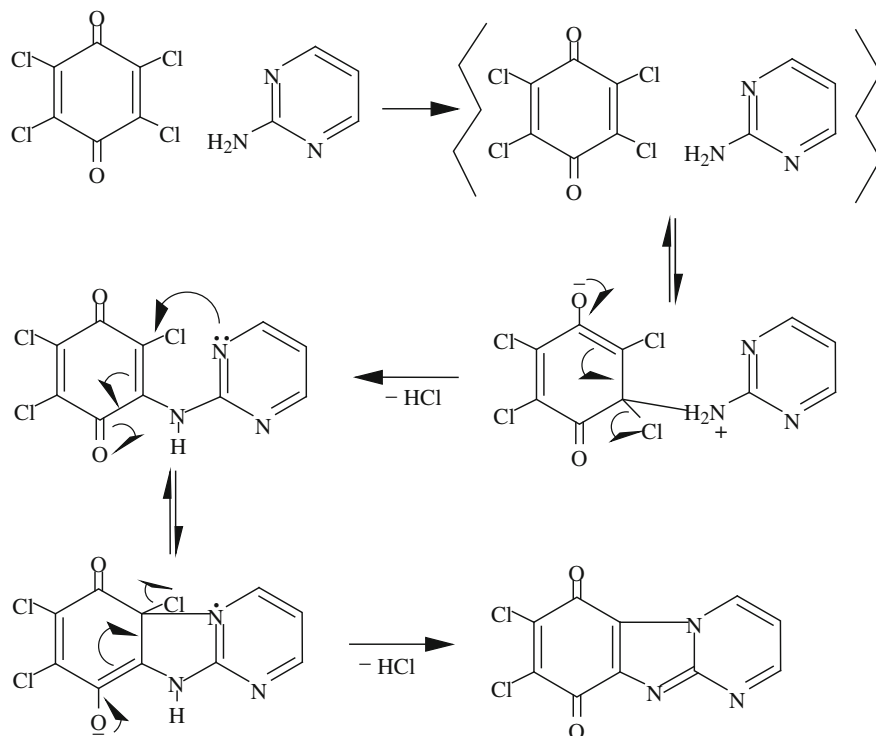


Scheme 3.3 Donor-acceptor confinement and stereospecificity in oxazine formation

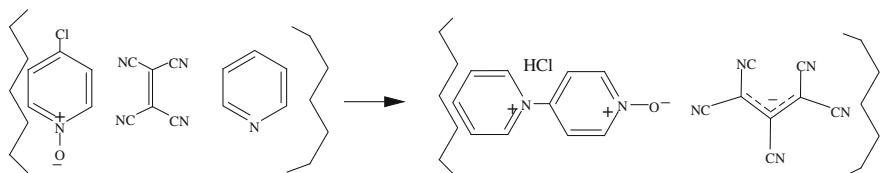
3.4 Substitution Within Charge-Transfer Complexes

Scheme 3.5 illustrates the role of complexation with tetracyanoethylene in a substitution reaction. Whereas the tetracyanoethylene interaction with 4-chloropyridine-1-oxide is inoperative, the substitution reaction does take place when the donor properties of the substrate are enhanced by dint of pyridine addition. This results in substitution of pyridinium for chlorine in 4-chloropyridine-1-oxide and in the formation of the pentacyanopropenide anion from tetracyanoethylene. Both products develop and exist within the charge-transfer complex (Scheme 3.5) (Ryzhakov et al. 2003).

Neeglund and Budni (2005) studied the interaction between 2,3-dichloro-1,4-naphthoquinone and *n*-butylamine. The reaction proceeds through three consecutive steps. Among them, the formation and conversion of reaction intermediates are extremely fast, whereas the formation of the final product proceeds at moderate



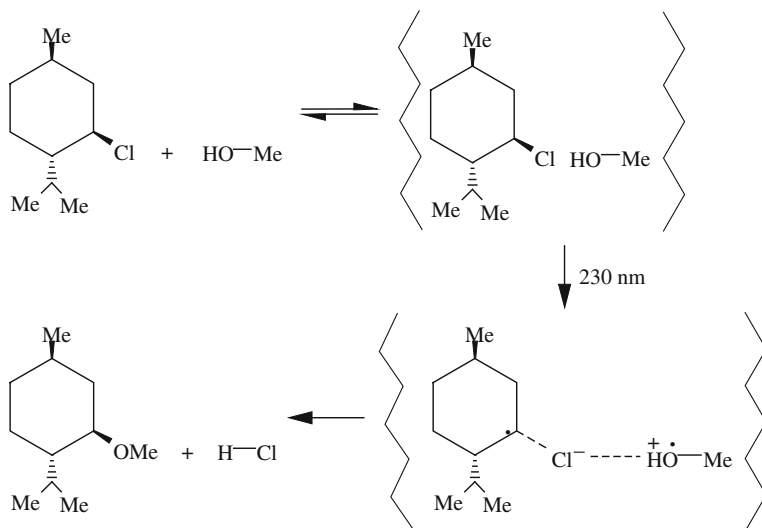
Scheme 3.4 Chloranil-aminopyrimidine charge-transfer complexation and charge separation on way to benzimidazolopyrimidine derivative



Scheme 3.5 Substitution reaction within charge transfer complexes

speed. The product formed in the reaction is 2-*N*(*n*-butylamino)-3-chloro-1,4-naphthoquinone. No disubstituted product is formed in this case.

In contrast to the latter reaction, the interaction between *p*-chloranil and dimethylamine (in aqueous dimethylformamide) includes the formation of a charge-transfer complex at the initial step, but undergoes the full charge separation and reaches the step of free ion-radicals. As a result, anion-radicals of *p*-chloranil transform into anion-radicals of 2,5-bis(dimethylamino)-3,6-dichloro-*p*-benzoquinone. During the reaction, consumption of the *p*-chloranil anion-radicals coincides with accumulation of the 2,5-bis(dimethylamino)-3,6-dichloro-*p*-benzoquinone anion-radicals (Kadirov et al. 2003).



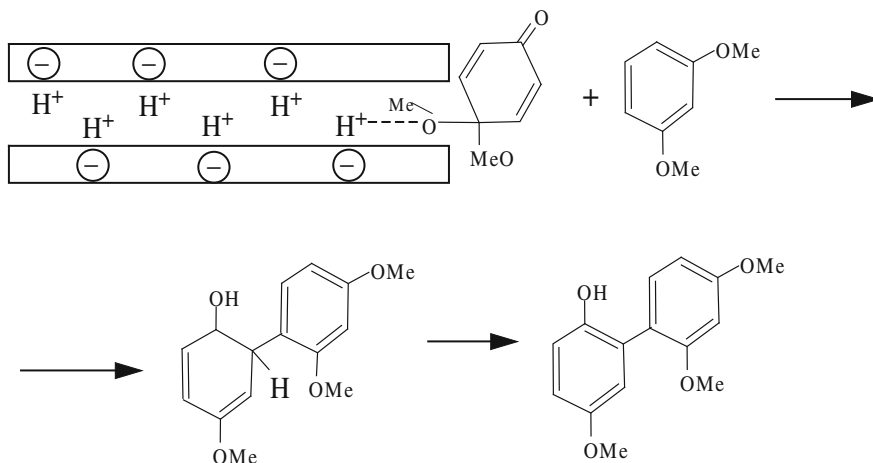
Scheme 3.6 Menthyl chloride-methanol charge-transfer complex, photogeneration of component ion-radicals and final S_N1 reaction between them with retention of initial steric configuration

Miller and Salvador (2002) reported photoinduced electron-transfer substitution reactions that proceed via unusual charge-transfer complexes. Scheme 3.6 introduces one of these reactions: the formation of methyl (1*R*,2*S*,5*R*)-menthylate from (1*R*,2*S*,5*R*)-menthyl chloride and methanol. Methanol forms a charge-transfer complex with menthyl chloride via the chlorine and develops the photosubstitution chromophore. Upon absorption of a photon, a zwitterionic diradical intermediate appears. This zwitterion remains associated within a solvent (methanol) cage. In the radicaloid part of the zwitterions, neither planarization nor rapid inversion takes place, and the starting configuration of the atoms about the stereocenter is kept as such. Hence, substitution occurs without the racemization common to S_N1 chemistry.

A formal but very curious analogy for the reaction within charge-transfer complexes is the unprecedented reaction of quinone monoacetals in a substitution conjugated with aromatization (Scheme 3.7) (Dohi et al. 2011). The reaction proceeds with participation of montmorillonite. This solid acid consists of anionic layers, in which a number of protons are confined. These protons acquire unusual activity and are capable of activating acetal moieties, enabling the unprecedented substitution with the formation of biaryl syntons.

3.5 Geometrical Isomerization of Alkenes Within Charge-Transfer Complexes

The electrochemical behavior of 4,4'-dimethoxystilbene was compared with the action of *p*-chloranil in solution (Todres and Ionina 1992). It was found that the *cis* and *trans* isomers of the compound form different charge-transfer complexes with

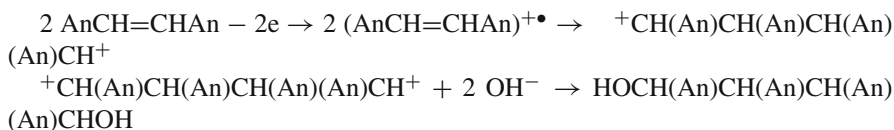


Scheme 3.7 Biaryl formation via reaction of resorcinol dimethyl ether and gem-dimethoxy benzoquinone confined by protonated montmorillonite

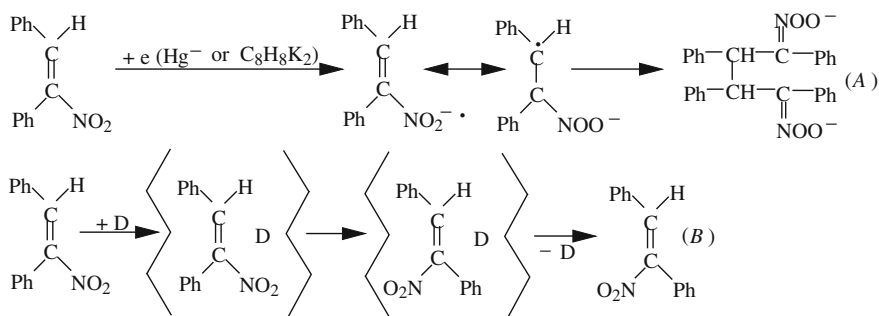
chloranil, which are unlike in color and can be interconverted. The conversion was found to be in the *cis*-to-*trans* direction. A reverse transition (from *trans* to *cis*) was not observed, and no cyclization like the one depicted in Scheme 3.2 was detected. Formation of charge-transfer complexes was observed in homogeneous solutions. Because of the limited solubility of chloranil, the reaction was performed in a boiling solvent. In hexane and methylene chloride [boiling points (b.p.) of 69 and 49 °C, respectively], the degree of *cis*-to-*trans* conversion was 50 and 30 %, respectively. No conversion was observed in the absence of chloranil, when 4,4'-dimethoxy-*cis*-stilbene was kept in these boiling solvents.

In the case of benzene as solvent (b.p. 80 °C), no conversion was observed even in the presence of *p*-chloranil. This is perhaps because benzene competes with dimethoxystilbene in binding with chloranil during the formation of a charge-transfer complex. In distinction to hexane and methylene chloride, benzene contains a circular contour of mobile π -electrons that is favorable for charge transfer.

During oxidation on a platinum anode, the same 4,4'-dimethoxystilbene ($\text{AnCH}=\text{CHAn}$) yields the cation-radical in the first step. According to Parker and Ebersson (1969), Steckhan (1978), and Burgbacher and Schaefer (1979), these cation-radicals are freely formed and dimerized even in the presence of nucleophiles (OH^-):



Another example concerns the transfer of a charge or an electron from donors to α -nitrostilbene (Todres et al. 1982, 1985; Todres and Tsvetkova 1987; Kraya et al. 2004). The electron transfer develops according to direction (A) in Scheme 3.8 if the



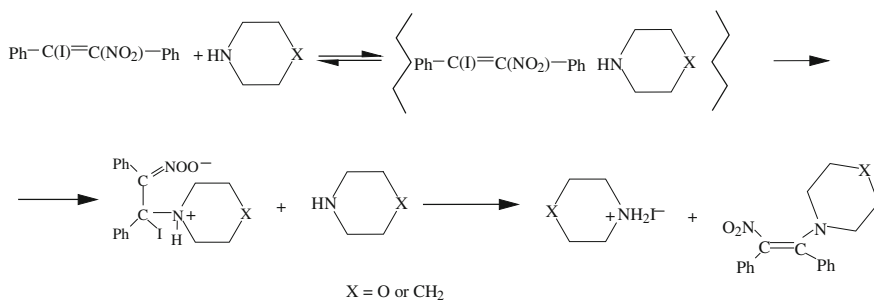
Scheme 3.8 α -nitrostilbene conversions upon electron transfer and within donor-acceptor complex

mercury cathode or cyclooctatetraene dianion is the electron source. When the same stilbene enters the charge-transfer complexes with uranocene or bis(pyridine)tungsten tetracarbonyl, the confined reaction follows direction (B). For direction (B), a charge-transfer band in the electron spectra is observed. So, the mentioned data reveal a basic difference in the fate of products resulting from electron transfer or charge transfer—the processes marked in Scheme 3.8.

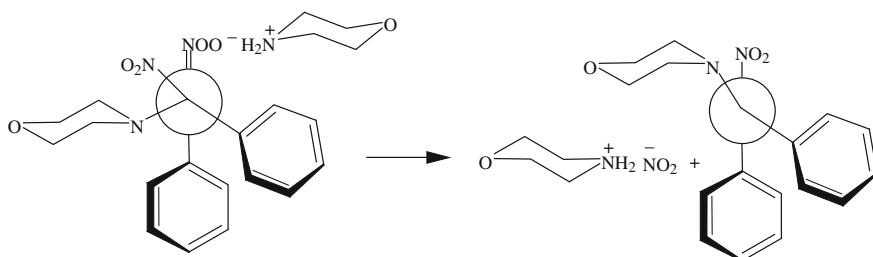
3.6 Role of Charge-Transfer Complexation in Vinylic Nucleophilic Substitution

The difference denoted in Scheme 3.8 for reactions (A) and (B) was used to reveal the charge-transfer step in reactions of nucleophilic vinylic substitution. Let us consider data on the general mechanism of these reactions, based on α -iodo- β -nitro- and α,β -dinitrostilbene interactions with morpholine or piperidine (Todres et al. 1990; Korotehev et al. 1992; Todres et al. 1992). The reactions lead to nitroenamines, which contain donor and acceptor groups in the conjugated chain. Such compounds are of interest for microelectronics and photonics and as intermediates for drug design.

For the reaction of Scheme 3.9 stereospecificity was studied along with the dependence of the final product yield on the solvent nature and the process temperature. It was found that both *cis* and *trans* isomers of iodonitrostilbene form the *cis*-substituted product only, without iodoaminostilbene: The reaction proceeds fully regioselectively and stereospecifically. As to the solvent effect, the more polar the solvent, the higher the yield of the product (for the experiments leading to less than quantitative yields). This means that polar intermediate states are formed in the course of the reaction. The temperature effect on the product yield has a clear-cut trend: The lower (not higher) the temperature, the greater the yield. (Such dependence is typical for reactions including the formation of charge-transfer complexes.)



Scheme 3.9 Charge transfer from morpholine or piperidine to alpha-iodo-beta-nitrostilbene and substitution reaction between participants



Scheme 3.10 Newman projections of intermediary and final products of reaction 3-9

The observed facts confirm Scheme 3.10, which is also in good agreement with the data on the kinetics of the interaction of α,β -dinitrostilbene with morpholine. The regioselectivity observed in the reaction of Scheme 3.10 can be explained by the formation of an intermediate that directly precedes the final product formation. As can be seen from Newman projection, this intermediate possesses the most favorable arrangement of fragments. The advantage consists not only in minimal steric stress: Additionally, the nitronate orbital (populated by a pair of electrons) overlaps with the orbital of the leaving nitro group; this facilitates transfer of the electron pair from the occupied orbital to the vacant one, making the removal of the nitrite anion energetically favorable. Note that this also predetermines the *cis* configuration of the product formed. This statement equally relates to the *cis* and *trans* isomers of the substrate, because they form the same intermediate during the reaction with morpholine.

Schemes 3.9 and 3.10 incorporate the intermediate formation of charge-transfer complexes. Electron transfer does not take place, and no paramagnetic particles were observed in the reaction sphere. The substrate (an acceptor) and the reactant (a donor) undergo charge-transfer complexation that proceeds reversibly. Namely, a part of the donor and the acceptor exist in the complex, but a part of the reactant and the substrate exist separately. If some part of the substrate remains noninvolved in the substitution reaction, it must in any way have a notch, entering for a while into the charge-transfer complex. Temporarily entering the complex, this substrate must undergo *cis/trans* conversion.

The reactions of *cis*- α,β -dinitrostilbene with piperidine or morpholine were tested. Because the products of both reactions are formed with almost quantitative yield, an artificial decrease of these yields was needed. For this purpose, the ratio of reactant to substrate was chosen as 1:1. The yields were decreased from 100 % to about 40 %. This opens the way to analyze the geometry of the substrate returned without substitution. Indeed, a mixture of *cis* and *trans* forms was obtained from the *cis* substrate; i.e., the charge-transfer complexation really took place.

Material balance data for the *cis*- α,β -dinitrostilbene reactions are the following: (1) With morpholine: α -(*N*-morpholino)- β -nitrostilbene is the sole product. In tetrahydrofuran at 25 °C, at 45 min duration and with reactant-to-substrate ratio of 1:1, this product is formed with 43 % yield, whereas the substrate return is 55 % (the balance reaching 98 %); (2) With piperidine: α -(piperidino)- β -nitrostilbene is the sole product. In tetrahydrofuran, at 45 min duration and with reactant-to-substrate ratio of 1:1, product yields were determined as a function of temperature. At +25 °C, the yield is 63 %, and the substrate returns with 35 % yield (the balance reaching 98 %). The content of the converted (*trans*) form in the returned substrate is 10 %. At -25 °C, the product yield is 65 %, and the yield of the returned substrate is 33 % (the balance reaching 98 %). The content of the converted (*trans*) form in the returned substrate is 10 %.

Based on the study of nucleophilic vinylic substitution in the nitrostilbene-amine system, the formation of charge-transfer complexes was established. This step precedes the substitution. Several independent methods were used to reveal the participation of these complexes (temperature and solvent effects, stereochemical analysis of the reactions), which was corroborated by the kinetic scheme of the process (comparison between experimental and calculated data by the approach of discriminative analysis of kinetic characteristics). The methods discussed here seem to be applicable for other reactions of vinylic substitution. In the considered cases, knowledge of the charge-transfer step allowed choice of the optimal conditions for preparation of the target products.

3.7 Role of Charge-Transfer Interaction in Oxidative Polymerization

Gelover-Santiago et al. (2005) obtained a promising result from inclusion of a charge-transfer dopant in the process of oxidative polymerization of 2,6-bis(2-thienyl)-1,4-dithiafulvalene in chloroform. Tetracyanoquinodimethane was used as a charge-transfer dopant. The polymer is obtained as a complex with the same dopant. This dopant forms charge-transfer complexes with the monomer, and the resulting charge-transfer complex gives rise to a polymer with improved molecular weight (by three times in comparison with polymerization without the dopant).

The polymer obtained in the presence of the dopant is completely soluble in dimethylsulfoxide, dimethylformamide, and acetone. The processability of this (doped) polymer turns out to be acceptable. The electric conductivity of the poly-

mer proves to be three orders of magnitude larger than that of the polymer prepared from 2,6-bis(2-thienyl)-1,4-dithiafulvalene without tetracyanoquinodimethane. Scheme 3.11 compares the structures of the undoped polymer and the polymer formed from the monomer charge-transfer complex with the tetracyanoquinodimethane dopant.

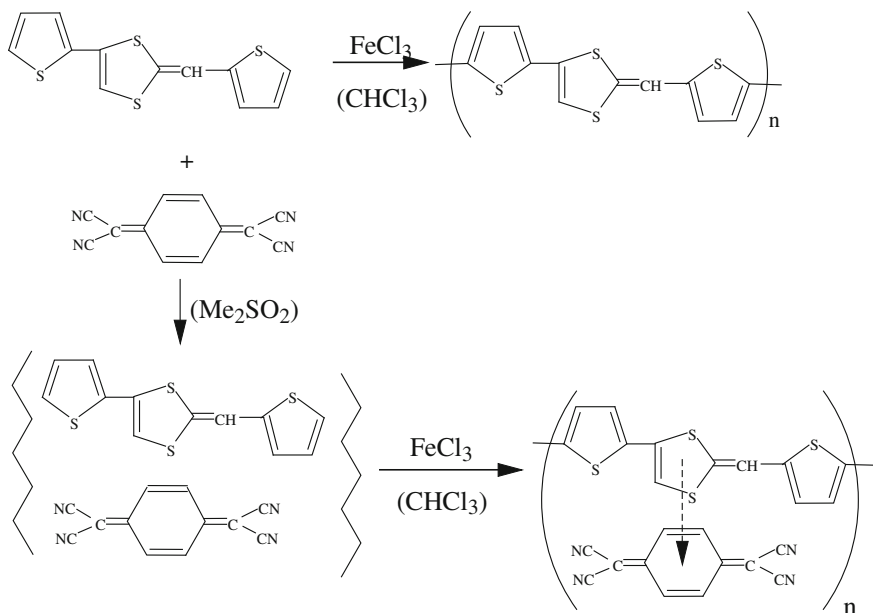
3.8 Organic Reactivity Within Crystals Containing Charge-Transfer Complexes

In the crystalline state, organic compounds have a unit cell containing several identical molecules. Upon laser illumination or mechanical shock, ionized states are generated within the cell (Kunz et al. 2002). Since the molecules are equivalent, a hole is fixed at one molecule and an electron is transferred to various other molecules in the same cell or to an adjacent one. This phenomenon has chemical consequences. Considering the explosive known as hexogen (1,3,5-trinitro-1,3,5-triazacyclohexane; industrial name: RDX), Tsiaousis and Munn (2005) calculated its dissociation energy in a crystal cell containing neutral hexogen, the hexogen cation-radical, and anion-radical. In the cell incorporating the charge-transfer states, total destruction of hexogen needs appreciably lower energy consumption relatively to that of the free (neutral) molecule. The destruction begins with rupture of the N–NO₂ bond. In this regard, new approaches are possible for the design of detonating materials and understandable preventions can be stated for treatment of organic crystals with pressure, mechanical activation, or laser illumination. (Note that it is both dangerous and illegal to participate in unauthorized experimentation with explosives.)

Importantly, organic molecules with smaller dipole moments are weak at trapping charge-transfer pairs within the crystal cell. This makes detonation-induced molecular rupture difficult. Thus, crystals of the nonpolar molecule 1,3,5-triamino-2,4,6-trinitrobenzene (TATB) are highly insensitive to detonation, even though TATB is a practical explosive material (Tsiaousis and Munn 2005) (Scheme 3.12).

Another charge-transfer interaction between equal molecules was described for *trans*-4-styrylpyridines (Scheme 3.13) (Yamada et al. 2012). The authors kept the starting materials as powder crystals in a desiccator filled with dried HCl gas and observed changes in the powder X-ray diffraction pattern. It was concluded that the transition of *trans*-styrylpyridines into their pyridinium salts led to ordering in the crystal lattice according to Scheme 3.13: The ordering is caused by a cation– π interaction. Irradiation of the resultant HCl salts with a 450-W high-pressure lamp (Yamada et al. 2007) gave *syn* head-to-tail dimers with excellent yield. The HCl gas-induced reorientation process in the crystals is conjugated with long-range interaction caused by charge transfer from the benzenoid to pyridinium component of the styrylpyridiniums under consideration. The crystallinity, on the microscale level, is sufficiently high to attain regio- and stereoselective photodimerization.

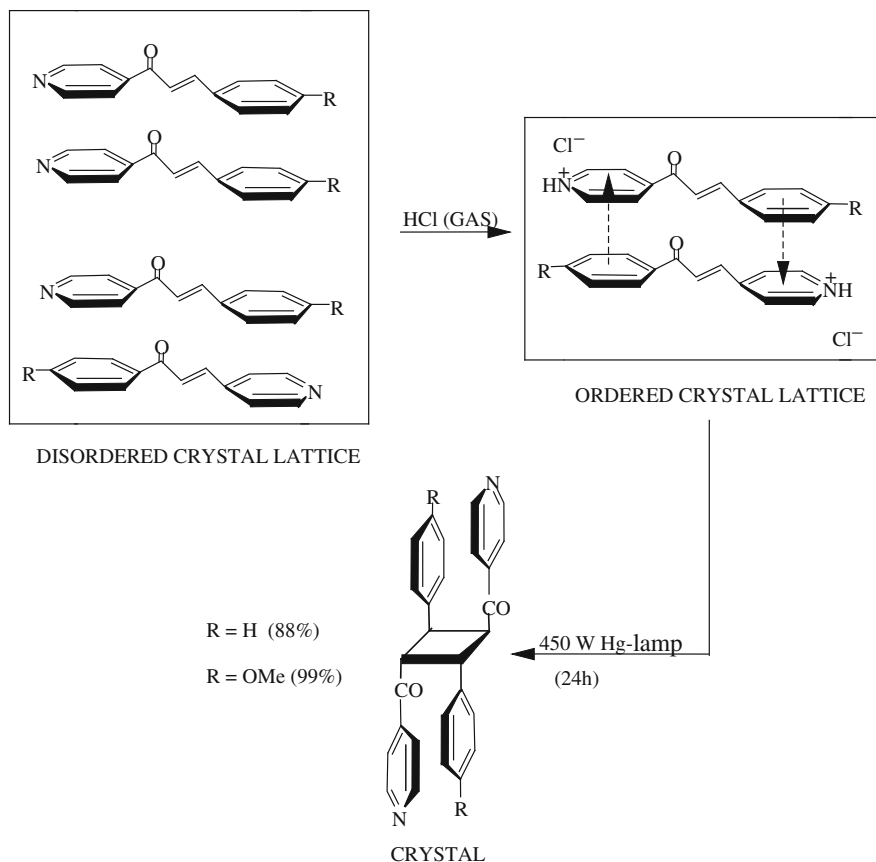
Interesting results were obtained in the search for catalytic effects for the solid-state Diels–Alder reaction between 1,4-benzoquinone and 9,10-dimethylanthracene.



Scheme 3.11 Role of charge-transfer complexation in oxidative polymerization of bis(thienyl)dithiafulvalene

Watanabe and Senna (2005) attempted to perform this reaction under vibrational milling. As it turned out, the reaction yield was relatively low when compared with the conventional solution reaction. However, the interaction of benzoquinone with dimethylantracene under mechanical stress resulted in the formation of a cycloadduct at almost *quantitative* yield when (*rac*)-1,1'-bis(2-naphthol) or 2-naphthol was added to the reaction mixture. The effect of these additives is based on the formation of a charge-transfer complex with strong hydrogen bonds between naphthol and benzoquinone. Using an X-ray diffraction method, the authors established that the charge-transfer complex incorporates dimethylantracene during vibrational milling. The catalytic role of the complex consists in the creation of a crystallographically ordered homogeneous reaction field that facilitates the cycloaddition.

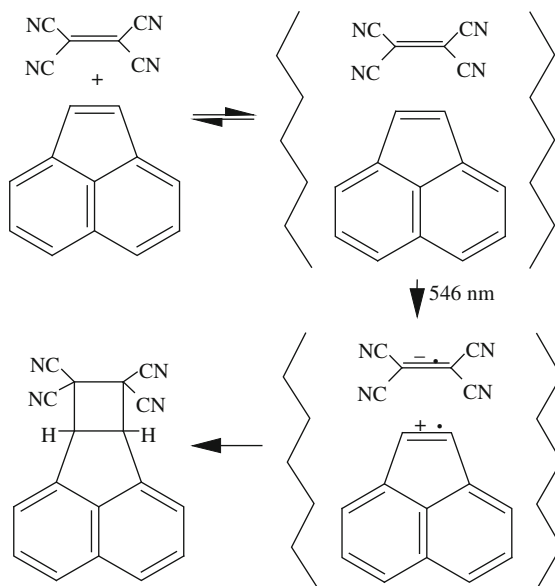
A principal difference between the reactivity of charge-transfer complexes in solution and in crystals was found during photoexcitation of the complex between acenaphthylene and tetracyanoethylene (Haga et al. 1998, 2002). Interaction of these two components in dichloroethane or in acetonitrile leads to the formation of a 1:1 complex. Photoexcitation at the charge-transfer band (at 546 nm) results in the formation of the acenaphthylene cation-radical and the tetracyanoethylene anion-radical as a contact pair. In solution, this contact ion-radical pair is converted into a solvent-separated pair. Between the solvent-separated particles, back electron transfer takes place. This returns the system to the initial neutral components; the system remains chemically inert, and no reaction products are formed. Removal of the solvent leads to the same 1:1 complex that was obtained in the crystalline state.



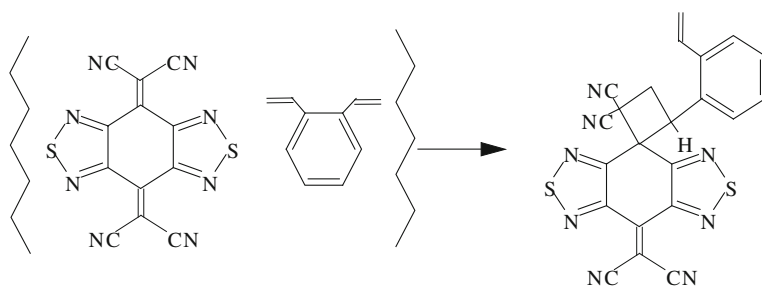
Scheme 3.12 Styrylpyridine hydrochloride photodimerization upon formation of inner charge-transfer complex

X-ray structural data indicate the presence of the two alkenic C=C double bonds in the acenaphthylene–tetracyanoethylene complex no further than 0.4 nm from each other. At the same time, 0.42 nm is the limit value to undergo reaction in the solid state (Haga et al. 1998). Being excited at 546 nm in the crystalline state, this formed contact ion-radical pair retards the deactivation and back electron transfer, but undergoes cycloaddition according to Scheme 3.13. It is the charge-transfer complexation that confines the components close to each other in the crystalline state. This kind of confinement provides rigid mobility to the components and proper proximity of the alkenic C=C double bonds. In the crystalline state, distinctive photoreactivity of the charge-transfer complex results in the ultimate formation of 6*b*,8*a*-dihydrocyclobutano[*a*]acenaphthylene-7,7,8,8-tetracyano.

Scheme 3.14 introduces the reaction between bis{[1,2,5]-thiadiazolo}tetracyanoquinodimethane and 1,2-divinylbenzene. The reaction proceeds in a confined environment, i.e., within the chiral crystal of the charge-transfer complex, upon light



Scheme 3.13 Tetracyanoethylene photocycloaddition to acenaphthylene within solid charge-transfer complex



Scheme 3.14 Bis(thiadiazolo) tetracyanoquinodimethane cycloaddition to divinylbenzene within solid charge-transfer complex

irradiation. The resulting cycloadduct is optically active and is formed in 95% *e, e* purity (Suzuki et al. 1994).

3.9 Closing Remarks

Let us sum up the features of organic chemistry in confined media of charge-transfer complexes. Such reactions proceed more efficiently at lower temperatures and in more polar solvents. Indeed, charge-transfer complexes play a decisive role in a series of chemical reactions that run at low temperatures (Serghehev 1970). Such

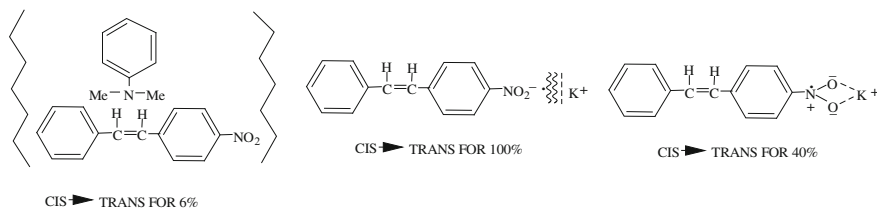
complexes are responsible for the negative temperature coefficients that are observed during halogen addition to double bonds. At low temperatures these additions sometimes proceed with explosive velocities (Serghehev et al. 1973). Charge-transfer complexation puts halogens and olefins in good order and explains the high reactivity of the reactants when added together (Serghehev and Batyuk 1978).

Charge-transfer complexation makes some unusual cyclizations possible and can improve practically useful properties of the obtained polymers. Elucidation of the step concerning the charge-transfer complex formation allows the choice of optimal conditions for vinylic substitution and explains its stereochemical outcome. Geometrical isomerization of alkenes within charge-transfer complexes can be attractive, too.

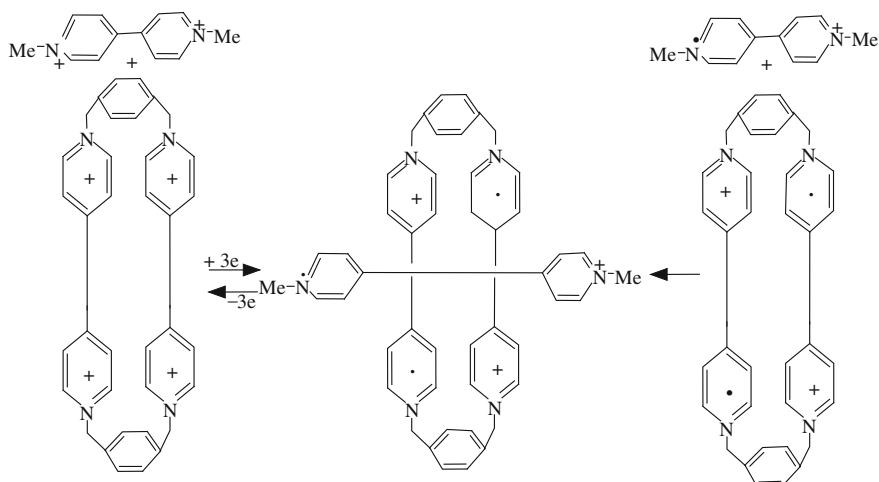
Considering the geometrical conversion of stilbene acceptors confined close to donors in charge-transfer complexes, some restrictions should also be taken into account. The main restrictions are caused by the reversibility of electron transfer and mechanical holding of the stilbene acceptor at the amine donor. Thus, the percentage conversion of 4-nitro-*cis*-stilbene into its *trans* isomer varies, being 6% in the charge-transfer complex with *N,N*-dimethylaniline (Dyusengaliev et al. 1981, 1995), 100% in the state of free anion-radical, and 40% in the state of the ion pair of this anion-radical with the potassium cation (Scheme 3.15) (Todres 1992).

Up to now, only donor-acceptor interaction was regarded as a driving force for charge-transfer complexation. Nevertheless, a pseudorotaxane (Fahrenbach et al. 2012) and a catenane (Zhu et al. 2012) in which donor-acceptor and radical-radical affinity play equal roles have been described. In particular, the middle part of Scheme 3.16 presents the cyclobis(paraquat-*p*-phenylene) bis(cation-radical) as a cavity and the *N,N*-dimethyl-4,4'-bipyridine cation-radical as a stopper. Reduction of the cavity component comes to a halt after reception of two electrons. Reduction of the stopper component discontinues after one-electron transfer. (The stopper component belongs to the class of viologens. In concentrated solutions, viologen cation-radicals exist in dimeric forms that give the violet color to the solutions. On dilution, the violet color recedes and becomes blue on account of the dissociation of the dimer to the monomer. Just the monomeric form of the dimethylviologen cation-radical appears in Scheme 3.16.)

The inclusion compound of Scheme 3.16 was obtained in two ways. In one way, zinc-dust reduction was performed (in acetonitrile and under argon) with the pair of compounds depicted on the left side of Scheme 3.16. Three-electron transfers result



Scheme 3.15 *cis*-4-Nitrostilbene *trans*-isomerization in charge-transfer complex, as free anion-radical and anion-radical pair with K^+



Scheme 3.16 Donor-acceptor and radical-radical interactions between viologen cation-radical and bis(cation-radical) of cyclobis(paraquat-phenylene)

in stopper penetration into the cavity. Reoxidation of the pseudorotaxane by oxygen results in the regeneration of the initial components (left side of Scheme 3.16).

In an alternative approach, the cation-radical of the guest and di(cation-radical) of the host were prepared independently by zinc-dust reduction of the starting materials (in acetonitrile and inside a glovebox). Combination of these individual solutions results in the formation of the 1:1 inclusion complex. In Scheme 3.16, this approach corresponds to movement from the right-side pair to the central pseudorotaxane. The studied system manifests amphiphilic behavior. Both donor-acceptor and radical-radical interactions ensure this type of noncovalent bonding.

References

- Al-Sou'od, Kh A. (2006). *Journal of Inclusion Phenomena and Macrocyclic Chemistry*, 54, 123.
- Burgbacher, G., & Schaefer, H. J. (1979). *Journal of the American Chemical Society*, 101, 7590.
- Dohi, T.; Washimi, N.; Kamitanaka, T.; Fukushima, K. -i., & Kita, Y. (2011). *Angewandte Chemie, International Edition*, 50, 6142.
- Dyusengaliev, K. I., Borisov, Yu A., & Todres, Z. V. (1981). *Izvestiya Akademii Nauk SSSR. Seriya Khimicheskaya*, 30, 1159.
- Dyusengaliev, K. I., Ermekov, D. S., & Todres, Z. V. (1995). *Zhurnal Obshchei Khimii*, 65, 858.
- Fahrenbach, A. C., Barnes, J. C., Lanfranchi, D. A., Li, H., Coskun, A., Gassensmith, J. J., et al. (2012). *Journal of the American Chemical Society*, 134, 3061.
- Gelover-Santiago, A., Naka, K., & Chujo, Y. (2005). *Journal of Polymer Science*, 43A, 6592.
- Haga, N., Nakajima, H., Takayanagi, H., & Tokumaru, K. (1998). *Journal of Organic Chemistry*, 63, 5372.
- Haga, N.; Takayanagi, H.; Tokumaru, K. (2002). *Journal of the Chemical Society, Perkin Transactions*, 2, 734.

- Kadirov, M. K., Nefed'ev, S. E., & Zuev, M. B. (2003). *Izvestiya RAN. Seriya Khimicheskaya*, 859.
- Kiselev, V. D., & Miller, J. G. (1975). *Journal of the American Chemical Society*, 97, 4036.
- Korotehev, S. V., Ermekov, D. S., Todres, Z. V., & Malievskii, A. D. (1992). *Izvestiya Akademii Nauk SSSR. Seriya Khimicheskaya*, 41, 78.
- Kraya, Ch., Singh, P., Todres, Z. V., & Evans, D. H. (2004). *Journal of Electroanalytical Chemistry*, 563, 171.
- Kunz, A. B., Kuklia, M. M., Botcher, T. R., & Russell, T. R. (2002). *Thermochimica Acta*, 384, 279.
- Lemaire, M.; Guy, A.; Imbert, D.; Guette, J.-P. (1986). *Journal of the Chemical Society, Chemical Communications*, 741.
- Miller, J. B., & Salvador, J. R. (2002). *Journal of Organic Chemistry*, 67, 435.
- Neeglund, G. M., & Budni, M. L. (2005). *Spectrochimica Acta*, 61A, 1729.
- Parker, V. D.; Ebersson, L. (1969). *Journal of the Chemical Society, Chemical Communications*, 91, 340.
- Rabie, U. M., Abou-El-Wafa, M. H., & Mohamed, R. A. (2007). *Journal of Molecular Structure*, 871, 6.
- Ryzhakov, A. V., Andreev, V. P., & Rodina, L. L. (2003). *Heterocycles*, 60, 419.
- Serghehev, G. B. (1970). In: *Modern Problems of Physical Chemistry—Sovremennye Problemy Fizicheskoi Khimii*, in Russian (vol. 4, p. 20). Moscow, Russia: Moscow State University Publishing.
- Serghehev, G. B.; Batyuk, V. A. (1978). *Cryochemistry—Kriokhimiya*, in Russian. Moscow, Russia: Khimiya Publishing.
- Serghehev, G. B.; Serguchyov, Yu. A.; Smirnov, V. V. (1973). *Russian Chemical Reviews—Uspekhi Khimii*, in Russian, 42, 1545.
- Steckhan, E. (1978). *Journal of the American Chemical Society*, 100, 3256.
- Suzuki, T., Fukushima, T., Yamashita, Y., & Miyashi, T. (1994). *Journal of the American Chemical Society*, 116, 2793.
- Todres, Z. V. (1992). *Journal of Organometallic Chemistry*, 441, 349.
- Todres, Z. V., Dyusengaliev, R. I., Buzlanova, M. M., Shklover, V. E., & Struchkov, Yu T. (1990). *Zhurnal Organicheskoi Khimii*, 26, 845.
- Todres, Z. V., Dyusengaliev, K. I., & Ustynyuk, N. A. (1982). *Izvestiya Akademii Nauk SSSR. Seriya Khimicheskaya*, 240, 1389.
- Todres, Z. V., Dyusengaliev, K. I., & Sevast'yanov, V. G. (1985). *Izvestiya Akademii Nauk SSSR, Seriya Khimicheskaya*, 1416.
- Todres, Z. V., & Ermekov, D. S. (1992). *Izvestiya Akademii Nauk SSSR. Seriya Khimicheskaya*, 41, 1214.
- Todres, Z. V., & Ionina, E. A. (1992). *Izvestiya RAN. Seriya Khimicheskaya*, 1271.
- Todres, Z. V., & Tsvetkova, T. M. (1987). *Izvestiya Akademii Nauk SSSR. Seriya Khimicheskaya*, 1553.
- Tsiaousis, D., & Munn, R. W. (2005). *Journal of Chemical Physics*, 122, 184708.
- Tyrkov, A. G. (2004). *Izvestiya Vysshikh Uchebnykh Zavedenii, Khimiya i Khimicheskaya Tekhnologiya*, 47, 103.
- Watanabe, H., & Senna, M. (2005). *Tetrahedron Letters*, 46, 6815.
- Yamada, Sh, Tokugawa, Y., Nojiri, Y., & Takamori, E. (2012). *Chemical Communications*, 48, 1763.
- Yamada, Sh, Uematsu, N., & Yamashita, K. (2007). *Journal of the American Chemical Society*, 129, 12100.
- Zhu, Zh, Fahrenbach, A. C., & Li, H.; Barnes, J. C., Liu, Zh., Dyar, S. M., Zhang, H., Lei, J., Carmieli, R., Sarjeant, A. A., Stern, Ch. L., Wasiliewski, M. R., Stoddart, J. F., (2012). *Journal of the American Chemical Society*, 134, 11709.

Chapter 4

Effects of Hydrogen Bonding

4.1 Introduction

Hydrogen bonds are characterized by interaction energies in the range from 5 to 30 kJ/mol. The following energetic characteristics can be extracted from the literature: For the weakest C–H···N and C–H··· π interactions, 6.28–10.47 kJ/mol; for N–H···O, N–H···N, O–H···O, and O–H···N, 12.57–29.33 kJ/mol (see, e.g., Zhang et al. 2011; He et al. 2012). Such energy is the largest among the noncovalent interactions. Although noncovalent interactions are weak, hydrogen bonding is able to govern the assemblage of organic guests at the correct distance and angle; see, for instance, Imai et al. (2008). Below are several principal examples of control with the help of hydrogen bonds.

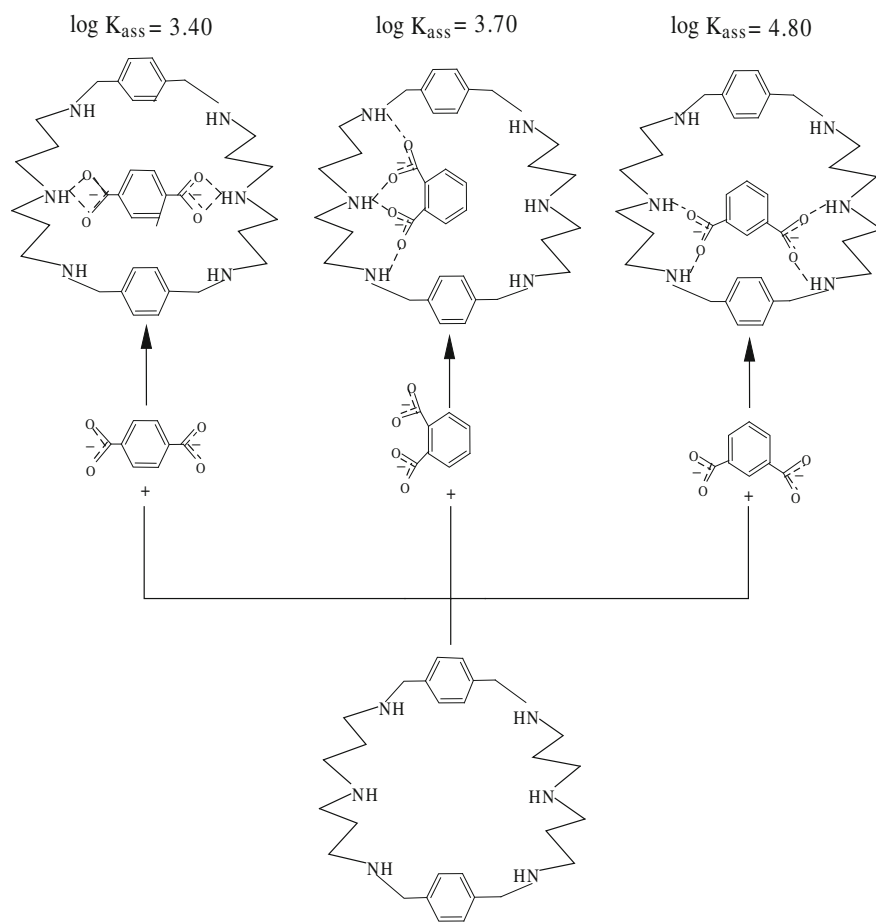
4.2 Host–Guest Arrangement in Hydrogen-Bond Complexes

In water solution at pH 5.0, the hexaazamacrocyclic of Scheme 4.1 binds isophthalate with selectivity of over 89 versus terephthalate (Arbuse et al. 2007). Through its carboxylate functions, isophthalate forms four hydrogen bonds with NH groups of the azamacrocyclic, whereas terephthalate forms only two such bonds. Phthalate with its three hydrogen bonds between carboxylate and the NH groups forms a complex which is slightly stronger compared with that of terephthalate. The complex with isophthalate remains the strongest one. This is also evident from the magnitudes of the corresponding association constants: log 4.80 for isophthalate, log 3.70 for phthalate, and log 3.40 for terephthalate; see also Scheme 4.1 (Arbuse et al. 2007).

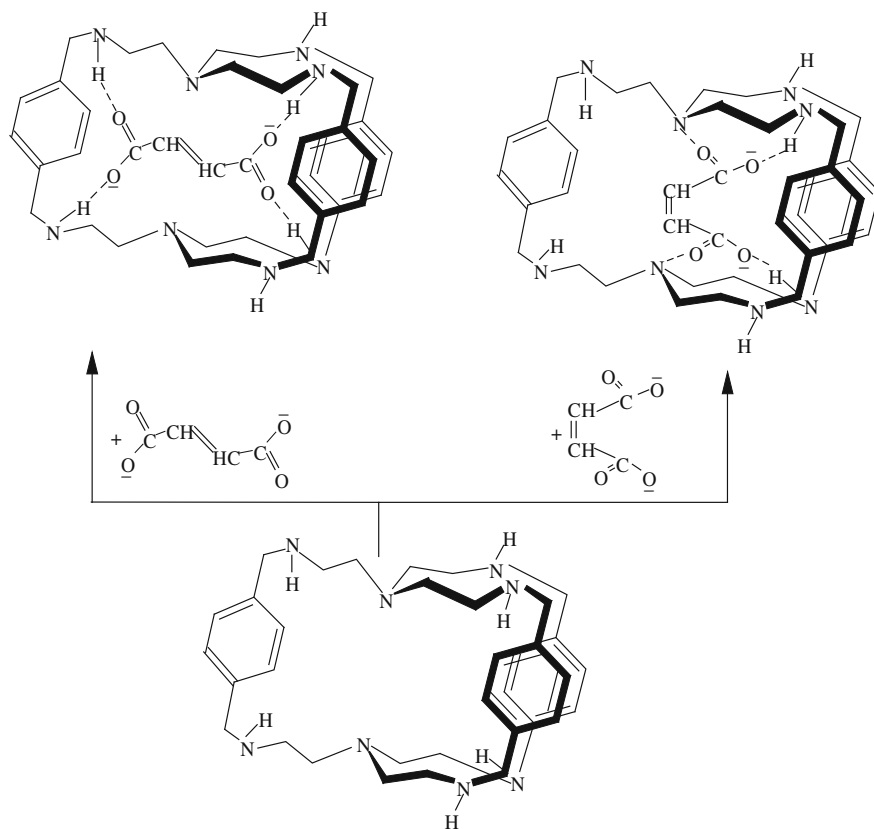
Methylation of the central secondary amino groups in the host of Scheme 4.1 reduces the log K_{ass} value for the isophthalate guest (from 4.80 to 3.02). This effect originates from the incapability of the central N–Me fragments to participate in hydrogen bonding and, besides, the lower capability for these fragments to rotate (Arbuse et al. 2007).

(Mateus et al. 2012) prepared polyamine macrobicyclic receptors that exhibit unprecedented selectivity for fumarate over other dicarboxylate competitors, including its *cis* isomer maleate (Scheme 4.2). The receptors work in water at pH of about 4. Oxalate, malonate, succinate, glutarate, maleate, and fumarate were tested. The authors ascribed the lower affinity of all of them (excluding fumarate) to worse fit to the receptor cavity arising from their own conformational preferences and flexibility. The fumarate anion has the right size, shape, and rigidity to fit into the cavity of the receptors. Namely, fumarate can be retained inside the cavity through four hydrogen bonds. Scheme 4.2 shows that maleate forms only two hydrogen bonds and two coordinative ones, therefore being held more weakly.

The search for receptors appropriate for fumarate remains an unresolved and very important medicobiological problem. Dicarboxylates are key intermediates of the



Scheme 4.1 H-bond complexation of benzene dicarboxylates with hexaazamacrocycle



Scheme 4.2 Fourfold H-bond fastening of fumarate against twofold H-bond and twofold coordinative fastening of maleate to polyamine macrocycle

Krebs cycle, the metabolic pathway used by all aerobic organisms for energy production. Fumarate is one such metabolic intermediate, formed by oxidation of succinate with the enzyme succinate dehydrogenase. Metabolically produced fumarate is then converted by the enzyme fumarase to malate, $^- \text{OCOCH}_2\text{CH}(\text{OH})\text{COO}^-$. From the review by Briere et al. (2006), mutations impairing the function of fumarase in humans cause accumulation of fumarate and are related to the development of cutaneous and uterine leiomyomas and papillary renal cell cancer. In addition, it was suggested that accumulation of fumarate competitively inhibits the 2-oxoglutarate-dependent dioxygenases, activating oncogenic hypoxia pathways that lead to tumor-formation predisposition (Ratcliffe 2007). It is clear that the design of a synthetic receptor that selectively binds fumarate in the presence of structurally similar or isomeric competitors is very important.

Condensation of 1-methoxy-4-(octyloxy)benzene (1 equivalent) and 1,4-dimethoxybenzene (4 equivalents) in dichloroethane solution containing paraform

(5 equivalents) and catalytic amounts of boron trifluoride etherate leads to copillar[5]arene with an octyloxy branch (Zhang et al. 2011). The crystal structure revealed that the product was not formed as a monomer. In this crystal structure, the octyl group of the copillararene penetrates deeply into the electron-rich cavity of another adjacent copillararene monomer, and the resulting dimer is connected with a third monomer through the octyl branch, and so on. The resulting rod-like head-to-tail supramolecular polymer runs across the entire crystal. Hydrogen atoms of the included octyl group form C–H $\cdot\pi$ bonds with copillararene benzene rings. In solution, NMR experiments corroborate this kind of interaction (Zhang et al. 2011). Scheme 4.3 outlines the reaction. The authors gave no data on the technical applicability of such a supramolecular polymer, but remarked that their study affords the first example of polymerization driven by C–H $\cdot\pi$ interactions.

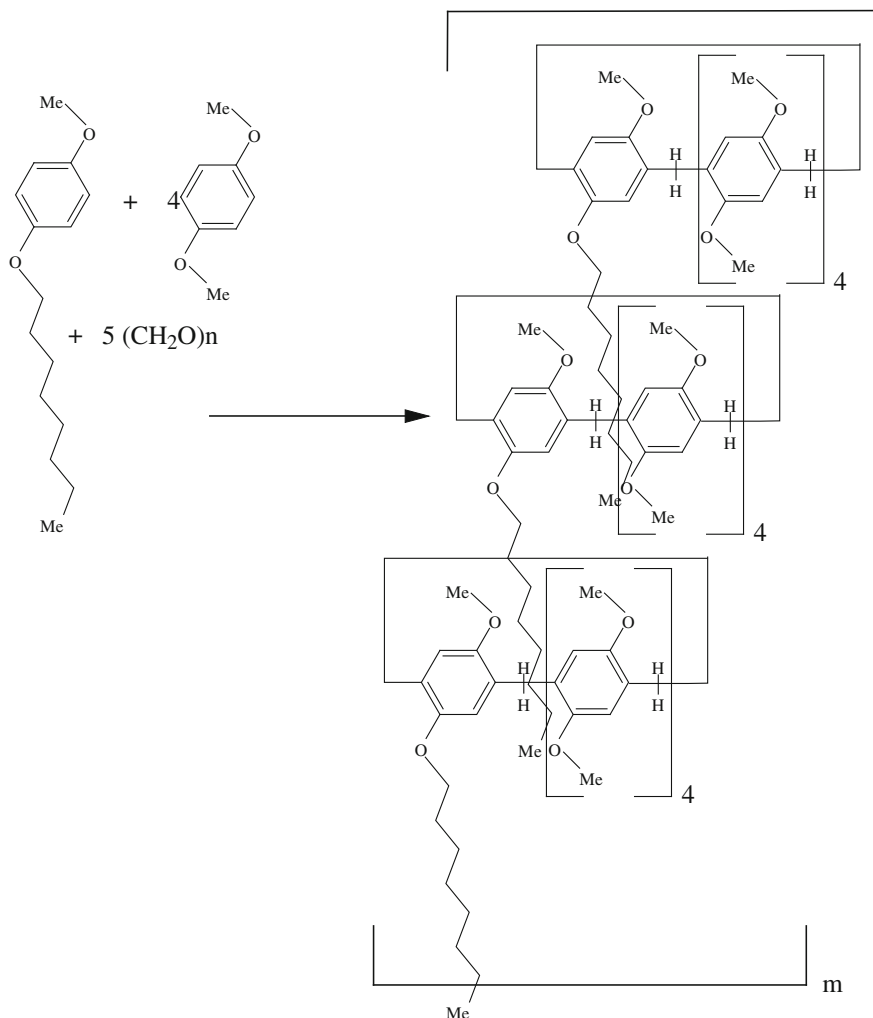
Scheme 4.4 presents photocyclization of dihydrochloride of a diaminobutane derivative. The reaction proceeds in water solution and is accompanied by coloring of the solution to yellow (the initial ring-opened compound being colorless). This coloring process is recommended for use in optical applications such as optical memory and switching devices (Liu et al. 2008). For optical devices, photofatigue is a limiting property. The process presented in Scheme 4.4 is indeed a photofatigue process. The point is that the dihydrochloride undergoes hydrolysis in the aqueous medium, resulting in the formation of the diamine in free (nonprotonated) form. The nonprotonated form is sensitive to air oxidation, especially in conditions of photoexcitation.

When the opened-chain initial compound was encapsulated into cucurbit[6]uril, hydrogen bonding took place between protons of both ammonium groups and the carbonyl groups surrounding the cucurbituril portal. This protects the ammonium chloride groups from hydrolysis but does not prevent photocyclization (Scheme 4.5). Closure and cleavage of the ring are observed at wave lengths 250 nm and 365 nm, respectively. Whereas unprotected compounds are destroyed during irradiation cycles, the ammonium-carbonyl hydrogen-bound (protected) compounds are stable for more than 200 irradiation cycles (Liu et al. 2008).

Sixfold hydrogen bonding of barbituric acceptors with tweezer-like merocyanine donors leads to head-to-tail bimolecular complexes with increased dipole moments. In these complexes, summation of dipole moments takes place. Enhancement of the dipole moment is highly desirable for building of nonlinear optical and photorefractive polymeric composite materials; for examples of this, see Schmidt et al. (2008).

4.3 Hydrogen-Bonding Effects on Reactivity of Confined Guests

When included into β -cyclodextrin, α -azido aryl ketones can be asymmetrically reduced by sodium borohydride in water. The resultant 2-azido-1-arylethanol is obtained in yields up to 95% with very high *e*, *e*-enantioselectivity up to 80% (Scheme 4.6) (Reddy et al. 2001). The authors ascribed the stereoselectivity of the reaction to hydrogen bonding between the substrate carbonyl group and wider-rim secondary

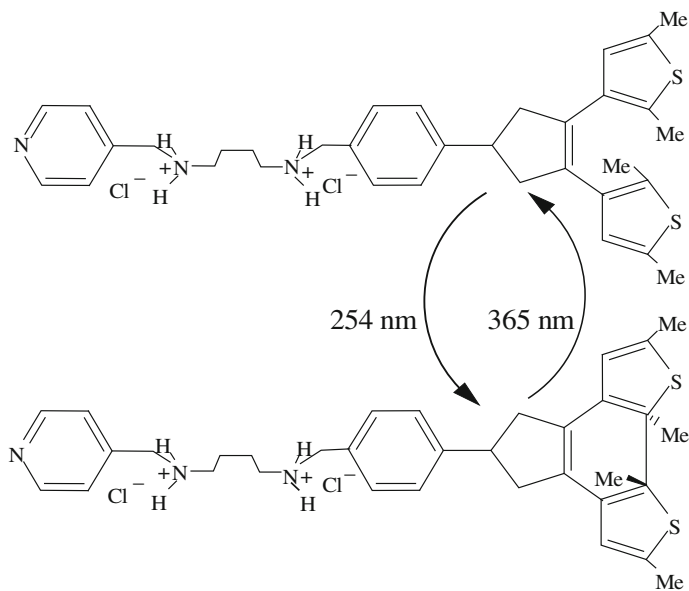


Scheme 4.3 Formation of polymeric pillar[5]arene from (octyloxy) benzene, paraform and dimethoxy benzene in crystal governing by [C—H (octyl)]-(benzene- π) H-bond interaction

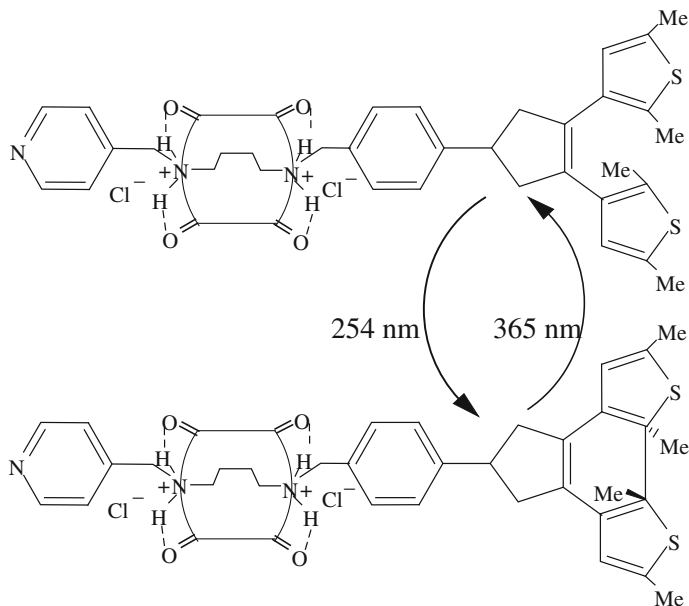
hydroxyl group of β -cyclodextrin. This fixes the outward position of the carbonyl with respect to the inserted aromatic component and decreases the degrees of freedom of the guest molecule (Scheme 4.6).

Generally speaking, the rims of the cyclodextrin pail have great potential to interact with guest molecules through hydrogen bonds under conditions of polar interaction supported by the hydrophobic nature of the pail cavity.

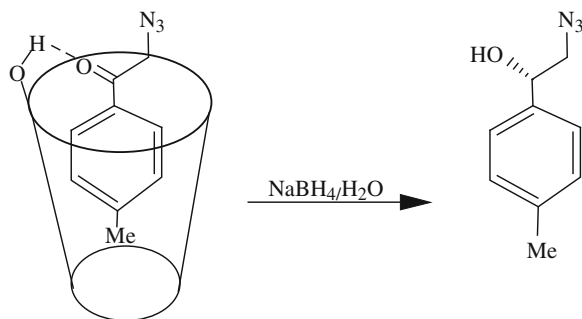
Azomethynes (imines or Schiff bases) react with amines so that amines of higher basicity displace amines of lower basicity. Scheme 4.7 gives an opposite example



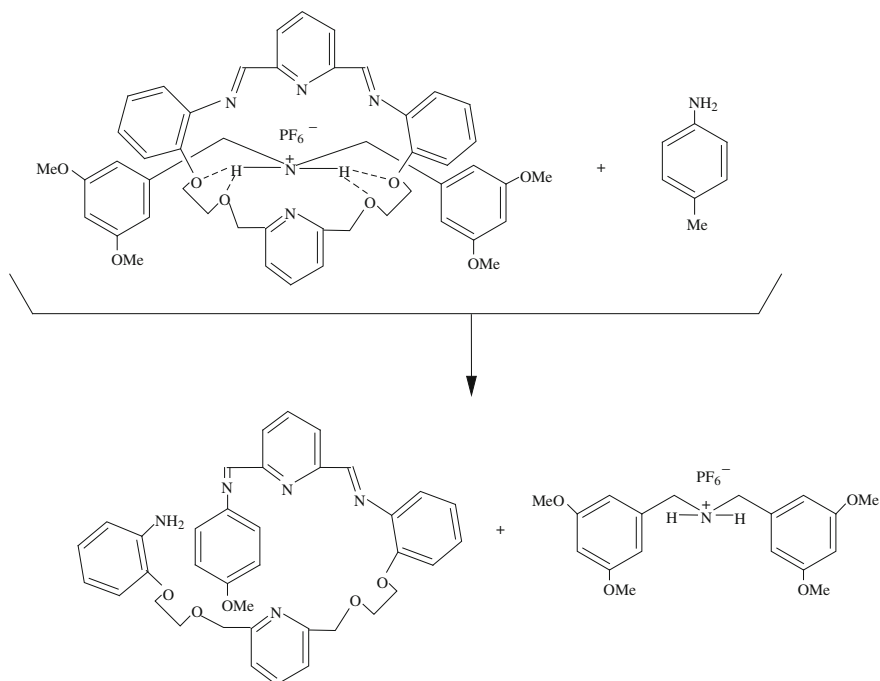
Scheme 4.4 Reversible inner condensation of diaminobutane dihydrochloride upon photoirradiation



Scheme 4.5 Prevention of hydrolysis in starting and final products by inclusion and H-bond complexation with cucurbituril



Scheme 4.6 Stereospecific reduction of azidoaryl ketone governing with H-bonding between guest ketone carbonyl and host (cyclodextrin) hydroxyl



Scheme 4.7 Azomethyne component displacement by 4-methylaniline specified with H-bond complexation

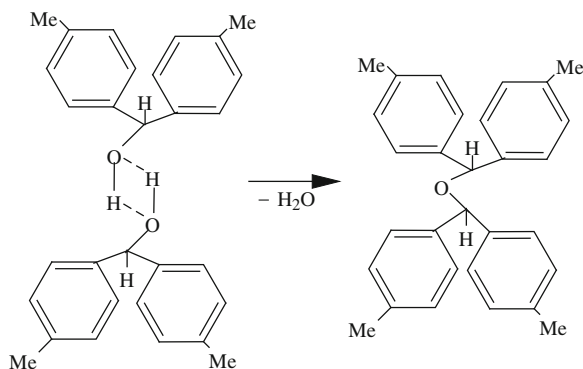
where the less basic amine, *para*-methylaniline, displaces the formally more basic amine, *ortho*-alkoxyaniline in a hydrogen-bonded rotaxane (Leung et al. 2010). Hydrogen bonding weakens the alkoxyaniline basicity, enabling its displacement by *para*-methylaniline.

When hydrogen bonding and ionic interactions act together, the host–guest binding energy is increased. Although the complexes formed by hydrogen bonds are

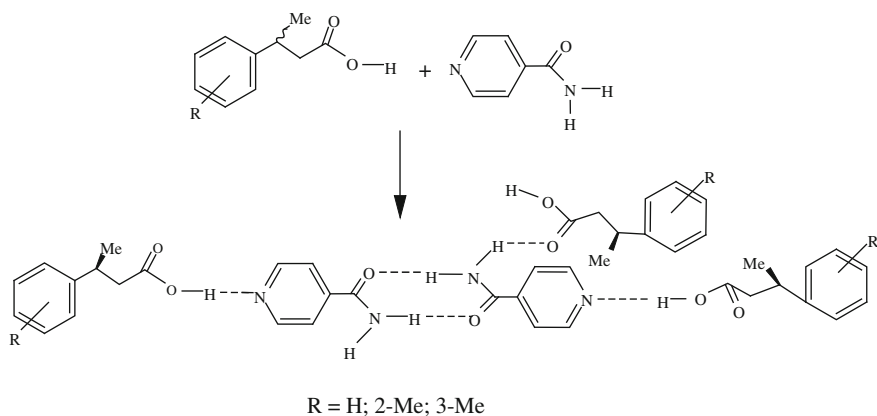
weak, they become stronger when several hydrogen bonds are established. Thus, 4-methylbenzohydrol molecules form a dimer that is well connected by two hydrogen bonds. The solid dimer is obtained upon recrystallization from ether or as a result of grinding in an agate mortar with a pestle. The structure of the dimer was established by X-ray crystallographic method at room temperature (Scheme 4.8). The H-bonded dimer is hydrolyzed upon the action of 4-methylbenzene-4-sulfonic acid (TosOH) at room temperature or even at 15°C during 10 min. The corresponding ether was obtained in 96% yield. When the reaction was performed using the same temperature and duration but in methanol, the yield was found to be lower, namely 10% (Toda et al. 1990; Toda and Okuda 1991). Due to the hydrogen bonding, the two alcohol molecules are held in close proximity. The action of TosOH on the pair of alcohols results in a carbonium ion from one of the alcoholic components. This carbonium ion, in the confined space and due to its close proximity, attacks the second alcoholic molecule. In the confined condition, the interaction of the alcohol with the carbonium ion facilitates etherification and makes it stereospecific. The obtained ethers retain the configuration of the starting alcohols. Methanol reduces the yield by partially destroying the H-bonded dimer and decreasing the carbonium participation.

4.4 Hydrogen-Bonding Effects in Organic Co-Crystals

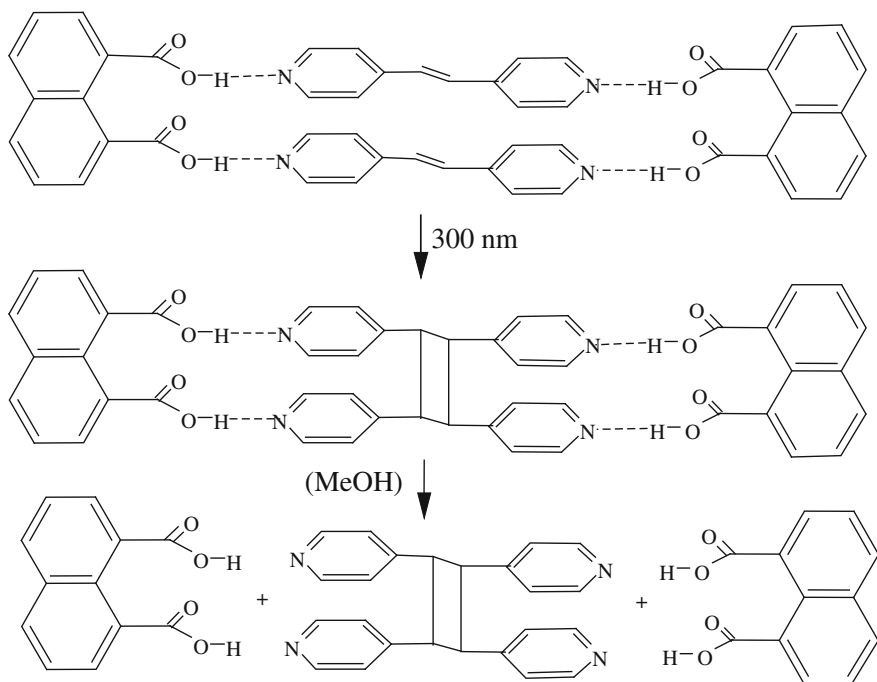
Eccles et al. (2011) proposed the use of the hydrogen-bonding effect in co-crystals for the determination of the absolute stereochemistry of substituted 3-arylbutanoic acid. This method requires small sample amounts; it is applicable to liquid substances and can serve as an alternative to salt formation. In this approach, the mentioned acids were ground with isonicotinamide in equimolar ratio, and the blend thus prepared was dissolved in 7:3 acetonitrile–acetone mixture. The solution was allowed to stand in ambient conditions, and co-crystals were obtained by slow evaporation of the



Scheme 4.8 Formation of benzhydrol dimer and role of H-bonding between neighboring two substrates in crystal

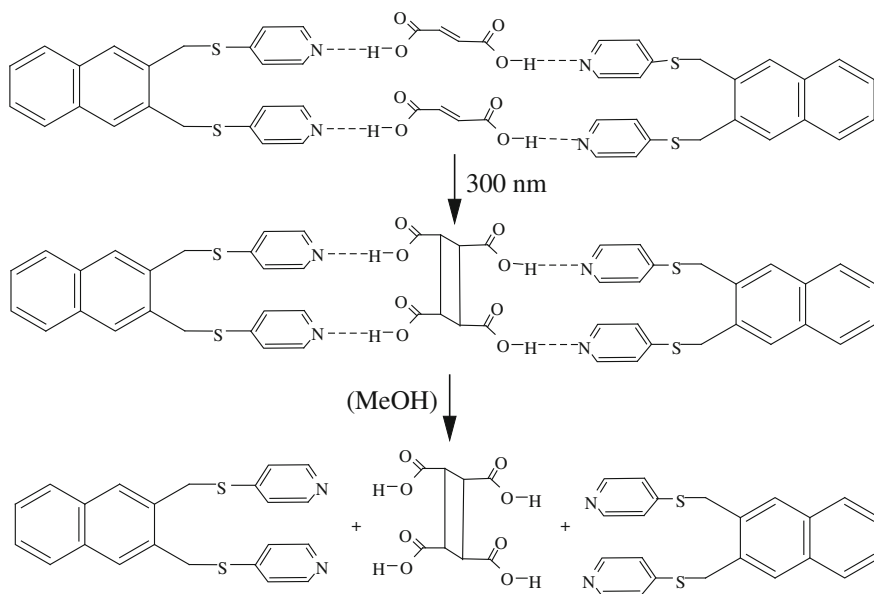


Scheme 4.9 Deracemization of beta-methyl-beta-aryl butanoic acid in its crystalline H-bond complex with isonicotinamide



Scheme 4.10 Photodimerization in crystalline complex formed by H-bonds

solvent. The resultant species were suitable for single-crystal diffraction. Using pure (*S*) isomers of the acid, the authors established retention of this (*S*)-configuration in the co-crystals. Acid racemates with isonicotinamide form pure co-crystals with the



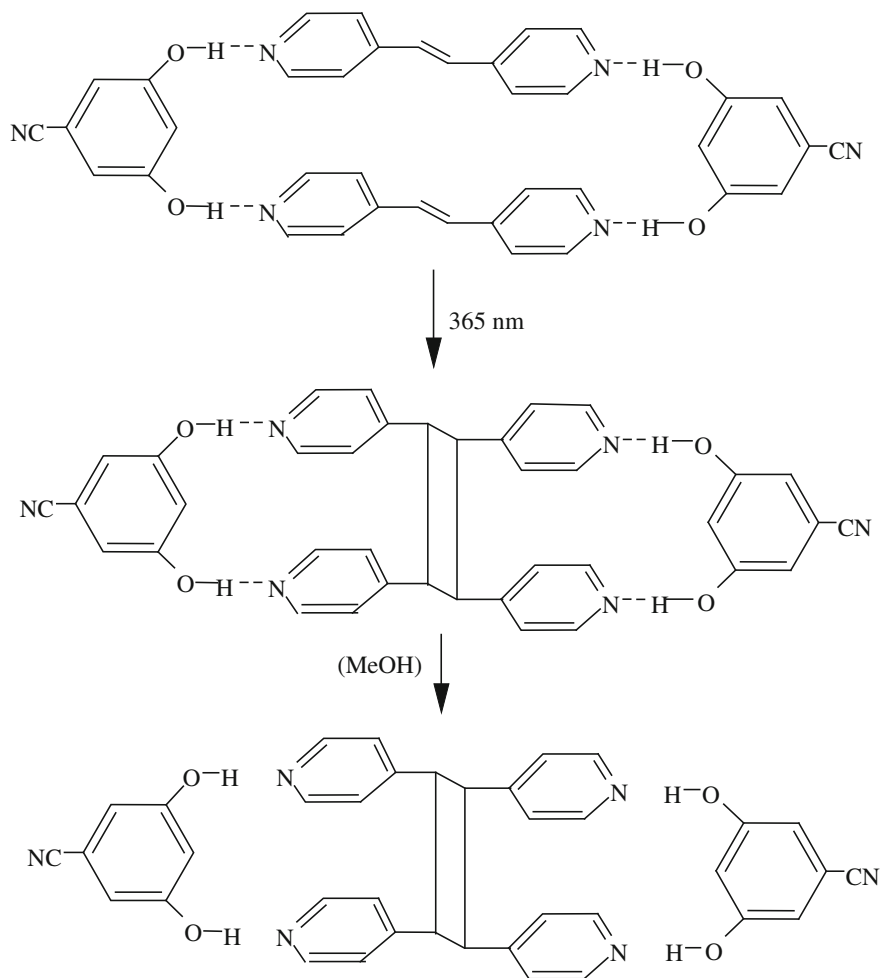
Scheme 4.11 Fumaric acid photodimerization in crystalline H-bond complex with pyridine moieties

(*S*)-enantiomers. Scheme 4.9 illustrates the role of hydrogen bonding in the formation of the co-crystal architecture.

Schemes 4.10 and 4.11 (MacGillivray 2008) and 4.12 (Karunatilaka et al. 2011) present photodimerization proceeding in crystalline complexes that contain confined organic components fastened by hydrogen bonds with donor and acceptor character. Release of the dimer formed from the H-bonded complexes takes place during dissolution in methanol (MacGillivray 2008).

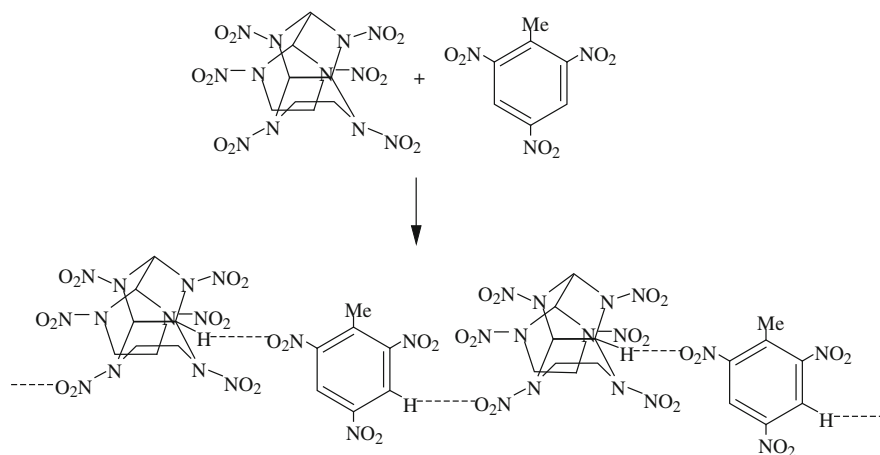
Similarly to the reaction of Scheme 4.12, the same tetrakis(pyridyl)cyclobutane was quantitatively obtained from the photoinitiated reaction of the co-crystal between 4,6-dichlororesorcinol (2 equivalents) and 1,2-bis(4-pyridyl)-*trans*-ethylene (also 2 equivalents). The equimolar mixture of the starting materials co-crystallizes from solution or on vortex grinding (Stojakovic et al. 2012).

Co-crystallization with trinitrotoluene (TNT) allows improved stability and functionality of a caged high-energy nitramine with the industrial name CL-20 (Bolton and Matzger 2011). The product has the structure depicted in Scheme 4.13 and is now being produced in France in quantities of 50–100 kg in an industrial pilot-scale plant (Akhavan 2010, p. 15). A nonaromatic cyclic nitramine, CL-20 features high density, high detonation velocity, and favorable oxygen balance. However, practical application of CL-20 as an explosive is complicated by safety standards: It detonates readily upon physical impact. At the same time, TNT has poor density, low oxygen balance, and modest detonation velocity, but features low sensitivity to impact (Akhavan 2010). In the co-crystal, CL-20 and TNT are bound preferentially by interactions involving nitro groups and aliphatic hydrogens of CL-20 with the 3-position

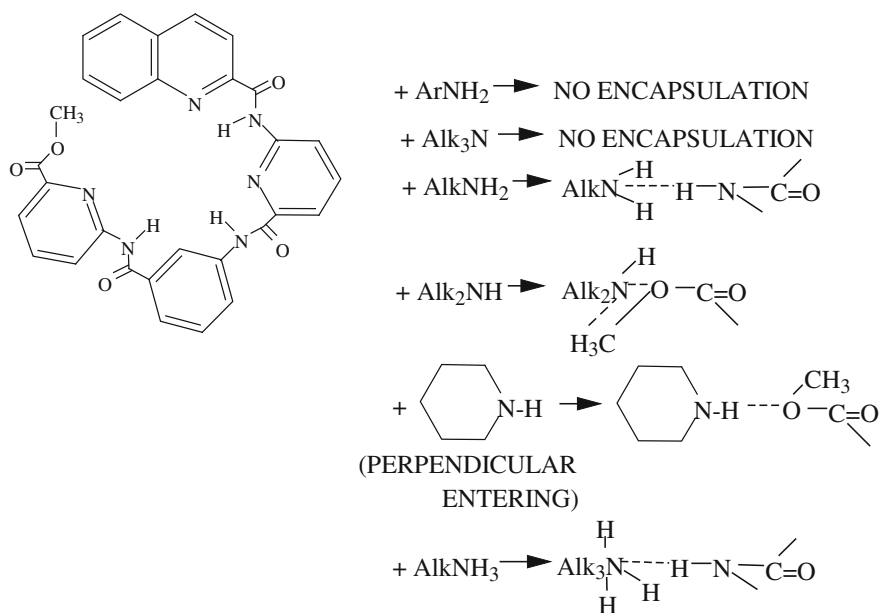


Scheme 4.12 Photodimerization of 1,2-dipyridylethylene in H-bond crystalline complex with resorcinol

hydrogen and the 6-nitro group of TNT. Scheme 4.13 shows the shortest contacts in the co-crystal (data from X-ray diffraction and Raman spectroscopy; Bolton and Matzger 2011). Incorporating insensitive TNT into a co-crystal with sensitive CL-20 greatly reduces its impact sensitivity and improves the viability of CL-20 in explosive applications. (Note that it is both dangerous and illegal to participate in unauthorized experimentation with explosives.)



Scheme 4.13 Hydrogen bonding between CL-20 and TNT explosives in their co-crystal



Scheme 4.14 Structure of amine or ammonium ions in connection with their possibility of entering into helical host cavity

4.5 Closing Remarks

It should be noted that the interaction between a host and a guest can proceed through nontrivial hydrogen-bonding interactions. The helical host of Scheme 4.14 was experimentally investigated using the nuclear Overhauser effect (in CDCl_3) and theoretically by an ab initio method at B3LYP/6-31G level (Ong et al. 2012). The cavity enclosed by these pyridine foldamers is ca. 0.25 nm in radius. The host is decorated by both H-bond donors (amide protons) and H-bond acceptors (pyridine N-atoms and ester O-atoms). Based on methods mentioned above, H-bond types were studied for complexes between this helical host and amines or alkylammonium ions. The main hydrogen-bonding interactions are shown in Scheme 4.14. A more detailed description of the H-bonds formed follows:

- (1) Tertiary and aromatic amines do not interact with the host. Tertiary amines contain no protons, and aromatic amines are too weak in basicity.
- (2) Primary amines sit in the cavity with the amine N-atom forming a strong H-bond with the amide proton.
- (3) Acyclic secondary amines form H-bonded complexes through the amine N-atom and the ester O-atom with weak participation of a methyl proton in OCOCH_3 fragment. There is also a weak interaction of these amines with protons of the three amide groups of the host.
- (4) The cyclic secondary amines (e.g., piperidine) enter almost perpendicularly into the cavity of the host. The N–H proton in piperidine forms a strong H-bond with the ester O-atom and a weak H-bond with the pyridine N-atom.
- (5) Alkylammonium ions interact with all three of the amide protons and also with the ester methyl group of the host.

These observations based on proton nuclear magnetic resonance experiments illustrate that different amine and ammonium guests each display a different binding mode with the host of Scheme 4.14. This should be taken into account in the design of new H-bonded complexes and when studying the reactivity of confined species.

References

- Akhavan, J. (2010). *The Chemistry of Explosives* (2nd ed.). Cambridge, UK: The Royal Society of Chemistry.
- Arbuse, A., Anda, C., Martinez, M. F., Perez-Miron, J., Jaime, C., Parella, T., et al. (2007). *Inorganic Chemistry*, *46*, 10632.
- Bolton, O., & Matzger, A. J. (2011). *Angewandte Chemie International Edition*, *50*, 8960.
- Briere, J.-J., Favier, J., Gimenez-Roqueplo, A.-P., & Rustin, P. (2006). *American Journal of Physiology. Cell Physiology*, *291*, C1114.
- Eccles, K. S., Deasy, R. E., Fabian, L., Marguire, A. R., & Lawrence, S. E. (2011). *Journal of Organic Chemistry*, *76*, 1159.
- He, Z., Liu, D., Mao, R., Tang, Q., & Miao, Q. (2012). *Organic Letters*, *14*, 1050.
- Imai, Yo, Murata, K., Sato, T., & Kuroda, R. (2008). *Organic Letters*, *10*, 3821.

- Karunatilaka, Ch., Bucar, D.-K., Dizler, L. R., Frisic, T., Swenson, D. C., MacGillivray, L. R., Tivanski, A. V. (2011). *Angewandte Chemie International Edition*, 50, 8642.
- Leung, K. Ch.-F., Wong, W.-Ya., Arico, F., Haussmann, Ph. C., & Stoddart, J. F. (2010). *Organic & Biomolecular Chemistry*, 8, 83.
- Liu, J., Xu, Y., Li, X., & Tian, H. (2008). *Dyes Pigments*, 76, 294.
- MacGillivray, L. R. (2008). *Journal of Organic Chemistry*, 73, 3311.
- Mateus, P., Delgado, R., Brandao, P., & Felix, V. (2012). *Journal of Organic Chemistry*, 77, 4611.
- Ong, W. Q., Zhao, H., Sun, Ch., Wu, J'.E., Wong, Z., Li, S.F.Y. et al. (2012). *Chemical Communications*, 48, 6343.
- Ratcliffe, P. J. (2007). *Cancer Cell*, 11, 303.
- Reddy, M. A., Bhanumathi, N., & Rao, K. R. (2001). *Chemical Communications*, 1974.
- Schmidt, J., Schmidt, R., & Wuerthner, F. (2008). *Journal of Organic Chemistry*, 73, 6355.
- Stojakovic, J., Farris, B. S., & MacGillivray, L. R. (2012). *Chemistry Communications*, 48, 7958.
- Toda, F., Okuda, K. (1991). *Journal of the Chemical Society, Chemical Communications*, 1212.
- Toda, F., Takumi, H., Akehi, M. (1990). *Journal of the Chemical Society, Chemical Communications*, 1270.
- Zhang, Z., Luo, Y., Chen, J., Dong, Sh., Yu, Y., Ma, Zh. et al. (2011). *Angewandte Chemie International Edition*, 50, 1397.

Chapter 5

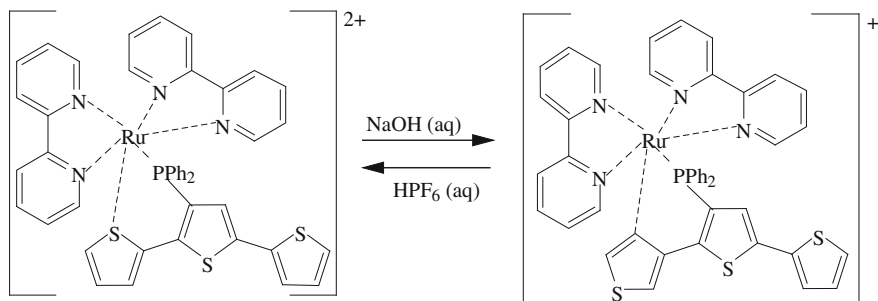
Effects of Coordination to Metals

5.1 Introduction

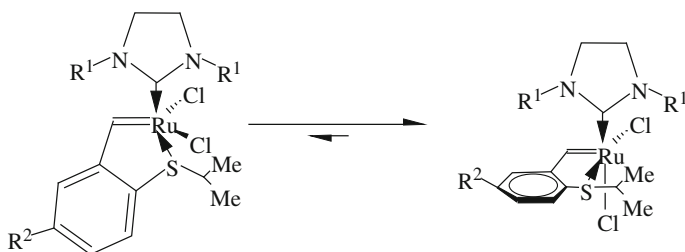
This chapter considers reactions taking place within organometallic complexes. These reactions are of great importance for cyclization of ligands governed by their coordination to a metallic center. The coordination can be temporary or permanent. This topic is well documented, and the most significant examples are cited in this chapter. Less well known are isomerization reactions such as the circle dance of coordinated ligands or changes in the geometry of the ligand surroundings. Several examples of these confined transformations are also presented to attract readers' attention to this problem.

5.2 Organic-Ligand Isomerization Within Metallocomplexes

Moorlag et al. (2002, 2005) prepared the metal complexes of Scheme 5.1, in which ruthenium bis(dipyridyl) was coordinated to 3'-phosphinoterthiophene via a diphenylphosphine linker and thienyl sulfur (P,S bonding). Upon treatment with a base, switching of the thiophene coordination from Ru-S (P, S-bonding) to Ru-C (P,C bonding) was observed. This process is reversible: Addition of acid regenerates the S-coordinated complex. The authors did not indicate a driving force for the reaction but pointed out that the P,C-bonding mode is flatter than the P,S-bonding. As can be seen from Scheme 5.1, the switching from the P,S to the P,C mode is accompanied by electron transfer from the base to the P,S-complex. Because the P,C-complex is flatter than the P,S-complex, the conditions for delocalization of the transferring electron become more favorable. Besides, it is suggested that reduction of the initial complex weakens bonds connected with the swinging thiophene ring, which could facilitate the observed switching.



Scheme 5.1 Change of ligand coordination (from P,S to P,C) within organoruthenium complex



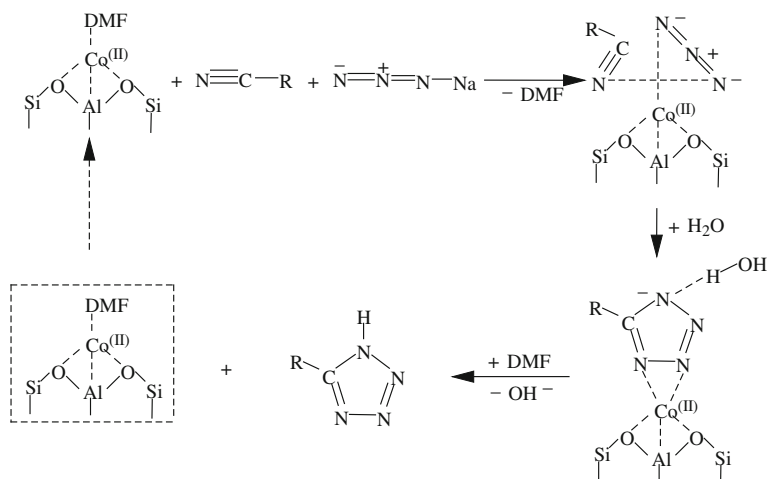
Scheme 5.2 Change of ligand disposition in dichlorosulfur benzylidene complex with ruthenium

As can be seen from Scheme 5.1, the circle dance of the coordinated thienyl fragment in the terthiophene ligand proceeds within the metallocomplex. This is an example of a confined reaction.

When dissolved, dichloro sulfur-chelated ruthenium benzylidenes undergo *cis*-dichloro \rightarrow *trans*-dichloro isomerization according to Scheme 5.2 (Aharoni et al. 2011). Analogous isomerization was established for dichloro oxygen-chelated ruthenium alkylidenes (Zirngast et al. 2011). The isomerization rate is dependent on the nature of the solvent. Although clearly defined correlation was not reported, it is obvious that the solvent can use the empty coordination site of the 16-electron ruthenium center. This causes electron redistribution within the whole complex and lowers the barrier for isomerization. The alkylidene ligand changes its conformation, and chlorine atoms alter their mutual orientation. The ligand bonds with the ruthenium atom retain their integrity.

5.3 Metal-Coordination Assemblage

There are reactions in which the structure of the forming monomolecular organic compound is defined by the coordination of the starting materials to a metal. The metallic center coordinates the reactants and thus orients them; see, for instance,



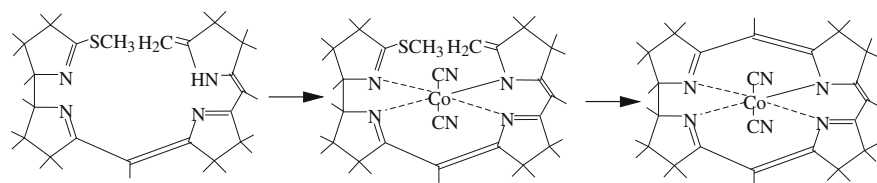
Scheme 5.3 Tetrazole formation from organyl nitriles and sodium azide via their coordination to cobalt in CoY zeolite

Cucciolito et al. (2008). Without the metal, the target product is not formed at all. This metal templating effect is used to prepare cyclic compounds.

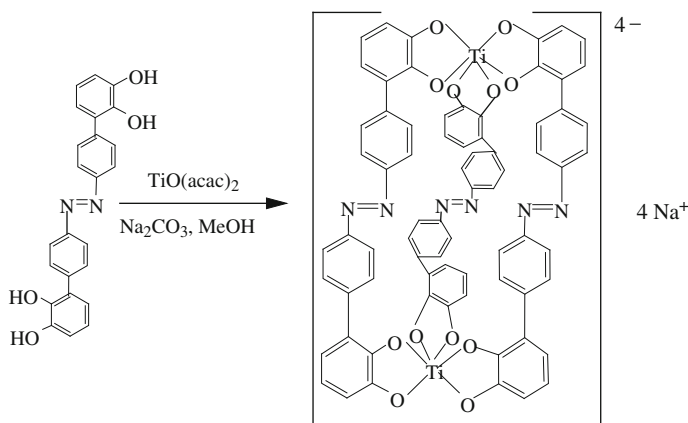
One simple example is the synthesis of 5-substituted 1*H*-tetrazoles based on reusable CoY zeolite Scheme 5.3 (Rama et al. 2011). The authors reported on the optimal reaction conditions as follows: dimethylformamide (DMF) as solvent, 120 °C, and 14h duration. Yields were good to excellent. Being bound to zeolite Y (to trivalent aluminum), cobalt(II) coordinates readily to nitriles and sodium azide, and this is the dominant factor in assemblage of the tetrazole five-membered cycle. Release of tetrazoles from the cobalt coordinative complex takes place as a result of hydrolysis. At the same time, the CoY zeolite is released for the next cycle of reactions, its structural integrity remaining unaltered.

Another example of metal-governed assemblage is the synthesis of corrin, the “core” for vitamin B₁₂ (Nelson and Cox 2000). Scheme 5.4 illustrates the template effect in corrin synthesis.

In the absence of the cobalt component, the starting compound transforms into the *endo* isomer, which is useless for further synthesis. When the required *exo* structure



Scheme 5.4 Corrin cyclization within open-ligand cobalt complex



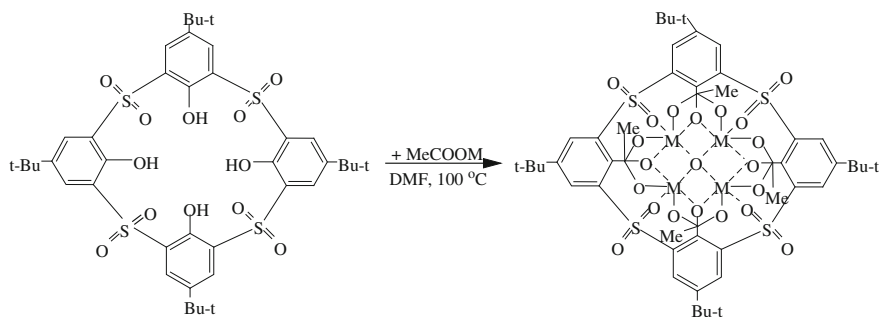
Scheme 5.5 Cage-like assemblage of bis(dihydroxyphenyl) trans-azobenzene complex with titanium oxyacetylacetonate

can be secured, the dicyanocobalt derivative can be obtained. In the complex, the cobalt provides spatial proximity of the thiomethyl and methylene groups, which is decisive for the corrin cycle formation. The cobalt is also needed in vitamin B₁₂.

Reaction of titanium^{IV} oxyacetylacetonate with 4,4'-bis (2,3-dihydroxyphenyl)-*trans*-azobenzene results in the cage-like assemblage depicted in Scheme 5.5 (Yamamura et al. 2012). The assemblage prevents *cis* → *trans* photoisomerization. Under the same conditions, the noncoordinated starting compound easily undergoes *cis* → *trans* photoisomerization. According to the authors, the inhibition of photoisomerization is based on either the conformational rigidity of the cage-like assembly or the tightening effect of the titanium-catecholate node (Yamamura et al. 2012).

Dai and Wang (2012) attempted the introduction of a class of metalorganic derivatives from calixarene analogs, in which the methylene units are replaced by sulfur linkages, Scheme 5.6. Sulfonylcalix[4]arenes bearing hydroxyl groups at the lower rim and *tert*-butyl substituents at *para*-positions of phenyl rings (at the upper rim) react with manganese, cobalt or nickel diacetate. As a result, the starting thiocalixarene container is bound with a metalorganic knot, where four phenoxo and four sulfonyl oxygen atoms coordinate to four metal ions that are further bound by four acetate groups and one μ_4 -hydroxo oxygen. Scheme 5.6. In other words, the resulting compound has both *endo* and *exo* domains. The authors replaced acetate by 1,3,5-benzenetricarboxylate and prepared the metalorganic domains as nanosized capsules. These symmetric and unique coordination capsules contain both internal and surface cavities, a trademark feature of viruses, which use the enclosed space to store genetic material (i.e., DNA or RNA) and the surface binding sites to recognize specifically targeted hosts. This makes such metalorganic sulfonylcalixarenes promising for allosteric catalysis, biosensing, and controlled drug delivery.

Template syntheses governed by alkali metal cations, as a rule, lead to macrocycles that are free from the metal; For instance, reaction of thiophene-2,5-dithiocyanate



Scheme 5.6 Knotting of sulfonyl calixarene with metal acetoacetate

with an equimolar amount of cyclooctatetraene dipotassium in tetrahydrofuran results in the formation of the potassium-free tetra(thienylene-2,5)-cyclooctadisulfide (Scheme 5.7 (Todres et al. 1973)).

The cyclic structure of the product was established by X-ray analysis. The diameter of the cavity of the obtained multiheterocycle matches twice the radius of the potassium cation. Nevertheless, the cation is absent from the final product (Todres et al. 1979a). The potassium cation again acts as a coordination center, but it leaves the cavity once the cyclization has been achieved.

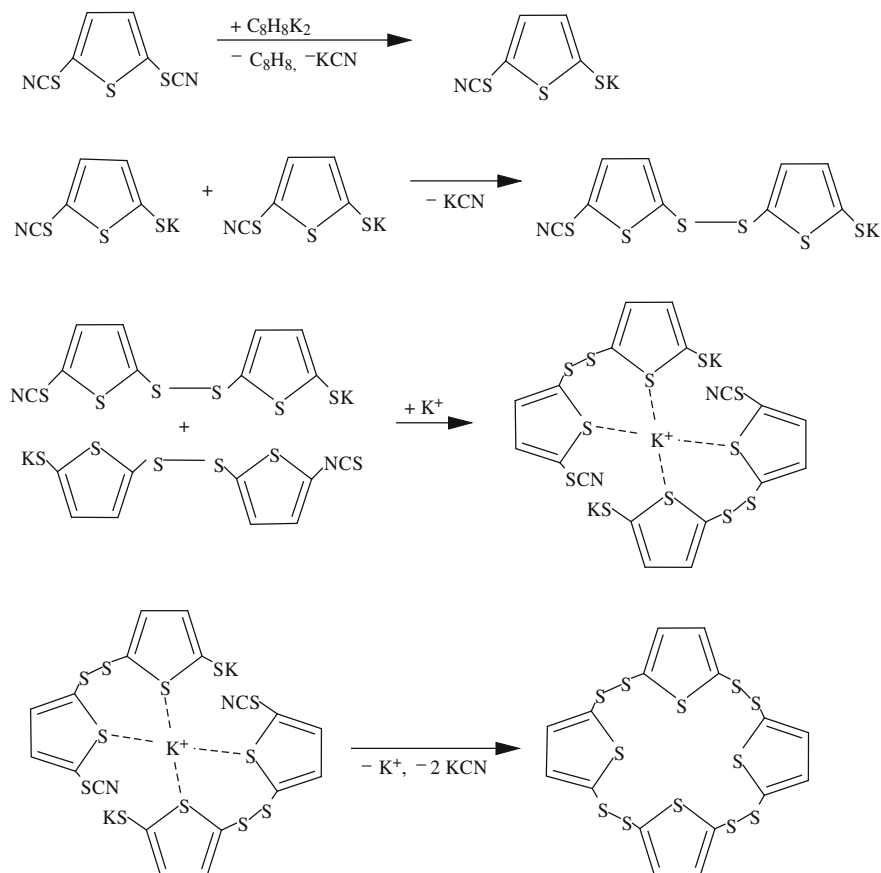
When thiophene-2,5-dithiocyanate reacts with an equimolar amount of cyclooctatetraene dipotassium in tetrahydrofuran solution containing 18-crown-6-ether, the product formed was found to be a linear polysulfide. The crown ether removes the potassium cation; the reaction changes its direction and leads to the formation of a linear product rather than a cyclic one (Scheme 5.8 (Todres et al. 1979b)).

Schemes 5.7 and 5.8 explain the results of furan condensation with acetone in acid medium. The reaction leads to a linear polymer (Scheme 5.9). In the presence of LiClO_4 , the macrocycle of Scheme 5.9 is formed (Chastrette and Chastrette 1973).

When the coordinative bond between a metal ion and a product is weaker than that between a metal ion and starting or intermediary compounds, the product easily separates from the metal ion. Thereafter, the starting or intermediary compound forms a new complex with the metal, and this complex is identical to the initial one. The classical Reppe's synthesis of cyclooctatetraene from acetylene upon the action of $\text{Ni}(\text{CN})_2$ proceeds just according to such a mechanism (Scheme 5.10 (Reppe et al. 1948)).

Schrauser's group proposed a modification of Reppe's synthesis, using triphenylphosphine along with nickel dicyanide (Schrauser and Eicher 1952; Schrauser et al. 1964). In the case of $\text{P}(\text{Ph})_3$, a complex in which there are only three vacancies for acetylene is formed. Accordingly, benzene rather than cyclooctatetraene is the final product (Scheme 5.11).

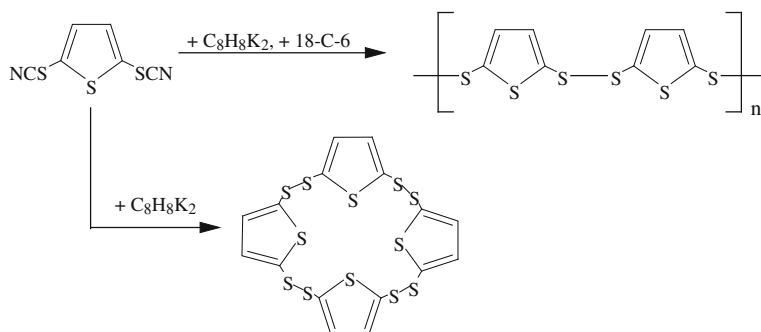
Metal-assisted assemblage provides reliable routes to molecular pseudorotaxanes, rotaxanes, catenanes, and knots (Sauvage 1990). As examples, works by Aucagne et al. (2006) and Barrel et al. (2008) should be mentioned. Scheme 5.12 outlines



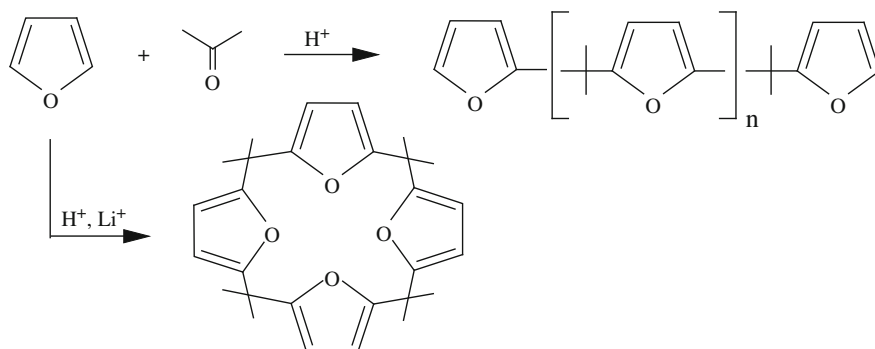
Scheme 5.7 Synthesis of tetra[thienylene cycloocta (disulfide)] based on thiophene dithiocyanate reaction with cyclooctatetraene dipotassium

the principal steps of this strategy. As seen, the bulky stopper group $R = (tert\text{-BuC}_6\text{H}_4)_3\text{CC}_6\text{H}_4$ and the copper coordination center ensure the growth and then splicing of the noninterlocked thread through the cavity of the starting macrocycle. Eventually, the new cycle is built around the cavity. Importantly, copper is released during the formation of the triazole fragment. The released copper participates in the formation of the new pseudorotaxane molecule, i.e., a catalytic effect takes place.

Cheng et al. (2011) reported that a 2,2':6',2''-terpyridylmacrocycle–Ni complex can efficiently mediate the threading of two alkyl chains with bulky end-groups in a homocoupling reaction, resulting in a rare example of a doubly threaded [3]rotaxane in up to 51 % yield. The unusual architecture was confirmed by X-ray crystallography and was found to be stable with respect to dethreading despite the large ring size of the macrocycle.

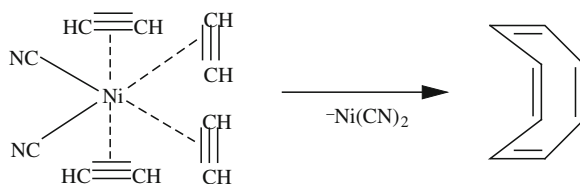


Scheme 5.8 Formation of linear thiophene polysulfide from thiophene dithiocyanate and cyclooctatetraene dipotassium in presence of crown ether

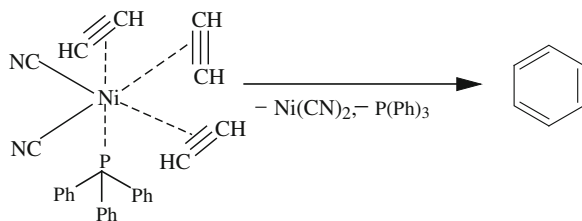


Scheme 5.9 Role of lithium cation in acetone-furan condensation

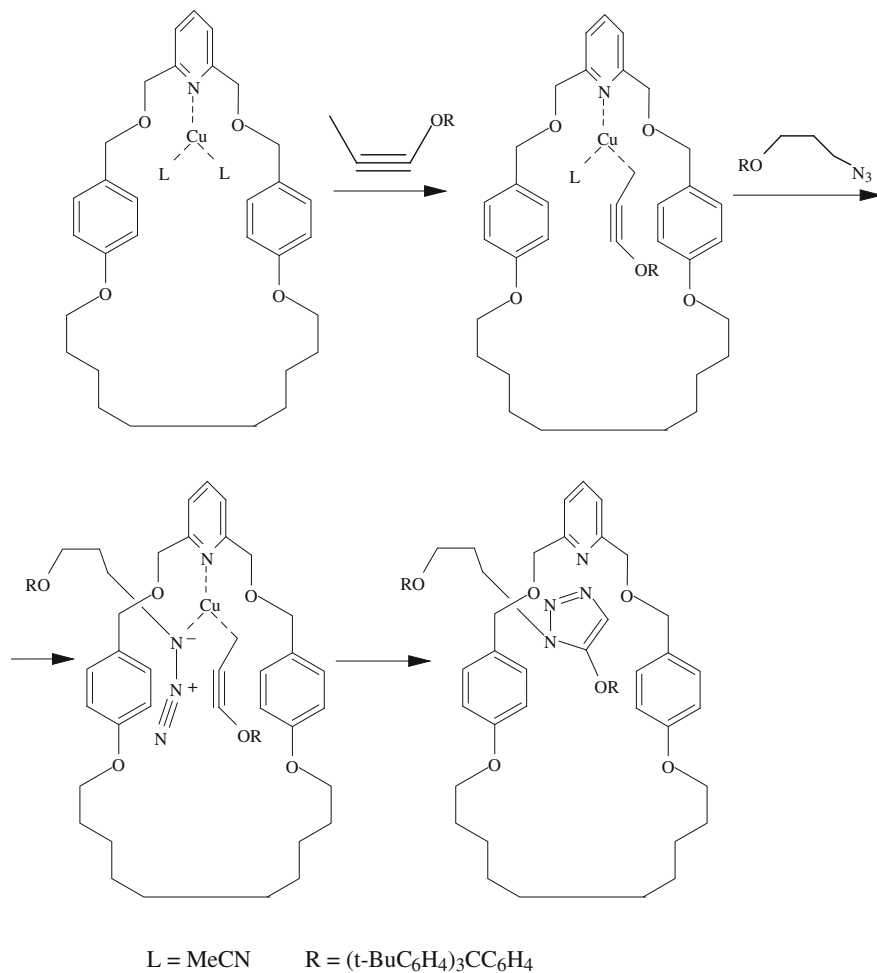
Zinc-pyridine coordination and hydrogen-bonding interactions have been used to assemble a [2]rotaxane (Hunter et al. 2001). Scheme 5.13 depicts this metal-governed molecular assemblage of the rotaxane (compound 36) from individual components, namely from 1 mole of compound 34 and 2 moles of compound 35. Scheme 5.13 was taken from a review by Faiz et al. (2009) with permission, with the authors' numbering of the reacting molecules.



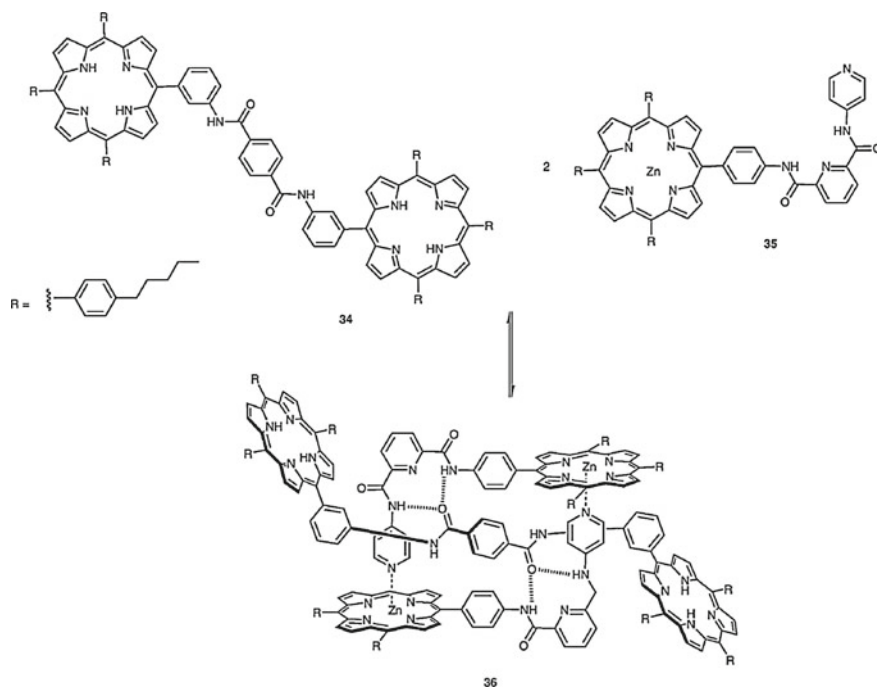
Scheme 5.10 Reppe's synthesis of cyclooctatetraene



Scheme 5.11 Modification of Reppe's synthesis by introduction of tri(phenyl)phosphine into reacting system



Scheme 5.12 Template synthesis of pseudorotaxane



Scheme 5.13 Zinc-pyridine coordination and hydrogen bonding in assemblage of rotaxane (Reproduced with permission from J.-P. Sauvage, the Author, on August 04, 2012) (Permission of August 04, 2012)

In sum, metal-coordination assemblage is being applied with the development and employment of subcomponent self-assembly toward the creation of increasingly more complex structures.

5.4 Closing Remarks

Whereas metal-coordination assemblage is well known, isomerization of organic ligands within metallocomplexes deserves further development both scientifically and in terms of applications; For instance, Chap. 3 described *cis* \rightarrow *trans* rearrangement of ethylenic compounds upon charge or electron transfer. It would be interesting to check such a possibility for ethylenic ligands coordinated to metals of changeable valence. It is clear that the ligands are capable of compensating for this valence change by acting as donors or acceptors of electron(s). The question is whether the ligand can undergo isomerization after an electron shift to (or from) the central metal within the coordinative complex. Reversible metal-to-ligand electron transfer (redox or valence isomerism) is reported for organic complexes with various d- and

f-metals, in solution as well as in the solid state (Sato et al. 2007; Trofimov et al. 2007). Recently, Fedushkin et al. (2012) observed this phenomenon for a complex of Yb with 1,2-bis[(2,6-diisopropylphenyl)imino]acenaphthene: upon lowering the temperature, an electron is transferred from the metal to the organic ligand. In the solid state, this electron transfer gives rise to marked shortening of the Yb-N bond and to a hysteretic jump in the magnetic moment.

It would be interesting to check the behavior of organic substrates in the pores of the zeolite-like materials resulting from reactions of zinc or cobalt nitrate with imidazole and its derivatives. Some such materials are capable of holding carbon dioxide (Banerjee et al. 2009). This could open the way to carbonization of organic compounds of appropriate size and reactivity.

Sometimes, coordination to a metallic center advantageously orients a reagent in relation to a substrate and thus facilitates a reaction between them. Advancement of this possibility could enrich synthetic methods of chemistry.

References

- Aharoni, A., Vidavsky, Yu., Diesendruck, Ch E, Ben-Asuly, A., Goldberg, I., & Lemcoff, N. G. (2011). *Organometallics*, 30, 1607.
- Aucagne, V., Haenni, K. D., Leigh, D. A., Lusby, P. L., & Walker, D. B. (2006). *Journal of the American Chemical Society*, 128, 2186.
- Banerjee, R., Furukawa, H., Britt, D., Knobler, C., O'Keefe, M., & Yaghi, O. M. (2009). *Journal of the American Chemical Society*, 131, 3875.
- Barrel, M. J., Leigh, D. A., Lusby, P. J., & Slawin, A. M. Z. (2008). *Angewandte Chemie International Edition*, 47, 8036.
- Chastrette, M., & Chastrette, F. (1973). *Journal of Chemical Society, Chemical Communications*. 534.
- Cheng, H. M., Leigh, D. A., Maffei, F., McGonical, P. R., Slawin, A. M. Z., & Wu, J. (2011). *Journal of the American Chemical Society*, 133, 12298.
- Cucciolito, M. E., de Renzi, A., Roviello, G., & Ruffo, F. (2008). *Organometallics*, 27, 1351.
- Dai, F.-R., & Wang, Zh. (2012). *Journal of the American Chemical Society*, 134, 8002.
- Faiz, J. A., Heitz, V., & Sauvage, J.-P. (2009). *Chemical Society Reviews*, 38, 422.
- Fedushkin, I. L., Maslova, O. V., Morozov, A. G., Dechter, S., Demeshko, S., & Meyer, F. (2012). *Angewandte Chemie (International ed. in English)*, 51, 10584.
- Hunter, C. A., Low, C. M. R., Packer, M. J., Spey, S. E., Vinter, J. C., Vysotsky, M. J., et al. (2001). *Angewandte Chemie International Edition*, 40, 2678.
- Moorlag, C., Clot, O., Wolf, M. O., & Patrick, B. O. (2002). *Chemical Communications*, 24, 3028.
- Moorlag, C., Wolf, M. O., Bohne, C., & Patrick, B. O. (2005). *Journal of the American Chemical Society*, 127, 6382.
- Nelson, D. L., & Cox, M. M. (2000). *Principles of Biochemistry* (3rd ed.). New York: Worth Publishing.
- Rama, V., Kanagaraj, K., & Pitchumani, K. (2011). *Journal of Organic Chemistry*, 76, 9090.
- Reppe, W., Schlichting, O., Klager, K., & Toepel, T. (1948). *Liebigs Annalen*, 560, 1.
- Sato, O., Tao, J., & Zhang, E.-J. (2007). *Angewandte Chemie (International ed. in English)*, 46, 2152.
- Sauvage, J.-P. (1990). *Accounts of Chemical Research*, 23, 319.
- Schrauzer, G. N., & Eicher, S. (1952). *Chemische Berichte*, 95, 550.
- Schrauzer, G. N., Glockner, P., & Eicher, S. (1964). *Angewandte Chemie*, 76, 28.

- Todres, Z. V., Furmanova, N. G., & Struchkov, Yu T. (1979a). *Phosphorus Sulfur*, *6*, 305.
- Todres, Z. V., Furmanova, N. G., Avagyan, S. P., Struchkov, Yu T, & Kursanov, D. N. (1979b). *Phosphorus Sulfur*, *6*, 309.
- Todres, Z. V., Stoyanovich, F. M., Gol'dfarb, Y. L., & Kursanov, D. N. (1973). *Khim* (p. 632). Soed.: Geterotsikl.
- Trofimov, A. A., Borovkov, I. A., Fedorova, E. F., Fukin, G. K., Larionova, J., Druzhkov, N. O., et al. (2007). *Chemistry—A European Journal*, *13*, 4981.
- Yamamura, M., Okazaki, Y., & Nabeshima, T. (2012). *Chemical Communications*, *48*, 5724.
- Zirngast, M., Pump, E., Leitgeb, A., Albering, J. H., & Slugovc, Ch. (2011). *Chemical Communications*, *47*, 2261.

Chapter 6

Effects of Sorption

6.1 Introduction

Sorption is a specific kind of confinement that governs the reactivity of organic and organometallic compounds. This chapter considers confinement by chemisorption or physisorption forces, including sorption upon electrodes as charged surfaces. Physisorption is due to the operation of forces between the solid surface and adsorbate molecules that are similar to the van der Waals forces between molecules. The energies of adsorption involved are of the order of 0.03–3 kJ/mol. In contrast to physisorption, chemisorption is the result of much stronger binding forces, comparable to those leading to the formation of chemical compounds. Such adsorption may be regarded as the formation of a sort of surface compound. The energies of chemisorption range from about 40 to 400 kJ/mol.

6.2 Chemisorption

As a typical example of chemisorption, the conversion of 1-fluorobenzo[*c*]fluoranthene to benzo[*ghi*]fluoranthene can be chosen. It was found that γ -Al₂O₃ displays pronounced activity in ring closure of the starting material (Scheme 6.1) (Amsharov et al. 2012). The cyclization is extremely sensitive to the pretreatment of the Al₂O₃. The best results were obtained after activation of γ -Al₂O₃ at 500 °C for 15 min at 10² Pa. Among several oxides tested (BeO, B₂O₃, MgO, Al₂O₃, SiO₂, Sc₂O₃, TiO₂, ZnO, SnO, Nb₂O₅, In₂O₃, and HfO₂), only Al₂O₃ showed high activity in condensation. Only alumina therefore ensures the required strength of substrate adsorption (Amsharov and Merz 2012).

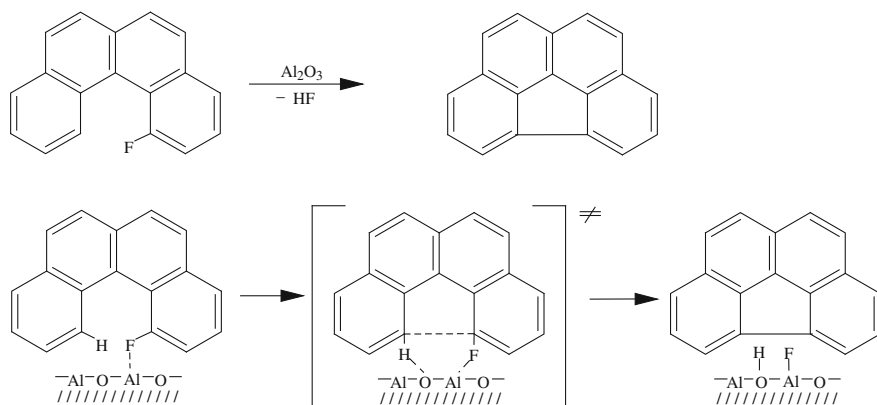
The transformation depicted in Scheme 6.1 must be considered as highly chemoselective and regioselective:

- (1) If the fluorine atom is not directly involved in the core region (2-fluorobenzo[*c*]fluoranthene), no reaction takes place and the compound remains completely intact.
- (2) If the starting fluoranthene bears two fluorine substituents at positions 1 and 4, only the fluorine at position 1 is involved in cyclization.
- (3) If the starting fluoranthene bears only a bromine atom at position 2, no reaction takes place.
- (4) If 1-fluoro-4-bromobenzo[*c*]fluoranthene is exposed to cyclization, only HF is eliminated. Despite the activity of C–Br in cleavage reactions, the C–F bond is widely believed to be the most passive functionality. Nevertheless, in Scheme 6.1, just the C–F bond is a functional group, allowing very effective carbon–carbon bond formation.
- (5) No fluorine-to-hydrogen exchange was observed, and no reactive intermediates were formed.

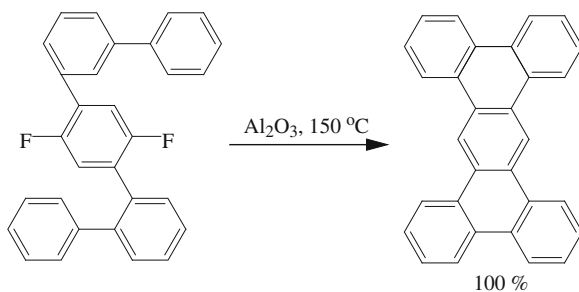
Not only brominated but also chlorinated substrates remain completely intact under Al_2O_3 -mediated condensation conditions up to 250°C (Amsharov et al. 2012). The desired products can be obtained in pure form after simple extraction, and no additional purification procedures are required. The higher tolerance to chlorine and bromine functionalities makes the described chemisorption reaction a very powerful tool for synthesis of halogenated polycyclic aromatic hydrocarbons. The latter can serve as building blocks for construction of more complex structures using known reactions involving the chlorine or bromine substituents.

All the results presented above make the cyclic transition state of Scheme 6.1 absolutely logical. The reaction proceeds according to the concerted mechanism.

As can be seen from Scheme 6.1, the reacting molecule should be in close contact with an active site of alumina. As small fluoroarenes melt below $150\text{--}200^\circ\text{C}$ (the temperature range used for condensation), there are obviously no obstacles to free diffusion. When both starting fluoroaromatic compounds and the condensation products have remarkably higher melting points than the temperature of the reaction, the



Scheme 6.1 Adsorption of fluorobenzo fluorene upon alumina and formation of defluorinated fluoranthene



Scheme 6.2 Alumina-promoted cyclization of bis(diphenyl)difluoro benzene into defluorinated tetrabenzanthracene

elimination can also be realized very effectively: The reacting molecules find mobility as a consequence of the Tamman temperature effect. In this case, diffusion of the mobile species to the alumina surface occurs at approximately halfway between the melting points of these species. Amsharov and Merz (2012) carried out reactions of extralarge substrates with the same efficiency in refluxing dodecane (b.p. 196 °C), 1,2,4-trichlorobenzene (b.p. 214.4 °C), or naphthalene (b.p. 218 °C). In these refluxing solvents, transport of the substrate to the alumina surface proceeds by means of convection.

Scheme 6.2 presents an example of multifold intramolecular cyclization resulting in the formation of a highly condensed polycyclic aromatic hydrocarbon (Amsharov and Merz 2012). In particular, the γ - Al_2O_3 chemisorption reaction is of great interest for rational synthesis of carbon-based nanostructures, including fullerenes, nanotubes, nanographenes, and nanoribbons.

6.3 Physisorption

As a typical example of physisorption, alkali-metal reduction of stilbenes can be chosen. The reactions usually proceed in liquid ammonia. When performed in homogeneous media, stilbenes form mixtures of enantiomers. At the same time, the ethylene bonds of stilbenes have affinity to the alkali-metal surface. When the metal is used as “pieces,” adsorption takes place. Based on these circumstances, a simple modification was proposed for the reduction of α -methyl- β -isopropyl stilbene with potassium in liquid ammonia (Collins and Hobbs 1983). The metal is not predissolved, as usual, but is added in small portions without trying to make the reaction medium homogeneous. Stereoselectivity is ensured by carrying out the reduction on the surface of the metal and not in the solution bulk.

Compounds containing π -systems have an affinity to the metallic surface and are arranged on the surface in a parallel manner. The ethylene bond of α -methyl- β -isopropyl stilbene is responsible for the adsorption, and the substituents deviate from the metallic surface. Alkali cations, when formed, have a strong tendency to be

solvated and are carried away into solvating solution. The remaining electrons jump onto the adsorbed substrate. Reduction of α -methyl- β -isopropyl stilbene consists of two consecutive one-electron steps resulting in the formation of a dianion. Being adsorbed, the dianion accepts two protons. A proton is a very small particle and is attracted by the dianion from the side where the negative charges are localized, namely along the metal surface. After protonation, the obtained product leaves the potassium surface. Therefore, regardless of the configuration of the initial stilbene, the reduction proceeds with predominant formation of an *erythro* product according to Scheme 6.3.

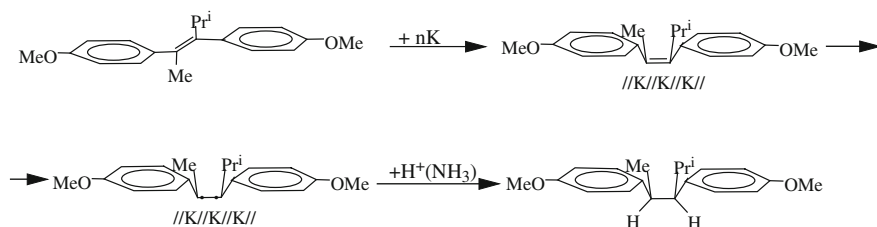
Scheme 6.3 foresees direct interaction of a species to be reduced with a metal reducing agent. Blocking the metal surface by other guests can change the course of reduction. Leger et al. (2008) studied styrene hydrogenation over rhodium nanoparticles in nonaqueous ionic liquids. In this case, the rhodium reducer was blocked by bipyridine isomers, $(\text{Py})_2$. Blocking the reducer, these isomers (abbreviated as IL) also stabilize the rhodium colloidal suspension:



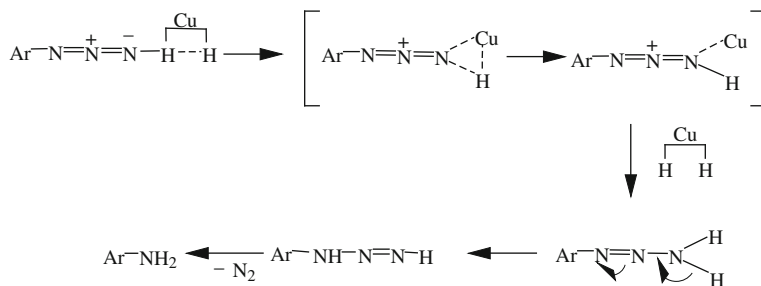
It turned out that styrene gave exclusively ethylcyclohexane when the blocking agents were 3,3'- and 4,4'-bipyridines. Blockage with 2,2'-bipyridine led to a 6:4 mixture of ethylcyclohexane with ethylbenzene. Whereas 3,3'- and 4,4'-bipyridines coordinate to rhodium through only one pyridinium nitrogen, 2,2'-bipyridine coordinates to rhodium by both nitrogens of the equal pyridinium rings. The bidentate coordination results in greater steric shielding of the rhodium nanoparticle surface and thus decreases the catalytic activity compared with the monodentate coordination of the 3,3'- and 4,4'-bipyridine isomers (Leger et al. 2008).

Ahmed et al. (2011) reported on an unusual case of selective transformation of the azido group into an amino function in adsorptive reduction taking place on copper nanoparticles in aqueous ammonium formate solution. The reaction is depicted in Scheme 6.4. The nanostate of copper is an indispensable condition. The reaction is clean and high-yielding. A combination of copper nanoparticles and ammonium formate in water at 100 °C is decisive for a successful reaction.

In full accordance with Scheme 6.4, a gradual change of the aqueous reaction medium was observed toward the acidic range with the progress of the reaction. Ahmed et al. (2011) assume that the copper nanoparticles dissociate H_2 mole-



Scheme 6.3 Stereoselective ethylenic bond hydrogenation of 1-methyl-2-isopropyl stilbene on potassium surface



Scheme 6.4 Reduction of organyl azides to amines upon copper nanoparticles in aqueous formate solution

cles, generated from ammonium formate, and adsorb dissociated hydrogen onto their surfaces. The Cu(0) nanoparticle, with its surface hydrogen, interacts with the azide, forming a type of weak adsorptive complex. Within the complex, transfer of hydride to azide takes place simultaneously with expulsion of a proton from the copper surface. This transfer process is repeated and eventually results in the formation of aryl amine. The hydrogen adsorbed onto the copper nanoparticle surface is moderately activated, thus facilitating reduction of azides with high selectivity. Reduction of the azide functionality appears to be more facile than that of the nitro group, which remains intact during the reaction. (The nitro group at the *ortho*-position to the azido function in the aromatic nucleus does not pose any steric constraint.) The nitrile, ketocarbonyl, alkyl carbonyl, and halogen functions also remain unaffected in the reduction of the corresponding aryl-substituted azides.

Abdelsayed et al. (2006) described radical-initiated polymerization of styrene vapor on nickel or ferric oxide nanoparticle surface and the incorporation of the metal and metal oxide nanoparticles within polystyrene polymers. In this approach, 2,2'-azobisisobutyronitrile (a radical initiator) was dissolved in acetone. Selected nanoparticles (prepared separately using the laser vaporization controlled condensation method) were sonicated in the initiator solution for a time appropriate to achieve homogeneity. The mixture was placed on a glass substrate, from which solvent was gently evaporated to obtain initiator-coated nanoparticles. The substrate was then heated (90 °C) inside a vacuum chamber into which styrene was admitted at a controlled rate. The olefin vapor was then polymerized by the activated initiator on the nanoparticle surface. The resulting polymer encapsulates the nanoparticles, forming a polymer coat on the surface.

6.4 Absorption at Water Surface

Organic substrates can be sorbed at a water surface. Karthaus et al. (1996) prepared a monolayer by spreading a dilute chloroform solution of an amphiphile onto water. The amphiphile used was the disodium 4,4'-pentadecylamido-2,2'-disulfonate

derivative of *trans*-stilbene. In this layer, both sulfonate groups remain parallel to the surface. When the monolayer was irradiated with 366 nm light, *trans*-to-*cis* conversion took place. Such a kind of conversion is usual for stilbenes under conditions of photoinitiation. In the case considered, absorption of the stilbene onto the water surface markedly retarded the conversion. However, this conversion is accelerated by alkaline-earth metal salts. The cause of the acceleration is a salting-out effect. Namely, salting-out promotes desorption of the monolayer from the water surface, facilitating photoisomerization.

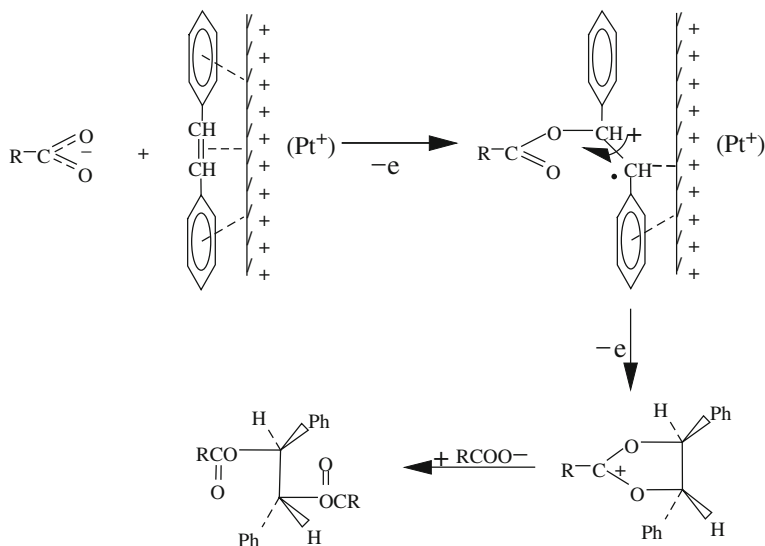
On the water surface, the concentration of hydroxide ions is higher than that in the water bulk. This can be important for water absorption of organic compounds with polar groups. L-Phenylalanine at the air–water surface is an illustrative example (Griffith and Vaida 2013).

6.5 Adsorption at Electrode Surfaces

For confinement within the dense part of the double layer near an electrode, significant overlap between substrate and electrode orbitals is needed; that is, a weak chemical bond has to be established. This implies that there must be a mutual electrode–depolarizer orientation effect and the depolarizer molecule must be fairly close to the electrode surface. These are features of such a kind of confinement. The following pairs of *cis* and *trans* substituted ethylenes were reported to exhibit identical reduction potentials: 1,2-dimethyl-1,2-diphenyl ethylenes (Weinberg and Weinberg 1968), 1,2-bis(4-cyanophenyl)-1,2-bis(4-methoxyphenyl) ethylenes (Leigh and Arnold 1981), and 1,2-bis-(4-acetylphenyl)-1,2-diphenyl ethylenes (Wolf et al. 1996). As free molecules, the *trans* isomer of 1,2-dimethyl-1,2-diphenyl ethylene is coplanar and the *cis* isomer is noncoplanar. However, both isomers are oriented in an identical manner within the pre-electrode space due to the electric field effect (Horner and Roder 1969). The energy needed for such orientation is not markedly reflected in the magnitude of the reduction potential. For oxidation potentials, there are also data showing that they are not sensitive to diastereoisomerism of depolarizers (Fukui et al. 2007).

At this point, a brief comparison of oxidative acyloxylation of *cis*- or *trans*-stilbene in electrochemical and chemical conditions is relevant. Oxidation of *cis*- or *trans*-stilbene at a platinum anode in the presence of acetic or benzoic acid gives *meso*-diacylates of hydroxybenzoin. Racemates are not formed. There was no evidence of isomerization of *cis*- to *trans*-stilbene under the electrochemical conditions employed (Mango and Bonner 1964; Koyama et al. 1969). The sequence of reaction steps in Scheme 6.5 was proposed.

As can be seen from Scheme 6.5, adsorption-controlled confinement can be the key step. One-electron oxidation generates the confined cation-radical. The latter interacts with an acylate to form an oxonium ion. The phenyl groups of the oxonium adopt *trans* mutual disposition, which is thermodynamically preferential. The *trans*-benzoxonium ion is the common intermediate for conversion of both *cis*- and



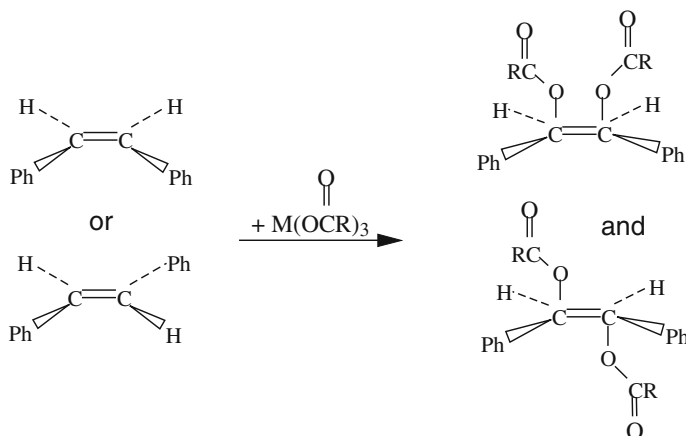
Scheme 6.5 Acyloxylation of stilbene isomers at platinum anode

trans-stilbenes. There is no passage of oxidized intermediates into the solution volume or following electron exchange with nonoxidized molecules of stilbene.

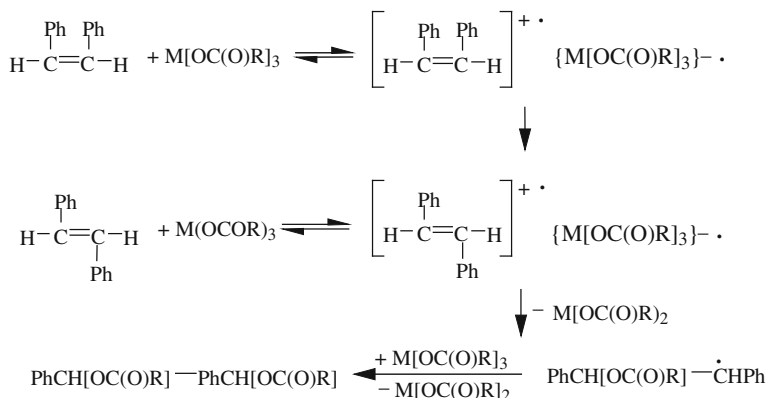
Chemical oxidation of *cis*- or *trans*-stilbene was comparatively studied in non-confined conditions (Vinogradov et al. 1976). The oxidant was cobalt or manganese triacetate and, in separate experiments, thallium tris(trifluoroacetate). Acetic or trifluoroacetic acid was used as solvent. This homogeneous oxidation was considered from the standpoint of the configuration of the recovered (nonreacted) substrate and the stereoisomeric composition of the products obtained. This allowed the desirable comparison of confined and nonconfined reactions.

The cation-radicals of stilbene have been detected by electron spin resonance spectroscopy. These cation-radicals are accumulated and then consumed in the course of consecutive reactions. The stereoisomeric composition of the final products is constant and does not depend on the configuration of the initial substrate: In both cases, a mixture of *meso*- and *dl*-hydrobenzoin is obtained. Acetoxylation of the olefinic bond in *cis*-stilbene is almost one order of magnitude slower than that in *trans*-stilbene. This kinetic feature deserves a special explanation, because *cis*-stilbene is less thermodynamically stable than *trans*-stilbene and should react faster. The products obtained are depicted in Scheme 6.6.

When the initial compound was *trans*-stilbene, the untrapped part was recovered with no change in configuration. When *cis*-stilbene was employed as the initial reactant, the recovered olefin was a mixture of *trans* and *cis* isomers. (In Chap. 3 we indicated such a phenomenon as a characteristic of the ion-radical mechanism of vinylic substitution reactions.) It is inferred that the *trans* configuration is more



Scheme 6.6 Chemical acyloxylation of stilbene isomers in homogenous solutions



Scheme 6.7 Mechanism of isomeric stilbene homogenous acyloxylation

favorable for oxidative acetoxylation than the *cis* configuration. In accordance with this conclusion, the mechanism shown in Scheme 6.7 was proposed.

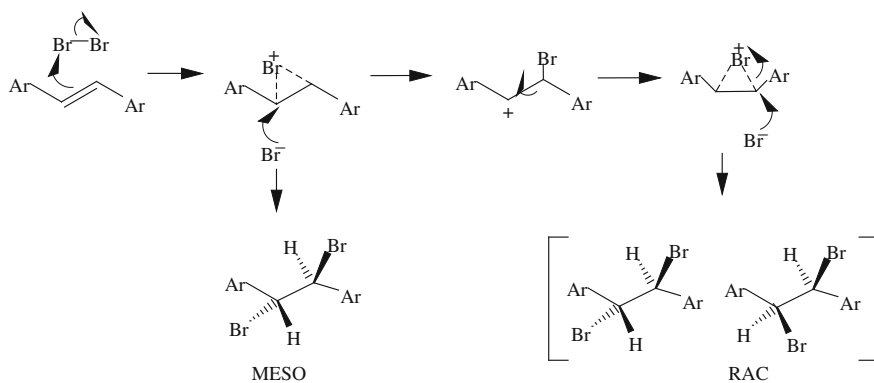
It is seen that the cation-radical of stilbene, but not stilbene itself, is subjected to acetoxylation. Stilbene in the neutral *trans* form yields the *trans* form of the cation-radical, which undergoes further reaction directly. The *cis* cation-radical first acquires the *trans* configuration and only then adds the carboxylate ion. It is the isomerization that causes the observed retardation of the *cis*-isomer reaction. It is the absence of confinement within the double electrode layer that allows the nonacetoxyated part of *cis*-stilbene to isomerize and to turn into the richer stereoisomeric set of final products. To support this point of view, one can mention the cation-radical epoxidation, cyclopropanation, and cycloaddition (Diels–Alder reaction) of stilbenes. Particularly, the stereochemistry of the Diels–Alder reaction is complicated by competing

cis-to-*trans* isomerization of the stilbene cation-radical (Yueh and Bauld 1995, 1996). In cycloadditions catalyzed by ammonium ions, *cis*-stilbenes react approximately 2.5 times slower than *trans*-stilbenes. In contrast, electrode oxidation reveals that *cis* isomers are more reactive (Kim et al. 1993; Bauld and Yueh 1994; Mirafzal et al. 1998; Adamo et al. 2000).

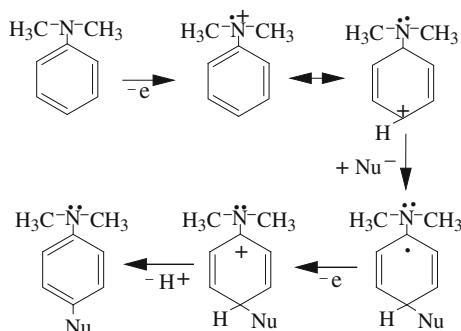
Let us return to Scheme 6.5. The formation of the *trans*-benzoxonium cyclic ion brings no controversy to the commonly accepted mechanism of vinylic addition; For instance, addition of halogens to stilbene includes the initially forming cyclic bromonium ion. Such an ion produces two sets of diastereomers, namely a racemic (*rac*) pair of (1*R*,2*R*)- and (1*S*,2*S*)-dibromo-1,2-diphenylethanes along with *meso*- (1*R*,2*S*)-dibromo-1,2-diphenylethane. The generally accepted polar mechanism of bromination in solution admits stereochemical scrambling. The scrambling originates from free rotation of the initially forming cyclic bromonium ion (Scheme 6.8) (Williamson 1989).

Works by Weinberg and Reddy (1968), Andreades and Zahnow (1969), as well as Kirchgessner et al. (2006) give a striking example of the difference between homogeneous and confined (electrode) oxidation of a substrate undergoing a further nucleophilic attack. Scheme 6.9 describes the oxidation with cupric perchlorate. Under these (nonconfined) conditions, the cation-radical formed takes part in the nucleophilic substitution at the *para* position of the phenyl ring (Kirchgessner et al. 2006).

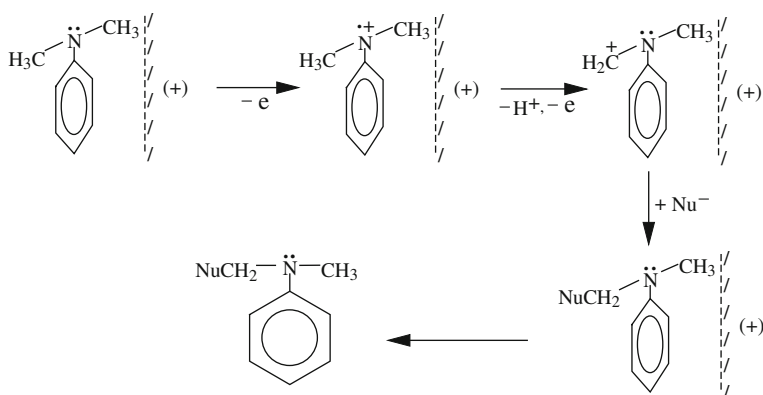
When anode is used as an oxidizer, the nucleophilic substitution involves the methyl group due to the formation of $\text{Ph-N}(\text{CH}_3)\text{CH}_2^+$ as a precursor of the final product (Scheme 6.10). Thus, the change in the orientation of the nucleophilic attack was explained by the strong adsorption of dimethyl aniline and its cation-radical on the anode (Scheme 6.10) (Weinberg and Reddy 1968; Andreades and Zahnow 1969).



Scheme 6.8 Scrambling of 1,2-dibromo-1,2-diphenyl ethane stereoisomers as products of *trans*-stilbene bromination



Scheme 6.9 One-electron chemical oxidation and nucleophilic substitution in aromatic ring of N,N-dimethylaniline

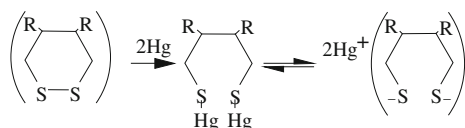


Scheme 6.10 One-electron anodic oxidation and nucleophilic substitution in N-methyl group of N,N-dimethylaniline

6.6 Confinement by Monolayers or Clathrates

Organothiolate-based self-assembled monolayers provide other important examples of chemistry in confined circumstances. Rajalingam et al. (2007) studied saponification of monoacetylated 4,4'-biphenyldimethyldithiols immobilized on gold via the thiolate groups. Whereas the free monoacetylated 4,4'-biphenyldimethyldithiol hydrolyzes in aqueous sodium hydroxide solution at room temperature in minutes, the corresponding reaction at the organic surfaces requires 3.5 days under the same conditions. This is a typical phenomenon for self-assembled monolayers of thiolates on metals (see review by Love et al. 2005). According to the data presented by Rajalingam et al. (2007), the deacetylation (hydrolytic) reaction starts at defects on the surface covered with the organic layer. The hydrolysis affects only one of the thioacetyl moieties, namely the thioacetyl that is next to the already deprotected

Scheme 6.11 Reduction at mercury cathode of dithiacyclohexane from monolayer with silica



one. The confined reaction occurs at a one-dimensional front and is significantly decelerated.

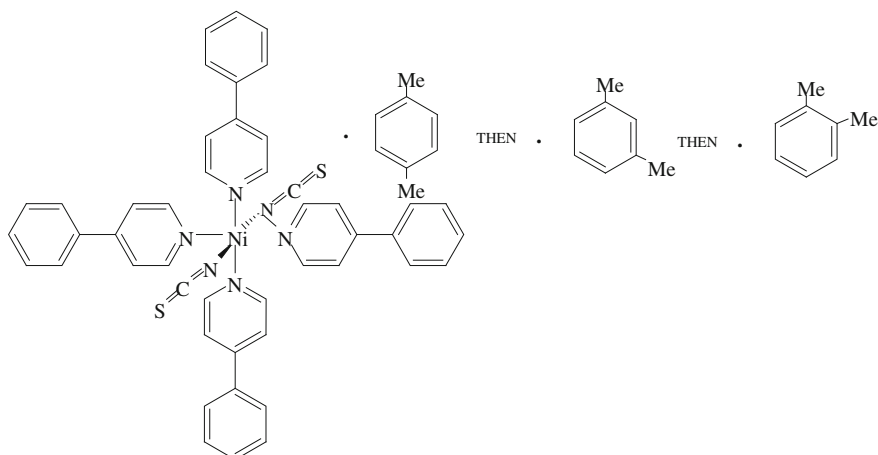
Other examples concern sorption (chemisorption) on a mercury electrode. On a mercury electrode, Salomon et al. (2004) prepared a monolayer of silicon oxide and a depolarizer that had a six-membered ring including a disulfide bond (Scheme 6.11). During monolayer formation, the disulfide bond breaks and two mercury–sulfur bonds are formed. The further step consists in reduction of mercury–sulfur bonds to give the dithiolate; this step is reversible. Once dithiolate is formed, the conductance across the monolayer drops. There are two reasons for the decrease in conductance: (1) after desorption, the contact between the depolarizer and the mercury electrode is worse, and (2) repulsion of the negative charges on the dithiolate and mercury cathode disrupts contact between them. The reverse process of dithiolate oxidation reinforces the conductivity. Confinement of the depolarizer through chemisorption allows modulation of the conduction across the monolayer.

In a similar way, confinement on a mercury electrode changes the reduction order of nitrophenyl sulfenates or the selectivity of carbon–sulfur bond splitting in dimethylbenzyl sulfonium ions (Todres 2009, Sect. 2.4.3).

Coordinative adsorption upon organometallic compounds also deserves attention. Lusi and Barbour (2012) reported adsorption of xylene isomers from vapor phase upon solid nickel tetrakis(*para*-phenylpyridine) bis(isothiocyanate) (Scheme 6.12). During adsorption, the xylene clathrates are formed and a rearrangement of the host molecule takes place. The adsorbed xylene guest molecules are reextracted from the polycrystalline adsorbate using hexane. Although the process leads to only separation of the xylene, without chemical changes, it should be included in our consideration due to its practical importance.

Xylenes occur in three isomeric forms (*ortho*, *meta*, and *para*). Together with ethylbenzene, they constitute the so-called C₈ aromatic compounds derived from crude oil that serve as starting materials for synthesis of many important chemical intermediates. Moreover, xylenes are often added to motor fuel as an antiknocking agent. It is important to use xylenes as individual isomers. Owing to their similar physical properties (boiling points of 144.5, 139.1, and 138.2 °C for *ortho*, *meta*, and *para* isomers, respectively), separation methods of the three isomers are expensive and inefficient.

Sorption upon the nickel complex of Scheme 6.12 shows remarkable discrimination between the isomers. The *ortho*-substituted compound removed, followed by *meta*-xylene and finally *para*-xylene. This means that *para*-xylene is held most strongly, followed by *meta*-xylene, whereas *ortho*-xylene is loosely bound (Scheme 6.12) (Lusi and Barbour 2012). According to the authors, the xylene



Scheme 6.12 Discrimination of xylene isomers via sorption upon nickel complex

selectivity is based on factors that allow the adsorbate to assume the most relaxed conformation, which varies from one isomer to another.

6.7 Closing Remarks

The particular reactions discussed in this chapter enable some important and nontrivial opportunities for chemical practice. Rational synthesis of carbon-based nanostructures, including fullerenes, nanographenes, etc., can be performed by means of chemisorption of aromatic compounds having fluoro substituents at the cove regions on thermally activated γ - Al_2O_3 . Sorption of xylene isomer mixture on solid metal-lococomplexes is of great interest for inexpensive and effective isolation of each isomer in its pure state. This is important for subsequent transformation of the isolated isomers. Redox reactions of organic and elementoorganic compounds are frequently modeled with the help of electrochemistry. Because adsorption of depolarizers onto an electrode changes their configuration, stereochemical aspects should be excluded from electrochemical modeling. At the same time, the *Handbook on Organic Electrochemistry* (Baizer and Lund 1983, p. 907) underlines that “When the stereochemistry of an electrochemical reaction is discussed, it is normally assumed that the geometry of the molecule in question remains essentially unchanged until bond breaking or bond transformation occurs. It should be recognized, however, that an electron transfer might entail significant changes in the geometry and bond strength of a molecule with concomitant implications for the stereochemistry of its reaction (Todres 1974). Unfortunately, this important area has not been extensively investigated.”

References

- Abdelsayed, V., Alsharaeh, E., & El-Shall, M. S. (2006). *Journal of Physical Chemistry B*, *110*, 10100.
- Adamo, M. F. A., Aggarwal, V. K., & Sage, M. A. (2000). *Journal of the American Chemical Society*, *122*, 8317.
- Ahmed, S., Saha, A., & Ranu, B. C. (2011). *Journal of Organic Chemistry*, *76*, 7235.
- Amsharov, K. Yu., & Merz, P. (2012). *Journal of Organic Chemistry*, *77*, 5445.
- Amsharov, K. Yu., Kabdulov, M. A., & Jansen, M. (2012). *Angewandte Chemie International Edition*, *51*, 4594.
- Andreades, S., & Zahnow, E. W. (1969). *Journal of the American Chemical Society*, *91*, 4181.
- Baizer, M. M., & Lund, H. (Eds.). (1983). *Organic electrochemistry* (2nd edn). New York: Marcel Dekker.
- Bauld, N. L., & Yueh, W. (1994). *Journal of the American Chemical Society*, *116*, 8845.
- Collins, D. J., & Hobbs, J. J. (1983). *Australian Journal of Chemistry*, *36*, 619.
- Fukui, M., Mori, T., Inoue, Y., & Rathore, R. (2007). *Organic Letters*, *9*, 3977.
- Griffith, E. C., & Vaida, V. (2013). *Journal of the American Chemical Society*, *135*, 710.
- Horner, L., & Roder, H. (1969). *Liebigs Annalen der Chemie*, *723*, 11.
- Karthus, O., Hioki, M., & Shimomura, M. (1996). *Journal of the American Chemical Society*, *118*, 9174.
- Kim, T., Mirafzal, G. A., Liu, J., & Bauld, N. L. (1993). *Journal of the American Chemical Society*, *115*, 7653.
- Kirchgesner, M., Sreenath, K., & Gopidas, K. R. (2006). *Journal of Organic Chemistry*, *71*, 9849.
- Koyama, K., Ebara, T., Tani, T., & Tsutsumi, Sh. (1969). *Canadian Journal of Chemistry*, *47*, 2484.
- Leger, B., Denicourt-Nowicki, A., Olivier-Bourbigou, H., & Roucoux, A. (2008). *Inorganic Chemistry*, *47*, 9090.
- Leigh, W. J., & Arnold, D. R. (1981). *Canadian Journal of Chemistry*, *59*, 3061.
- Love, J. Ch., Estroff, L. A., Kriebel, J. K., Nuzzo, R. G., & Whitesides, G. M. (2005). *Chemical Reviews*, *105*, 1103.
- Lusi, M., & Barbour, L. J. (2012). *Angewandte Chemie International Edition*, *51*, 3928.
- Mango, F. D., & Bonner, W. A. (1964). *Journal of Organic Chemistry*, *29*, 1367.
- Mirafzal, G. A., Loseva, A. M., & Olson, J. A. (1998). *Tetrahedron Letters*, *39*, 9323.
- Rajalingam, K., Bashir, A., Badin, M., Schroeder, F., Hardman, N., Strunskus, Th., et al. (2007). *ChemPhysChem*, *8*, 657.
- Salomon, A., Arad-Yelin, R., Shanzer, A., Karton, A., & Cahen, D. (2004). *Journal of the American Chemical Society*, *126*, 11648.
- Todres, Z. V. (1974). *Russian Chemical Reviews*, *43*, 1099.
- Todres, Z. V. (2009). *Ion-radical organic chemistry—principles and applications*. Boca Raton, FL: CRC Press, Taylor and Francis Group.
- Vinogradov, M. G., Todres, Z. V., Il'ina, G. P., Rutavichus, A. I., Kursanov, D. N., & Nikishin, G. I. (1976). *Izvestiya Akademii Nauk SSSR, Seriya khimicheskaya*, 1331.
- Weinberg, N. L., & Reddy, T. B. (1968). *Journal of the American Chemical Society*, *90*, 91.
- Weinberg, N. L., & Weinberg, H. R. (1968). *Chemistry Reviews*, *68*, 470.
- Williamson, K. (1989). *Macroscale and microscale experiments* (2nd edn). Lexington, MA: D. C. Heath.
- Wolf, M. O., Fox, H. H., & Fox, M. A. (1996). *Journal of Organic Chemistry*, *61*, 287.
- Yueh, W., & Bauld, N. L. (1995). *Journal of the Chemical Society, Perkin Transactions*, *2*, 871.
- Yueh, W., & Bauld, N. L. (1996). *Journal of the Chemical Society, Perkin Transactions*, *2*, 1761.

Chapter 7

Micellar Effects

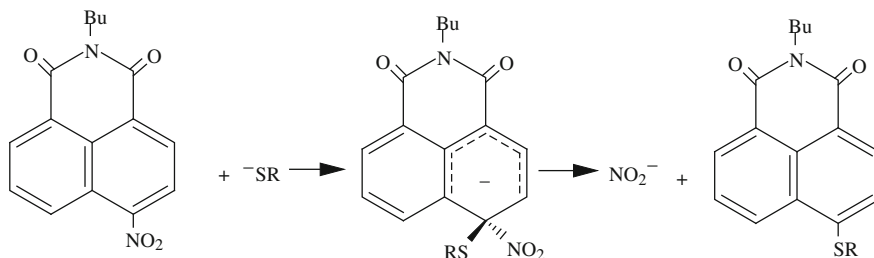
7.1 Introduction

The simplest micelles are constructed from the sodium and potassium salts of long-chain carboxylic acids. In aqueous solution, these salts aggregate as spherical clusters. Water–surfactant micelles are energetically stable particles because the hydrophilic groups (e.g., the carboxylate functionalities) are hydrogen-bonded to the surrounding water. At the same time, the hydrophobic groups (e.g., the long hydrocarbon chains) are shielded within the interior of the micelle, interacting with other hydrophobic groups. These micelles belong to the anionic type. Other micelles are constructed from halides of long-chain alkylammonium cations, belonging to the cationic type. Micelles based on such substances but that can ionize to form either anions or cations belong to the amphiphilic type. Ampholytic detergents (e.g., aminoamylene glycol) are cationic in acid media but anionic in basic media. In strongly apolar media, the polar groups of the detergents become lyophobic. The formation of so-called reverse micelles takes place: All the polar groups are gathered in the center of a micelle. In reverse micelles, the aggregation number is less than that in micelles formed in the presence of water.

7.2 Micellar Effects on Guest Reactivity

Incorporation of organic reactants into micelles retards or deters their diffusion within the solvent pool. This creates self-assembled reactors of nanometer or micrometer size. Water–surfactant micelles establish a confined environment that controls organic reactivity, making organic substrates and reactants soluble and also bringing them into close proximity. The efficiency of chemical transformation increases.

Thiolysis of nitronaphthalimides within cationic micelles is a relevant example. Namely, cetyltrimethylammonium chloride water micelles provide five-order acceleration of the reaction between 4-nitro-*N*-butyl-1,8-naphthalimide and alkyl or aryl



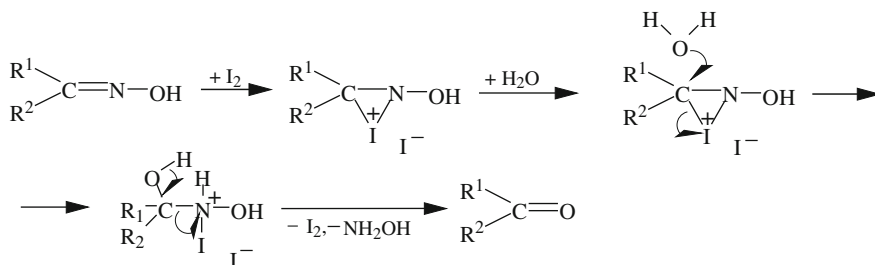
Scheme 7.1 Micelle-promoted substitution of thiolate for nitro group in nitronaphthalimides

thiolate as compared with the same reaction in aqueous methanol without the surfactant (Triboni et al. 2003). This kind of thiolysis is depicted in Scheme 7.1. Having a positive charge, the micelle fixes thiolate anions at the micellar surface. The cavity of the micellar interior incorporates the hydrophobic nitronaphthalimide molecules that are more mobile as compared with the thiole molecules and are homogeneously distributed in the micelle. Interaction of the reactant and the substrate is facilitated and leads to the formation of an intermediary Meisenheimer complex as depicted in Scheme 7.1. This complex has a more diffuse negative charge, and its binding to micelles is weakened. The complex separates into the nitrite anion and a thioether of nitronaphthalimide. These thioethers are highly fluorescent, allowing use of this reaction for quantitative determination of thiols.

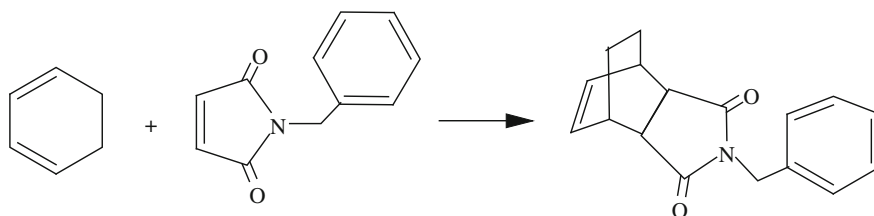
Perylene confined in an aqueous micelle containing cetylpyridinium chloride surfactant acquires the possibility to reduce the pyridinium headgroup of this surfactant under photoexcitation (Singh et al. 2005). The perylene molecules (reductants) are localized at or near the micellar surface, where they coexist with the pyridinium moieties (the oxidative parts of the surfactant molecules). Such confinement promotes electron transfer. This process of electron transfer (forward transfer) proceeds in the ultrafast regime. Perylene transforms into the cation-radical (in its excited state). Because the cation-radical bears a positive charge, it is forced to leave the positively charged headgroup space and to move into the neutral zone of the cetyl chains within the micelle. Accordingly, back electron transfer becomes less probable.

Gogoi et al. (2005) used an environmentally friendly method by applying iodine-sodium dodecyl sulfate water micelles for transformation of oximes and imines into the corresponding carbonyl compounds at 25–40 °C, with 60–90% yields. This reaction does not proceed without the surfactant. Within the micelle, iodine activates C=N bond hydration, probably forming an organoiodonium ion. The ion is attacked by water to form carbonyl compounds. At the same time, iodine is regenerated. No iodinated side-products are formed, and no overoxidation takes place. Scheme 7.2 illustrates the mechanism proposed for the reaction under consideration. The steric availability of the C=N bond carbon atom defines the kinetics of the reaction. Bulky substituents predictably retard the reaction.

In the water-cetyltrimethylammonium bromide micellar microreactor, the reaction between aldoximes and iodosobenzene leads to nitrile oxides. The latter are



Scheme 7.2 Transformation of ketoximes into ketones in aqueous micelles containing iodine and sodium dodecyl sulfate



Scheme 7.3 Diels-Alder reaction between cyclohexadiene and maleimide

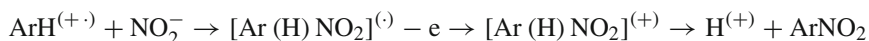
unstable; they were trapped with alkenes, giving 4,5-dihydroisoxazoles with high yields. Iodobenzene is a side-product of the reaction. In the absence of the surfactant mentioned, the reaction did not proceed in aqueous media (Chatterjee et al. 2008).

Ionic liquids in mixtures with water form micellar systems that in some cases can overcome issues of water or ionic liquids as sole solvents. Thus, the Diels-Alder reaction between 1,3-cyclohexadiene and *N*-benzylmaleimide (Scheme 7.3) in aqueous 1-tetradecyl-3-methylimidazolium chloride at room temperature was accelerated by more than four times as compared with the same reaction in pure water or in water containing conventional cationic, anionic or zwitterionic surfactants (Bica et al. 2012).

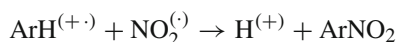
7.3 Micellar Effects in Regulation of Guest Reactivity

The works by Okamoto et al. (2001) and Bharathy et al. (2005) showed how one could regulate ion-radical (nonphotochemical) reactions by construction of cationic, anionic or neutral micelles. A combination of electrochemical and micelle-confined methods can be exemplified as an approach to elucidate the mechanism of anode nitration of 1,4-dimethoxybenzene (ArH) with $NaNO_2$ (Laurent et al. 1984). The reaction was performed in the presence of water micelles with corresponding surfactants. It was established that 1,4-dimethoxy-2-nitrobenzene (the product) was formed only in the region of potentials corresponding to simultaneous electrooxidation of the substrate to the cation-radical and the nitrite ion to the nitrogen dioxide radical,

namely at 1.5 V versus saturated calomel electrode. At potentials of oxidation of only the nitrite ion (0.8 V), no nitration was observed. Consequently, reaction of $\text{NO}_2^{(\cdot)}$ with the neutral ArH does not take place. Two feasible mechanisms remain for addition to the cation-radical form, as follows:



or

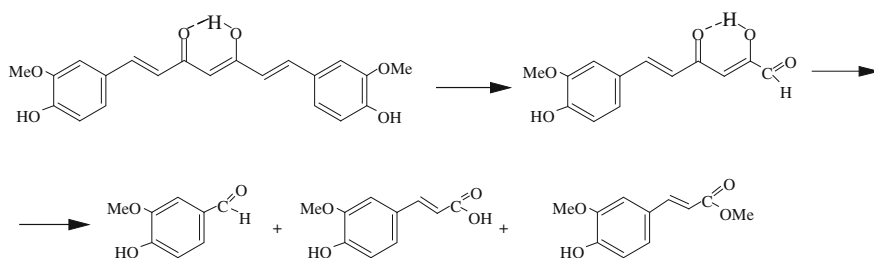


Confinement within micelles was used to operate a choice between these two mechanisms. When an ion-radical has a charge opposite to that of the micelle surface, it is trapped by the micelle. In the presence of a surface-active compound, the aromatic substrate is nitrated in the very depth of a micelle, and the reaction rate depends on the local concentration of the nitrating agent on phase boundaries between the micelle and solution. A positively charged micelle will have a higher concentration of the nitrite *anion*. However, such a micelle is less likely to include the substrate *cation-radical*, which also bears a positive charge. A negatively charged micelle should assist in the insertion of the *cation-radical* and repel the nitrite *anion*. If the reaction proceeds with participation of the *neutral radical* $\text{NO}_2^{(\cdot)}$, the sign of the micelle charge cannot be decisive.

For the anode process under comparable conditions, the yield of 1,4-dimethoxy-2-nitrobenzene depends distinctly on the electrical nature of the micelle, namely the yield is 30, 40, and 70% for positive, negative, and neutral micelles, respectively. The observed micellar effect corroborates the mechanism that includes the 1,4-dimethoxybenzene cation-radical and the nitrogen dioxide radical as preferential reacting species.

Another very demonstrative example of the micellar effect concerns coupling of 4-chlorobenzene diazonium hydrogen sulfate with sodium 2-naphthol-3,5-disulfonate. The reaction proceeds in aqueous solution and gives rise to sodium 1-(4-chlorobenzene)-azo-2-naphthol-3,5-disulfonate. In the presence of sodium dodecyl sulfate (SDS), the anionic micelle is formed. This micelle effectively draws the diazonium cation in and prevents the naphthol disulfonate from participating in azocoupling. Strong inhibition of the reaction was observed: The rate constant was smaller by 50-fold than that in the absence of SDS (Shinkai et al. 1987).

It should be underlined that charged micelles create medium polarity. The reaction of bilirubin with peroxy radicals is an outstanding example. In biological systems, bilirubin acts as an antioxidant. It has also been termed a “major physiologic antioxidant cytoprotectant” (Baranano et al. 2002). Hartfield and Barclay (2004) established that bilirubin shows very weak antioxidant activity in nonpolar media. In contrast, bilirubin exhibits strong antioxidant activity in aqueous sodium dodecyl sulfate micelles, containing phosphate buffer (pH 7.4). At this pH, the pyrrole fragments of bilirubin retain their strong electron-donor ability. Reaction between bilirubin and



Scheme 7.4 Hydrolysis of Curcumin (in keto-enol H-bonded form)

peroxy radicals leads to formation of bilirubin cation-radicals and peroxides. Peroxides are acceptors of protons, whereas bilirubin cation-radicals are very strong proton donors. Being generated in the micelle confines, these species find themselves in close contact and interact according to a proton-transfer scheme. The bilirubin cation-radicals transform into pyrrole-centered radicals, and the peroxides turn into hydroperoxides. These transformations lead to annihilation of the peroxy radical with their malignant action.

7.4 Drug-Protective and Drug-Delivery Properties of Polymer-Based Micelles

Curcumin is recognized as a potential chemotherapeutic agent against a variety of tumors. However, clinical application of curcumin is hindered by its poor water solubility and fast hydrolytic degradation. Hydrolysis of curcumin [1,7-bis(4-hydroxy-3-methoxyphenyl)-1,6-heptadien-3,5-dione (in the keto-enol form)] leads to 6-(4-hydroxy-3-methoxyphenyl)-2,4-dioxohexan-1-al (in the aldo-enol form). The hexanal further decomposes to vanillin, ferulic acid, and the acid methyl ester (Scheme 7.4) (Wang et al. 1997). The results presented below show how inclusion of curcumin in polymer-based micelles protects the drug against hydrolysis and improves its bioavailability.

Amphiphilic block copolymer micelles of poly(ethylene oxide)/poly(ϵ -caprolactone) (PEO-PCL) (Ma et al. 2008) have been used as vehicles for solubilization, stabilization, and controlled delivery of curcumin (a free-radical scavenger and antioxidant). PEO-PCL micelles solubilize curcumin effectively, protect the encapsulated curcumin from hydrolytic degradation in physiological matrix, and control the release of curcumin over a few days. PEO-PCL micelle-encapsulated curcumin retained its cytotoxicity against B16-F10, a mouse melanoma cell line, and SP-53, Mino, and JeKo-1 human mantle lymphoma cell lines.

Scheme 7.4 shows that curcumin reacts in the keto-enol form. In alkaline medium, all three of the hydroxyl groups are fully deprotonated and the compound undergoes alkaline hydrolysis. The hydrolytic process was studied in cationic and anionic mi-

celles (Leung et al. 2008). At pH 13 and in anionic micelles containing sodium dodecyl sulfate, the curcumin trianion rapidly degrades. In contrast, alkaline hydrolysis of curcumin is greatly suppressed when the micelles are cationic (containing cetyltrimethylammonium or dodecyltrimethylammonium bromide). The degrees of suppression are close to 90%. These results obtained by Leung et al. (2008) are revealing: as long as the curcumin trianion remains encapsulated in the cationic micelles, it cannot be incorporated by the anionic micelle and remains in the aqueous phase at pH 13. Lack of encapsulation and stabilization inside the sodium dodecyl sulfate micelle results in rapid hydrolysis of curcumin.

Mixed polymeric micelles based on Pluronic P123/Pluronic F127 also improve drug solubility and delivery and prolong drug action. Pluronics are a family of (polyethylene oxide)/poly(propylene) amphiphilic block copolymers. Incorporation within such polymeric micelles significantly raises the therapeutic activity of Paclitaxel as a mitotic inhibitor during cancer treatment (Zhang et al. 2011).

7.5 Closing Remarks

As a whole, this chapter was designed so as not to overburden or distract the reader with excessive detail. Incorporation of organic reactants into micelles retards or deters their diffusion within the solvent pool. This creates self-assembled reactors of nanometer or micrometer size. Water–surfactant micelles establish a confined environment that controls organic reactivity, making organic substrates and reactants soluble and also bringing them into close proximity. The efficiency of chemical transformation increases.

This chapter has provided information on the micellar effects on guest reactivity and considers the regulation of this reactivity by proper choice of the micelle container. Illustrative examples were given concerning the drug-protective and drug-delivery properties of polymer-based micelles. Some attention is focused on use of the micelle nature in studies of reaction mechanisms. Such an approach to mechanism investigation is still in its infancy but is undoubtedly of particular interest: Although a chemist's heart is devoted to mechanisms, public demands for chemistry originated due to the need for new substances and reactions.

References

- Baranano, D. E., Rao, M., Ferris, C. D., & Snyder, S. H. (2002). *Proceedings of National Academy of Sciences USA*, 99, 1093.
- Bharathy, J. R. B., Ganesan, T. K., Rajkumar, E., Rajagopal, S., Manimaran, B., Rajendran, T., et al. (2005). *Tetrahedron*, 61, 4679.
- Bica, K., Gaertner, P., Gritsch, Ph J., & Ressmann, A. K. (2012). *Chemical Communications*, 48, 5013.
- Chatterjee, N., Pandit, P., Halder, S., Patra, A., & Maiti, D. K. (2008). *Journal of Organic Chemistry*, 73, 7775.

- Gogoi, P., Hazarika, P., & Konwar, D. (2005). *Journal of Organic Chemistry*, 70, 1934.
- Hartfield, G. L., & Barclay, L. R. C. (2004). *Organic Letters*, 6, 1539.
- Laurent, E., Rauniyar, G., & Tomalla, M. (1984). *Bulletin de la Societe Chimique de France*, 78.
- Leung, M. H. M., Colangelo, H., & Kee, T. W. (2008). *Langmuir*, 24, 5672.
- Ma, Z. S., Haddadi, A., Molavi, O., Lavasanifar, A., Lai, R., & Samuel, J. (2008). *Journal of Biomedical Materials Research A*, 86A, 300.
- Okamoto, K., Hirota, N., Tominaga, T., & Terazima, M. (2001). *The Journal of Physical Chemistry A*, 105, 6586.
- Shinkai, S., Mori, S., Araki, K., & Manabe, O. (1987). *Bulletin of the Chemical Society of Japan*, 60, 3679.
- Singh, A. K., Mondal, J. A., Ramakrishna, G., Ghosh, H. N., Bandypadhyay, T., & Palit, D. K. (2005). *The Journal of Physical Chemistry B*, 109, 4014.
- Triboni, E. R., Politi, M. J., Cuccovia, I. V., Chaimovich, H., & Filho, P. B. (2003). *Journal of Physical Organic Chemistry*, 16, 311.
- Wang, Y.-J., Pan, M.-H., Cheng, A.-L., Lin, L.-L., Ho, Y.-S., Hsieh, C.-Y., et al. (1997). *Journal of Pharmaceutical and Biomedical Analysis*, 15, 1867.
- Zhang, W., Shi, Y., Ye, J., Sha, X., & Fang, X. (2011). *Biomaterials*, 32, 2894.

Chapter 8

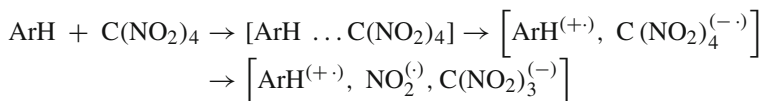
Cage Effects of Solvents, Proteins, and Crystal Lattices

8.1 Introduction

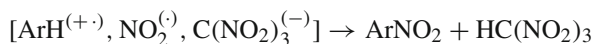
The concept of cage effects is usually connected with the Franck–Rabinovitch phenomenon: If the amount of molecules disintegrated during a thermal, photoinitiated or radiative reaction is the same, the amount of free radicals observed in solution is always significantly less than that in the gas phase. This phenomenon is caused by partial recombination of radical pairs in the solvent cage where the radicals were formed. By this means, cage effects lead to the formation of products originating from radical recombination inside their initial housing (i.e., inside the solvent cage).

8.2 Solvent-Cage Effects

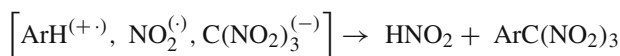
Ion-radical organic chemistry provides some prominent examples of cage effects. Nitration with tetranitromethane proceeds along the ion-radical route. It is typical for nitration of highly activated substrates such as perylene, azulene, *N, N*-dialkylaniline, etc.:



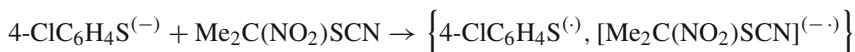
The activity of the $\text{NO}_2^{(\cdot)}$ radical is quite moderate. The leading role belongs to the $\text{C}(\text{NO}_2)_3^{(\cdot-)}$ anion. Having escaped from the solvent cage, this anion carries a proton (a light particle) away:



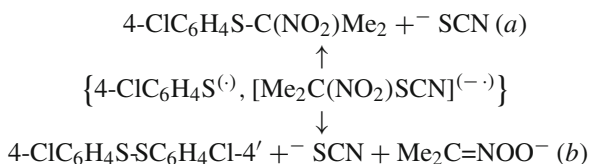
When the reaction proceeds within the solvent cage, disengagement of nitrous acid takes place with the formation of trinitromethylated products (Sankararaman and Kochi 1991):



Photoinduced electron transfer from 4-chlorophenylthiolate to 2-nitro-2-thiocyanato propane leads to the formation of the following radical–anion–radical pair (Al-Khalil and Bowman 1984):



The nature of the solvent determines the direction of the reactions proceeding within solvent cages. In dimethylsulfoxide, the main process is innercage recombination (route *a*) whereas a minor process consists of radical–anion–radical pair disintegration after its diffusion into the solvent pool (route *b*):



When methanol is used as a solvent, it protonates $[\text{Me}_2\text{C}(\text{NO}_2)\text{SCN}]^{(-\cdot)}$ within the solvent cage and thus stabilizes this anion–radical part of the pair. Such stabilization prevents inner-cage recombination and contributes to diffusion of the whole radical–anion–radical pair into the solvent pool, providing the pair disintegration according to route *b*.

For solvent-cage-confined reactions, the transformation within the contact pair must have a lower barrier than that for separation of the components of the contact pair to give individually solvated species. Generally, the barriers for diffusion of the constituents of contact pairs into the bulk solution are estimated to be on the order of 12 kJ/mol (Brunner et al. 2012) and references therein.

8.3 Interplay Between Salt- and Solvent-Cage Effects

Hubig et al. (1994) studied three distinct classes of substitution reactivity discerned in halogenation of methyl-substituted methoxybenzenes (ArH) by iodine monochloride (ICl), namely exclusive iodination, exclusive chlorination, and mixed iodination–chlorination. The prior formation of an $[\text{ArH} \cdot \cdot \text{ICl}]$ complex was established. The complex suffers electron transfer to afford the reactive triad, i.e., $\text{ArH}^{(+\cdot)}$,

$I^{(\cdot)}$, and $Cl^{(-)}$. Chlorination and iodination result from quenching of the aromatic cation-radical by chloride anion and iodine atom, respectively. Iodination versus chlorination thus represents the competition between radical- and ion-pair collapses of the reactive triad. This competition could be modulated through the dissociating ability of the solvent and by adding a “foreign” salt (Hubig et al. 1994). In nondissociating solvents (CCl_4 and CH_2Cl_2), the collapse of the ion pair was enhanced, leading to a higher proportion of the chlorinated product. In contrast, when the ions were readily separated and stabilized by solvation with a polar solvent such as acetonitrile, the radical type of collapse became predominant, making iodination competitive. The $[ArI]/[ArCl]$ ratio is equal to 90/10 in CH_3CN ($\epsilon = 36$) or 60/40 in CH_2Cl_2 ($\epsilon = 8.9$). If CH_2Cl_2 contains 0.2 M $Bu_4N^{(+)}PF_6^{(-)}$, the ratio changes from 60/40 to 40/60. Due to preferential ion pairing with the chloride anion of the reactive triad, the cation $Bu_4N^{(+)}$ makes the $ArH^{(\cdot)}$ cation-radical approachable for attack by the $I^{(\cdot)}$ radical.

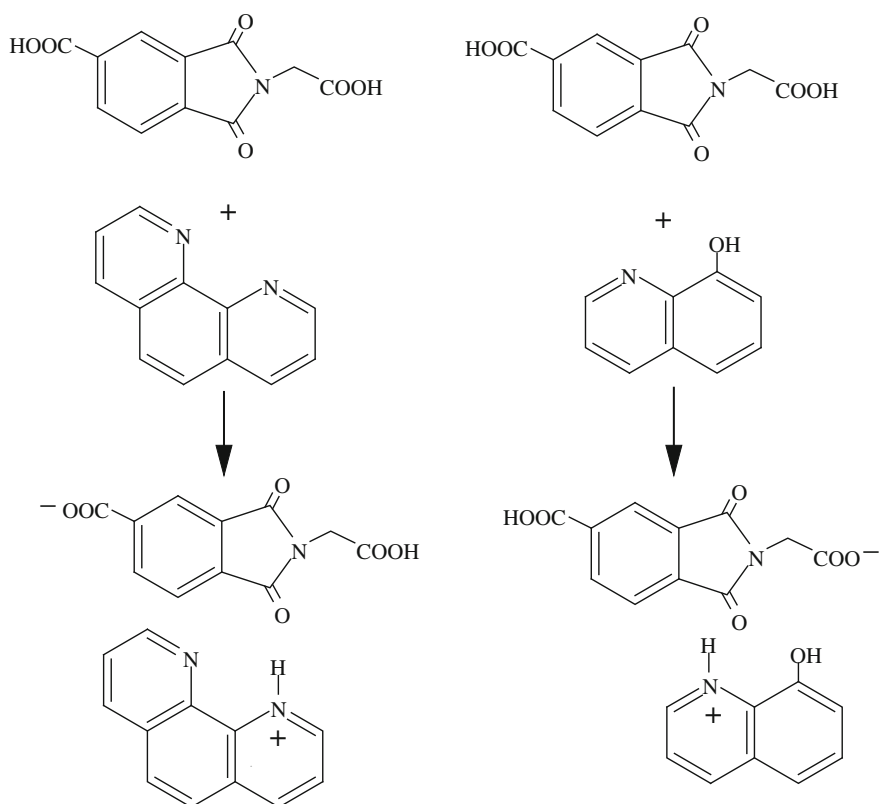
8.4 Protein-Cage Effects

Proteins are complex, large polymers containing carbon, hydrogen, oxygen, nitrogen, and usually sulfur. Proteins comprise chains of amino acids connected by peptide linkages ($-CO-NH-$). Proteins occur in the cells of all living organisms and in biological fluids (blood plasma, protoplasm). Proteins form colloidal solutions, and protein subunits develop spherical nanoparticles. The protein subunits are arranged symmetrically in a shell that encloses an interior compartment. A protein cage provides a versatile molecular scaffold, upon which chemical reactants can be introduced in a spatially defined manner.

Abedin et al. (2009) demonstrated that a cross-linked branched polymer can be synthesized within the interior cavity of a protein cage. The authors used a protein cage made of heat shock protein from *Methanococcus jannaschii*. Polymerization was initiated by reaction of *N*-propargyl bromoacetamide with a genetically engineered cysteine located on the interior of the cage-like architecture. The exposed alkyne was subsequently reacted with 2-azido-1-azidomethyl ethylamine to give S-exposed amidotriazinyl azidomethylamine. The terminal azido group was treated with tri(propargyl)amine, followed by repeated attacks by 2-azido-1-azidomethyl ethylamine and tri(propargyl)amine. As a result, branched dendritic structures were synthesized and completely filled the cavity in an ordered sequential fashion. Protein cages encapsulating the branched polymer maintained their native shape and size distribution. Meanwhile, this kind of cage filling greatly enhances thermostability. The authors anticipate application of these materials in drug delivery and imaging (Abedin et al. 2009).

8.5 Cage Effects of Crystal Lattices

Formation of close-packed structures can also define a suitable geometry for anion-cation interaction within a crystallographic cage. A relevant example consists of salt formation between the dicarboxylic acid of Scheme 8.1 and 9,1,10-phenanthroline or 8-hydroxyquinoline (Barooh et al. 2008). Of the two carboxylic groups of the diacid, one is directly bound to aromatic ring while the other adjoins the heterocycle via the methylene bridge. It is clear that the two carboxylic groups must have different acidities. However, packing in the crystalline cage determines a preferential order of acid deprotonation. This order is shown in Scheme 8.1. We see some reversal of acidity between the two asymmetrically disposed carboxylic groups. Ammonium cations occupy different places within the lattices of the formed salts. This defines the observed thermodynamic preference of proton removal from either carboxylic group.



Scheme 8.1 Order of deprotonation for aryl- and alkyl-bound carboxylic groups under action of phenanthroline or quinoline within co-crystals

8.6 Closing Remarks

Solvent-cage effects are well determined, and this chapter uses some specific examples to present generalizations. At the same time, Sects. 8.3–8.5 present points of view beyond routine considerations. In this regard, the interplay between salt- and solvent-cage effects deserves special attention. It is also important to develop our knowledge on cage effects of crystal lattices. This chapter presents an example of unpredictable deprotonation of two different carboxylic functionalities depending on the positions of the counteranions in the crystallographic cages. Development of further examples of this type would have important implications both scientifically and practically.

References

- Abedin, M. J., Liepold, L., Suci, P., Young, M., & Douglas, T. (2009). *Journal of the American Chemical Society*, 131, 4346.
- Al-Khalil, S. I., & Bowman, R. (1984). *Tetrahedron Letters*, 25, 461.
- Barooah, N., Singh, W. M., & Baruah, J. B. (2008). *Journal of Molecular Structure*, 875, 329.
- Brunner, H., Muschiol, M., Tsuno, T., Ike, H., Kurosawa, T., Koyama, K. (2012). *Angewandte Chemie International Edition*, textit51, 1067.
- Hubig, S. M., Jung, W., & Kochi, J. K. (1994). *Journal of Organic Chemistry*, 59, 6233.
- Sankararaman, S., Kochi, J. K. (1991). *Journal of the Chemical Society, Perkin Transactions 2*, 1.

Chapter 9

Pore Effects

9.1 Introduction

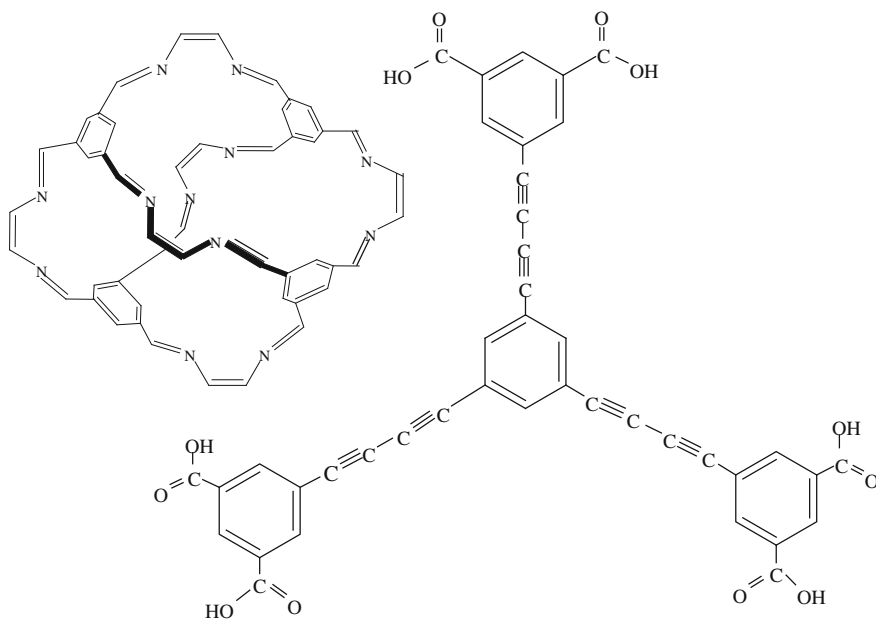
The International Union of Pure and Applied Chemistry (IUPAC) classifies pore size as follows: *micropores* (under 0.2 nm), *mesopores* (0.2–50 nm), and *macropores* (over 50 nm). The general term *nanopore* is associated with nanometer-size dimension. The presence of large pores in some coordination networks allows the design of chemical reactions to be carried out in the pores. These networks can be termed “crystalline molecular flasks,” in which organic substrates can be efficiently trapped and allowed to undergo chemical transformations. In virtue of their crystalline nature, fixing the substrates at predetermined positions enables the reactions in the pores to be topochemically controlled. However, unlike host–guest interactions in solution, substrates in porous coordination networks often only fill the spaces in the structure, rather than interacting with specific sites in the pores.

9.2 Porous Organic Frameworks

Porous organic frameworks are interesting due to their nanoporosity. The nanoporosity is retained when the material is desolvated, despite the large solvated cavity volume (Cooper 2011). Not only are organic materials highly porous, but they also demonstrate other interesting properties.

The structures of Scheme 9.1 are relevant to this chapter: The molecule on the right is a building block for an organometallic framework. Organometallic frameworks will be considered in Sect. 9.3. The molecule on the left of Scheme 9.1 represents porous organic frameworks: In the solid state, it forms a porous network and displays polymorphism.

Polymorphism emerges when a guest is taken up into molecular-sized channels in a crystalline sample of an organic framework, as depicted by the structure on the left of Scheme 9.1. Depending on the chemical nature of the guest, three different



Scheme 9.1 Examples of porous organic network (*left structure*) and of organic support for inorganic nodes to form porous crystals (*right structure*)

polymorphs can be stabilized: nonporous, selectively porous, and nonselectively porous. The porosity of the former two polymorphs can be interconverted reversibly in the solid state. The nonselectively porous form shows only limited reversibility. Most importantly, the porosity of the solid network based on the metal-free cage species of Scheme 9.1 can be switched on and off in response to a chemical stimulus. Jones et al. (2011) described this kind of porosity change in detail. On–off porosity switching might be useful in the future for controlling permeation or in capturing particular guests in a “molecular mousetrap.”

Hydrogen bonding is also a useful strategy to form permanently porous organic crystals with a huge surface area of extrinsic intermolecular porosity. Crystals of this type are formed when triptycene-like tris(benzimidazolone) self-assembles through H bonds (Cooper 2012).

9.3 Porous Organometallic Frameworks

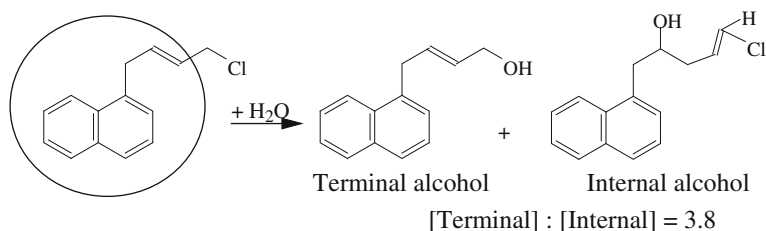
The chemical and structural diversity of organometallic frameworks is one of the most notable characteristics of these materials. They are hybrid materials composed of inorganic nodes and organic struts. The most intriguing examples exhibit large internal surface areas, ultralow density, permanent porosity, and uniformity of

channels, cavities, and voids. As an example, the paddle-wheel crystalline material with $[\text{Cu}_3(\text{L}(3))(\text{H}_2\text{O})_3]_n$ composition can be mentioned. This material was proposed by Farha et al. (2012). The structure of the organic support (i.e., L in this empiric formula) is depicted in the right half of Scheme 9.1.

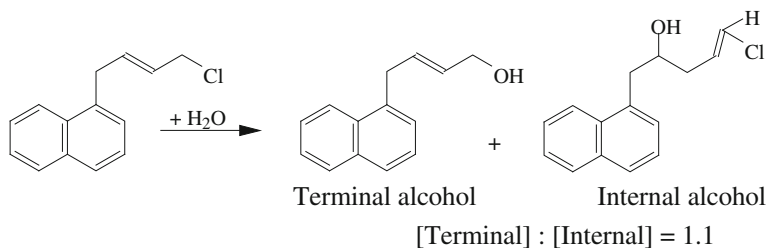
Another organometallic framework is $[\text{Zn}_2(\text{OBA})_2\text{BPY}]\bullet\text{DMA}$, where OBA stands for 4,4'-bis(hydroxybenzoate), BPY for 4,4'-bipyridyl, and DMA for *N,N*-dimethyl-acetamide (Pramanik et al. 2011). The framework contains micropores capable of including guest molecules of the appropriate size. The network has π -electronic structure. Upon photoexcitation, it serves as an electron donor when a guest has electron-withdrawing groups and as an electron acceptor when a guest bears electron-donating groups. This donor-acceptor electron-transfer interaction between the host and guest can occur upon an appropriate difference in their redox potentials and when strong overlap is possible between the corresponding π -orbitals. The described photoinduced electron-transfer reactions have been used in analytical applications: The authors exposed solid crystals of the synthesized microporous organometallic network to the vapor of guest molecules and studied the changes in the fluorescence of the starting crystals. They observed fluorescence quenching upon exposure to the vapor of acceptor aromatics (including nitroaromatic compounds) and fluorescence enhancement upon exposure to the vapor of donor aromatics. Interestingly, nitro-containing *nonaromatic* guests had a negligible effect on the fluorescence of the microporous organometallic framework. With respect to the host π -system, overlapping of the π -orbital of an aromatic guest is much stronger than that of the σ -orbital of a nonaromatic guest. The microporous effect described by Pramanik et al. (2011) illustrates the unprecedented ability of the host for sensing and detection of high explosives and aromatic compounds.

Methylviologen can be inserted into the zinc-isophthalate framework, being located at the center of the metallorganic framework (MOF) cavity. The formed diad has empirical formula $[\text{Zn}_3(\text{isophthalate})_4]\text{-methylviologen}$ (Zeng et al. 2012). In the crystal, all pyridinium ring atoms lie in the same plane, and they are parallel to the rings of the isophthalate ligands in the host frame. The plane-plane distance was determined as 0.350(5) nm. Both planes stack in π - π mode. The plane-plane distance is small enough and the orientation between host and guest molecules satisfies the requirements for intermolecular electron transfer (Yao et al. 2009). Upon visible-light irradiation (in the range of 500–700 nm) or heating above 120 °C, the crystalline sample shows irreversible color change from yellow to blue. The blue color is characteristic for the methylviologen cation-radical. ESR measurements support that external irradiation or heating is accompanied by generation of spin-bearing species. These species are stable at room temperature for weeks. The methylviologen cation-radicals exist in the monomeric, not dimeric, form and are resistant to air oxidation (Zeng et al. 2012). In the system considered, the carboxylate group acts as an electron donor to the methylviologen dication. At the same time, the metalorganic network protects the embedded methylviologen cation-radical from dimerization and reverse oxidation.

An organometallic porous network constructed from six (1,10-phenanthroline)-palladium nodes connected via 1,3,5-triazinopyridyl links was used as a noncovalent



Scheme 9.2 Reaction with water of naphthylmethylallyl chloride confined in metal-organic network

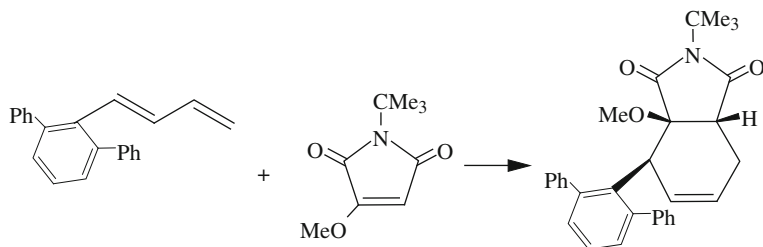


Scheme 9.3 Formation of terminal and internal allylic alcohols during reaction with water without confining metal-organic network

protective group in nucleophilic substitution of aryl-allyl chlorides (Kohyama et al. 2012). This cage is represented as a circle in Scheme 9.2. The cage accommodates 1-naphthyl-(3-methylallyl) chloride, forming a 1:1 inclusion compound. On treatment with aqueous solution containing the cage and silver nitrate at 70°C in the dark for 24 h, the substrate is completely converted to terminal and internal allylic alcohols in ratio of 3.8. As this takes place, the cage appears empty. (In a control experiment without the cage mentioned above, the ratio of terminal to internal allylic alcohols was 1.1; Scheme 9.3.) Inclusion of the substrate in the porous cage results in shielding of the internal reaction site while the external one is exposed (Scheme 9.2).

The coordination network consisting of ZnI_2 and 1,3,5-tris(4-pyridyl)triazine ligand (L) displays high molecular recognition ability in the pores (Ohmori et al. 2004; Kawamichi et al. 2008). Ikemoto et al. (2011) showed that this network, which has the formula $[(ZnI_2)_3(L)_2]$, incorporates the diene and dienophile of Scheme 9.4 and forms a common crystal with them. In this crystal, the diene and dienophile are oriented in such a manner that the bicyclic product of Scheme 9.4 is formed (upon heating) with 80% isolated yield. The orientation of the diene and dienophile prior to the reaction has been established by X-ray crystallography.

In stark contrast to the reaction within the pores, the Diels–Alder adduct was not formed in control experiments in solution or even under neat conditions despite heating. To perform the reaction in Scheme 9.4, the diene must be included in the pore of the coordination network and the inclusion compound must be crystallized. According to X-ray data, the diene was geometrically well fixed in the pore and no disorder was observed even for the flexible diene molecule. Efficient π – π interaction



Scheme 9.4 Butadiene-maleimide cycloaddition inside co-crystal with metal-organic network

was evidenced between the diene and 1,3,5-tris(4-pyridyl)triazine ligand (L). Then, the maleimide dienophile was introduced by diffusion from solution. X-ray study revealed that the two carbonyl oxygens of the maleimide were in close proximity to the edges of two triazine moieties of L. Additionally, the maleimide was also fixed by C–H•••O bonds between the carbonyl oxygens and Py-H β protons of the ligand L. As a result, both reactants were oriented in a parallel fashion within the pore and their interfacial separation did not exceed 0.4 nm. This distance is ideal for Diels–Alder reactions. The crystalline flask described above captures the reactants through host–guest stoichiometric inclusion into crystals. This makes the Diels–Alder reaction of Scheme 9.4 possible and highly effective (Ikemoto et al. 2011).

Principal results were obtained by Furutani et al. (2009) upon photoirradiation of adamantane placed in a cage resulting from self-assembly of the platinum or palladium complex with 2,2'-dipyridyl and 2,4,6-tris(pyridyl)triazine ligands. Such a cage accommodates four molecules of adamantane. Photolysis of the guest–host system in solution (water or acetonitrile) as well as in the solid state initiates single-electron transfer from the guest to the host. In this process, the extremely electron-deficient triazine component of the host acts as an electron acceptor, while adamantane acts as an electron donor. The cage (i.e., host) is not simply a vessel for this reaction, because it is transformed into the anion-radical state. An electronically altered reaction field is formed that promotes the following transformation of the confined adamantane cation-radical: It loses a proton and gives rise to a σ -radical. The generated σ -radical is trapped by water or air oxygen to give 1-adamantyl hydroperoxide or 1-adamantol. The total yield of photoproducts per cage was about 25%, indicating that only one of the four guest adamantanes was oxidized. Although four triazine ligands surround the metal, only one of them undergoes single-electron gain under experimental conditions. (Although there is no direct π -conjugation between the ligands, the single-electron redox wave in the cyclic voltammogram of the adamantane-free cage indicates that there is electronic communication among the cage constituents.) Since only one triazine constituent transforms into the cation-radical state, only one adamantane anion-radical is generated and only this sole species turns into the products of subsequent oxidation. It is worth noting that the cage-filled complex is unique and particularly well suited for guest-to-host photoelectron transfer. Furutani et al. (2009) underline that “First, the triazine core of the panel ligands is very electron-poor because of the three coordinated pyridine moieties and thus is

a good electron acceptor. Second, the four guest molecules are tightly bound and packed within the cage cavity. As a result of this cage effect, the adamantane molecules are held in very close proximity to the triazine panels, facilitating the unusual photoelectron transfer.”

The coordination polymer of $\text{Al}(\text{OH})(\text{ndc})_n$ type (where ndc stands for 1,4-naphthalene dicarboxylate) contains straight pores. If histamine [2-(1*H*-imidazol-4-yl)ethanamine] is introduced as a proton-donating/accepting molecule, effective proton conductivity is observed. Under anhydrous conditions at 150 °C, this conductivity was measured to be above 10^{-3} S/cm (Umeyama et al. 2011). The authors underline that the histamine molecules are densely packed within the one-dimensional (1D) channels, have an appropriate conformation for proton hopping, and thus form a real ion-transporting path. With its low activation energy, the material is regarded as a superionic conductor.

The homochiral metalorganic network of $\text{Zn}_2(\text{bdc})(\text{S-lac})(\text{DMF})$ is capable of enantioselective sorption of *S*-1-phenyl-1-ethanol against *R*-1-phenyl-1-ethanol by dint of their different orientation in the porous channels of $\text{Zn}_2(\text{bdc})(\text{S-lac})(\text{DMF})$. Here, bcd stands for 1,4-benzene dicarboxylate, *S*-lac for L-(-)-lactate, and DMF for *N,N*-dimethylformamide. Only *S*-PhEtOH can form a hydrogen bond with the methyl group of the surrounding ligand, and this anchors the guest inside the porous host (Suh et al. 2012).

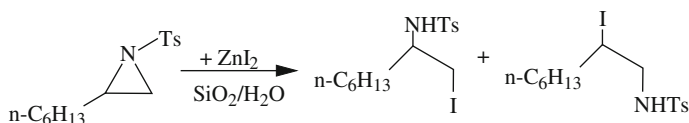
From the synthetic point of view, it is important to note the ability of metalorganic networks to enhance the solubility of reacting gas in organic solvents when the solvents are confined within the network. Thus, hydrogen uptake at 298 K and 3×10^6 Pa in *n*-hexane confined by a chromium-terephthalate network was found to be 22 times larger than in sole *n*-hexane (Clausier et al. 2012).

9.4 Silica Porous Materials

Commercial porous silica can be impregnated with rhodamine 6G ethanol solution as a result of capillary adsorption. Within the pores, the guest interacts with the polar surface. At the same time, the molecules adsorbed on the porous silica surface retain a certain degree of mobility. This enables aggregation of the incorporated rhodamine molecules. Physical dimers are formed. This phenomenon could have prospective technological applications in the fields of solid-state lasers and optical memory devices (Carbonaro et al. 2009). At the same time, both monomers and dimers remain isolated within the pore. Importantly, the isolated molecules are characterized by greater photostability than nonisolated molecules.

Porous material such as Silica Gel 60 is effective as an organic reaction medium in water, as exemplified by Scheme 9.5 (Minakata et al. 2006). After 48 h of stirring, two products were obtained: the first with 90% yield, and the second with 6% yield.

The reaction of Scheme 9.5 is based on the absorptive nature of silica gel. The reactants are collected at the external surface and within the pores, greatly facilitating the interaction between them.



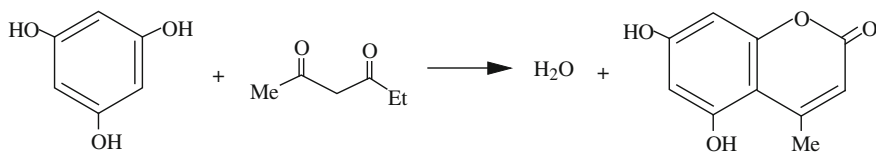
Scheme 9.5 Reductive ring opening in aziridine promoted by Silica Gel

Generation of silica-surface functional groups inside the channels allows uniform tuning of the activity of these nanoreactors. Thus, modification of SBA-15 with phenylpropyl sulfonic acid (PhPrSO₃H) along with phenyl moiety (Ph) enables enhancement of the efficacy of Pechmann condensation. Scheme 9.6 presents the condensation of phloroglucinol (1,3,5-benzenetriol) with ethylacetoacetate. (SBA-15 is Santa Barbara Amorphous material with a hexagonal array of pores.) Within such modified SBA-15, the condensation proceeds without a solvent, requires 10 min duration at 130 °C, and leads to pure 4-methyl-5,7-dihydroxy-2*H*-1-benzopyrane-2-one in 94% isolated yield. The modified SBA-15 was used in 7 mol% amount for 10 mmol phloroglucinol and, after recovery, showed practically the same activity in six successive runs (Karimi and Zareyee 2008).

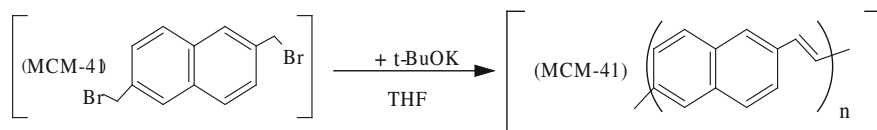
Currently, high-area, large-hollow silicas are available. They are used to perform polymerization of arylenevinyl monomers within hollow silica spheres. The resulting polymers exhibit electroconductivity and are important materials for organic transistors and electroluminescent devices. Incorporation of the polymers obtained within the internal voids of a rigid, inorganic host protects the polymer from attack by oxygen and moisture under conditions in which a film of pure polymer is promptly degraded (Alvaro et al. 2006).

Another attractive material is MCM-41 (MCM means Mobil Composition Matter). Being composed of amorphous silica walls, MCM-41 possesses a long-range ordered framework composed of uniform monospheres with pore diameter of 3.5 nm. Using MCM-41 as a host material, Peris et al. (2008) synthesized individual conjugated poly(2,6-naphthylidenevinylene) (PNV). The polymerization proceeds in the interior of the hollow silica spheres (Scheme 9.7). After deposition of a water suspension of PNV-loaded MCM-41 onto a glassy surface, most of the polymer chains were evacuated from the pores into the aqueous solvent. Eventually, a monolayer film was formed (Peris et al. 2008).

Among the various inorganic supports, microporous (pore diameters <2 nm) and mesoporous (pore diameters 2–50 nm) silicas have attracted much attention. Large



Scheme 9.6 Promotion of condensation between phloroglucinol and methyl ethyl acetoacetate with SBA-15



Scheme 9.7 Transition of 2,6-bis(bromomethyl)naphthalene into vinyl-containing polymer upon action of potassium tert-butyrate within hollow silica spheres

pore diameters allow grafting of bulky organic moieties or several fragments of small molecules. Mesoporous silica nanoparticles have a wormlike arrangement of pores, which are radially oriented from the center to the outer surface (Haskouri et al. 2002).

Thus, porous siloxane with shell interior diameter of 2 nm is capable of tethering 7-9-amino fragments from aminopropyl groups. The protonation constants of these groups in bulk solution are about 10, but within the cage the constants increase by 5–7 pH units (Henao et al. 2008). This arises because protonation of more than one amino fragment within the high local concentration inside the nanocages is prevented by electrostatic repulsion. This is caused by the brush-bristle density and restricted mobility of amines within the confined space.

The inner walls of porous silicas are covered with silanol groups ($\equiv\text{Si}-\text{OH}$) that can be functionalized. Such functionalization usually maintains the original mesoporosity, although there are some exceptions to this rule (Lee et al. 2009). Importantly, functionalization can lead to the formation of single-site, chiral, catalytically active centers. The review by Thomas and Raja (2008) describes diverse heterogeneous enantioselective conversions under spatial restrictions. The conversions proceed within nanocavities upon the inner-wall immobilized catalyst. Kidder and Buchanan (2008) used MCM-41 of 1.6 or 2.8 nm pore size to pyrolyze 4-(3-phenylpropyl)phenol in the presence of 2- or 3-hydroxyfluorene. Both reactants were covalently attached to the silica inner surface through the oxygen bridge. The pyrolysis leads to breakage of one C–H bond in the propylidene fragment. The resultant dehydrogenated radicals react with the fluorenyl hydrogen donors and transform into toluene and styrene. As follows from the pyrolysis rates, the pore confinement and curvature of the inner surface play a decisive role in the mutual orientation of the silica-supported reactants, controlling the selectivity of the homolytic hydrogen atom elimination. Sharma et al. (2008) revealed a marked catalytic effect of MCM-41 mesoporous silica grafted with amino groups on the inner walls on the Henry reaction between *p*-hydroxybenzaldehyde and nitromethane, leading to the formation of *p*-hydroxy- ω -nitrostyrene (100% conversion within 15 min).

Especially interesting is the functionalization of inner surfaces of nanoporous silica with well-defined polymers. Polymer formed in mesopores or micropores serves as an anchor for the polymer layer. These layers are not readily available in bulk systems but have implications for use in the fields of electronics and control of heterogeneous catalysis. Recently, a method was proposed to obtain polymer chains inside the pores. The formation of very thin, uniform poly(acrylonitrile) of controlled thickness was achieved within the high surface area of silicas named SBA-15 (cylindrical pores of diameter ~ 10 nm) or FDU-1 (spherical pores of diameter ~ 15 nm).

Kruk et al. (2008) generated silica–polymer composites with accessible porosity and appreciable surface area and pore volume.

Mesoporous silica nanoparticles have garnered a great deal of attention as potential carriers for therapeutic payloads. However, achieving triggered drug release from mesopores in vivo has been challenging. Singh et al. (2011) described the synthesis of stimulus-responsive polymer-coated mesoporous silica nanoparticles and the loading of therapeutics into both the core and shell domains. From them, doxorubicin is released in response to proteases present at a tumor site in vivo, resulting in cellular apoptosis. These data demonstrate the utility of polymer-coated nanoparticles in specifically delivering an antitumor payload.

Muhammad et al. (2011) employed acid-decomposable, luminescent ZnO quantum dots to seal the nanopores of mesoporous silica nanoparticles in order to inhibit premature drug (doxorubicin) release. After internalization into HeLa cells, the ZnO quantum dot lids are rapidly dissolved in the acidic intracellular compartments, and as a result, the loaded drug is released into the cytosol from the mesoporous silica nanoparticles. The ZnO nanolids behave as a dual-purpose entity that not only acts as a lid but also has a synergistic antitumor effect on cancer cells. These nanoparticles may be a significant step toward the development of a pH-sensitive drug-delivery system that minimizes drug toxicity.

9.5 Single Crystals as Porous Materials

Single crystals are also interesting as porous materials; For instance, they can be prepared by reaction of a triazine ligand with zinc iodide in the presence of 2-aminotriphenyl (Kawamichi et al. 2008). The material crystallizes into a robust network with large pores into which even bulky 2-aminotriphenyl can fit. The amino reactive groups intrude into the pores. Upon dipping the material into cyclohexane solution of acetic anhydride, acetylation of the amine molecules takes place inside the pores. No heating (as used in usual acetylation in solution) is needed. The robust nature of the crystal network tolerates the rapid diffusion of acetic anhydride into the pores. The amine–amide conversion proceeds completely. The pores also accommodate the larger octanoic anhydride, and after diffusion into the pores, the octanoic amide is obtained. Surprisingly, the pores also allow diffusion of the bulky phenyl isocyanate, and the bound aminotriphenylene is quantitatively converted into the corresponding phenyl urea. These results indicate that even large molecules have considerable mobility in the crystal pores.

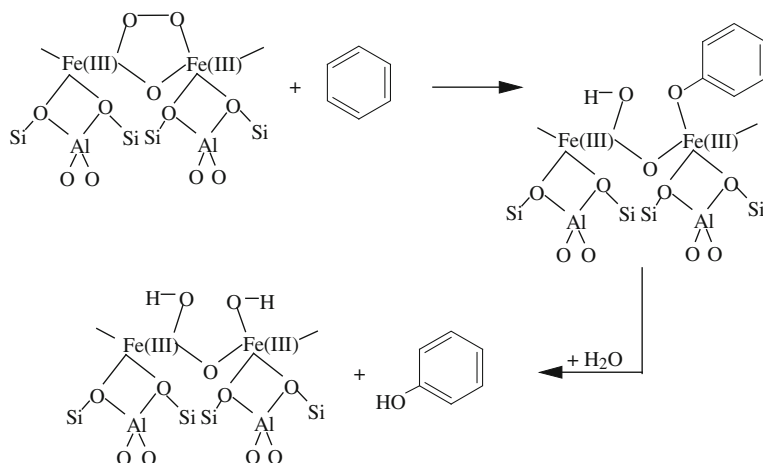
Jones and Bauer (2009) performed gas–solid bromination of *trans*-stilbene-4,4'-dicarboxylic acid confined within a cubic porous complex with zinc. As in the regular reaction, the bromination results in the formation of cyclic bromonium ion. In the solution, this bromonium ion can rotate. Inside the pores of the complex, C–C rotation of the bromonium ion is, however, prohibited due to strong ligand coordination within the framework. As a result, the cyclic bromonium ion is accessible to back-side attack by Br[−]. All these factors lead to the exclusive formation of the *meso* product, namely *meso*-4,4'-(1,2-dibromoethane-1,2-diyl)benzoate.

It is interesting to compare the results mentioned above with bromination of crystalline *trans*-stilbene with gaseous bromine (Kaupp and Mathies 1987). In this gas–solid reaction, if the bromide ion cannot migrate within the crystal to give back-side attack on the cyclic bromonium species, then *cis* addition to give the *rac*-dibromide becomes possible. Experimentally, the heterogeneous gas–solid reaction turned out to be not so selective and gave a *meso/rac* ratio of 2:1. Contrarily, a mixture with *meso/rac* ratio of 4:1 was obtained from homogeneous reaction in solution of dichloromethane.

Dawn et al. (2011) reported the synthesis and self-assembly of an expanded bisurea macrocycle to give crystals with columnar channels. Constructed from two C-shaped phenylethynylene units and two urea groups, the macrocycle affords a large pore with diameter of ~ 0.9 nm. Despite its increased size, the macrocycles assemble into columns with high fidelity to afford porous crystals. The porosity and accessibility of these channels have been demonstrated by gas adsorption studies and by the uptake of coumarin to afford solid inclusion complexes. Upon ultraviolet (UV) irradiation, these inclusion complexes facilitate conversion of coumarin to its *anti* head-to-head photodimer with high selectivity. This is contrary to what is observed upon solid-state irradiation of nonincluded coumarin, which affords photodimers with low selectivity and conversion. The reader is directed to the original paper by Dawn et al. (2011) for the complex picture of the described transformations.

9.6 Zeolites as Confining Materials

From the chemical point of view, zeolites as porous materials are especially interesting. They are crystalline aluminosilicates characterized by strictly regular porous structure. Zeolites have a large free intracrystalline volume consisting of channels and cages, sometimes interconnected. The faujasite and pentasil family of zeolites are widely used in petrochemical processes such as cracking, isomerization, alkylation, and alkene oligomerization. The zeolite lattice is a three-dimensional network of tetrahedral $[\text{SiO}_4]^{4-}$ and $[\text{AlO}_4]^{5-}$ with Si or Al atoms at centers and O atoms in each corner. The combination of $[\text{SiO}_4]^{4-}$ and $[\text{AlO}_4]^{5-}$ within the zeolite framework creates a negative charge. Consequently, silicon–aluminum zeolites bear cations to be electrically neutral. In most cases, Na^+ appears as such a cation, but there are zeolites with H^+ , NH_4^+ , K^+ , Ca^{2+} , etc. These cations are accommodated in an inner cavity and are loosely bound to the zeolite framework. The loosely bound cations can be exchanged for transition-metal cations. Such trapping of transition-metal cations gives zeolites additional catalytic functions due to the high chemical reactivities of transition-metal cations (some such catalytic reactions are considered in this Chapter). Zeolites can be artificially prepared or used as naturally occurring minerals found in volcanic rocks, where they have been formed by hydrothermal processes. Upon heating, natural zeolites release a large amount of water. This feature explains the name “zeolites,” which was derived from the Greek words *zein* (to boil) and *litos* (stone). Of course, when the water is liberated, zeolites



Scheme 9.8 Formation of phenol from benzene upon action of ZSM-5 containing oxygen atoms and ferric cations

can actively trap organic molecules with sizes that correspond to the pore volumes. In this sense, zeolites should be considered as solid solvents in terms of the partition coefficient of reactants inside and outside the pore system.

So-called solid solvation in fact consists in adsorption of any guest molecule on a zeolite. This is the first step of the interaction considered, and adsorption takes place onto the external surface. After that, size–shape–selective diffusion occurs, inside the internal pores. Moscatelli et al. (2008) proved an improved model in which the external surface of zeolites is composed of strong binding sites, located on the pore openings, and weak binding sites, situated between the pores. The high porosity and openness of the zeolite structures provide the medium for chemical transformations of guests. These transformations have the possibility of proceeding in precise and well-defined spatial arrangements.

On the other hand, zeolites can trap the intermediates of catalytic reactions inside the channels and prolong their contact time with the catalysts. This results in the formation of another gamut of products. Thus, syngas ($\text{CO} + \text{H}_2$) gives longer-chain C_{5+} hydrocarbons over catalysts encapsulated inside supercages of faujasite compared with the reaction over the outside catalyst (Tang et al. 2004). The same effect of confinement was observed in Fischer–Tropsch synthesis over iron catalyst inside carbon nanotubes (Chen et al. 2008). The zeolite Socony Mobil-5 (ZSM-5) containing oxygen atoms and ferric cations is an excellent catalyst that transforms benzene into phenol at room temperature (Xia et al. 2008). Scheme 9.8 outlines the transformation.

ZSM-5 containing platinum (Pt-ZSM-5 zeolite) provides *trans*-preferential partial hydrogenation of fatty-acid chains. This allows the preparation of healthier fats/oils (low in *trans*, high in *cis*) with desirable melting properties, from real feedstocks (Philippaerts et al. 2011). Vegetable oils are made up of triglycerol molecule mixtures, comprising three fatty acids esterified to a glycerol backbone. It is important to

prepare *partially* hydrogenated products with significantly low *trans* admixtures because the latter lead to a serious risk of cardiovascular disease. It is commonly accepted that triacylglycerols are sorbed onto zeolite in a fork shape. The more linear the prong of the fork, the more easily it penetrates into the zeolite pore. Olefinic compounds in *trans* configuration are slightly more linear than their *cis* counterparts. This explains the *trans* preference in the partial hydrogenation of triacylglycerol molecules.

Sastre et al. (2011) proposed a method for selective, room-temperature methane oxygenation by deep-ultraviolet photolysis over zeolites in air in the presence of water. Liquid C₁ oxygenated products are formed with selectivities above 95 % at 13 % conversion. Pure silica zeolites, and more specifically β -zeolite with a large number of internal silanol groups, are active and selective, while amorphous silica with no micropores is much less efficient. Ultraviolet irradiation initiates the homolytic cleavage of surface hydroxyl groups, leading to silyloxyl radicals that will generate methyl radicals from methane. The selectivity arises from the occurrence of the reaction in a confined space restricting the mobility of the radical intermediates that will be mostly attached to the solid surface. The energy consumption of the process is on the order of 7.2 Gcal/mol, which compares very favorably with the energy required for transforming methane to syngas (15.96 Gcal/mol).

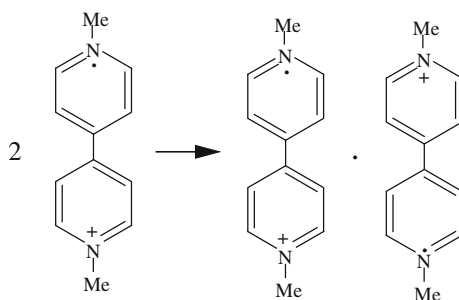
Zeolites can also act as microreactors with enhanced chemical selectivity. In fact, reactants and products often differ in their diffusion ability as well as in the preferential adsorption of molecules in the zeolite channels and cavities (as a function of their polarity). This leads to selective activation of organic compounds. Once trapped, the molecules tend to optimize their configuration towards the most favorable van der Waals interaction with the cavity or channel walls. When the formed products have a huge volume, exceeding the pore/cavity size, this can prevent the development of the reaction. Within zeolites, conversion of methanol into lightweight hydrocarbons is prohibited by the formation of bicyclic arenes (Olsbye et al. 2012) or adamantane derivatives (Wei et al. 2012).

When the molecular size of the adsorbate is close to the dimension of the cavity or channel, its frontier molecular orbitals are strongly affected. This reinforces the corresponding acidity or basicity and increases the reactivity. Trapping of organic compounds by zeolites from solution is accompanied by frustration of the hydrogen-bonding network and by decrease in the solution density. These effects (induced by confinement) facilitate penetration of the organic compounds inside the zeolite channels.

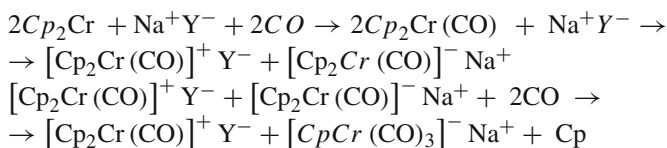
In zeolites, ionic pairs of cations and anions are not tight, so that electron migration can occur over the electron-deficient sites in pentasil zeolites such as sodium cations (e.g., in Na-ZSM-5) or over the aluminum centers. Alternatively, hole migration (redistribution of positive charge) can occur via electron-rich sites, such as oxygen sites in the zeolite framework. All these processes indeed take place during trapping of organic substrates by zeolites.

Differing from isotropic media, in which the direction and magnitude of electric field fluctuate around a solvated molecule, cations in a zeolite cavity generate a stronger, anisotropic, and more stable electric field. The presence of high internal

Scheme 9.9 Formation and dimerization of viologen cation-radical within zeolite pores



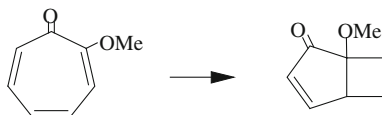
electric fields and coordinatively unsaturated Na^+ extraframework cations in the zeolite interior offers a unique reaction environment to encapsulated molecules. This was demonstrated by carbonylation of chromocene, Cp_2Cr (Estephane et al. 2009). In experiments, chromocene was molecularly dispersed inside NaY zeolite supercages and, for comparison, inside polystyrene nanopores. In contrast to NaY zeolite, the polystyrene matrix acts as a solid solvent only. In both cases, Cp_2Cr was simply encapsulated as a neutral Cp_2Cr molecule with no further reaction. Upon addition of CO ($P_{\text{CO}} = 150\text{Torr}$) to Cp_2Cr , $[\text{Cp}_2\text{Cr}(\text{CO})]$ is formed. Having formed inside the polystyrene matrix, this product is stable at room temperature. Within the NaY zeolite supercage, $[\text{Cp}_2\text{Cr}(\text{CO})]$ undergoes rapid evolution at the same temperature. In this case, electron transfer and ligand exchange take place to yield the $[\text{Cp}_2\text{Cr}(\text{CO})]^+ \text{Y}^-$ and $[\text{CpCr}(\text{CO})_3]^- \text{Na}^+$ species. Taking into consideration that each NaY supercage can absorb two molecules of chromocene, the following mechanism was proposed (Estephane et al. 2009):



In other words, zeolitic pores can act as nanoscale reaction chambers for guest molecules. In this regard, the reaction of dried, dimethylviologen-doped zeolites with solvated electrons in diethyl ether should also be mentioned (Park et al. 2000). Dimethylviologen readily transforms into the corresponding cation-radical within the zeolite pores. Two dimethylviologen cation-radicals dimerize in this confined environment with the formation of a p -type complex consisting of two dimethylviologen cation-radicals, as depicted in Scheme 9.9.

Cations present in zeolites, being only partially coordinated to the surface oxygens, are free to interact with guest molecules. The sodium cation plays a special role during accommodation of organic molecules. A guest such as phenylalanine, for instance, exhibits the following types of interaction with Na^+ : $\text{Na}^+ \bullet \bullet \bullet \pi$, $\text{Na}^+ \bullet \bullet \bullet \text{O}=\text{C}$, and $\text{Na}^+ \bullet \bullet \bullet (:) \text{N}$. Importantly, these types of interaction conjointly restrict

Scheme 9.10 Methoxytropone rearrangement upon photoirradiation within zeolite



the conformational mobility of Na^+ -bound phenylalanine. In solution, the influence of the alkali ions is prevented by coordination of the cations to solvent molecules. The conformations of free and Na^+ -bound phenylalanine are different (Sivaguru et al. 2003).

In 1998, Joy et al. prepared chirally modified zeolites and used them as chiral hosts for asymmetric photoreactions; For example, a mixture of NaY zeolite, 2-methoxytropone, and (-)-2-amino-1-phenyl-1-propanol (norephedrine, a chiral inductor) in dichloromethane–hexane was stirred for 12 h and filtered to give the zeolite containing both the reactant and chiral inductor. Using a medium-pressure mercury lamp, this filled zeolite as hexane slurry was photoirradiated for 2 h to yield the optically active bicyclic product of Scheme 9.10 at up to 50% *e.e.* Apparently, not all reactant molecules occupied the inner sphere, and therefore 100% enantioselectivity was not observed.

The authors enumerate the following anchoring points that ensure the achieved enantioselectivity: the hydroxyl, amino, and aryl groups of norephedrine, the carbonyl and methoxy groups of methoxytropone, and the sodium cations of the zeolite. Moreover, hydrogen bonding occurs between norephedrine and methoxytropone, whereas electrostatic interaction also connects the zeolite cation and the norephedrine phenyl group. This view reveals that one of the faces of methoxytropone is fairly open while the other is encumbered by the zeolite surface. This is the reason for the enantioselectivity mentioned Joy et al. (1998).

Organic molecules spontaneously form corresponding cation-radicals during inclusion within activated zeolites (Yoon and Kochi 1988; Yoon 1993; Pitchumani et al. 1997). As zeolites act as electron acceptors due to the presence of Lewis- or Brønsted-acid sites, confined organic compounds are electron donors. Frequently, the interaction of electron donors with electron-acceptor centers spontaneously generates cation-radicals and traps the ejected electrons. Of course, the electron-donor ability of organic compounds is important for these reactions.

The formation of organic cation-radicals leads to their further deprotonation. Negatively charged framework oxygen stabilizes the formed hydrocarbon cations. Generally, the formation of cation-radicals in porous media allows the most correct data on their reactivity to be obtained; For example, organic cation-radicals are usually very sensitive to surrounding nucleophilic reagents. This results in their consumption before deprotonation. In channels of redox-active zeolites, the cation-radical deprotonation proceeds preferably because competing reactions with outside reagents are precluded. Catalytic transformation of organic hydrocarbons in zeolites is practically very important for petroleum refining processes. (Every molecule of petrol passes through the pores of a zeolite.) Particularly, a key problem is which positions are

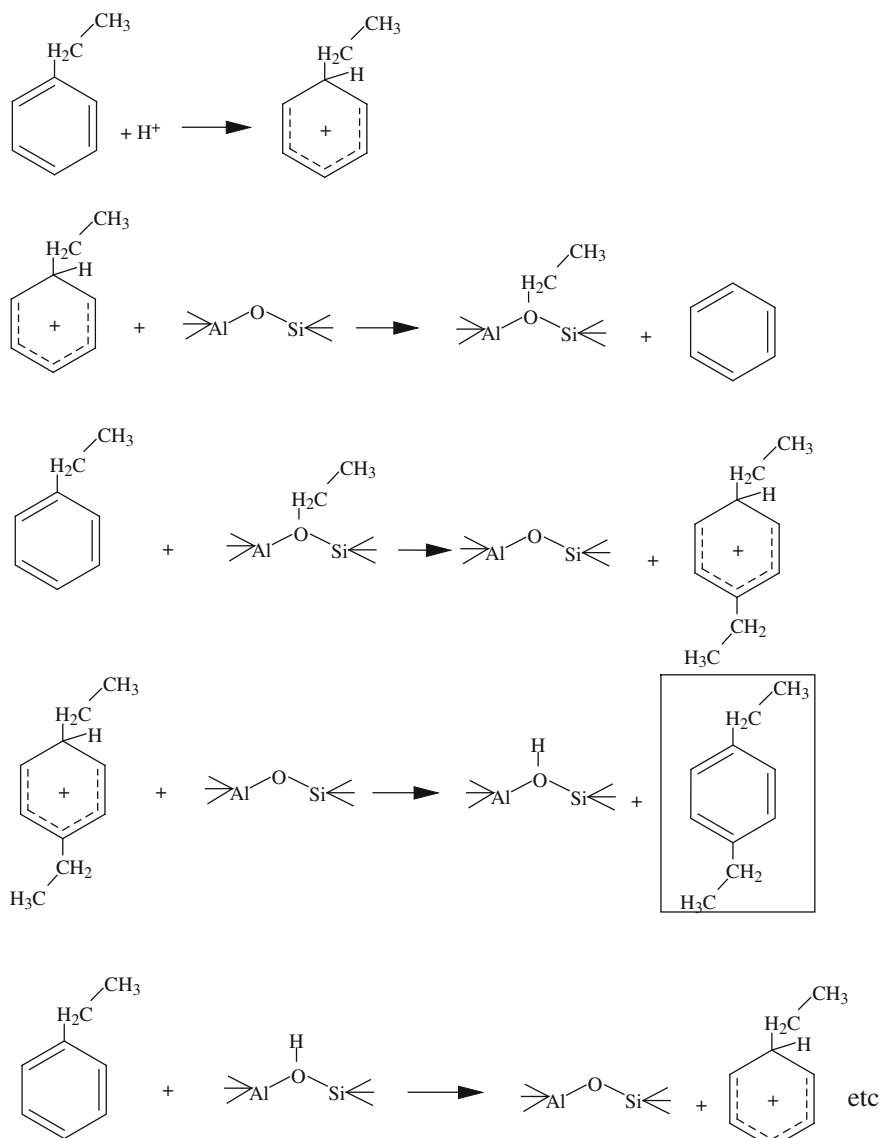
active in the deprotonation, or in other words, which radical is generated after proton abstraction from the initial hydrocarbon cation-radical.

The electron spin resonance spectra of alkane cation-radicals show that the dominant hyperfine constant is caused by hydrogen atom of *terminal* methyl groups that lie in the plane of the carbon skeleton in its extended conformation. The proton loss from the cation-radical is thought to involve the C–H bond of the highest electron density (Toriyama et al. 1982). Calculations show that spin enrichment of the C–H bond leads to its elongation. This leads to weakening of the C–H binding and facilitates the bond disruption (Shchapin and Chuvylkin 1996).

For instance, the completely expanded cation-radical of *n*-heptane forwards its terminal proton to the neutral parent molecule if both participants are neighbors in the zeolite cavity: $\text{RH}^{(+\bullet)} + \text{RH} \rightarrow \text{R}^{(\bullet)} + \text{RH}_2^{(+)}$. This reaction results in selective formation of the 1-heptyl radical (Demeyer et al. 1993). In the case of *trans*-oct-2-ene, the cation-radical deprotonation predominantly leads to allyl radical formation (Fel'dman et al. 1993): $[\text{CH}_3\text{CH}=\text{CH}-(\text{CH}_2)_4-\text{CH}_3]^{(+)} \rightarrow \rightarrow \text{H}^{(+)} + (\text{CH}_2-\text{CH}-\text{CH})^{(\bullet)} - (\text{CH}_2)_4\text{CH}_3$. Further reactions consist in splitting the expanding radicals and in recombination of splinters with each other or with atomic hydrogen. The resultant products are obtained from the industrial cracking process.

Besides cracking, thermal condensation can proceed within porous materials if its cages are large-sized; For instance, formation of heptamethylbenzenium ion was established as a result of methane passing over molecular sieves of SAPO type, $\text{Si}_{0.144}\text{Al}_{0.493}\text{P}_{0.362}\text{O}_2$ (Li et al. 2012). The authors did not provide a mechanism for the process inside the porous material, but underlined that ample supercages (~ 0.1 nm in diameter) and extremely high concentration of Brønsted acids were responsible for the stabilization of this bulky intermediate in the cages of the sieve.

Disproportionation of aromatic hydrocarbons is also an important petrochemical process. Thus, ethylbenzene disproportionation is used to produce the valuable *para* isomer of diethylbenzene. This reaction strongly depends on the acidic properties and pore shape of zeolites. It is also used as a standard reaction for acidity characterization according to the International Zeolite Association (IZA) method. Huang et al. (2008) described a mechanism of *p*-diethylbenzene formation that takes into account participation of a medium-sized zeolite ZSM-5 as the ethyl-group carrier (Scheme 9.11). The disproportionation begins with protonation of the ethylbenzene aromatic ring and develops the ethylcyclohexyl carbonium ion. At higher temperatures, the carbonium ion splits off an ethyl cation and produces unsubstituted benzene. The ethyl cation is stabilized by a nearby Si–O–Al site to form a Si–O(CH₂CH₃)–Al fragment. The latter combines with the second molecule of ethylbenzene within the pore to yield the *p*-diethylphenyl cation containing an additional proton at the aromatic ring. This proton migrates to the nearby Si–O–Al site, producing diethylbenzene as the final product. *p*-Diethylbenzene is the most preferred product, because the formation of *o*- and *m*-isomers is restricted by the pore size of zeolite ZSM-5. The reaction on zeolite pores is a clean process without side-reactions, which is interesting for industrial applications. It should also be mentioned that the zeolite-governed reactions can sometimes proceed at the pore mouth, under conditions of partial



Scheme 9.11 Mechanism of 1,4-diethylbenzene formation from ethylbenzene inside Na-ZSM-5 pores

confinement (i.e., guest molecules penetrate small zeolite channels only partially as they react). The partial confinement of a hydrocarbon into such zeolite pores leads to a configurational preference for cracking at terminal C–C bonds (Gounder and Iglesia 2009).

It should be noted, however, that diverse zeolites differ in their electron-acceptor power. Cation-radicals are formed along with carbocations, but the carbocation generation can be diminished by selection of an appropriate zeolite and activation method; For instance, Ca(Y) zeolite activated by heating above 400° C on a high-vacuum line was found to be ideal for cation-radical generation when a diarylethene was sorbed from cyclohexane solution. The generation proceeds even in the absence of light, with minimum interference from carbocations (Pitchumani et al. 1997).

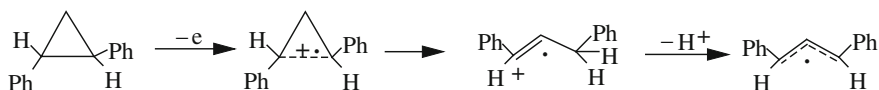
To develop this theme, it would be interesting to compare H-ZSM and M-ZSM zeolites with different cations, on the one hand, and organic electron donors of variable ionization potentials, on the other hand. Zeolite H-ZSM-5 generates cation-radicals from substrates with oxidation potential of up to +1.65 V (Ramamurthy et al. 1991).

Thus, solid tetracene is introduced into the dehydrated medium-porous H-ZSM-5 by direct exposure under dry and inert atmosphere without any solvent. The rod-shaped tetracene fits tightly into the pore size of the zeolite. Inside H-ZSM-5, a slow reaction takes place consisting of tetracene cation-radical formation and aluminum electron trapping. Charge recombination is hindered, and the electron-hole combination is stabilized efficiently (Marquis et al. 2007).

Important results were obtained during incorporation of *N,N'*-diphenylhydrazine into H-ZSM-5: Azobenzene and aniline were formed (Marti et al. 2000). The authors rationalized these two products by two competing mechanisms. One mechanism consists of the formation of the *N,N'*-diphenylhydrazine cation-radical that loses a proton and then the hydrogen atom; The other (competing) mechanism includes protonation of *N,N'*-diphenylhydrazine by H-ZSM-5 followed by N–N bond cleavage in the resultant hydrazonium ion. These reactions take place within the pores of the zeolite, where intermediary forms are protected from alien reagents that would cause their decay.

Al-ZSM-5 zeolites, calcified in an atmosphere of oxygen or argon, adsorb naphthalene. Two occluded particles—the naphthalene cation-radical and isolated electron—are formed. Both particles were determined by the electron spin resonance method. The back reaction between the oppositely charged particles proceeds extremely slowly, and both signals persist over several weeks at room temperature (Moissette et al. 2003).

Easily ionizable anthracene forms a cation-radical as a result of preliminary sorption within M-ZSM-5 (Marquis et al. 2005). Anthracene is sorbed as it is without ionization. Among the counterbalancing alkali cations, only Li⁺ can induce sufficient polarization energy to initiate spontaneous ionization at the moment of anthracene sorption. The lithium cation has the smallest ionic radius, and its distance to the oxygen net is the shortest. The ejected electron appears to be delocalized in a restricted space around the Li⁺ ion and Al and Si atoms in the zeolite framework. The anthracene cation-radical appears to be in proximity to the space where the electron is delocalized. This opens the possibility for the anthracene cation-radical to be stabilized by the electron negative field. In other words, a special driving force for one-electron transfer is formed in the case of Li-ZSM-5.

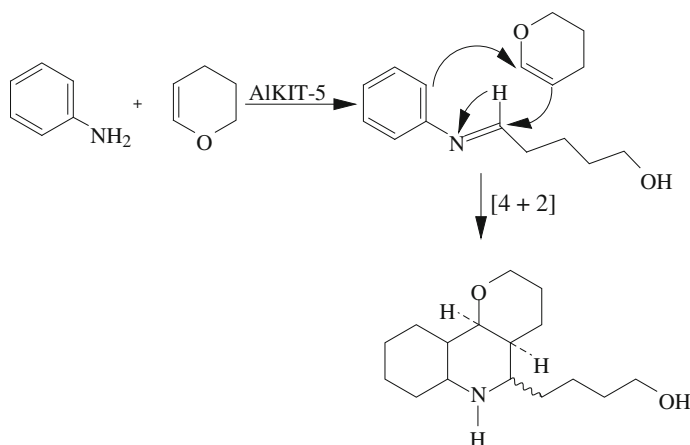


Scheme 9.12 Consecutive steps in formation of diphenyl allyl radical from *trans*-diphenylcyclopropane within Na-ZSM-5 hollow spheres

An important feature of zeolites is their selectivity with respect to substrate shape and conformation. The internal cavity system of a zeolite can host organic guest molecules. The type of guests sorbed depends on the chemical nature, dimensions, and topology of the zeolite channels and cages; For instance, zeolite ZSM-5 is bidirectional because its internal space is constituted by two systems of oval channels—one straight ($0.53 \times 0.56 \text{ nm}^2$) and the other sinusoidal with an elliptical opening ($0.51 \times 0.55 \text{ nm}^2$)—crossing each other at right angles (Garcia and Roth 2002; Moissette et al. 2007). Accordingly, *trans*-1,2-diphenylcyclopropane is readily incorporated into the channels of Na-ZSM-5, whereas the *cis* counterpart remains unconfined (Herbertz et al. 2000). The *trans* isomer fits into the zeolite channel (whose internal diameter is approximately 0.55 nm), whereas the *cis* isomer appears to be too bulky. On reaction with the zeolite, the incorporated *trans* isomer consecutively undergoes one-electron oxidation, ring opening, and hydrogen migration (benzylic protons occur adjacent to one of the phenyl groups). In this way, the benzyl-containing cation-radical is formed. The latter loses a proton to give an *exo,exo*-1,3-diphenylallyl radical as the final product. The allyl radical is more or less stable and is protected against contact with other reactants by being incorporated into the zeolite interior. Scheme 9.12 illustrates the whole transformation (Herbertz et al. 2000).

A tight fit of the organic substrate within the zeolite pore or channel is essential for generation of long-lived cation-radicals; For instance, biphenyl fits tightly at the intersections between the straight and sinusoidal channels of Na-ZSM-5. When biphenyl is sublimated into zeolite under vacuum and then photoirradiated, the cation-radical is formed. Its lifetime within the pore reaches days, much longer than that in acetonitrile solution (Moissette et al. 2007).

Cation-radicals, stabilized in zeolites, are excellent one-electron oxidizers for alkenes. The back electron transfer is, as a rule, decelerated (see, for instance, Zhang et al. (2009) and references therein). In the direct electron-transfer reaction, only those oxidizable alkenes can give rise to cation-radicals, which are able to penetrate into the zeolite channels. Of two dienes, 2,4-hexadiene and cyclooctadiene, only the linear one (with cylindrical width of 0.44 nm) can reach the biphenyl cation-radical or encounter it in the channel (if the biphenyl cation-radical migrates from its site toward the alkene donor). The eight-membered ring is too large to penetrate into the Na-ZSM-5 channels. Cyclooctadiene can be confined if the cylindrical width is 0.61 nm; however, the width of the channels in Na-ZSM-5 is only 0.55 nm. No cyclooctadiene reaction with the confined biphenyl cation-radical was detected despite the fact that, in solution, one-electron exchange between cyclooctadiene and biphenyl^(+•) proceeds readily (Morkin et al. 2003).



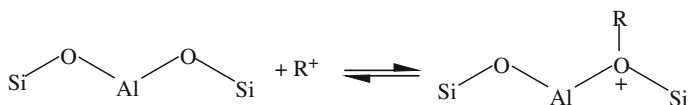
Scheme 9.13 Co-condensation of aniline with dihydrofuran in nanocages of AIKIT-5 aluminosilicate (Reproduced with permission from Georg Thieme Verlag on September 13, 2012)

Size compatibility is not the sole factor defining the possibility of cation-radical generation. Although the estimated width of 2,3-dihydrofuran is 0.38 nm, this cycloalkene ether does not react with the biphenyl cation-radical confined in Na-ZSM-5 zeolite. (In solution, this electron exchange proceeds easily.) As Morikin et al. (2003) pointed out, it is possible that the preferred location of oxygen-containing dihydrofuran in zeolite is very different from that of 2,4-hexadiene. Particularly, the lone-pair electrons on the dihydrofuran oxygen can coordinate with the metal cations located on the external surface of zeolite. This inhibits diffusion of dihydrofuran into the zeolite channels and prevents the possible electron exchange.

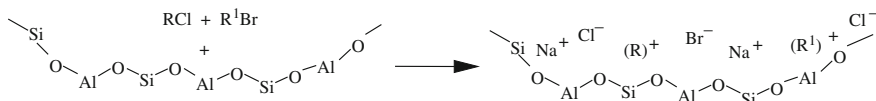
In contrast, nanoporous three-dimensional aluminosilicate AIKIT-5 is capable of incorporating 2,3-dihydrofuran (2 equivalents) and aniline (1 equivalent) from acetonitrile solution. After 5 h at 25 °C, a furo[3.2-*c*]quinoline derivative is formed with 92% yield as an *edo* (95%) and *exso* (5%) isomeric mixture (Chauhan et al. 2012). This cycloaddition happens within the nanocage of AIKIT-5. The cage provides high surface area, large pore volume, and a well-defined porous structure with strong Brønsted acidity. Notably, no reaction was observed at 25 °C in the absence of AIKIT-5. Obviously, aniline within the cage transforms into its cation-radical. The cation-radical loses protons, reacts with dihydrofuran, and yields 2-azodiene. The latter intermediate accepts another molecule of dihydrofuran and gives the fused quinoline derivative. The fully analogous reaction was observed between aniline and 3,4-dihydro-2*H*-pyran to afford a pyrano[2.3-*c*]quinoline derivative (Scheme 9.13) (Chauhan et al. 2012). AIKIT-5 was found to be highly stable and could be used several times without affecting its activity to confine and sterically organize this imino Diels–Alder process.

Scheme 9.13 (permission of September 13, 2012)

The restriction on the nucleophiles that can penetrate and react with a confined cation-radical sometimes leads to unexpected results. Comparing the reactions of



Scheme 9.14 Anchorage of carbocations to zeolite internal surface as approach to protect them



Scheme 9.15 Role of NaY zeolite in stabilization of two different carbocations from pair of organyl halides

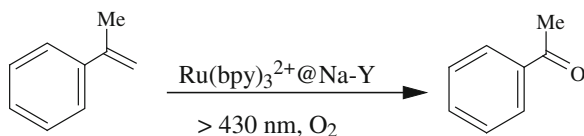
thianthrene cation-radical, (Randgappa and Shine 2006) referred to the zeolite situation. When thianthrene is adsorbed by zeolites, either by thermal evaporation or from solution, the thianthrene cation-radical is formed. The adsorbed cation-radical is stable for a very long time. If isooctane (2,2,4-trimethylpentane) was used as a solvent, *tert*-butylthianthrene was formed in high yield. The authors noted “it is apparent that the solvent underwent rupture, but the mechanism of the reaction remains unsolved.”

Another unexpected reaction inside zeolites was found by Franko et al. (2008). The authors injected an equimolecular mixture of *tert*-butyl chloride and *sec*-butyl bromide into a N₂ stream, and passed it over NaY zeolite at room temperature. As a result, *tert*-butyl bromide and *sec*-butyl chloride were formed. The same reactions were observed for several alkyl halide pairs. These reactions are, on the face of it, general; they have never been reported in solution. Obviously, within the zeolite any pair of alkyl halides forms carbocations that then take part in the halogen switch described. On the zeolite internal surface, these carbocations are reversibly stabilized, forming alkoxides according to Scheme 9.14 (cf. Scheme 9.11).

In solution, the substrate is completely surrounded by solvent molecules, and scrambling of carbocations and halides is retarded by the solvation shells. Therefore, either the solvent or the leaving group (internal return) attacks the carbocation formed. On zeolites, the pore structure permits the concentration of two different alkyl halide molecules inside the cavities, allowing the formed carbocations to interact with two different leaving groups (nucleophiles), as pictured in Scheme 9.15.

As seen in Scheme 9.15, the halogen switch occurs inside the pores of the zeolite, due to confinement, which localizes the carbocation between two different nucleophiles.

Another interesting aspect deals with the reactivity of a guest filled inside cages of zeolites with no space for other chemicals. Using a cation-exchange procedure, Na⁺-Y zeolite was filled with Ru(NH₃)₆Cl₃ in the absence of oxygen. The prepared Ru/Na⁺-Y was refluxed in ethylene glycol solution containing 2,2'-bipyridine (bpy) to obtain Ru(bpy)₃²⁺ encapsulated in Na⁺-Y (Mori et al. 2008). The estimated diameter of Ru(bpy)₃²⁺ is ~1.2 nm, so this complex occupies most of the volume of the Na⁺-Y zeolite supercage (the supercage diameter is ~1.3 nm). In other words, the encapsulated material was prepared via a “ship-in-a-bottle” method. The acetonitrile solution of the encapsulated material and 2-phenyl-1-propene was bubbled with



Scheme 9.16 Acetophenone formation upon phenylpropene photooxidation with oxygen and ruthenium complex inside NaY zeolite

oxygen and then UV photoirradiated at $\lambda > 430 \text{ nm}$. This excitation generates a triplet state of the encapsulated complex. The latter reacts with out-of-cage oxygen and 2-phenyl-1-propene at room temperature with the formation of acetophenone (Scheme 9.16) (Mori et al. 2008). In the reaction, a superoxide anion ($\text{O}_2^{\bullet-}$) was proven to be the main reactive species. This $\text{O}_2^{\bullet-}$ species was produced by an excited ruthenium (confined) complex reacting with O_2 via photoinduced electron transfer. Interaction between superoxide anion and 2-phenyl-1-propene eventually results in the acetophenone formation. Out-of-cage electron-transfer reactions proceed in this case just as was noted for the incarcerated guest in Sect. 1.3.

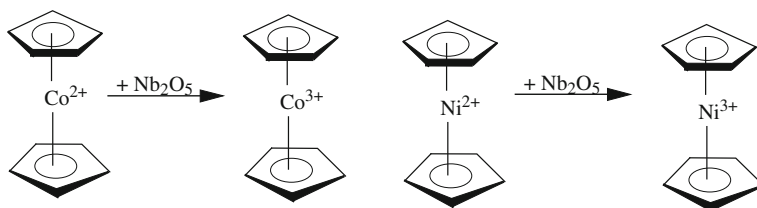
9.7 Confinement Within Porous Metal Oxides

Mesoporous transition-metal oxides are also materials with confinement ability. Such metal oxides can be obtained by hydrolysis of acetylacetonate complexes with metal isopropylates in aqueous solution containing potassium tetradecyl phosphate (a surfactant) at pH 4–6 and aging at 80°C for several days (Antonelli and Ying 1995). The resultant materials possess pore size of 2–5 nm and surface areas of up to $1,200 \text{ m}^2/\text{g}$.

Mesoporous samples of niobium pentoxide were prepared by hydrolysis of niobium pentachloride in the presence of Pluronic block copolymers. Under these conditions, gels or sols are formed and, upon aging, provide structurization of the oxide within templates. The resulting oxide samples were removed from the templates by long-time thermolysis at 110°C (Aydhya et al. 2008), by spray pyrolysis at 200°C using nitrogen as a carrier gas (Konopka et al. 2010), or merely by solvent-extraction treatment (Nakajima et al. 2010).

Mesoporous materials present specific effects. These materials have pore diameters in the range of 2.0–50.0 nm, which is much larger in general than that of zeolites and is certainly beyond the size of normal organic substrates. Reductions of mesoporous niobium oxide by cobaltocene and nickelocene are relevant examples. The sandwich molecules undergo one-electron oxidation (Scheme 9.16) (Skadchenko and Antonelli 2006). Niobium(V) is partly reduced to niobium(IV) and transforms into a material in the pores of which there are both niobium(IV) and niobium(V) centers. The electron captured by Nb_2O_5 is not tightly bound to the one niobium center.

Although Scheme 9.17 does not distinguish between the resulting metalloceniums, the difference really exists (Skadchenko and Antonelli 2006). Namely, the



Scheme 9.17 One electron oxidation of cobaltocene or nickelocene by mesoporous niobium pentoxide

one-oxidation potential of cobaltocene is lower than that of nickelocene. Cobaltocene is oxidized more easily than nickelocene. All of the cobaltocene molecules are intercalated and wholly oxidized by the niobium site with strong oxidizing strength. The resulting cobaltocenium is retained in the pores containing delocalized electrons (and therefore charged negatively). The authors determined that a supermagnetic material (Skadchenko and Antonelli 2006) somewhat resembling a double electric layer is formed (cf. Bottenus et al. 2009).

Nickelocene is oxidized incompletely and nickelocenium is incompletely retained within the pores. The authors describe the resulting material as a spin glass, in which the spins are in random orientation (Skadchenko and Antonelli 2006). No similar double electric layer is formed.

9.8 Confinement Within Carbon and Polymer Nanopores

A chemical reaction confined to a nanoscale environment can have a different outcome compared with the same reaction in the bulk phase; For instance, the content of nanopores generally has a higher density than that in the bulk. Le Chatelier's principle predicts that this results in an increase in yield for reactions in which there is a decrease in the total number of moles. Conversely, a drop in yield occurs for reactions for which the total number of moles increases. A classic example is the equilibrium between NO and N_2O_2 : In the vapor phase this conversion proceeds for less than a few percent, whereas in nanoporous carbons, the dimer can be obtained with many-time increased yields (Lisal et al. 2008).

It is interesting to compare data on the equilibrium between NO and N_2O_2 that takes place in carbon nanopores with data on the equilibrium between NO_2 and N_2O_4 that takes place in the internal microporous cavities in polymers. Groppo et al. (2008) exposed commercial poly(4-vinylpyridine) to 2.7 kPa NO_2 and observed that NO_2 dimerizes in the pores, giving rise to N_2O_4 . The latter disproportionates into the ionic $NO^+NO_3^-$ species. The nitrosonium cation NO^+ thereupon reacts with the pyridine unit of the polymer, in its internal pores, and forms poly[*N*-(4-nitrosopyridinium)] nitrate. Other mechanisms of the $NO^+NO_3^-$ reaction with

poly(4-vinylpyridine) are also allowable, but the mechanism just described is simple, logical, and understandable.

9.9 Closing Remarks

This chapter described interesting properties of metalorganic frameworks (MOFs) as confining matrices. In this regard, it should be mentioned that one MOF has been put into application using readily available sources, namely γ -cyclodextrin and potassium hydroxide with empirical formula $[(C_{48}H_{80}O_{40})(KOH)_2]_n$ (Smaldone et al. 2010). This MOF was prepared by combining 1.0 equivalents of γ -CD with 8.0 equivalents of KOH in aqueous solution under ambient temperature and pressure. After diffusion of methanol into the solution during 2–7 days, colorless, cubic, single crystals were deposited. The crystals have 1.7-nm-sized pores. These large, spherical pores reside at the center of each γ -CD and are connected by a series of smaller voids to form a porous framework. For future uses, it is important that this MOF is thermally stable up to 175 °C and that its porosity does not change (Smaldone et al. 2010).

References

- Alvaro, M., Ferrer, B., Garcia, H., & Peris, E. (2006). *The Journal of Physical Chemistry B*, 110, 16887.
- Antonelli, D. M., & Ying, J. Y. (1995). *Angewandte Chemie International Edition*, 34, 2014.
- Ayudhya, S. K. N., Soottitantawat, A., Praserttham, P., & Satayaprasert, Ch. (2008). *Materials Chemistry and Physics*, 110, 387.
- Bottenus, D., Oh, y.-J., Han, S. M., & Ivory, C. F. (2009). *Lab on a Chip*, 9, 219.
- Carbonaro, C. C., Meinardi, F., Ricci, P. C., Salis, M., & Anedda, A. (2009). *The Journal of Physical Chemistry B*, 113, 5111.
- Chauhan, S., Mane, G. P., Anand, C., Dhawale, D. S., Subba Reddy, B. V., Zaidi, S. V. J., et al. (2012). *SYNLETT*, 23, 2237.
- Chen, W., Fan, Zh, Pan, X., & Bao, X. (2008). *Journal of the American Chemical Society*, 130, 9414.
- Clausier, S., Ho, L. N., Pera-Tlitus, M., Coasne, B., & Farruseng, D. (2012). *Journal of the American Chemical Society*, 134, 17369.
- Cooper, A. I. (2011). *Angewandte Chemie International Edition*, 50, 996.
- Cooper, A. I. (2012). *Angewandte Chemie International Edition*, 51, 7892.
- Dawn, S., Dewal, M. B., Sobransingh, D., Paderes, V. C., Wibowo, A. C., Smith, M. D., et al. (1993). *Journal of Physical Chemistry*, 97, 1477.
- Estephane, J., Groppo, E., Damin, A., Vitillo, J. G., Gianolio, D., Lamberti, C., et al. (2009). *Journal of Physical Chemistry C*, 113, 7395.
- Farha, O. K., Wilmer, Ch E, Eryazici, I., Hauser, B. G., Parilla, Ph A, O'Neil, K., et al. (2012). *Journal of the American Chemical Society*, 134, 9860.
- Fel'dman, V. I., Ulyukina, E. A., Sukhov, F. F., & Slovokhotova, N. A. (1993). *Khimicheskaya Fizika*, 12, 1613.
- Franco, M., Rosenbach, N., Ferreira, G. B., Guerra, A. C. O., Kover, B., Turci, C. C., et al. (2008). *Journal of the American Chemical Society*, 130, 1592.

- Furutani, Yu., Kandori, H., Kawano, M., Nakabayashi, K., Yoshizawa, M., & Fujita, M. (2009). *Journal of the American Chemical Society*, *131*, 9172.
- Garcia, H., & Roth, H. D. (2002). *Chemical Reviews*, *102*, 3947.
- Gounder, R., & Iglesia, E. (2009). *Journal of the American Chemical Society*, *131*, 1958.
- Grosso, E., Uddin, M. J., Zavorotynska, O., Damin, A., Vitillo, J. G., Spoto, G., et al. (2008). *Journal of Physical Chemistry C*, *112*, 19493.
- Haskouri, J. E., Zarate, D. O., Guillem, C., Lattore, J., Caldes, M., Bertran, A. et al. (2002). *Chemical Communications*, 330.
- Henao, J. D., Suh, Y.-W., Lee, J. K., Kung, M. C., & Kung, H. H. (2008). *Journal of the American Chemical Society*, *130*, 16142.
- Herbertz, T., Lakkaraju, P. S., Blume, F., Blume, M., & Roth, H.D. (2000). *European Journal of Organic Chemistry*, 467.
- Huang, J., Jiang, Y., Marthala, V. R. R., & Hunger, M. (2008). *Journal of the American Chemical Society*, *130*, 12642.
- Ikemoto, K., Inokuma, Y., & Fujita, M. (2011). *Journal of the American Chemical Society*, *133*, 16806.
- Jones, J. T. A., Holden, D., Mira, T., Hasell, T., Adams, D. J., Jelfs, K. E., et al. (2011). *Angewandte Chemie International Edition*, *50*, 749.
- Jones, S. C., & Bauer, Ch A. (2009). *Journal of the American Chemical Society*, *131*, 12516.
- Joy, A., Scheffer, J. R., Corbin, D. R., & Ramamurthy, V. (1998). *Chemical Communications*, 1379.
- Karimi, B., & Zareyee, D. (2008). *Organic Letters*, *10*, 3989.
- Kaupp, G., & Mathies, D. (1987). *Chemische Berichte*, *120*, 1897.
- Kawamichi, T., Kodama, T., Kawano, M., & Fujita, M. (2008). *Angewandte Chemie International Edition*, *47*, 8030.
- Kidder, M. K., & Buchanan, A. C. (2008). *Journal of Physical Chemistry C*, *112*, 3027.
- Kohyama, Y., Murase, T., & Fujita, M. (2012). *Chemical Communications*, 48, 7811.
- Konopka, D. A., Pylpenko, S., Atanassov, P., & Ward, T. L. (2010). *ACS Applied Materials Interfaces*, *2*, 86.
- Kruk, M., Dufour, B., Celer, E. B., Kowalewski, T., Jaroniec, M., & Matyjaszewski, K. (2008). *Macromolecules*, *41*, 8584.
- Lee, D.-H., Choi, M., Yu, B.-W., & Ryoo, R. (2009). *Chemical Communications*, 74.
- Li, J., Wei, Y., Chen, J., Tian, P., Su, X., Xu, Sh, et al. (2012). *Journal of the American Chemical Society*, *134*, 836.
- Lisal, M., Cosoli, P., Smith, W. R., Jain, S. K., & Gubbins, K. E. (2008). *Fluid Phase Equilibria*, *272*, 18.
- Marquis, S., Moissette, A., Vezin, H., & Bremard, C. (2005). *The Journal of Physical Chemistry B*, *109*, 3723.
- Marquis, S., & Moissette, A. (2007). *The Journal of Physical Chemistry B*, *111*, 17346.
- Marti, V., Fornes, V., Garcia, H., & Roth, H. D. (2000). *European Journal of Organic Chemistry*, 473.
- Minakata, S., Hotta, T., & Komatsu, M. (2006). *Journal of Organic Chemistry*, *71*, 7471.
- Moissette, A., Vezin, H., Gener, I., & Bremard, C. (2003). *The Journal of Physical Chemistry B*, *107*, 8935.
- Moscatelli, A., Liu, Zh, Lei, X., Dyer, J., Abrams, L., Ottaviani, M. F., et al. (2008). *Journal of the American Chemical Society*, *130*, 1134.
- Muhammad, F., Guo, M., Qi, W., Sun, F., Wang, A., Guo, X., et al. (2011). *Journal of the American Chemical Society*, *133*, 8778.
- Moissette, A., Bremard, C., Hureau, M., & Vezin, H. (2007). *Journal of Physical Chemistry C*, *111*, 2310.
- Mori, K., Kawashima, M., Kagohara, K., & Yamashita, H. (2008). *Journal of Physical Chemistry C*, *112*, 19449.
- Morkin, T. L., Turro, N. J., Kleinman, M. H., Brindle, Ch S, Kramer, W. H., & Gould, I. R. (2003). *Journal of the American Chemical Society*, *125*, 14917.

- Nakajima, K., & Fukui, Ts. (2010). *Chemistry of Materials*, 22, 3332.
- Ohmori, O., Kawano, M., & Fujita, M. (2004). *Journal of the American Chemical Society*, 126, 16292.
- Olsbye, U., Svelle, S., Bjorgen, M., Beato, P., Janssens, T. V. W., Joensen, F., Bordiga, S., & Lillerud, K. P. (2012). *Angewandte Chemie International Edition*, 51, 5810.
- Park, Y. S., Lee, K., Lee, Ch., & Yoon, K. B. (2000). *Langmuir*, 16, 4470.
- Peris, E., Hernando, J., Llabres i Xamena, F. X., van Hulst, N. F., Boudelande, J. L., & Garcia, H., (2008). *Journal of Physical Chemistry C*, 112, 4104.
- Philippaerts, A., Paulussen, S., Breesch, A., Turner, S., Lebedev, O. I.; Van Tendeloo, G., Sels, B., Jacobs, P. (2011). *Angewandte Chemie International Edition*, 50, 3947.
- Pitchumani, K., Lakshminarasimhan, P. H., Presvost, N., Coebin, D. R., & Ramamurthy, V. (1997). *Chemical Communications*, 181.
- Pramanik, S., Zheng, Ch., Zhang, X., Emge, Th J, & Li, J. (2011). *Journal of the American Chemical Society*, 133, 4153.
- Ramamurthy, V., Caspar, J. V., & Corbin, D. R. (1991). *Journal of the American Chemical Society*, 113, 594.
- Randgappa, P., & Shine, H. J. (2006). *Journal of Sulfur Chemistry*, 27, 617.
- Sastre, F., Fornes, V., Corma, A., & Garcia, H. (2011). *Journal of the American Chemical Society*, 130, 17257.
- Sharma, K. K., Buckley, R. P., & Asefa, T. (2008). *Langmuir*, 24, 14306.
- Shchapin, I. Y., & Chuvylkin, N. D. (1996). *Izvestia RAN, Seria khimicheskaya*, 321.
- Singh, N., Karambelkar, A., Gu, L., Lin, K., Miller, J. S., Chen, Ch S, et al. (2011). *Journal of the American Chemical Society*, 113, 19582.
- Sivaguru, J., Natarajan, A., Kaanumalle, L. S., Shailaja, J., Uppili, S., Joy, A., et al. (2003). *Accounts of Chemical Research*, 36, 509.
- Skadchenko, B. O., & Antonelli, D. M. (2006). *Canadian Journal of Chemistry*, 84, 371.
- Smaldone, R. A., Fogan, R. S., Furukawa, H., Gassenmith, J. J., Slawin, A. M. Z., Yaghi, O. M., et al. (2010). *Angewandte Chemie International Edition*, 49, 8630.
- Suh, K., Yutkin, M. P., Dybtsev, D. N., Fedin, V. H., & Kim, K. (2012). *Chemical Communications*, 48, 513.
- Tang, Q. H., Zhang, Q. H., Wang, P., Wang, Y., & Wan, H. L. (2004). *Chemistry of Materials*, 16, 1967.
- Thomas, J. M., & Raja, R. (2008). *Accounts of Chemical Research*, 41, 708.
- Toriyama, K., Nunome, K., & Iwasaki, M. (1982). *Journal of Chemical Physics*, 77, 5891.
- Umeyama, D., Horike, S., Inukae, M., Hijikata, Y., & Kitagawa, S. (2011). *Angewandte Chemie International Edition*, 50, 11706.
- Wei, Y., Li, J., Yuan, C., Xu, Sh, Zhou, Y., Chen, J., et al. (2012). *Chemical Communications*, 48, 3082.
- Xia, H., Sun, K., Sun, K., Feng, Zh, Li, W. X., & Li, C. (2008). *Journal of Physical Chemistry C*, 112, 9001.
- Yao, Q.-X., Ju, Zh-F, Jin, X.-H., & Zhang, J. (2009). *Inorganic Chemistry*, 48, 1266.
- Yoon, K. B., & Kochi, J. K. (1988). *Journal of the Chemical Society*, 110, 6586.
- Yoon, K. B. (1993). *Chemical reviews*, 93, 321.
- Zeng, Y., Fu, Zh, Chen, H., Liu, Ch., Liao, Sh, & Dai, J. (2012). *Chemical Communications*, 48, 8114.
- Zhang, H., Rajesh, Ch S, & Dutta, P. K. (2009). *Journal of Physical Chemistry C*, 113, 4263.

Chapter 10

Stereochemical Outcomes of Confinement

10.1 Introduction

Steric aspects of confinement allow investigation of the influence of effects such as penetration into cavities or the dense part of the double layer near the electrode, as physisorption or chemisorption, as well as fixation of organic molecules within charge-transfer complexes. Incorporation of a host into micelles also causes conformational reorganization and thereby can increase the capability of the host to accept guests (Javor and Rebek 2011). All these effects have been considered in the corresponding chapters as applied to particular reactions. This chapter is devoted to the stereochemical outcomes of confinement phenomena that were found out of these considerations.

10.2 Effects of Guest Confinement on Host Configurations

It is widely accepted that a snug fit for a guest corresponds to $55 \pm 0.09\%$ of the host internal volume. Sometimes, hosts distend their walls to accommodate larger occupants (Purse and Rebek 2006). For definite features of the nature of the host, structural reorganization is possible, depending on the size of the guest, even though the guest is placed entirely inside the cavity. If the guest is too small, steric effects are too small to deform the shape of the interior cavity. Conversely, if the guest is too large but can, nevertheless, be encapsulated, distortion of the host interior cavity is possible.

Cyclodextrins (CBs) can also be sterically changed upon inclusion of guests. CBs are presently considered not as rigid molecules but as flexible ones. Their flexibility is related to local fluctuations of the individual glucose rings and distortions of the macrocyclic structure (Lipkowitz 1991). Interestingly, while α -CB and γ -CB are almost equally prone to distortion, β -CB undergoes restricted macrocyclic ring

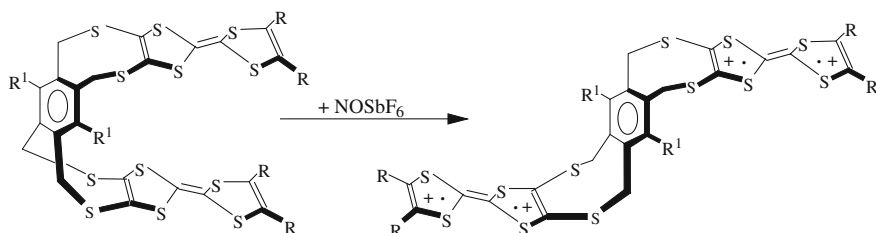
motion and relaxes significantly faster than other members of the CB family (Naidoo et al. 2004).

For instance, the α -cyclodextrin ring was reported to deviate from the hexagonal geometry to a configuration with ellipsoid cross-section upon inclusion of 4,4'-biphenyl dicarboxylic acid (Kamitori et al. 1998). This ellipsoid-shaped distortion is attributable to the planar structure of the guest phenyl ring.

Sgarlata et al. (2009) studied inclusion of aromatic and aliphatic anions into a cationic water-soluble calix[4]arene in water solution. The calix[4]arene used was 5,11,17,23-tetrakis[(dimethylamino)methyl]-25,26,27,28-tetrahydroxy-calix[4]arene. As anions, they utilized benzoate, butyrate, benzene sulfonate, and propyl sulfonate. As established by potentiometric, electrophoretic, and ^1H NMR analysis in D_2O at pD 7.1, all four amino groups of the host were still protonated and all the organic acids used as guests existed as the corresponding anions. All of the guests were included in the host cavity thanks to concerted hydrophobic and electrostatic effects. The aromatic anions formed stronger complexes than the aliphatic ones. The tighter binding of the aromatic guests is due to a π - π host-guest interaction that usually is more effective than the CH - π interaction occurring in the aliphatic host-guest complexes. To fit the guest better, the host somewhat changes its shape. The stereochemical result was most significant at pH 2. Under these conditions, the inclusion complexes become tighter.

Cucurbit[8]uril, CB[8], encapsulates 1,7-dimethyl-1,4,7,10-tetraazacyclododecane tetra(hydrochloride). The guest—a macrocyclic polyammonium compound—enters the host cavity entirely. The average planes of the inner and outer macrocycles are almost perpendicular to each other. The outer macrocycle, i.e., CB[8], changes from a round ring to an ellipse. Usually, the cucurbituril entrance diameter is defined as the distance between two opposite carbonyl oxygens of one rim. In the free state, CB[8] has a cavity entrance diameter of 0.99 nm. The resulting ellipse acquires two different axes of 0.93 and 1.07 nm, respectively (Wu et al. 2010). It is worth noting that the guest aza macrocycle shows antitumor activity. The complex of these two macrocycles is expected to have practical importance as a drug carrier in the field of medicine.

When included in a tweezers-like complex, an organic compound can change its polarizability, as was noted for Scheme 1.42. When such a polarizable interaction leads to the formation of charge-transfer complexes between host and guest, the distance between the pincers can be dramatically reduced. An example was recently given by Legouin et al. (2009). An electron getting into a host molecule can be identified as a guest. This corresponds to reduction of the host. From the same point of view, oxidation introduces a hole into a host, and such a hole can be considered as a guest. Scheme 10.1 outlines the hole-induced conformational change of a tetrathiafulvalene molecular tweezers based on a 1,2,4,5-tetramethylenebenzene scaffold. In the neutral form, this host adopts the closed, tweezers-like conformation. Oxidation results in the formation of tetrakis(tetrathiafulvalene) tetracation-tetraradical product. The cation-radical moieties experience strong electrostatic repulsion and come apart with the formation of an open conformation. Reduction of the cation-radical restores the tweezer-like, closed form (Azov et al. 2008). This property makes the

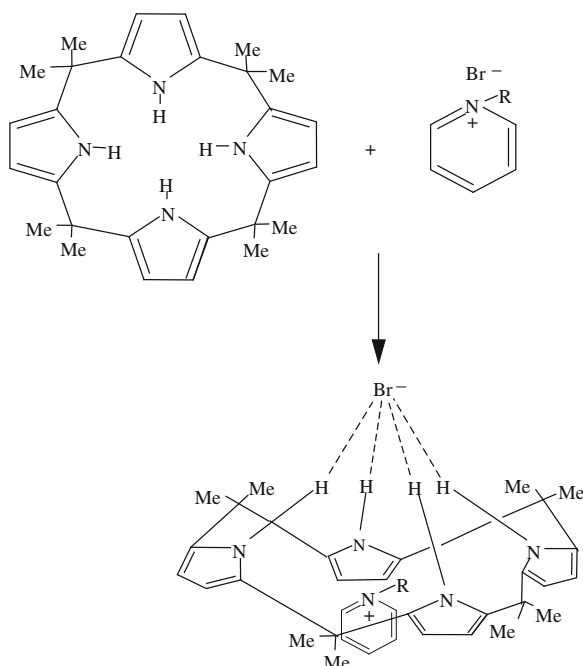


Scheme 10.1 Hole-induced conformational change in tetrathiafulvalene tweezers

tweezers of Scheme 10.1 a valuable switching block for construction of functional dynamic molecular architectures.

If a cavitand is likened to a solvent cage, it becomes clear that an encapsulating substrate can organize an appropriate “solvent environment” around itself, namely can induce the folding of the host to its vase conformation. The resultant inclusion complex is made rugged by steric effects. This phenomenon was outlined by Restor and Rebek (2008). As a particular example, reaction of *meso*-octamethylcalix[4]pyrrole with pyridinium bromide can be mentioned. The pyrrole binds bromide via four $\text{NH} \cdots \text{Br}^-$ hydrogen bonds and adopts the vase conformation. The pyridinium cation enters the cavity formed and is fixed there. Scheme 10.2 illustrates this wonderful case of self-organization to confine an organic salt as an ion pair (Caltagirone et al. 2010; Custelcean et al. 2005). In cases of interaction of *meso*-tetramethyltetraarylcalix[4]pyrroles (the hosts) with pyridine *N*-oxide derivatives (the guests), the host preorganization aims towards the vase conformation with a deep aromatic cavity (Verdejo et al. 2009). Such preorganization provides a combination of $\text{NH} \cdots \text{O}$ bonding, π - π , $\text{CH}-\pi$, and hydrophobic interactions between the hosts and the guests. The corresponding complexes turn out to be very stable, with the guest playing a fastening role.

As seen, the conformation of the host must supply a strong interaction with the guest at appropriate distances and angles. If a host does not undergo a significant conformational change upon complexation, it is preorganized. On the other hand, high flexibility of the host consumes energy, which is then not available for the binding process. Of course, conformationally flexible hosts are able to adjust rapidly to complexation conditions, and both complexation and decomplexation become possible and rapid. It is worth noting that, for successful complexation, the host’s conformation must provide not only sufficient interior concave surface but also an entry suitable for the guest to enter. The well-known host *p*-tertbutylcalix[4]arene provides an outstanding example of stereochemical changing: When the host–guest attraction is strong enough and when the host–guest geometrical-fitting requirements are satisfied, the rotation of the host *tert*-butyl groups produces a turnstile effect to make entry of the guest possible (Thallapally et al. 2005).

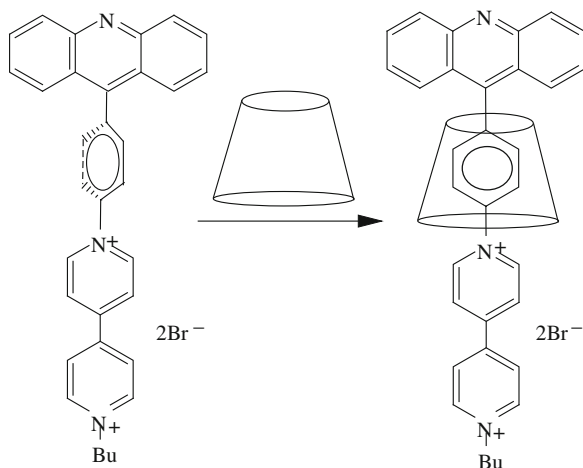


Scheme 10.2 Inclusion of pyridinium cation in cavity resulting from H-bond formation between bromide anion and calix[4]pyrrole

10.3 Stereochemical Changes of Guests Upon Their Inclusion into Hosts

Scheme 10.3 presents an unusual planarization of a spacer in an electron donor–acceptor diad. The spacer is the phenylenyl group having 65° dihedral angle with the acridine chromophore. Once encapsulated into β -CD, the spacer undergoes a rotation and thereby becomes almost coplanar with acridine. This unusual planarization as compared with the uncomplexed diad enhances electron transfer between the donor and acceptor moieties. Experimentally, encapsulation results in significantly decreased both fluorescence quantum yield and lifetime of the excited state. Electrochemical reduction of the viologen moiety has also been impeded after diad confinement (Hariharan et al. 2007).

An unprecedented fluorescence enhancement was observed in aqueous solutions of the complex formed by cucurbit[7]uril (CB[7]) and viologen carrying two *para*-tolyl groups on the quaternized nitrogens. Without CB[7], this viologen in aqueous solutions manifests very weak fluorescence: The free host acquires a conformation in which one *para*-tolyl ring and two rings of the 4,4'-bipyridinium core are coplanar and exhibit a quinonoid structure with alternating bond lengths. For this reason, the S_1 state turns out to be relaxed. Encapsulation in CB[7] guards the mentioned rings



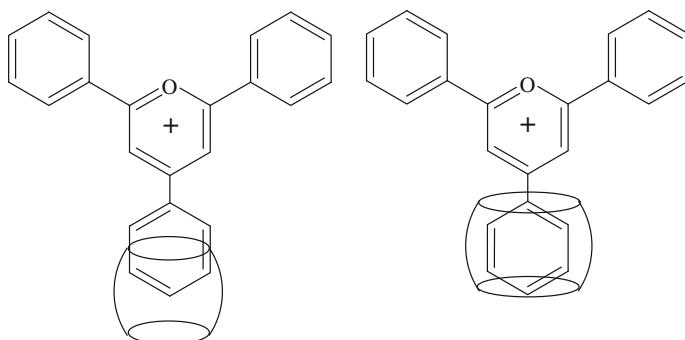
Scheme 10.3 Planarization of phenylbenzyl spacer in acridine-viologen dye after encapsulation in cyclodextrin

against rotation, prevents the guest molecule from adopting the quinonoid geometry, and results in dramatically increased fluorescent emission (Freitag et al. 2012). The authors noted that the viologen complex described can bind to nanostructured metal oxide films. Such organic–inorganic layers have good prospects for use in light-emitting diode applications.

The intrinsic fluorescence of *trans*-stilbene remains unchanged upon inclusion into a large capsule of 0.24 nm length and 0.620 nm³ volume. The fluorescence of the same guest is quenched after inclusion into a small capsule of 0.17 nm length and 0.245 nm³ volume (Ams et al. 2009). As follows from the theoretical calculations by Tzeli et al. (2012), the geometry of *trans*-stilbene in its ground state as well as its first excited singlet state is unaffected by encapsulation in the large cage, and consequently the absorption and emission spectra are similarly unaffected. In the small cage, the ground state of the encapsulated *trans*-stilbene is distorted, with the two phenyl groups twisted. The geometry of the excited state is conical, with interruption of the conjugation along the guest molecule. After inclusion of *trans*-stilbene into the small capsule, the former emission changes into nonradiative decay.

Nilsson et al. (2008) studied complexation between α -CD or β -CD and alkyl-bis(trimethylammonium) dibromides (bolaform surfactants with alkyl chains containing 8, 10, and 12 carbon atoms). The two positively charged ammonium groups of bolaforms pass through the hydrophobic CD cavity. Since the two charges at the bolaform ends must reside outside the CD cavity, this leads to stretching of the hydrocarbon chain when it enters the cavity.

In contrast to cyclodextrins, cucurbiturils can bend alkyl chains inside their capsules: When CB[8] includes alkyl-trimethylammonium bromides with alkyl chains containing 8, 10, and 12 carbon atoms, the long aliphatic chains are buried deep inside the capsule. X-ray structural analysis of these host–guest complexes provided



Scheme 10.4 Effects of cucurbit[7]uril and cucurbit[8]uril internal volume on triphenyl pyrilium penetration degree

unequivocal proof of the U-shaped conformation of the long alkyl chains, despite the high internal strain developed. This strained U-shaped conformation is stabilized by electrostatic and van der Waals interactions of the long chain with the carbonyl-lined portal and hydrophobic cavity of CB[8]. The ammonium group of the guests is located just outside of the portal, while leaning toward a narrow circle of the portal to maximize its interaction with the carbonyl groups of the host (Ko et al. 2008).

The internal hydrophobic cavity of CB[7] is smaller than that of CB[8]. Encapsulation of 2,4,6-triphenylpyrilium by these cucurbituril takes place through the phenyl group at position 4 of the pyrilium cation. Compared with CB[7], CB[8] provides deeper penetration for this phenyl ring into the cavity (cf. left and right structures of Scheme 10.4). When CB[7] is used as a host, the rotation of the 4-phenyl group is significantly restricted while the phenyl rings at positions 2 and 6 rotate freely. When CB[8] is used as a host, the 4-phenyl ring is able to rotate whereas the rotation of the external 2- and 6-phenyl rings is strongly impeded. These external rings are not included in the CB[8] capsule, but the proximity of their *ortho* hydrogen atoms to the portal carbonyl groups strongly interferes sterically with their conformational mobility. Therefore, the conformation of the 2- and 6-rings is locked by a high-energy barrier. The mentioned difference between CB[7] and CB[8] inclusion complexes with 2,4,6-triphenylpyrilium is clearly manifested in their spectral properties (Montes-Navajas et al. 2008).

A demonstrative example concerns flattening of thioflavin T. Thioflavin T is 4-(3,6-dimethyl-1,3-benzothiazol-3-ium-2-yl)-*N,N*-dimethylaniline chloride. As a free compound, thioflavin T prefers a nonplanar conformation with a torsional angle between the two aromatic parts of $\sim 35^\circ$. This is a yellow basic dye that exhibits yellow to yellowish-green fluorescence when excited by ultraviolet light. Staining with thioflavin T has been used for identification of amyloid fibrils. Amyloid is a protein polymer that deposits in human tissues as a result of long-term disturbance in nourishment, during chronic suppuration, or upon Alzheimer's disease, syphilis, or tuberculosis. When thioflavin T is confined in sheets of amyloid oligomers, the dye undergoes a characteristic blueshift of its emission spectrum. This blueshift is

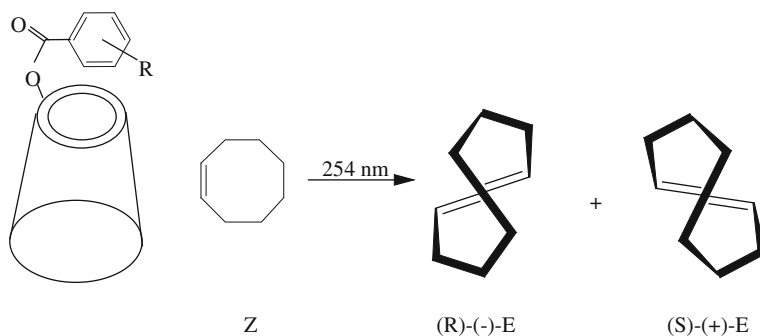
only observed if amyloid fibrils are present and serves as a diagnostic feature. The blue fluorescence is a consequence of complete flattening of the thioflavin molecule when the unfolding of the two aromatic parts attains 180° . Such a structure is stabilized in an amyloid cavity that supplies the fluorescent probe with an appropriate diameter (0.8–0.9 nm) and a sufficient depth (~ 1.4 nm) to cover the entire length of the thioflavin ions. The steric shroud for thioflavin T provided by the amyloid fibrils leads to the flattening considered above (Groenning 2010 and references therein).

Cyclodextrins are used to achieve water solubility and to enhance the bioavailability of many drugs. In particular, the problem of phenylalanine encapsulation in β -CD deserves mention. This guest exists in L and D forms. Whereas the L form is an essential component of human nutrition and is occasionally included in mixed medications, the D form is utilized very little by the human organism. Under some conditions, the L-to-D configurational change is possible. For this reason, it is useful to bear in mind that β -CD binds D-phenylalanine more tightly than L-phenylalanine, so that the mentioned enantiomerization can receive an additional impulse. The inclusion proceeds through the amino-acid part of phenylalanine in its zwitterionic form. The fact that inclusion of the D enantiomer is more favorable than that of the L enantiomer was established experimentally by Sompornprist et al. (2001) and supported theoretically by Fatiha et al. (2008).

Cyclodextrins have been used as modifiers for polymeric films prepared from 10,12-pentadecadiynoic acid. The side acid chains of the polymer are drawn into cyclodextrin cavities to form inclusion complexes. This induces a blue-to-red transition in fluorescence (Kim et al. 2005; Ahn and Kim 2008). Once such complexes have been formed, the cyclodextrins disrupt the densely packed, self-assembled structure of the polydiacetylene, disturbing the hydrogen bonding between the carboxylic headgroups. As a consequence, the effective conjugation length of the polymer is altered. The stress generated by the formation of the inclusion complexes provides a sufficient energetic driving force to promote the color change observed.

In *N*-methyl-2-pyrrolidone solution, β -CD encapsulates the polyaniline chain, forming an insulated molecular wire. Polyaniline has potential for use in molecular electronics. In the noninsulated state, polyaniline suffers from interchain interaction, coiling, and insufficient stability. These problems were solved by encapsulation of the polymer by β -CD (Frampton and Anderson 2007). Two effects accompany the encapsulation. The first consists of formation of a nanotube from several cyclodextrins that are close packed. The second effect consists of changing the polyaniline configuration from coil to rod; this configuration is required to realize high electric conductivity. Although the formation of this insulated molecular wire hinders oxidative doping of polyaniline with iodine, it does not prevent protonic doping. Acidification of the nanotube successfully leads to the formation of emeraldine salts, opening the way to an organic current-carrying conductor (Frampton and Anderson 2007).

Lu et al. (2008a,b) have studied cyclooctene photoisomerization within methoxybenzoyl derivatives of cyclodextrins. The methoxybenzoyl moiety acts as a photosensitizer and also as a space filler. The position of the methoxy group was varied as follows: R = *o*-MeO, R = *m*-MeO, or R = *p*-MeO. (*Z*)-cyclooctene was fully encapsulated. The authors did not calculate the mutual orientation of the filler and the



Scheme 10.5 Z-to-E photoisomerization of cyclooctene within methoxybenzoyl cyclodextrin

guest molecule, but admitted that the space filler can adjust the depth/position and orientation of guest penetration into the cyclodextrin cavity. Naturally, the structure of the filler moiety substantially affected the chirality induced in the guest substrate. The cyclodextrin bearing *meta*-methoxy moiety was the most effective to produce enantiomeric excess of (*E*)-cyclooctene formed from (*Z*)-cyclooctene (Scheme 10.5), namely chiral (*E*)-isomers were obtained in 46% enantiomeric excess.

10.4 Closing Remarks

Reactions within host–guest complexes are often considered as chemical interactions proceeding inside “molecular flasks”. This chapter has shown that these “flasks” can be flexible and can change their configuration upon guest inclusion. On the other hand, the guests, on inclusion into a host, can alter their spatial arrangement. This chapter has provided many examples of such alteration.

Williams et al. (2004) postulated that the driving force for guest binding does not have to come entirely from direct host–guest interactions. Instead, a major part may derive from strengthening of existing interactions *within* the host through the guest conformational change. Thus, Asadi et al. (2011) reported synthesis of a cavitand featuring thiourea hydrogen-bonding sites and its dimerization in the presence of suitable guests. Dimerization creates a capsule host, in which long-chain alkanes can be accommodated. Specifically, *n*-C₁₅H₃₂ is encapsulated, but this guest is folded *within* the host; as deduced from NMR studies, the guest turned out to be contorted.

References

- Ahn, D. J., & Kim, J.-M. (2008). *Accounts of Chemical Research*, 41, 805.
 Ams, M. R., Adjami, D., Craig, S. L., Yang, J.-S., & Rebek, J. (2009). *Beilstein Journal of Organic Chemistry*, 5, 79.
 Asadi, A., Ajami, D., & Rebek, J. (2011). *Journal of the American Chemical Society*, 133, 10682.

- Azov, V. A., Gomez, R., & Stelten, J. (2008). *Tetrahedron*, *64*, 1909.
- Caltagirone, C., Bill, N. L., Gross, D. E., Light, M. E., Sessler, J. L., & Galle, Ph A. (2010). *Organic & Biomolecular Chemistry*, *8*, 96.
- Custelcean, R., Delmau, L. H., Moyer, B. A., Sessler, J. L., Cho, W.-S., Gross, D. E., Bates, G. W., Brooks, S. J., Light, M. E., Gale, Ph. A. (2005). *Angewandte Chemie*, *117*, 2593.
- Fatiha, M., Djameleddine, Kh, & Leila, L. (2008). *Oriental Journal of Chemistry*, *24*, 43.
- Frampton, M. J., & Anderson, H. L. (2007). *Angewandte Chemie International Edition*, *46*, 1028.
- Freitag, M., Gundlach, L., Piotrowiak, P., & Galloppini, E. (2012). *Journal of the American Chemical Society*, *134*, 3358.
- Groenning, M. (2010). *Journal of Chemical Biology*, *3*, 1.
- Hariharan, M., Neelakandan, P. P., & Ramaiah, D. (2007). *Journal of Physical Chemistry B*, *111*, 11940.
- Javor, S., & Rebek, J. (2011). *Journal of the American Chemical Society*, *133*, 17473.
- Kamitori, Sh, Muraoka, Sh, Kondo, Sh, & Okuyama, K. (1998). *Carbohydrate Research*, *312*, 177.
- Kim, J.-M., Lee, J.-S., Lee, J.-S., Woo, S.-Y., & Ahn, D. J. (2005). *Macromolecular Chemistry and Physics*, *206*, 2299.
- Ko, Y. H., Kim, Y., & Kim, K. (2008). *Angewandte Chemie International Edition*, *47*, 4106.
- Legouin, B., Uriac, Ph, Tomasi, S., Toupet, L., Bondon, A., & van de Weghe, P. (2009). *Organic Letters*, *11*, 745.
- Lipkowitz, K. B. (1991). *Journal of Organic Chemistry*, *56*, 6357.
- Lu, R., Yang, Ch., Cao, Y., Wang, Zh, Wada, T., Jiao, W., et al. (2008). *Chemical Communications*, 374.
- Lu, R., Yang, Ch., Cao, Y., Tong, Y., Jiao, W., Wada, T., et al. (2008a). *Journal of Organic Chemistry*, *73*, 7695.
- Montes-Navajas, P., Teruel, L., Corma, A., & Garcia, H. (2008). *Chemistry: A European Journal*, *14*, 1762.
- Naidoo, K. J., Chen, J. Y.-J., Jansson, J. L. M., & Maliniak, A. (2004). *Journal of Physical Chemistry B*, *108*, 4236.
- Nilsson, M., Valente, A. J. M., Olofsson, G., Soederman, O., & Bonini, M. (2008). *Journal of Physical Chemistry B*, *112*, 11310.
- Purse, B. W., & Rebek, J. (2006). *Proceedings of the National Academy of Sciences*, *103*, 2530.
- Restorp, P., & Rebek, J. (2008). *Journal of the American Chemical Society*, *130*, 11850.
- Sgarlata, C., Bonaccorso, C., Gulino, F. G., Zito, V., Arena, G., & Sciotto, D. (2009). *Tetrahedron Letters*, *50*, 1610.
- Sompornprist, P., Deechalao, N., & Vongsvivit, J. (2002). *ScienceAsia*, *28*, 263.
- Thallapally, P. K., Wirsig, N. B., Barbour, L. J., & Atwood, J. L. (2005). *Chemical Communications*, 4420.
- Tzeli, D., Teodorakopoulos, G., Petsalakis, I. D., Adjami, D., & Rebek, J. (2012). *Journal of the American Chemical Society*, *134*, 4346.
- Verdejo, B., Gil-Ramirez, G., & Ballester, P. (2009). *Journal of the American Chemical Society*, *131*, 3178.
- Williams, D. H., Stephens, S. E., O'Brien, D. P., & Zhou, M. (2004). *Angewandte Chemie International Edition*, *43*, 6596.
- Wu, X., Hu, K., Meng, X., & Cheng, G. (2010). *New Journal of Chemistry*, *34*, 17.

Chapter 11

The Role of Solvents in Confined Organic and Organometallic Reactions

11.1 Introduction

The preceding chapters have described driving forces that govern host–guest complexation. Solvents are media where this complexation is most commonly carried out. In principle, encapsulation of species insulates them from solvents. At the same time, solvation and desolvation play an important role in reactivity under confinement. Sometimes, the equilibrium of the host–guest complexation depends on the nature of the solvent. The solvent may play the role of a filler upon guest coinclusion. This can significantly modify the orientation of the guest in the host cavity.

Generally, the encapsulation process, which leads to a loss of conformational freedom, is inherently accompanied by entropic loss. On the other hand, before encapsulation, both the free host and the free guest molecules were solvated. In the solvation shell, the solvent molecules around the host and the guest are highly oriented. During encapsulation, both the host and the guest have to lose their solvation shells, and the solvent molecules of the shells become disordered. In the solvent pool, this process causes the common disorder to increase and thus leads to a favorable entropy gain, which compensates the entropic loss of conformational freedom upon encapsulation (Liu et al. 2008).

11.2 Hydration/Dehydration Upon Confinement

Water is the most attractive solvent for confined chemistry: It is cheap and easily available. Water is an environmentally benign medium for organic synthesis. Complexation of a guest to a host proceeds without formation or rupture of covalent bonds and includes the following main processes:

- (1) Partial breaking of the hydration shells.
- (2) Exclusion of cavity-bound water molecules.

- (3) Conformational changes of the guests (e.g., deviation from symmetry and restriction of conformational flexibility).
- (4) Direct binding of the guest due to noncovalent interaction by H-bonding, van der Waals forces, hydrophobic effects, and electrostatic interactions.
- (5) Hydration of the inclusion complex formed.

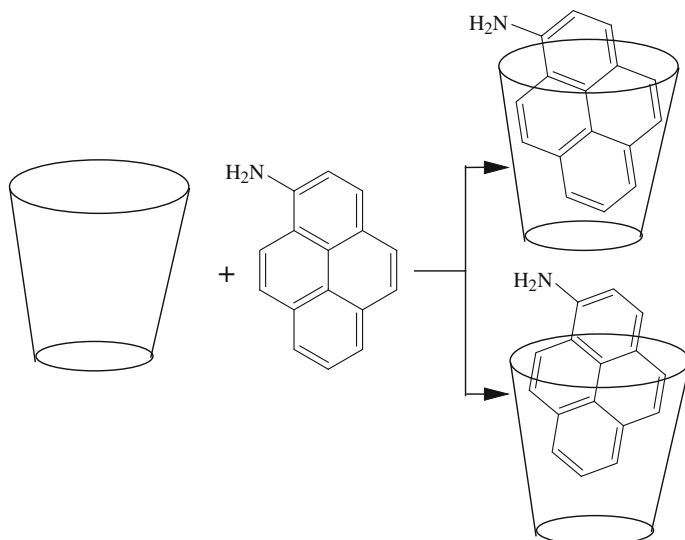
Solution molecules bound within the capsule are in dynamic equilibrium with free ones. In particular, the release of cavity-bound water molecules is connected with a release of energy (Zhang et al. 2008). When located inside a lipophilic cavity, water molecules cannot satisfy their hydrogen-bonding potential. Therefore, they have higher enthalpy than bulk water molecules located in the aqueous environment. The main driving force for complex formation in the case of the most frequently used β -CD appears to be release of these enthalpy-rich water molecules from the CD cavity, which lowers the energy of the system (Rafati and Safatian 2008). Thermodynamic analysis of cucurbit[7]uril complexation with bicyclo[2.2.2]octane or adamantane guests bearing ammonium substituents indicates that this pattern is consistent with the release of water molecules which are electrically oriented (Moghaddam et al. 2011).

According to estimations made by means of molecular dynamics techniques by Rodriguez et al. (2008), the amount of water (ρ_W) trapped inside β -CD typically fluctuates between four and six molecules. Olivera et al. (2007) confirmed this estimation experimentally, giving $\rho_W = 5$ on average. Interestingly, for dimethylsulfoxide (DMSO) this number drops to practically one unit, $\rho_{\text{DMSO}} = 1$. The values of ρ_W and ρ_{DMSO} coincide roughly with the differences in the bulk densities—or equivalently molecular sizes—of these two solvents at ambient conditions: $\rho_W/\rho_{\text{DMSO}} \sim 4$.

Molecular dynamics simulations established that, in a cavity with diameter of 0.12 nm, the dielectric constant of confined water is smaller by a factor 2 than that of bulk water (Senapati and Chandra 2002). For encapsulated water, the reduction of the dielectric constant is just a result of confinement because no electrostatic interaction between water and the cavity surface was introduced in these calculations. Of course, such a reduction can substantially define reaction conditions within the cavity.

Hydration of the inclusion complex formed can depend on the guest orientation, as was shown for 1-aminopyrene covered with a β -CD sleeve (Hansen et al. 1992). These authors measured the rates of proton transfer from surrounding water to the amino function of the guest under photoexcitation in the ultraviolet range. The experiments revealed that two complexes were formed, as illustrated in Scheme 11.1.

When the amino function of the guest is located near the hydroxyl rim of β -CD, it is involved in hydrogen bonding with the rim hydroxyl. The affinity of the NH_2 to an external proton rises. For the orientation where the amino function is further away from the hydroxyl rim, the proton affinity of this function drops off. This decrease of the affinity is caused by blockade of the amino function by the hydration shell, because the function is surrounded by water molecules. In the latter case, the proton transfer rate is not affected by inclusion of aminopyrene into β -CD. In contrast, the rate of water-to-aminopyrene proton transfer was enhanced by a factor 2 when the amino group was brought closer to the hydroxyl rim of the β -CD sleeve.



Scheme 11.1 Formation of two aminopyrene complexes with cyclodextrin depending on degree of guest penetration into host

It is interesting to compare α -CD, β -CD, and γ -CD in terms of their inclination to trap water molecules within their hydrophobic cavities. While the α -CD and γ -CD molecules exhibit marked flexibility, the β -CD counterpart is distinguished by its rigidity. The constrained motion of β -CD results in a greater readiness to trap water molecules within its hydrophobic cavity and in the first hydration shell compared with the relatively flexible γ -CD, which interferes only to a minor degree with the surrounding solvent. Accordingly, α -CD and γ -CD are 9 and 11 times more soluble in water than β -CD (Naidoo et al. 2004).

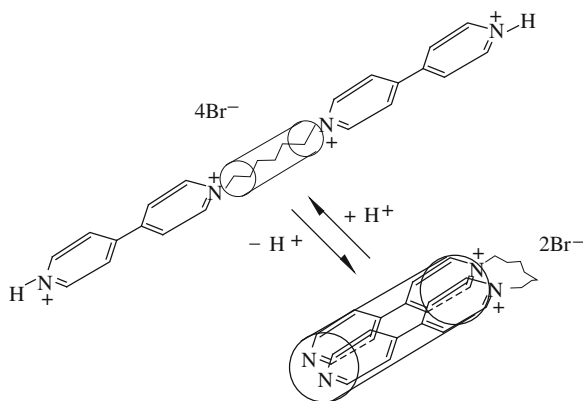
Dehydration processes can also play a decisive role in reactions of confined organic compounds. The outstanding example is the β -cyclodextrin-regulated reduction of mononitroarenes by hydroxide ion in water (Lu et al. 2006). Without β -cyclodextrin, hydroxide cannot transform a nitroarene even into its anion-radical. This inability originates from stabilization of the hydroxide as a result of hydration. Pearson (1986) estimated the stabilization energy as 420 kJ/mol. Nevertheless, the electronegative nature of the nitroarene permits the formation of an encounter complex with the negative hydroxide ion still in the water environment. β -Cyclodextrin sucks up this complex through the upper (wider) rim, leaving the water shell just above the rim. Being deprived of stabilization by hydration, the hydroxide acquires the ability to reduce the nitroarene. The corresponding anion-radical is formed. Reacting with water and hydroxide in the closed external sphere, this anion-radical transforms into the corresponding azoxyarene, which appears as the resultant product. The described reactions open the way to enhanced reducing ability of metal hydroxide in water. Water is the only solvent for metal hydroxides.

X-ray crystallographic study established that the solid complex of α -cyclodextrin with 4-fluorophenol contains the OH group of phenol inside the cyclodextrin cavity (Shibakami and Sekiya 1992). In aqueous solution, however, the F substituent is located inside and the OH substituent outside the cyclodextrin cavity, as proven by NMR (Alderfer and Elseheh 1997). Molecular orbital calculations (Liu et al. 2000) showed that, though the hydroxy group of 4-fluorophenol can be hydrogen-bonded to the glycosidic oxygen of cyclodextrin in the solid state, in aqueous solution it is more likely to form a hydrogen bond with water in the bulk. It is hydrogen bonding with the bulk water that changes the orientation of the substrate inside the cavity.

Besides hydration/dehydration, the affinity of the encapsulating species to the solvent plays an important role. Thus, CB[6] differentiates well between saturated and unsaturated hydrocarbons: alkenes show four to ten times weaker binding. This drop is definitely due to the three to five times higher water solubility of alkenes, which reduces the driving force for inclusion. Scheme 1.27 can again be mentioned to illustrate this specificity, as exemplified by pyridin-4-yl indolizine included into β -cyclodextrin (Becuwe et al. 2007). In neutral aqueous medium, the hydrophobic pyridinyl fragment is incorporated into the hydrophobic cavity of the receptacle. When the unsubstituted pyridinyl nitrogen is positively charged, exclusion of the moiety takes place: from the receptacle to the bulk water environment. The positive charge deprives the pyridinyl moiety of its hydrophobicity but generates affinity to the polar bulk. Analogously, N-protonation induces guest release from kinetically stable complexes of cycloalkenes encapsulated into resorcin[4]arene bearing quinone and quinoxaline fragments (Pochorovski et al. 2012).

Controllable molecular self-assembly behavior was reported for the cucurbit[8]uril and bispyridinium derivatives of Scheme 11.2 (Zhang et al. 2011). When the tetracation form is encapsulated by CB[8], the nonaromatic linker $[(\text{CH}_2)_6]$ occupies the host cavity. However, in neutral solution, the tetracation form loses protons at the terminal nitrogen atoms. The resulting inner dication bends into a loop so that the bispyridinium folded part is encapsulated but the linker is kept outside the CB[8] cylinder. This conformation changes from a molecular loop to a [2]pseudorotaxane in the presence of acid as a result of disruption of the CB[8]-induced homoguest pair and the high mutual affinity of CB[8] and the linker. Ion-dipole and hydrophobic interactions play a crucial role in controlling the conformational changes that occur upon interaction of the guest with neutral or acidic media. Zhang et al. (2011) also synthesized an acceptor-donor-acceptor linear molecule containing one electron-rich naphthoxy unit and two viologen units. Upon deprotonation/protonation, the CB[8] complex of this molecule undergoes principally the same transformations as depicted in Scheme 11.2. Interestingly, through the noncovalent interaction with CB[8], one naphthoxy and one viologen unit can be jointly located inside the guest sleeve.

Nishimura et al. (2008) revealed a very curious aspect of the influence of water on the rotation of the α -cyclodextrin cuff around a diphenylacetylene axis. One end of the axis was attached to a glass support, while the other end of the axis had a stopper. This prevents the cuff from coming off. The α -cyclodextrin cuff bore fluorescein covalently linked to cyclodextrin. This permits observation of the rotation of the



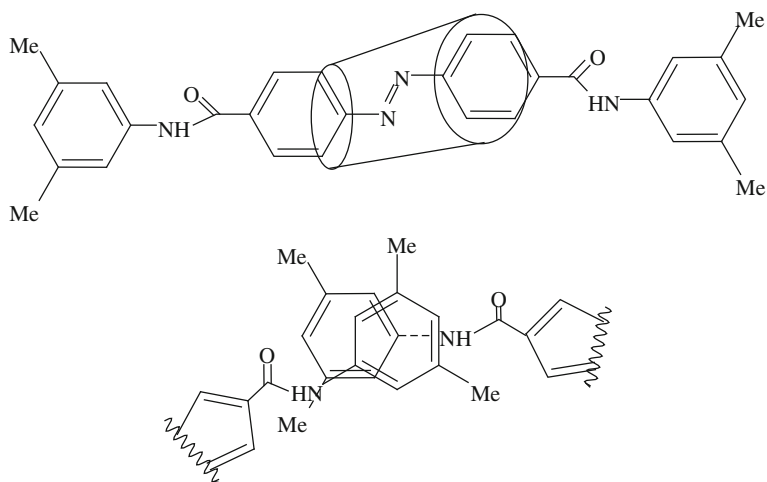
Scheme 11.2 Bending of bis(dipyridinium) tetracation encapsulated with cucurbituril upon losses of two terminal protons

cuff around the axis using a microscopy technique called defocused wide-field total internal reflection fluorescence microscopy. It turned out that the cuff of the rotaxane did not rotate if the sample was dry. However, when it was water-wet, very rapid rotational and vibrational motion was observed. (The term “rotaxane” originates from the Latin *rota*, meaning wheel, and Greek *axon*, meaning axis.) The authors did not provide any explanation for this water effect. It is logical to presuppose that water acts as a lubricant that makes the cuff rotation possible.

11.3 Organic Solvents

Organic solvents can have specific effects on the chemistry of confined organic and elementoorganic compounds. Thus, the arylazobenzene of Scheme 11.3 forms a rotaxane with α -cyclodextrin (Maniam et al. 2008). The fluorescent properties of this rotaxane are different in water and in methanol or dimethylsulfoxide.

In water: The macrocycle encompasses the axis between bulky blocking groups. The blocking groups prevent the cuff and axis from dissociating. The blocking groups of the dumbbell are almost coplanar with the axis, so there is extended conjugation along the length of the encapsulated chromophore. In water, the inclusion compound manifests applicable fluorescence emission and other spectroscopic characteristics that are not peculiar to the uncuffed azobenzene. The uncuffed chromophore is non-fluorescent in aqueous solution at room temperature, because radiative deactivation of the photoexcited azobenzene is not competitive with its photoisomerization. In water, the rotaxane dumbbells assemble as molecular fibers, linearly aligned along the single axis and insulated by cyclodextrins. The fibers come into contact with adjacent dumbbells through their blocking groups according to the schematic at the bottom of Scheme 11.3.



Scheme 11.3 Fiber-like alignment of azobenzene-based rotaxan in cyclodextrin cavity and intermolecular π - π stacking of dumbbell blocking groups

As seen from the schematic at the bottom of Scheme 11.3, the blocking groups are π - π stacked, with the centroid of one ring lying over one carbon of the other. The aggregation of the ready-made cuffed azobenzene results in very strong fluorescence emission (100 μ M water solution, room temperature, $\lambda_{\text{ex}} = 480$ nm).

In methanol or dimethylsulfoxide: When water as the solvent was replaced with methanol or dimethylsulfoxide, this emission disappears because these solvents disrupt π - π stacking (Maniam et al. 2008).

11.4 Mixed Solvents

Adding a cosolvent with increased solvation ability towards both guest and host can greatly reduce the binding constants of inclusion complexes. If such an addition decreases the polarity of the mixed solvent, this enhances the electrostatic interaction of ion pairs and also changes the course of the reaction. In cases of water-alcohol mixed solvents, the alcohol brings about extrusion of water from the capsule cavity and makes the cavity more hydrophobic. At the same time, however, inner-cavity desolvation is weakened and host-guest binding deteriorates too (Liu et al. 2008). It is also mentioned that the presence of methanol disrupts the hydrogen-bond network of some host capsules (Lledo et al. 2011).

The literature gives dissimilar standpoints on the effect of alcohols on reducing the constants characterizing the stability of cyclodextrin inclusion complexes with organic guests. Thus, Patrika et al. (2001) admitted the formation of a weak ternary (coincluded) complex, whereas Franchi et al. (2008) discarded the formation of a ternary complex and confirmed the formation of a binary complex alcohol@

cyclodextrin competing with the complex between an organic guest and cyclodextrin. However, the nature of the organic guest may play its own decisive role (other conditions being equal).

The macroscopic surface tension of solvent mixtures also controls the formation of encapsulation complexes. The stability constants of these complexes decrease as the surface tension values decrease. Thus, the inclusion complex of Methyl Orange with β -cyclodextrin is less stable in water–acetonitrile and in water–dimethylformamide than in water–dimethylsulfoxide mixture. The compared mixtures contained equal concentration of each organic cosolvent (Sueishi et al. 2003). The following values taken from handbooks allow comparison of the surface tension values at 25 °C (in mN/m) and dielectric constants (in parentheses) at 20 °C: water 72.0 (76.6), dimethylsulfoxide 42.9 (48.9), dimethylformamide 35.2 (36.0), and acetonitrile 28.7 (38.8). From this comparison of the dielectric constants, it can be inferred that the inclusion equilibria are more shifted towards complex formation with increasing solvent polarity.

Moreover, organic cosolvents strongly reduce the affinity of an organic guest for the CD cavity, compared with water. In fact, azobenzene rotaxination with cyclodextrins is effective in 9:1 water–dimethylsulfoxide mixture but does not take place in 1:9 water–dimethylsulfoxide mixture (Ma et al. 2007).

11.5 The Specific Role of Organic Solvents in Trapping by Porous Materials

The role of the solvent is more specific in organic and organometallic reactions proceeding within zeolites. Trapping of organic compounds by zeolites from solutions is accompanied by frustration of the hydrogen-bonding network and by decrease in the solution density. These effects (induced by trapping) facilitate penetration of the organic compounds inside the zeolite channels.

Surprisingly, preliminary inclusion of organic solvents into mesoporous γ -alumina enhances trapping of organic guests. An increase was observed for trapping of methane or ethane by mesoporous γ -alumina that already contained carbon tetrachloride or disulfide (Miachon et al. 2008).

An analogous effect of enhanced trapping was observed during sorption of hydrogen by γ -alumina mesopores into which ethanol had been previously introduced. This effect was measured microvolumetrically based on alumina with 10.9 nm mean pore size, at hydrogen pressure of 101 kPa and loading less than 100%. Compared with the corresponding bulk value (at the same hydrogen pressure), the solubility in the confined system increases dramatically, namely up to five times (Miachon et al. 2008). This phenomenon was used to explain the apparent H₂-zero-order kinetics for the nitrobenzene hydrogenation reaction (Pera-Titus et al. 2008).

As already mentioned, inclusion of guests in porous cavities is conjugated with preliminary displacement of internal portions of a solvent. In this case, a specific problem can be encountered. In metalorganic framework materials, bonds, which

define the porosity, are often weak. Typically, these materials are prepared in solution, and the solvent needs to be removed to allow guests to enter the pores. Depending on its volatility, the solvent can be removed by heating or reducing the pressure. However, if the network-forming bonds are thermally unstable or reactive to the solvent, remnants of the destroyed framework can block the channels. Loss of the solvent can also create a surface tension that drives the pores to collapse. Nelson et al. (2009) proposed to treat such systems with liquid supercritical carbon dioxide. This method relies on the solvent molecules being miscible with the carbon dioxide liquid. The initial solvent is replaced by the supercritical liquid. The latter is in turn simply released by depressurization to leave the empty pores; For instance, coordinative bonds between metal and polydentate carboxylate linkers retain their integrity whereas pore accessibility is fully guaranteed (Nelson et al. 2009).

11.6 Solvent–Matrix Effects

Solvent–matrix effects can be illustrated by the monomolecular reaction of the acetylene anion-radical generated in a glassy 2-methyltetrahydrofuran (MeTHF) or 3-methylpentane matrix by ionizing radiation (^{60}Co) at 77 K. On illumination of the MeTHF follipops with light of wavelength 430 nm, intramolecular hydrogen transfer takes place: $(\text{CH}\equiv\text{CH})^{\cdot-} \rightarrow \text{CH}_2=\text{C}^{\cdot-}$ (Itagaki and Shiotani 1999). When 3-methylpentane was used for follipop preparation, no such hydrogen transfer was observed. This could be due to the nature of 3-methylpentane, which gives a non-polar, soft matrix. MeTHF is a polar molecule, which forms a rigid, glassy matrix. The anion-radical $(\text{CH}\equiv\text{CH})^{\cdot-}$ as well as its isomeric form $\text{CH}_2=\text{C}^{\cdot-}$ (generated by ionizing radiation and hydrogen transfer) are both stabilized in MeTHF. The features of MeTHF as a confined medium may be responsible for the described phenomenon.

11.7 Closing Remarks

This chapter considers confinement processes that take place in water, in organic solvents, in water–organic mixtures, in rigid glassy matrices, and within porous material previously filled with organic solvents. This chapter gives some orientation for selection of the appropriate solvent to start a confinement event. Of course, confinement disengages the solvent shells around substrates in the final phase of the process, but the preceding phases define its general thermodynamics. As exemplified by hydration/dehydration, the thermodynamic features of confinement are considered in detail.

Organic solvents are, in principle, similar to organic substrates in their ability to occupy internal chambers of host molecules. Selection of the correct volume defines the fate of the included solvent molecules. If the internal volume is large enough to hold molecules of a solvent, a substrate, and an entering reactant, no removal of

the solvent is needed. In other cases the solvent must be evacuated. Sometimes, this evacuation requires precautions: The porous structure of the metalorganic network is destroyed upon direct evacuation of the solvent.

Entry of organic substrates into zeolites is facilitated when their channels are preliminarily filled with some solvent. Basically, the solvent sucks in the substrate by means of dissolution. Therefore, the choice of a solvent for a zeolite must take into account the solubility of the substrate in the given solvent or solvent mixture.

References

- Alderfer, J. L., & Elseheev, A. V. (1997). *Journal of Organic Chemistry*, 62, 8225.
- Becuwe, M., Cazier, F., Bria, M., Woisel, P., & Delattre, F. (2007). *Tetrahedron Letters*, 48, 6186.
- Franchi, H., Pedulli, G. F., & Lucarini, M. (2008). *Journal of Physical Chemistry A*, 112, 8706.
- Hansen, J. E., Pines, E., & Fleming, G. R. (1992). *Journal of Physical Chemistry*, 96, 6904.
- Itagaki, Y., & Shiotani, M. (1999). *Journal of Physical Chemistry A*, 103, 5189.
- Liu, L., Li, X.-S., & Guo, Q.-X. (2000). *THEOCHEM*, 530, 31.
- Liu, Y., Cao, R., Chen, Y., & He, J.-Y. (2008). *Journal of Physical Chemistry B*, 112, 1445.
- Lledo, A., Kamioka, S., Sather, A. C., & Rebek, J. (2011). *Angewandte Chemie International Edition*, 50, 1299.
- Lu, Y., Liu, J., Diffie, G., Liu, D., & Liu, B. (2006). *Tetrahedron Letters*, 47, 4597.
- Ma, X., Qu, D., Ji, F., Wang, Q., Zhu, L., Xu, Y., et al. (2007). *Chemical Communications*, 1409.
- Maniam, S., Cieslinski, M. M., Lincoln, S. F., Onagi, H., Steel, P. J., Willis, A. C., et al. (2008). *Organic Letters*, 10, 1885.
- Miachon, S., Syakaev, V. V., Rakhmatullin, A., Pera-Titus, M., Caldarelli, S., & Dalmon, J.-A. (2008). *ChemPhysChem*, 9, 78.
- Moghaddam, S., Yang, Ch., Rekharsky, M., Ko, Yo H, Kim, K., Inoue, Yo, et al. (2011). *Journal of the American Chemical Society*, 133, 3570.
- Naidoo, K. J., Chen, J. Y.-J., Jansson, J. L. M., & Maliniak, A. (2004). *Journal of Physical Chemistry B*, 108, 4236.
- Nelson, A. P., Farha, O. K., Mulfort, K. L., & Hupp, J. T. (2009). *Journal of the American Chemical Society*, 131, 458.
- Nishimura, D., Takashita, Yo., Aoki, H., Takahashi, T., Yamaguchi, H., Ito, Sh., et al. (2008). *Angewandte Chemie International Edition*, 47, 6077.
- Olivera, A., Perez-Casas, S., & Costas, M. (2007). *Journal of Physical Chemistry B*, 111, 1197.
- Patrika, M., Boo, H. A., & Evans, C. H. (2001). *Journal of Photochemistry and Photobiology A*, 140, 67.
- Pearson, R. G. (1986). *Journal of the American Chemical Society*, 108, 6109.
- Pera-Titus, M., Miachon, S., Dalmon, J.-A. (2008). *American Institute of Chemical Engineers Journal*, 55, 434.
- Pochorowski, I., Boudon, C., Gisselbrecht, J.-P., Ebert, M.-O., Schweizer, W. B., & Diederich, F. (2012). *Angewandte Chemie International Edition*, 51, 262.
- Rafati, A. A., & Safatian, F. (2008). *Physics and Chemistry of Liquids*, 46, 587.
- Rodriguez, J., Rico, D. H., Domenianni, L., & Laria, D. (2008). *Journal of Physical Chemistry B*, 112, 7522.
- Senapati, S., & Chandra, A. (2002). *Journal of Physical Chemistry B*, 105, 5106.
- Shibakami, M., & Sekiya, A. (1992). *Journal of the Chemical Society, Chemical Communications*, 1742.
- Sueishi, Y., Kasahara, M., Inoue, M., & Matsueda, K. (2003). *Journal of Inclusion Phenomena and Macrocyclic Chemistry*, 46, 71.
- Zhang, Q.-F., Jiang, Z.-T., Guo, Y.-X., & Li, R. (2008). *Spectrochimica Acta*, 69A, 65.
- Zhang, Zh-J, Zhang, Y.-M., & Liu, Y. (2011). *Journal of Organic Chemistry*, 76, 4682.

Chapter 12

Conclusions

The chemistry of confined organic and organometallic compounds spans a wide range of scientific and engineering interest. The peculiarities of organic chemistry in a confined environment clearly differ from conventional chemistry in the bulk phase with respect to reactivity and selectivity. There is much interest in designing molecular-sized containers that influence and facilitate chemical reactions within their nanocavities. On top of the advantages of improved yield and selectivity, studies of reactions in confined conditions also provide important clues that extend our basic understanding of chemical processes. Temporarily confining a guest by a host within a fixed space keeps the guest isolated from solution and directs the guest's reactivity, regioselectivity, and stereospecificity.

Guest's functional groups that reside inside a host cap are less reactive compared with the same groups when located in such a manner as to be accessible to outer reactants. The reactivity of bulk-phase reactants depends on their size and shape relative to the dimensions of the host's volume and equatorial portals. Molecular containers enable investigation of highly strained and reactive molecules under normal working conditions by generating them in the protective inner phase. In this way, species that usually would rapidly decompose or polymerize even at low temperatures can be stored under ambient conditions, especially when the guest has no chance to escape its host. Encapsulation can control the reactant conformation, control the orientation between reactants, and select molecules according to their size and shape.

Accordingly, complexation is based on a combination of several intermolecular interactions depending on the solvent and the nature of the host and guest. The following factors can be enumerated: steric fit, van der Waals interactions, dispersive forces, dipole–dipole connection, charge-transfer phenomena, electrostatic relations, and hydrogen bonding.

A practically very important aspect of confined organic chemistry consists in therapeutically improved formulations of medications. Drug-delivery systems have been developed to overcome the disadvantages of conventional drug dosage forms; For instance, one of the typical applications of confined drugs is localized delivery

of anticancer remedies. Such confined remedies can be used for passive targeting via the reticuloendothelial system of the liver and of cells that are pathologically active.

In the future, the wealth of methods available, most of which are described in this monograph, will find relevant applications in the synthesis of enantiomerically pure drug candidates and targeted natural products. It is certainly possible to state that such applications will be realized in the near future.

In this book, the “now” and “then” of confined organic and organometallic chemistry have been indicated. From a more practical and optimistic perspective, global development of the branch of chemistry advocated herein may soon provide tools available for chemists. The challenge now lying before the community is to find ever more ingenious and diverse applications or niches for this enduringly fascinating and newly developed branch of organic chemistry.

Index

A

Acetazolamide, 34
Acetylation
Acridine, 172, 173
Acyloxylation
Adamantanes, 147
Aldo-enols, 133
Alkylation, 33, 152
Amination
 dehydrative, 6
Amines
 monomethylation, 10, 11
Anion-radicals, 31, 75
Aryl radicals, 2
Azocompounds, 67
Azocoupling, 67, 132
Azomethylns, 95

B

Barbiturates, 92
Bicyclooctanes, 180
Bilirubin, 132, 133
Bolaforms, 173
Bromination
 cyclodextrin-assisted, 31

C

Camptothecins, 54
Caratenoids
 ion-radicals of, 75, 76, 83, 121, 132, 137
Carbonylation, 155
Carboprost, 33
Catalysis in confined systems
 by transition metals, 47, 152, 163
 by phase transfer, 7, 19, 40
Cation-radicals, 21, 22, 43, 54, 85, 121, 133,
 145, 155, 156, 157, 159, 160

Chemisorption, 110, 117
Choline
 derivatives, 7, 8, 19, 21, 31, 33, 35, 112,
 154, 175, 182
Chromocene, 155
CL-20, 98–100
Corrin, 105, 106
Coumarins, 150, 151
Cracking
Cross-linkage
 physical, 19, 27, 35, 54, 98, 125, 148
Crystals as molecular flasks, 143, 176
Curcumin, 133, 134
Cycloaddition, 2, 15, 82–84, 122, 123,
 147, 161
 alkene-nitrile oxide, 130
 azide-alkyne, 2
 azide-nitrile, 119
 Diels-Alder reaction, 17, 18, 122, 131, 146,
 147, 161
 Pechmann condensation, 149
Cyclobutadiene, 14
Cyclobutanes, 15, 98
Cyclooctatetraenes, 77, 107–109
Cyclooctenes, 175, 176
Cyclopropanes, 122, 160
Cysteamine, 48
Cystine-cysteine interconversion, 47

D

Deacylation
 hydrolytic, 124
Dehydration, 6, 7, 179, 181, 182
Diazenyl radicals, 20
Diazonium cations, 69, 132
Dibucaine, 45
Dicloxacillin, 25
Dimerization

- Dimerization (*cont.*)
 chemical, 48
 photoinitiated, 16, 98
 physical
- Diphenylhydrazine, 159
- Disulfides, 10, 48
- Dithiotretiol, 28
- Doxorubicine, 151
- Drug carriers, 170, 190
- E**
- Effects
 Frank-Rabinovich
 salt, 9, 25, 28, 34, 38
 solvent, 9, 24, 26, 35, 36, 40, 41, 54
 Tamman, 117
- Electric conductivity, 7, 80
- Electron transfer to guest compounds, 12
- Emeraldine, 175
- Energy
 chemisorption of
 encapsulation of, 7, 19, 24, 41, 57, 175
 host-guest binding of, 96
 hydrogen bonds of, 89, 96
 production, in Krebs cycle, 91
 physisorption of, 115, 117, 169
 steric of confined compounds, 16
- Experimental technique for measuring encapsulation, 14
- F**
- Faujasite, 152, 153
- FDU-1, 151
- Ferrocenes, 3, 4, 24, 46
- Ferroceniums, 3, 46
- Ferulic acid, 133
- Fisher-Tropsch synthesis, 153
- Fluoresceine, 182
- Fullerenes
 ion-radicals of, 117, 126
- Fumarates, 90, 91, 98
- Furazans, 2, 3, 66, 67
- Furoxans, 161
- G**
- Glutarates, 90
- Glutathiones, 21
- H**
- Hemithioindigo, 16
- Henry reaction, 150
- Homocarnosine, 32
- Housane, 38, 39
- Hydration, 6, 14, 17, 18, 35, 41, 130, 179
- Hydrogenation, 118, 153, 154, 185
- Hydrogen-bonded template, 21, 95, 129, 182
- Hydrolysis, 17, 25, 92, 94, 124, 133
- I**
- Ion pairs, 42
 intimate, 9
 loose, 9
- Ionic liquids, 7, 42, 118, 131
- Isomerization, 15, 46, 56, 77, 85, 103, 104
- Isonicotinamide, 96–98
- Isotope exchange, 25
- IZA method, 157
- K**
- Keto-enols, 133
- L**
- Ligand-template approach, 106, 107, 109
- Ligand exchange, 155
- Lomefloxacin, 5
- M**
- Macropores, 143
- Malates, 91
- Maleates, 90, 91
- Malonates, 90
- MCM-41, 149, 150
- Mercaptans, 9
- Merocyanines, 23, 92
- Mesopores, 143, 151, 185
- Methyl orange, 185
- Micelles
 normal, 163, 189
 reverse, 77, 125, 129, 145
- Micellization, 27
- Micropores, 143, 145, 149, 151, 154, 164
- Molecular recognition, 2, 50, 57, 146
- Montmorillonite, 76, 77

N

Nanopores, 151, 155, 164, 165
Naproxen, 51
Nickelocene, 163, 164
Nitration, 131, 132, 137
Norephedrine, 156
Novocaine, 45

O

Octa acid, 12, 14, 15
Oligomers
 amiloid, 174, 175
Oxadiazoles
 N-oxides of, 72
Oxalates, 90
Oxidation, 3, 9, 10, 21, 22, 26, 31,
 41, 46, 48

P

Pentasil, 152, 154
Phenazines
 ion-radicals of, 31
Phenylalanine, 120, 155, 156, 175
Photolysis, 13–15, 21, 38, 40, 44
Phthalates, 89
Physisorption, 115, 117, 169
pi-Complexes, 72
pi-Stacks, 14, 53, 145, 184
Pluronics
 P 123, 134
 F 127, 134
Polyaniline, 175
Prilocaine, 45
Progesterone, 25
Proston, 33
Proteins, 139
Protonation
 of guests, host-assisted, 33, 38, 118, 150,
 157, 159
Pseudorotaxanes, 107
Pyranine, 26
Pyrenes, 14, 27
Pyriliums, 41

R

Racemization, 79
Radical-radical donor-acceptor
 interaction, 8, 44

Reduction, 12, 20, 23, 43, 48, 49, 54

Rhodamines
 B, 23
 6G, 148
Rotaxanes, 51, 107

S

SAPO, 157
Self-organized compositions, 5
Silica Gel 60, 148
Syngas, 153
Solubility in water
 cucurbiturils of, 37
 cyclodextrins, native of, 33
 methylcyclodextrins of, 21, 26
Stabilization of reactive intermediates, 57
Stilbenes, 117, 120, 122
Substitution
 vinyl-nucleophilic, 78
Succinates, 54, 90, 91
Sulfenic acids, 10
Surfactants, interactions with
 cavitands, 44

T

Tamman temperature, 117
Taxol, 134
Tenoxicam, 25
Tetracaine, 45
Thiabenzazole, 38
Thianthrene, 162
Thiazines
 ion-radicals of, 21
Thioflavin T, 174, 175
Thiolysis, 129, 130
Thiophenes, 103, 104, 106–109
TNT, 98–100
Tolans, 19, 35
Triazoles, 19

V

Vanillin, 133
Viologens cation-radicals
 dimers, 143, 155
 monomers, 84, 145, 155
 cation-radical dimers of, 121
 cation-radicals of
Vitamins

Vitamins (*cont.*)B₁₂, 105K₃, 5**W**

Wang resin, 65, 66, 69

Water, thermodynamics of release from
cavities, 180**Z**

Zeolites

acidity of, IZA-method determination, 157

chemical reaction within, 156

ZSM-5, 153, 157–161